

Synthesis of novel low-molecular-weight polytetrafluoroethylene and tetrafluoroethylene copolymers for pyrotechnic applications

Gerard Jacob Puts

**Faculty of Engineering, Built Environment and
Information Technology**

Department of Chemical Engineering

University of Pretoria

A thesis submitted in partial fulfilment of the requirements
for the degree of

Doctor of Philosophy in Chemical Engineering

Doctoral advisors:

Prof. Philip Crouse

Dr Bruno Ameduri

October 2017

Deo Patri sit gloria, et Filio qui a mortuis surrexit,
ac Paraclito in saeculorum saecula.

Vaarwel aan mijn Vader, zonder uwe was deze onderneeming niet
mogentlik. Rust zacht, wij hebben beide een strijd voleindigt.

Bedankt aan mijn Moeder, zonder uwe hat ik niet deze dag kunne zien.
Wij zulle bijde de vruchte deze onderneeming nog in dit leven proeven.

Acknowledgements

Firstly I would like to acknowledge my supervisors, Prof. Philip Crouse and Dr Bruno Ameduri, as without them, this research would never have come to pass. In particular, I want to extend my gratitude to Prof. Crouse, whose guidance and care made of me a saner and more productive human being.

Secondly, I would like to acknowledge the technical help of Mr William Victor Venner: Victor, your assistance in the laboratory during my administrative absences is appreciated in the utmost. I also acknowledge and thank Mrs Suzette Seymore, as without her, the procurement processes would have been an insurmountable nightmare. Furthermore, I would like to extend my thanks to Prof. Walter Focke for the multiple discussions on the requirements for the proper formulation of metal/fluorocarbon pyrotechnics.

Thirdly, a special thank you goes also to the *École Nationale Supérieure de Chimie de Montpellier* for hosting me in their laboratories during my academic exchange period. The experience gained in France is of an inestimable value to the South African Fluorochemical Industry.

Finally, I would also like to thank the various funding bodies, including the Department of Science and Technology, The National Research Foundation and Pelchem SOC, for contributing the funds and materials by which this research was conducted.

Executive summary

At present, the explosives industry in South Africa makes extensive use of heavy metal oxide pyrolants in the time-delay elements of detonators used in mining activities. There is a drive towards the use of safer and more environmentally benign pyrolants in the form of metal/fluorocarbon pyrotechnic formulations. However, high-molecular-weight polytetrafluoroethylene (PTFE) is the current industry standard and pyrolants made with this polymer cannot be easily processed as it cannot be melt-extruded owing to the exceptionally high melt viscosity of PTFE.

The research detailed herein was aimed at developing a low-molecular-weight PTFE capable of being used for extrudable pyrotechnic formulations, without suffering the drawbacks of poor thermal stability associated with low-molecular-weight fluorocarbons. The end result of this endeavour was the development of a low-molecular-weight PTFE, marginally bridged with butanediol divinyl ether, having sufficiently low molecular weight to be classified as a wax, while retaining sufficient thermal stability to be useful in pyrolant formulations. Additionally, this polymer also showed increased reactivity towards silicon metal due to the liberation of small amounts of HF from the non-fluorinated end-groups and the bridging agent, which helped remove the passivation layer of SiO₂ on the surface prior to the ignition of the metal fluorine exchange reaction.

This research starts with an in-depth review of the English language literature regarding the homopolymerisation of tetrafluoroethylene and also details the design and construction of the equipment for the safe and facile generation of up to 100 g of tetrafluoroethylene as well as the equipment for the polymerisation of tetrafluoroethylene, both in a Carius tube, and in an autoclave.

The work then relates the batch-type synthesis of low-molecular-weight PTFE by conventional free-radical polymerisation. The conventional process was unable to produce a polymer with a sufficiently low molecular weight, such that it could be easily melt-extruded. It was noticed that, although the molecular weight of the polymer decreased with initiator concentration, as evidenced by the TGA curves, the M_n calculated by DSC increased with initiator concentration. This discrepancy is due to the mass transfer effects present within the polymerisation reactor. An attempt was made at deriving a kinetic expression for the polymerisation of TFE under a mass-transfer-limiting regime, but this endeavour was abandoned in favour of a more experimental solution to the low-molecular-weight problem.

The use of a persistent-radical perfluorinated initiator capable of generating $\cdot\text{CF}_3$ radicals was investigated for the purpose of providing a tracer end-group that will permit the measurement of the molecular weight of the polymers directly by NMR spectroscopy. The usefulness of CF_3 end-groups as labels for molecular weight determination in poly(CTFE-*alt*-iBVE) copolymers by ^{19}F NMR spectroscopy was demonstrated and compared to results obtained by SEC. The persistent-radical perfluorinated initiator was not applied to TFE homopolymers due to technical issues regarding NMR spectroscopic analysis.

The penultimate part of this thesis relates the use of a RAFT/MADIX agent (O-ethyl-S-(1-methyloxycarbonyl)ethyl xanthate) for the control of the molecular weight of PTFE, as studied *via* GPC using the copolymer of tetrafluoroethylene and isobutyl vinyl ether for a model polymer system. The effectiveness of RAFT/MADIX techniques in the control of the molecular weight of TFE-based polymers was demonstrated.

Finally, low-molecular-weight PTFE marginally bridged with butanediol divinyl ether was synthesised by RAFT/MADIX techniques. The tailored PTFE was tested as the fuel in a fluoropolymer/silicon metal mixture. The tailored PTFE showed enhanced reactivity towards the silicon metal as compared to commercial- and low-molecular-weight PTFE synthesised by conventional free-radical polymerisation.

The PTFE developed here is of significant commercial importance to the South African fluorochemical industry and will enable the South African explosives industry to greatly improve the safety and environmental friendliness of their detonators.

The work reported here is limited to the synthesis and characterisation of the polymers, and only briefly touches the pyrochemical behaviour. In depth investigation of this aspect, as well as the rheological characterisation of the product polymer is left for subsequent researchers.

Table of contents

Acknowledgements.....	vi
Executive summary	vii
List of abbreviations	xvi
Table of figures	xix
List of tables	xxv
List of schemes.....	xxvii
Research outputs.....	xxix
Chapter 1 General introduction.....	1
References	5
Chapter 2 Literature review: The homopolymerisation of tetrafluoroethylene.....	7
Notes on the research strategy	8
2.1 Introduction.....	9
2.2 Synthesis of TFE and concomitant safety aspects.....	12
2.2.1 Ultra-fast pyrolysis of CF ₂ ClH.....	13
2.2.2 Dehalogenation of halofluorocarbons.....	14
2.2.3 Pyrolysis of perfluoropropionic acid salts	14
2.2.4 Pyrolysis of PTFE under vacuum	14
2.2.5 Tetrafluoroethylene process safety.....	17
2.2.6 Conclusions.....	20
2.3 Polymerisation process and equipment	20
2.3.1 Polymerisation procedures	21
2.3.2 Polymerisation equipment.....	22
2.3.3 Reaction mechanisms and kinetics.....	24
2.3.4 Conclusion	27
2.4 Polymerisation initiators.....	27
2.4.1 Inorganic free-radical generating initiators.....	28

2.4.2	Organic free-radical-generating initiators	28
2.4.3	Free-radical generating redox initiators	29
2.4.4	Fluorinated free-radical generating initiators	30
2.4.5	Miscellaneous free-radical generating initiators	31
2.4.6	Photoinitiators	31
2.4.7	Other initiators	32
2.4.8	Ziegler-Natta catalysts	35
2.4.9	Conclusions.....	35
2.5	Reaction conditions	36
2.5.1	Monomer purity	36
2.5.2	Solvent environment	36
2.5.3	Temperature and pressure	42
2.5.4	Agitation.....	43
2.5.5	Polymerisation additives	43
2.5.6	Conclusions.....	49
2.6	Telomerisation and reversible-deactivation radical polymerisation of TFE.....	49
2.6.1	Telomerisation of TFE	49
2.6.2	Reversible-deactivation radical polymerisation of TFE	51
2.7	Properties of PTFE.....	51
2.7.1	Molecular weight.....	53
2.7.2	Morphology	55
2.7.3	Chemical and thermal properties.....	64
2.7.4	Mechanical properties	70
2.7.5	Hydrophobicity and surface properties	71
2.7.6	Tribology and friction coefficients.....	73
2.7.7	Electrical properties.....	73
2.7.8	Conclusions.....	74
2.8	Polymer analysis techniques	74

2.8.1	Spectroscopic techniques.....	75
2.8.2	Microscopy and particle analysis.....	77
2.8.3	Diffraction and light scattering.....	77
2.8.4	Rheology.....	78
2.8.5	Thermal analysis.....	78
2.8.6	Standard specific gravity techniques	79
2.8.7	Conclusions.....	80
2.9	Applications of PTFE	81
2.9.1	Electrical and electronic applications.....	81
2.9.2	Pipes, tubing, gaskets, seals, filters, and machined parts.....	82
2.9.3	Tribological applications.....	83
2.9.4	Chemically resistant, hydrophobic coatings and textiles.....	84
2.9.5	Medical applications	85
2.9.6	Pyrotechnic applications	86
2.9.7	Conclusions.....	86
2.10	Perspectives.....	86
2.11	References	89
Chapter 3 Tetrafluoroethylene generator and Carius tube manifold design.....		107
3.1	Introduction.....	108
3.2	Design philosophy	109
3.2.1	Depolymerisation reactor system	109
3.2.2	Carius tube system	111
3.3	Depolymerisation reactor design	112
3.3.1	Design overview.....	112
3.3.2	Depolymerisation vessel mechanical design.....	114
3.3.3	Cold trap sizing	119
3.3.4	Safety calculations.....	128
3.3.5	Mechanical support stand for the depolymerisation system	129

3.4	Carius tube system design.....	131
3.4.1	Design overview.....	131
3.4.2	Carius tube design.....	132
3.4.3	Tube loading masses.....	133
3.4.4	Mounted housing for the Carius tube system.....	134
3.4.5	Explosion containment system.....	135
3.5	Summary.....	136
3.6	References	138
Chapter 4 Synthesis of low-molecular-weight polytetrafluoroethylene waxes.....		141
4.1	Introduction.....	142
4.2	Experimental.....	145
4.2.1	Materials	145
4.2.2	Polymerisation apparatus.....	145
4.2.3	Synthesis of PTFE by free-radical polymerisation.....	145
4.2.4	Differential scanning calorimetry	148
4.2.5	Thermogravimetric analysis.....	148
4.2.6	Fourier-transform infrared analysis.....	148
4.2.7	Pyrotechnic burn tests.....	149
4.3	Results & discussion	149
4.3.1	Molecular weight.....	150
4.3.2	Kinetic modelling of the TFE polymerisation process	154
4.3.3	Pyrotechnic behaviour.....	160
4.3.4	Rheological characterisation.....	164
4.4	Conclusions.....	165
4.5	References	166
Chapter 5 Radical copolymerisation of chlorotrifluoroethylene with isobutyl vinyl ether initiated by the persistent perfluoro-3-ethyl-2,4-dimethyl-3-pentyl radical		169
5.1	Introduction.....	170

5.2	Experimental.....	172
5.2.1	Materials	172
5.2.2	Polymerisation apparatus.....	172
5.2.3	Radical polymerisation procedure	172
5.2.4	Product purification.....	173
5.2.5	Nuclear magnetic resonance spectroscopic characterisation.....	174
5.2.6	Thermogravimetric analysis.....	174
5.2.7	Differential scanning calorimetry (DSC).....	174
5.2.8	Size-exclusion chromatography (SEC)	174
5.3	Results and discussion	175
5.3.1	Nuclear magnetic resonance spectroscopic characterisation.....	177
5.3.2	Addition preferences of $\bullet\text{CF}_3$ radicals to the CTFE/iBuVE charge transfer complex 180	
5.3.3	Reaction of iBuVE with PPFR elimination products.....	182
5.3.4	Effect of initiator concentration on molecular weight.....	182
5.3.5	Thermal properties of CF_3 terminated poly(CTFE- <i>alt</i> -iBuVE) copolymers.....	184
5.4	Conclusions.....	187
5.5	References	189
Chapter 6 Free-radical and controlled-radical copolymerisation of tetrafluoroethylene with isobutyl vinyl ether.....		
6.1	Introduction	192
6.2	Experimental.....	194
6.2.1	Materials	194
6.2.2	Free-radical copolymerisation of tetrafluoroethylene with isobutyl vinyl ether ...	194
6.2.3	Copolymerisation of TFE with iBuVE by RAFT/MADIX	195
6.2.4	Nuclear magnetic resonance spectroscopy	195
6.2.5	DP_n and $\text{M}_{n(\text{NMR})}$ calculations using benzoyl end-group analysis	195
6.2.6	DP_n and $\text{M}_{n(\text{NMR})}$ calculations using R and Z end-group analysis	196

6.2.7	Theoretical molecular weight	196
6.2.8	Differential scanning calorimetry	197
6.2.9	Thermogravimetric analysis.....	197
6.2.10	Size-exclusion chromatography	197
6.2.11	Particle-size analysis.....	197
6.2.12	Maldi-TOF Spectroscopy	197
6.3	Results and discussion	198
6.3.1	Free-radical copolymerisation of tetrafluoroethylene with isobutyl vinyl ether ...	198
6.3.2	Copolymerisation of TFE with iBuVE by RAFT/MADIX	209
6.4	Conclusions	219
6.5	References	221
Chapter 7 Radical copolymerisation of tetrafluoroethylene with 1,4-butanediol divinyl ether and isobutyl vinyl ether.....		
		225
7.1	Introduction	226
7.2	Experimental.....	227
7.2.1	Materials	227
7.2.2	Free-radical copolymerisation of TFE with BDDVE.....	228
7.2.3	Free-radical terpolymerisation of TFE with BDDVE and iBuVE.....	228
7.2.4	Free-radical synthesis of low-molecular-weight bridge PTFE in water, dimethyl carbonate, and perfluoroheptane.....	229
7.2.5	Synthesis of low-molecular-weight bridged PTFE in water, dimethyl carbonate, and perfluoroheptane by RDRP.....	229
7.2.6	Thermogravimetric analysis.....	230
7.2.7	Differential thermal analysis.....	230
7.2.8	Swelling tests.....	230
7.2.9	Pyrotechnic burn tests.....	230
7.3	Results and discussion	230
7.3.1	Copolymerisation of tetrafluoroethylene and butanediol divinyl ether	230

7.3.2	Terpolymerisation of tetrafluoroethylene, isobutyl vinyl ether, and butanediol divinyl ether	234
7.3.3	Synthesis of low-molecular-weight tetrafluoroethylene polymers marginally bridged with 1,4-butanediol divinyl ether	237
7.3.4	Pyrotechnic behaviour of low-molecular-weight tetrafluoroethylene polymers marginally bridged with 1,4-butanediol divinyl ether	239
7.4	Conclusions	241
7.5	References	242
Chapter 8	General conclusions	245

List of abbreviations

Monomers

TFE	Tetrafluoroethylene	$\text{CF}_2=\text{CF}_2$
HFP	Hexafluoropropylene	$\text{CF}_2=\text{CF}-\text{CF}_3$
CTFE	Chlorotrifluoroethylene	$\text{CF}_2=\text{CFCl}$
VDF	Vinylidene fluoride	$\text{CF}_2=\text{CH}_2$
iBuVE	Isobutyl vinyl ether	$\text{CH}_2=\text{CH}-\text{O}-\text{CH}_2-\text{CH}(\text{CH}_3)_2$
BDDVE	Butanediol divinyl ether	$\text{CH}_2=\text{CH}-\text{O}-(\text{CH}_2)_4-\text{O}-\text{CH}=\text{CH}_2$

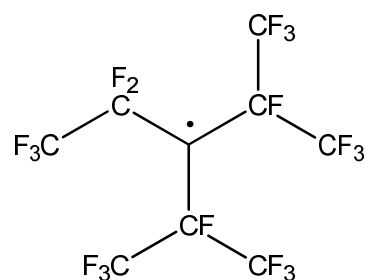
Polymers

PTFE	Polytetrafluoroethylene	$-(\text{CF}_2-\text{CF}_2)_n-$
------	-------------------------	---------------------------------

Initiators

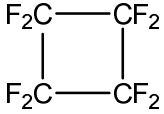
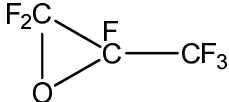
APS	Ammonium persulfate	$\text{NH}_3^+ \text{ } ^-\text{O}-\text{SO}_2-\text{O}-\text{O}-\text{SO}_2-\text{O}^- \text{ } ^+\text{NH}_3$
-----	---------------------	---

PPFR	Persistent perfluoro-3-ethyl-2,4-dimethyl-3-pentyl radical
------	--



BPO	Benzoyl peroxide	$\text{Ph}-(\text{C}=\text{O})-\text{O}-\text{O}-(\text{C}=\text{O})-\text{Ph}$
-----	------------------	---

Other fluorinated compounds

OFCB	Octafluorocyclobutane	
PFIB	Perfluoroisobutene	$\text{CF}_2=\text{C}(\text{CF}_3)_2$
HFPO	Hexafluoropropylene oxide	

Solvents

DMC	Dimethyl carbonate	$\text{CH}_3\text{-O-(C=O)-O-CH}_3$
PFH	Perfluoroheptane	$\text{CF}_3\text{-(CF}_2)_5\text{-CF}_3$

Characterisation techniques

NMR	Nuclear magnetic resonance
GPC/SEC	Gel-permeation chromatography / size-exclusion chromatography
DSC	Differential scanning calorimetry
TGA	Thermogravimetric analysis
FTIR	Fourier transform infrared

Polymerisation techniques

RDRP	Reversible deactivation radical polymerisation
RAFT	Reversible addition-fragmentation chain transfer
MADIX	Macromolecular design via the interchange of xanthates
ITP	Iodine-transfer polymerisation

Polymerisation related terms

DP	Degree of polymerisation
M_n	Number-average molecular weight
M_w	Weight-average molecular weight
PDI	Polydispersity index
CTA	Chain-transfer agent

Other abbreviations

AEL	African Explosives Limited
DST	Department of Science and Technology
FEI	Fluorochemical Expansion Initiative
Depol	Depolymerisation

Table of figures

Figure 1:	<i>Number of publications per year relating to tetrafluoroethylene homo- and heteropolymerisation (compiled via the Sci-Finder database).....</i>	<i>11</i>
Figure 2:	<i>Number of publications per language category relating to tetrafluoroethylene homo- and heteropolymerisation (compiled via the Sci-Finder database).....</i>	<i>11</i>
Figure 3:	<i>The kilogram-scale PTFE pyrolysis reactor built at the University of Pretoria.....</i>	<i>16</i>
Figure 4:	<i>Examples of 1-L bench-top type autoclaves (both glass and stainless steel) suited to the polymerisation of TFE (Images courtesy of AMAR Equipments PVT. Ltd.).....</i>	<i>23</i>
Figure 5:	<i>Head section of an industrial 40-kL polymerisation reactor (Images courtesy of International Process Plants).....</i>	<i>24</i>
Figure 6:	<i>Free surfactant concentration (in mol·L⁻¹) of the lithium salts of the homologous series of perfluorinated carboxylic acids from 7 to 10 carbons in length [136].....</i>	<i>46</i>
Figure 7:	<i>Gas chromatogram of the total product mixture from the redox telomerisation of TFE with CCl₄.....</i>	<i>51</i>
Figure 8:	<i>Differential-molecular-weight-distribution curves for Teflon® 6 and 7A, obtained by viscoelastic spectroscopy [199].....</i>	<i>54</i>
Figure 9:	<i>Helical chain structure of PTFE in phase II crystal form [202].....</i>	<i>55</i>
Figure 10:	<i>Pressure-temperature phase diagram for the crystal structure of PTFE [202].....</i>	<i>56</i>
Figure 11:	<i>Low dose, high resolution, negative contrast electron micrograph of rod-like PTFE particles showing the linear nature of the PTFE chains and their ordered long distance packing [208] (reprinted with permission from John Wiley and Sons).....</i>	<i>58</i>
Figure 12:	<i>Transmission electron micrograph of spherical PTFE particles that has been beam etched at 200 kV with a cumulative dose of 40 electrons.Å² [208] (reprinted with permission from John Wiley and Sons).....</i>	<i>58</i>
Figure 13:	<i>Transmission electron micrograph of a PTFE ribbon taken from a batch of emulsion polymerised PTFE [203] (reprinted with permission from John Wiley and Sons).....</i>	<i>59</i>
Figure 14:	<i>Chain arrangements of PTFE in an elementary fibril and fibril arrangement in a rod-like particle for PTFE in phase II crystal form.....</i>	<i>59</i>
Figure 15:	<i>Spherical PTFE particle formation by roll-up of a PTFE ribbon structure [203] (reprinted with permission from John Wiley and Sons).....</i>	<i>60</i>
Figure 16:	<i>Hexagonal platelets typically observed dispersion polymerised oligomeric PTFE [210].....</i>	<i>60</i>
Figure 17:	<i>Mesostructure of expanded PTFE showing the elementary fibrils (courtesy of W.L. Gore & Associates).....</i>	<i>61</i>

Figure 18:	<i>Polymer chain arrangements in PTFE at the amorphous to crystalline transition, showing the different types of amorphous region [195].</i>	69
Figure 19:	<i>¹⁹F SS NMR spectrum of PTFE synthesised in sc-CO₂ using bis(perfluoro-2-n-propoxypropionyl) peroxide as initiator [101].</i>	76
Figure 20:	<i>Polytetrafluoroethylene insulated co-axial cable (image courtesy of Bhawal Cables Company).</i>	81
Figure 21:	<i>Cut-open film capacitor showing the PTFE dielectric roll (image courtesy of RuTubes Audio Components Company).</i>	82
Figure 22:	<i>Polytetrafluoroethylene filter cartridges showing the PTFE membranes (image courtesy of the American Melt Blown & Filtration Company).</i>	83
Figure 23:	<i>Diagram of a PTFE sliding expansion bearing for road bridge applications (image courtesy of Nippon Pillar Singapore).</i>	84
Figure 24:	<i>Polytetrafluoroethylene lined pipe reducer (image courtesy of JCS Line Piping Products).</i>	85
Figure 25:	<i>Example of an ePTFE vascular graft (image courtesy of the Terumo Corporation).</i>	85
Figure 26:	<i>Magnesium/Teflon/Viton (MTV) countermeasure flare cartridges mounted in a C-130 Hercules.</i>	86
Figure 27:	<i>Bulk fluoropolymer market value for the period 1998 to 2018 (the 2018 value is an estimate).</i>	87
Figure 28:	<i>Distribution of fluoropolymer market share by polymer type in 2013.</i>	88
Figure 29:	<i>Flow diagram detailing the general process from depolymerisation to polymer synthesis.</i>	110
Figure 30:	<i>Flow diagram detailing the general process for the use of Carius tubes in polymer synthesis.</i>	111
Figure 31:	<i>Piping diagram for the depolymerisation reactor system.</i>	112
Figure 32:	<i>Depolymerisation vessel thermal geometry detailing the various temperature zones.</i>	117
Figure 33:	<i>Longitudinal temperature profile in the tube wall for the section of exit tube protruding from the tube furnace.</i>	118
Figure 34:	<i>Mechanical overview of the depolymerisation vessel.</i>	120
Figure 35:	<i>Detailed mechanical drawing of the depolymerisation vessel furnace insert.</i>	121
Figure 36:	<i>Experimental vapour pressure curve for TFE between its normal boiling and critical points [16-20].</i>	124
Figure 37:	<i>Comparison between the experimental- and calculated saturated liquid volumes of TFE using the Peng-Robinson EOS.</i>	124
Figure 38:	<i>Comparison between the experimental- and calculated saturated gas volumes of TFE using the Peng-Robinson EOS.</i>	125
Figure 39:	<i>The calculated two-phase region for TFE using the Peng-Robinson EOS with a B-spline fitted to represent the continuous data.</i>	125

Figure 40:	<i>Depolymerisation reactor system pressure as a function of the molar amount of TFE in the system at selected isotherms for a 250-mL catch vessel (475 mL total volume).</i>	126
Figure 41:	<i>Depolymerisation reactor system pressure as a function of the molar amount of TFE in the system at selected isotherms for a 500-mL catch vessel (775 mL total volume).</i>	127
Figure 42:	<i>Depolymerisation reactor system pressure as a function of the molar amount of TFE in the system at selected isotherms for a 750-mL catch vessel (975 mL total volume).</i>	127
Figure 43:	<i>Depol reactor system pressure as a function of the molar amount of TFE in the system at the adiabatic reaction temperature for a 250-, 500- and 750-mL catch vessel (475, 725 and 975 mL total volume).</i>	129
Figure 44:	<i>Photograph of the fully assembled, mounted depolymerisation apparatus and tube furnace as installed in the FMG laboratory.</i>	130
Figure 45:	<i>Piping diagram for the Carius tube manifold.</i>	131
Figure 46:	<i>Design schematic for the Carius tubes used at ENSCM in France.</i>	133
Figure 47:	<i>Photograph of the fully assembled, mounted Carius manifold as installed in the FMG laboratory.</i>	135
Figure 48:	<i>Copper Carius shield tube for containment of "live" Carius tubes, assembled with off-the-shelf fittings.</i>	136
Figure 49:	<i>Mass-pressure relations at 20 °C for TFE, HFP and VDF, assuming a working loading vessel volume of 160 mL.</i>	137
Figure 50:	<i>Graphical representation of the experimental design for the non-transfer, uncontrolled free-radical synthesis of PTFE using APS in water.</i>	148
Figure 51:	<i>Photograph showing an example of the PTFE synthesised by aqueous, free-radical polymerisation at 80 °C.</i>	150
Figure 52:	<i>Molecular weight of PTFE, as determined by DSC, as a function of the square root of the initiator concentration at 65 °C isothermal conditions, produced by aqueous, batch free-radical polymerisation using ammonium persulfate as initiator.</i>	152
Figure 53:	<i>Thermograms for PTFE synthesized at 65 °C at 1, 2.3, 5.5, 8.7, 10, and 20 mol % APS.</i>	152
Figure 54:	<i>The transmission mode FTIR spectrum of a disc of PTFE produced by aqueous, batch free-radical polymerisation at 65 °C using 5.5 % ammonium persulfate as initiator.</i>	153
Figure 55:	<i>Possible shapes of a molecular-weight-distribution curve for PTFE.</i>	155
Figure 56:	<i>Post-reaction Carius tubes loaded with TFE and with VDF using 1 % APS as initiator at 65°C.</i>	158

Figure 57:	<i>Comparison of the experimental pressure drop with the predicted pressure drop during the homopolymerisation of PTFE in water at 75 °C using 10 % APS as initiator.</i>	160
Figure 58:	<i>Structure of an MTV combustion wave (image taken from Koch [3]).</i>	162
Figure 59:	<i>Temperature profile and structure of the heat transfer mechanisms for the combustion of an MTV pyrolant (image taken from Koch [3]).</i>	162
Figure 60:	<i>Schematic representation of the gaseous reactions mediating fluorine exchange between fluorocarbons and magnesium in an MTV combustion reaction (image taken from Koch [3]).</i>	163
Figure 61:	<i>Structure of the perfluoro-3-ethyl-2,4-dimethyl-3-pentyl persistent radical (PPFR).</i>	171
Figure 62:	<i>¹⁹F NMR spectra of poly(CTFE-alt-iBuVE) copolymers showing the progression of the CF₃ ¹⁹F NMR signal with increasing initiator concentration from 1 mol % (top spectrum) to 20 mol % (bottom spectrum).</i>	178
Figure 63:	<i>¹H NMR spectra of poly(CTFE-alt-iBuVE) copolymers at 1 % and 10 % PPFR concentration compared to that of isobutyl vinyl ether (top spectrum).</i>	179
Figure 64:	<i>Size-exclusion chromatograms showing the number-average molecular weights of poly(CTFE-alt-iBuVE) copolymers prepared from various amounts of PPFR radical molar percentages.</i>	183
Figure 65:	<i>Correlation of M_n decrease as PPFR ratio increases as determined by both SEC (Δ) and ¹⁹F NMR spectroscopy (■).</i>	184
Figure 66:	<i>TGA thermograms for the poly(CTFE-alt-iBVE) copolymers under N₂ at 10 °C/min.</i>	186
Figure 67:	<i>Fourier-transform infrared spectrum of the evolved gases from the thermal decomposition of the poly(CTFE-alt-iBuVE) alternating copolymers, taken at the point of maximum absorbance, showing, among other species, the evolution of HF, HCl, CO and CO₂.</i>	187
Figure 68:	<i>¹H NMR spectra of poly(TFE-alt-iBuVE) copolymers achieved from 1 and 30 % BPO (recorded in CDCl₃).</i>	203
Figure 69:	<i>Expansion of the ¹H NMR spectra of poly(TFE-alt-iBuVE) copolymer achieved from 1 % BPO (3.00 to 3.50 ppm) showing the stereochemistry of the polymer backbone as viewed from the CF₂ group.</i>	204
Figure 70:	<i>¹⁹F NMR spectrum of poly(TFE-alt-iBuVE) copolymers at 1 % BPO (recorded in CDCl₃).</i>	204
Figure 71:	<i>¹⁹F NMR spectrum of poly(TFE-alt-iBuVE) copolymers at 30 % BPO (recorded in CDCl₃).</i>	205

Figure 72:	Enlargement of the region from -110 to -125 ppm for the ^{19}F NMR spectrum of poly(TFE- <i>alt</i> - <i>i</i> BuVE) copolymers at 1% BPO, showing the multiplicities and coupling constants.....	205
Figure 73:	<i>Stereochemistry of the polymer backbone of poly(TFE-<i>alt</i>-<i>i</i>BuVE) copolymer as viewed from the C-H group.</i>	206
Figure 74:	<i>Negative ion MALDI-TOF mass spectrum of poly(TFE-<i>alt</i>-<i>i</i>BuVE) synthesised by free radical copolymerisation (Table 15, experiment 5) with DCTB as matrix and LiCl as cationic agent.</i>	208
Figure 75:	<i>Correlation of M_n decrease as BPO ratio increases, determined by both SEC (■) and ^{19}F NMR spectroscopy (Δ).</i>	210
Figure 76:	<i>TGA thermograms of poly(TFE-<i>alt</i>-<i>i</i>BuVE) copolymers synthesised with 1, 5, 10, 15, and 30 mol % BPO under an N_2 atmosphere.</i>	210
Figure 77:	<i>Expected structure of poly(TFE-<i>alt</i>-<i>i</i>BuVE) alternating copolymer from the RAFT copolymerisation reaction of TFE and <i>i</i>BuVE initiated by benzoyl radical and controlled by O-ethyl-S-(1-methyloxycarbonyl)ethyl xanthate.</i>	211
Figure 78:	<i>^1H NMR spectrum of RAFT copolymerisation of TFE with <i>i</i>BuVE controlled by xanthate, taken at 15 min (recorded in CDCl_3).</i>	214
Figure 79:	<i>^{19}F NMR spectrum of the total product mixture of the radical copolymerisation of TFE with <i>i</i>BuVE initiated by BPO and controlled xanthate, controlled poly(TFE-<i>alt</i>-<i>i</i>BuVE), taken at 15 min (recorded in CDCl_3).</i>	214
Figure 80:	Enlargement of the region from 1 to 4.75 ppm for the ^1H NMR spectrum of poly(TFE- <i>alt</i> - <i>i</i> BuVE) copolymer controlled by xanthate, taken at 15 minutes (recorded in CDCl_3).	215
Figure 81:	<i>Evolution of selected ^1H and ^{19}F NMR signals with conversion of poly(TFE-<i>alt</i>-<i>i</i>BuVE) copolymers synthesised via MADIX polymerisation using a 1:1 ratio of monomers and a $[\text{Monomers}]_0:[\text{CTA}]_0:[\text{BPO}]_0$ ratio of 20:1:0.1, with O-ethyl-S-(1-methoxycarbonyl)-ethylidithiocarbonate as CTA.</i>	215
Figure 82:	<i>Negative ion MALDI-TOF mass spectrum of poly(TFE-<i>alt</i>-<i>i</i>BuVE) synthesised by MADIX polymerisation (Table 16, experiment 1) with DCTB as matrix and LiCl as cationic agent.</i>	216
Figure 83:	<i>Evolution of M_n and \mathcal{D} as a function of conversion for the MADIX copolymerisation of TFE and <i>i</i>BuVE using a 1:1 ratio of monomers and a $[\text{Monomers}]_0:[\text{CTA}]_0:[\text{BPO}]_0$ ratio of 20:1:0.1, with O-ethyl-S-(1-methoxycarbonyl)-ethylidithiocarbonate as CTA.</i>	218

Figure 84:	<i>TGA thermograms of poly(TFE-<i>alt</i>-iBuVE) copolymers prepared via RAFT/MADIX using O-ethyl-S-(1-methoxycarbonyl)-ethyldithiocarbonate at 15, 30, 60, 120, and 1440 minutes reaction time under N₂ atmosphere.....</i>	<i>219</i>
Figure 85:	<i>Fluorescence of poly(TFE-co-BDDVE) under the action of a camera flash.....</i>	<i>233</i>
Figure 86:	<i>Thermograms for the decomposition of poly(TFE-co-BBVE) copolymers under N₂ atmosphere.....</i>	<i>234</i>
Figure 87:	<i>Photograph detailing the rubbery, non-fluorescing poly(TFE-<i>ter</i>-iBuVE-<i>ter</i>-BDDVE) terpolymer.....</i>	<i>236</i>
Figure 88:	<i>¹H NMR spectrum for poly(TFE-<i>ter</i>-iBuVE-<i>ter</i>-BDDVE) terpolymer synthesised at 85 °C with a monomer ratio [TFE]:[iBuVE]:[BDDVE] of 20:20:1.....</i>	<i>236</i>
Figure 89:	<i>¹⁹F NMR spectrum for poly(TFE-<i>ter</i>-iBuVE-<i>ter</i>-BDDVE) terpolymer synthesised at 85 °C with a monomer ratio [TFE]:[iBuVE]:[BDDVE] of 20:20:1.....</i>	<i>237</i>
Figure 90:	<i>Thermograms for selected PTFE samples decomposed under nitrogen atmosphere.</i>	<i>239</i>
Figure 91:	<i>Differential temperature curves for uncontrolled, low-molecular-weight PTFE/Si- and RAFT controlled, bridged PTFE/Si mixtures.....</i>	<i>240</i>

List of tables

Table 1:	<i>The physical and chemical properties of tetrafluoroethylene (CAS No: 116-14-3).....</i>	12
Table 2:	<i>Radical generating initiators used in the polymerisation of tetrafluoroethylene.....</i>	33
Table 3:	<i>Solvents employed in the free-radical polymerisation of tetrafluoroethylene.</i>	41
Table 4:	<i>Dispersive agents used in the aqueous emulsion polymerisation of tetrafluoroethylene.</i>	47
Table 5:	<i>Chain-transfer agents employed in aqueous free-radical polymerisation of tetrafluoroethylene.</i>	48
Table 6:	<i>Physical and chemical properties of PTFE.....</i>	52
Table 7:	<i>Comparison of the molecular weights obtained for commercial PTFE resins by various techniques.</i>	53
Table 8:	<i>The reported glass-transition temperatures for PTFE, indicating the scope of the controversies regarding this property of PTFE.</i>	70
Table 9:	<i>Bill of materials for the depolymerisation reactor.....</i>	113
Table 10:	<i>Schedule 40 pipe outer diameters at ambient and maximum operation temperature.</i>	115
Table 11:	<i>Bill of materials for the Carius tube manifold.</i>	132
Table 12:	<i>Experimental conditions for the synthesis of PTFE via non-transfer uncontrolled free-radical polymerisation.....</i>	147
Table 13:	<i>Summary of experimental conditions and results obtained.....</i>	176
Table 14:	<i>CF₃ signal assignments and percentage relative abundance in the copolymer made with 20 % PPF.</i>	181
Table 15:	<i>Experimental conditions and results obtained for the free-radical copolymerisation of TFE with <i>i</i>BuVE initiated by BPO at 85 °C in DMC.....</i>	201
Table 16:	<i>Experimental conditions and results obtained for the RAFT copolymerisation of TFE with <i>i</i>BuVE in a 1:1 ratio initiated by BPO at 85 °C controlled by O-ethyl-S-(1-methyloxycarbonyl)ethyl xanthate. [Monomers]₀: [CTA]₀: [BPO]₀ ratio of 20:1:0.1.....</i>	212
Table 17:	<i>Molecular weights of xanthate controlled poly(TFE-<i>alt</i>-<i>i</i>BuVE) copolymers as determined by NMR spectroscopy and by GPC versus the theoretical molecular weight.</i>	217
Table 18:	<i>Summary of experimental conditions and results obtained for the free-radical copolymerisation of tetrafluoroethylene with butanediol divinyl in DMC.....</i>	232
Table 19:	<i>Summary of experimental conditions and results obtained for the free-radical terpolymerisation of tetrafluoroethylene with butanediol divinyl ether and isobutyl vinyl ether using benzoyl peroxide as initiator.</i>	235
Table 20:	<i>Summary of open-air ignition tests, and burn rates with electrical ignition, for selected PTFE samples with powdered silicon.</i>	240

List of schemes

Scheme 1:	<i>Common synthetic routes for the production of tetrafluoroethylene.</i>	13
Scheme 2:	<i>The route for the industrial synthesis of tetrafluoroethylene via the ultra-fast pyrolysis of chlorodifluoromethane (R-22).</i>	13
Scheme 3:	<i>Mechanism of PTFE breakdown by thermal chain scission to eliminate difluorocarbene.</i> ...	15
Scheme 4:	<i>Gaseous radical reactions occurring during PTFE pyrolysis that leads to the formation of TFE and fluorocarbon by-products.</i>	15
Scheme 5:	<i>Thermal decomposition mechanisms of poly(hexafluoropropylene oxide) peroxide to yield two fluorinated radical species that may initiate polymerisation.</i>	30
Scheme 6:	<i>The formation of the various microparticle types found within PTFE produced by dispersion polymerisation.</i>	63
Scheme 7:	<i>Mechanism of carboxylic acid end-group formation by persulfate initiators.</i>	67
Scheme 8:	<i>Decomposition pathways of carboxylic acid end-groups in PTFE to produce various secondary end-groups.</i>	68
Scheme 9:	<i>Unimolecular reaction mechanism proposed for formation of zwitterionic intermediate that leads to formation of acyl fluoride groups.</i>	68
Scheme 10:	<i>Reaction of PTFE breakdown products with Si particles, showing the HF stripping of the SiO₂ passivation layer.</i>	164
Scheme 11:	<i>β-scission elimination mechanism for the generation of $\bullet\text{CF}_3$ from PPFR.</i>	175
Scheme 12:	<i>Expected copolymerisation reaction of CTFE and <i>i</i>BuVE initiated by $\bullet\text{CF}_3$ to yield a poly(CTFE-<i>alt</i>-<i>i</i>BuVE) alternating copolymer.</i>	175
Scheme 13:	<i>Possible addition reactions of $\bullet\text{CF}_3$ radicals onto the CTFE/<i>i</i>BuVE.</i>	180
Scheme 14:	<i>Possible polymerisation reaction between <i>i</i>BuVE and perfluoroolefin A.</i>	182
Scheme 15:	<i>Mechanism of reversible addition-fragmentation chain transfer polymerisation (RAFT) / macromolecular design via the interchange of xanthates (MADIX).</i>	193
Scheme 16:	<i>Radical copolymerisation of tetrafluoroethylene with isobutyl vinyl ether initiated by benzoyl peroxide (BPO) in dimethyl carbonate (DMC) leading to a poly(TFE-<i>alt</i>-<i>i</i>BuVE) alternating copolymer.</i>	198
Scheme 17:	<i>Mechanism of proton transfer from DMC onto macroradicals to produce a polymer dead chain and radical fragments.</i>	200
Scheme 18:	<i>Non-trivial modes for the termination by recombination of macroradicals for poly(TFE-<i>alt</i>-<i>i</i>BuVE) copolymer.</i>	206
Scheme 19:	<i>Thermal decomposition process of benzoyl peroxide [45-47].</i>	207

Scheme 20:	<i>Possible addition reactions of benzoyl radicals onto the TFE/iBuVE mixture.</i>	207
Scheme 21:	<i>Expected copolymerisation reaction of TFE and BDDVE initiated by benzoyl radical to yield a poly((TFE-alt-BDDVE)-co-TFE) polymer.</i>	232

Research outputs

Publications in peer-reviewed journals:

- 1) Puts, G., Crouse, P., and Ameduri, B. *Thermal Degradation and Pyrolysis of Polytetrafluoroethylene*, in *Handbook of Fluoropolymer Science and Technology*. 2014, John Wiley & Sons, Inc. p. 81-104.
- 2) Puts, G.J., Lopez, G., Ono, T., Crouse, P.L., and Ameduri, B.M. "Radical copolymerisation of chlorotrifluoroethylene with isobutyl vinyl ether initiated by the persistent perfluoro-3-ethyl-2,4-dimethyl-3-pentyl radical" *RSC Advances*, 2015. **5**(52): 41544-41554.

Conference contributions:

- 1) Puts, G., Grobler, M., Potgieter, G., Focke, W., Crouse, P. *Low-molecular-weight PTFE for pyrotechnic applications* in, *Fluoropolymer*. 2-5 October 2016. New Orleans, Louisiana, USA: The American Chemical Society.

Manuscripts in preparation:

- 1) Puts, G.J., Venner, W.V., Ameduri, B.M., and Crouse, P.L. "Polytetrafluoroethylene: Synthesis and characterization of the original extreme polymer" *Chemical Reviews*.
- 2) Puts, G.J., Venner, W.V., Gimello, O., Ameduri, B.M. and Crouse, P.L. "Free-radical and controlled-radical copolymerisation of tetrafluoroethylene with isobutyl vinyl ether" *Macromolecules*.
- 3) Puts, G.J., Venner, W.V., Crouse, P.L. "Kinetic expressions for the batch-type homopolymerisation of tetrafluoroethylene" *Journal of Fluorine Chemistry*.

Chapter 1

General introduction

Fluorine-containing compounds underpin the technologies supporting modern society; without them the human species would not have developed much past the level of the 1920s [1]. Fluoromaterials are found in application areas such as medicine, energy storage and energy conversion, electronics, metallurgy, refrigeration, and engineering plastics.

Unlike materials such as iron or silicon, or hydrocarbons derived from oil, the fluorine value chain is quite involved, requiring the processing of fluorine-containing minerals into first hydrogen fluoride, then into elemental fluorine, and from these two into a myriad of other compounds [2-4]. The synthetic processes are quite lengthy, but also require that the means of production be built from special materials capable of handling the corrosive- or unstable nature of the fluorinated intermediates and the high pressures and temperatures employed in their production. This processing complexity imparts a significant cost to the finished products. The fluorochemical industry was worth €14 billion annually in 2009 [5].

Although there are several minerals from which fluorine may be extracted, the most significant commercial source of fluorine is the mineral fluorspar or fluorite (CaF_2) and it is from this mineral that the fluorine value chain starts. South Africa possesses the world's largest reserves of fluorspar (41 million tons), but mined only about 177 thousand tons per annum in 2009 [6]. At present, most of the mined fluorspar is exported, shipped mainly to China, Mexico, and Spain, where it is beneficiated to higher-value products that South Africa then re-imports.

The Government of South Africa has, *via* the Fluorochemical Expansion Initiative (FEI) program, embarked on a process of encouraging local beneficiation of our fluorite resources for the benefit of the national economy [7]. In particular, the production of fluoropolymers was identified as a key area in which technical expertise should be built.

Besides the usual uses for fluoropolymers, mixtures of the fluoropolymer polytetrafluoroethylene (PTFE) with silicon, magnesium or aluminium metal are used as high-energy pyrolants, finding application in missile-countermeasure flares, thermal lances and as fuse material in demolitions time-delay elements [8]. These time-delay elements are employed extensively in the mining industry as part of the explosives packages used in the blasting process, both underground and in surface mining.

Most of the explosives and their accessories (*i.e.* detonators, ripcord *etc.*) used in the South African mining industry are produced by African Explosives Ltd (AEL). Currently, all the time-delay components in the detonators manufactured by AEL consist of bismuth- and lead-based pyrolants, and AEL is sponsoring the development of detonators that incorporate more environmentally benign fluoropolymer-based pyrolants in an effort to reduce the negative

environmental effects of mining. AEL faces a further issue in that the detonator units are produced at a factory and then transported by truck to the blasting site. There have been several incidents where the detonators have spontaneously exploded, destroying the transport as well as damaging nearby roads and killing bystanders. From a safety perspective, it would be preferable to transport the inert raw materials to the blasting site and compound the metal-fluorocarbon composite on site. Furthermore, from a demolitions perspective, it is desired that the composites be formed into whatever shape the demolition project requires.

A difficulty faced by AEL, and indeed, all manufacturers of metal-fluorocarbon-based pyrolant mixtures, is that the facile extrusion and molding methods for such mixtures are still non-existent, as non-melt-processable, high-molecular-weight PTFE is employed. The use of low-molecular-weight PTFE or other fluorocarbon waxes has been stymied by pre-ignition evaporation of the polymer, resulting in a reduced reaction temperature, variable burn times, or in extreme cases, total removal of the fluorocarbon and subsequent ignition failure.

It would be of immense commercial importance to the South African mining- and fluorochemical industries if a perfluoropolymer could be synthesised that would permit extrusion moulding while overcoming the difficulties encountered when using low-molecular-weight waxes.

The aim of this doctoral research is to develop a synthetic strategy for the facile production of a melt-extrudable, low-molecular-weight, TFE-based polymer for use as pyrolant in time-delay elements, applicable to the South African mining industry. The end user has specified that the target melt viscosity of the polymer should lie in the region of 10^4 Pa·s at 200 °C (as opposed to the 10^{11} Pa·s for high-molecular-weight PTFE), and the target bulk decomposition temperature should be 560 – 590 °C (the same as for high-molecular-weight PTFE) with less than 10 % mass loss before polymer/fuel ignition is achieved. Furthermore, the product polymer should have sufficient mechanical strength to undergo rod extrusion and spool winding.

A secondary, but vitally important objective of this doctoral research was to develop competency in the synthesis and characterisation of fluoropolymers, a skill set that is nearly completely absent in the South African fluorochemical industry.

After extensive review of the literature on the homopolymerisation of tetrafluoroethylene, summarised in Chapter 2, it was found that there is a dearth of information in the open literature regarding the effects of polymerisation conditions on the molecular-weight distribution of polytetrafluoroethylene and, concomitantly, of the effect of molecular-weight distribution on the thermal properties of PTFE. The results of the literature review and the experimental results of

the homopolymerisation of TFE showed that lowering the molecular weight of PTFE alone cannot produce a polymer that meets the requirements of the end user. To permit both facile extrusion and maintain thermal stability of the polymer, it is required that the low-molecular-weight PTFE chains be bridged so that they may undergo entanglement, thus imparting some mechanical strength to the polymer and mitigating the deleterious effect the low molecular weight has on the thermal stability of the polymer.

This work demonstrates the effect of the polymerisation conditions on the molecular-weight distribution of PTFE *via* its influence on the thermal stability of the polymer, as well as the development of a bridged tetrafluoroethylene polymer. The document consists of:

- 1) A review of the state-of-the-art concerning the homopolymerisation of tetrafluoroethylene;
- 2) An investigation into the effect that polymerisation conditions have on the molecular-weight distribution of a TFE homopolymer prepared by conventional precipitation polymerisation to ascertain the limits of tailored molecular weight achievable by the conventional, uncontrolled polymerisation process;
- 3) An investigation into the suitability of persistent perfluoro-3-ethyl-2,4-dimethyl-3-pentyl radical as an end-group label for use in determining the number-average molecular weight of a fluorinated polymer by ^{19}F NMR spectroscopy. This work focuses on using chlorotrifluoroethylene (CTFE) and isobutyl vinyl ether as model monomers to permit the correlation of the NMR spectroscopy results with GPC data. This work also served as technology transfer to the University of Pretoria of the research methods used for the synthesis and characterisation of fluoropolymers, as practiced at the Institute Charles Gerhardt in Montpellier, France;
- 4) A demonstration that the molecular weight of a TFE/iBuVE copolymer can be controlled using *O*-ethyl-*S*-(1-methyloxycarbonyl)ethyl xanthate and that a monodisperse polymer can be produced using this xanthate;
- 5) An investigation into the structure of poly(TFE-*co*-1,4-butanediol divinyl ether) copolymer and poly(TFE-*ter*-iBuVE-*ter*-1,4-butanediol divinyl ether) terpolymer to demonstrate the suitability of this divinyl ether as bridging agent for tetrafluoroethylene polymers, and the synthesis of a TFE polymer marginally bridged with 1,4-butanediol divinyl ether in dimethyl carbonate, both with and without xanthate control agent.

The final aim is to develop a strategy for the facile synthesis of a tetrafluoroethylene polymer of sufficiently low molecular weight so as to be safely compoundable with metal fuels, but having sufficient thermal stability so as to not evaporate before the reaction ignition temperature.

The research laid out here is restricted to the synthesis of the polymer, and limited pyrotechnical characterisation using differential thermal analysis and burn-rate tests using high-speed cameras. Proper investigation into the compounding of the polymer with the metals and full determination of the burn characteristics are left to other, subsequent investigators.

References

- [1] Dolbier, W.R., Jr, "Fluorine chemistry at the millennium", *Journal of Fluorine Chemistry*, 2005, 126 (2), 157-163.
- [2] Jaccaud, M., Faron, R., Devilliers, D., and Romano, R., 2000, "Fluorine", in (eds.), *Ullmann's Encyclopedia of Industrial Chemistry*, Wiley-VCH Verlag GmbH & Co. KGaA, Weinheim, Germany.
- [3] Aigueperse, J., Mollard, P., Devilliers, D., Chemla, M., Faron, R., Romano, R., and Cuer, J.P., 2000, "Fluorine compounds, inorganic", in (eds.), *Ullmann's Encyclopedia of Industrial Chemistry*, Wiley-VCH Verlag GmbH & Co. KGaA, Weinheim, Germany.
- [4] Siegemund, G., Schwertfeger, W., Feiring, A., Smart, B., Behr, F., Vogel, H., McKusick, B., and Kirsch, P., 2000, "Fluorine compounds, organic", in (eds.), *Ullmann's Encyclopedia of Industrial Chemistry*, Wiley-VCH Verlag GmbH & Co. KGaA, Weinheim, Germany.
- [5] Hayes, T. "Industry Study 2496 Fluoropolymers", **2009**.
- [6] Bride, T., Gunn, G., Brown, T., and Rayner, D. "Fluorospar commodity profile", **2011**.
- [7] Medupe, S. "Media Statement by the South African Government on the Establishment of a Pharmaceutical Manufacturing Plant in South Africa", **2012**.
- [8] Koch, E.C., 2012, *Metal-Fluorocarbon Based Energetic Materials*, Wiley, New York.

Chapter 2
Literature review:
The homopolymerisation of
tetrafluoroethylene

Notes on the research strategy

The Chemical Abstracts Service SciFinder database, Scopus, Elsevier Reaxys, Google Scholar, Science Direct, SpringerLink, Wiley Online Library, and Google Patents were employed to search for literature pertaining to the homopolymerisation of tetrafluoroethylene, as well as the decompositional behaviour of polytetrafluoroethylene.

Although there were some peer-reviewed research articles available in the open literature, many of them were written in either Russian, Mandarin or Japanese. Articles in the English language were sparse, particularly in the early literature, with most of the English language, publically accessible literature consisting of patents or technical reports from the Manhattan Project. Patent documents are not good primary sources of scientific and technical data as they are not peer reviewed and specific technical data may be omitted, or they may contain wilful falsification of results for the sake of misleading the competition. Nonetheless, these documents were consulted as primary literature due to the dearth of proper peer-reviewed articles and due to the fact that the patent literature is the primary indicator of the research direction within the major commercial entities who are virtually the sole drivers of research into tetrafluoroethylene polymerisation.

There is considerable duplication in the literature, with patents being filed firstly in the country of the originating commercial entity and subsequently in other countries, most commonly the US and the UK. In such cases, the earliest English language version of the publication, or, the earliest US Patent document where such a document is the only English version, were consulted. German language documents were consulted directly.

Furthermore, in cases where a publication contradicts the known behaviour of tetrafluoroethylene, as taught by experience, that publication was set aside, and is not mentioned in this review. Fortunately, such instances were few.

This review is meant to be comprehensive, and efforts were made to ensure that all literature was consulted. However, as there are almost 3000 publications on the topic logged in the public databases, it stands to reason that some publications may have been missed. Nevertheless, it is believed that this review spans the bulk of the relevant literature and includes the most important features of tetrafluoroethylene homopolymerisation.

2.1 Introduction

Fluorinated polymers are niche macromolecules that play an integral role in modern life [1]. Largely due to the properties of fluorine (including, among others, large electronegativity, low polarizability, and small van der Waals radius (1.32 Å)) and to the strong C–F bonds (485 kJ·mol⁻¹), they exhibit unique and remarkable attributes. Their applications span engineering thermoplastics and elastomers for the chemical-process, automotive, and aeronautics industries, weather-proof coatings, biomedical materials, membranes for use in Li-ion batteries, membranes in fuel cells, and many more [2-12].

Among the fluoropolymers, polytetrafluoroethylene (the homopolymer of tetrafluoroethylene) and its marginally modified derivatives rank first, comprising some 60 % of the total international fluoropolymer market in 2015 [13, 14], with a global production increase of *ca.* 7 % per annum. These polymers, both high-molecular-mass materials and waxes, are chemically inert, hydrophobic, and exhibit superb thermal stability as well as an exceptionally low coefficient of friction. Numerous companies, such as Asahi Glass, Solvay Specialty Polymers, Daikin, Chemours (formerly part of E.I. du Pont de Nemours and Company, hereafter collectively referred to as DuPont/Chemours), Juhua, 3F, 3M/Dyneon, Gore, *etc.*, produce TFE homopolymers. These polymers find use in applications ranging from coatings and lubrication to pyrotechnics, and extensive industries (electronic, aerospace, wires and cables, as well as textiles) have been built around them.

In 1941, Plunkett [15] pioneered the polymerisation of tetrafluoroethylene (TFE) under autogenous pressure at 25 °C. The gas was found to autopolymerise at 25 °C, forming white, dusty powders and formed foamy, low-molecular-weight waxes in the presence of AgNO₃ and AgNO₃ / MeOH mixtures. Plunkett's patent also contained the first known report of PTFE depolymerisation, stating that the foamy product formed in the presence of AgNO₃ decomposed to TFE, leaving behind only a small amount of proper polymer.

Brubaker [16] subsequently published, comprehensively, the method for free radical suspension polymerisation of TFE in an aqueous medium, using alkali or ammonium persulfate (at 0.1 % mass basis or 0.3 % mol basis) as well as an alkaline buffer (0.5 to 1 % by mass of TFE).

A large number of publications on the homo- and copolymerisation of TFE followed (*cf.* [9, 17-33]), spanning processes such as free-radical-, coordination- [34], and electrochemical polymerisation [35, 36], with even plasma-type polymerisation being reported [37-40]. So far, almost 3000 publications have been logged in the publically accessible databases. Figure 1

summarises the number of publications each year related to the homo- and heteropolymerisation of tetrafluoroethylene, which is seen to be increasing with time, indicating the continued importance of tetrafluoroethylene in commercial fluoropolymer research. The breakdown of the number of publications per language category is presented in Figure 2. English remains the language with the most number of publications, with Japanese and Mandarin in second and third place, respectively.

It must be noted here that the publications originating from universities and other academic institutions are done mostly in collaboration with these commercial entities. As far as is known, only Clemson University in the USA, the University of Ottawa in Canada, and the University of Pretoria in South Africa have direct access to multi-gram quantities of tetrafluoroethylene and operate independently from commercial entities.

Free-radical polymerisation remains the most commonly employed method for synthesising TFE high polymers and though suspension polymerisation retains the lion's share of the market, emulsion polymerisation using fluorinated surfactants is also widely employed.

Every commercial producer of PTFE has its own synthesis strategies, and there have been many contradictions in the literature regarding the most effective initiators, optimal reaction conditions, and polymer properties as a function of reaction conditions.

The objective of this review is to summarise the literature regarding the homopolymerisation of tetrafluoroethylene. For the sake of convenience to the experimentalist, the literature is discussed in divisions organised around the important features of the polymerisation procedure, starting with an overview of the various routes to synthesise tetrafluoroethylene, before discussing the engineering aspects, including safety, of the polymerisation process, followed by an overview of the initiators employed with TFE, then a discussion on the reaction conditions, with special emphasis on monomer purity, solvent environment, temperature and pressure as well as the various polymer additives. Thereafter, the properties of PTFE, as a function of the polymerisation conditions are discussed, and the chapter closes with a summary of the analytical techniques particular to the analysis of PTFE.

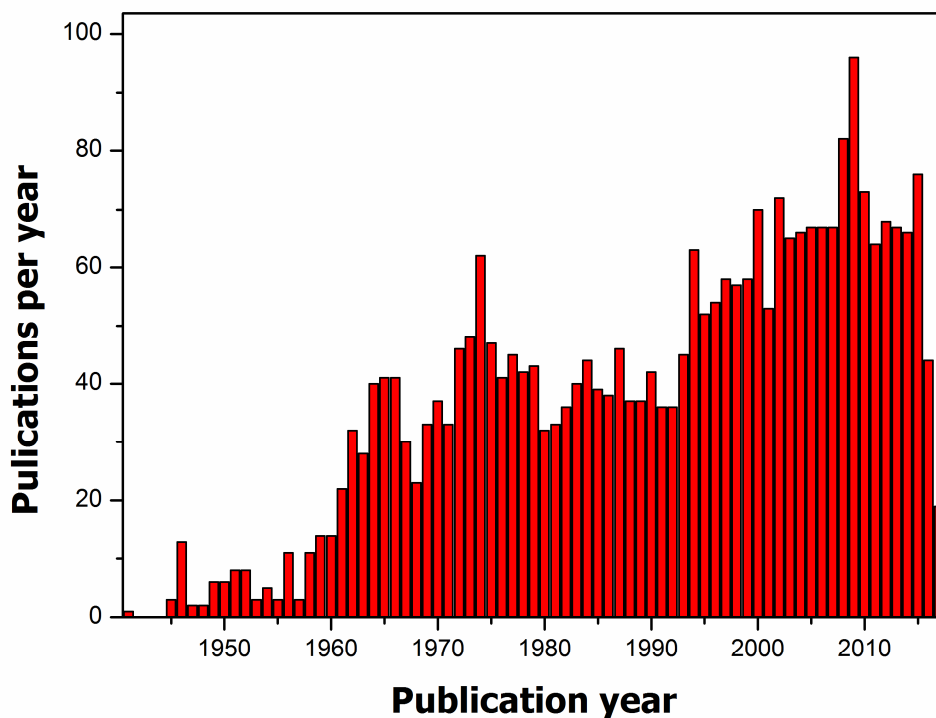


Figure 1: *Number of publications per year relating to tetrafluoroethylene homo- and heteropolymerisation (compiled via the Sci-Finder database).*

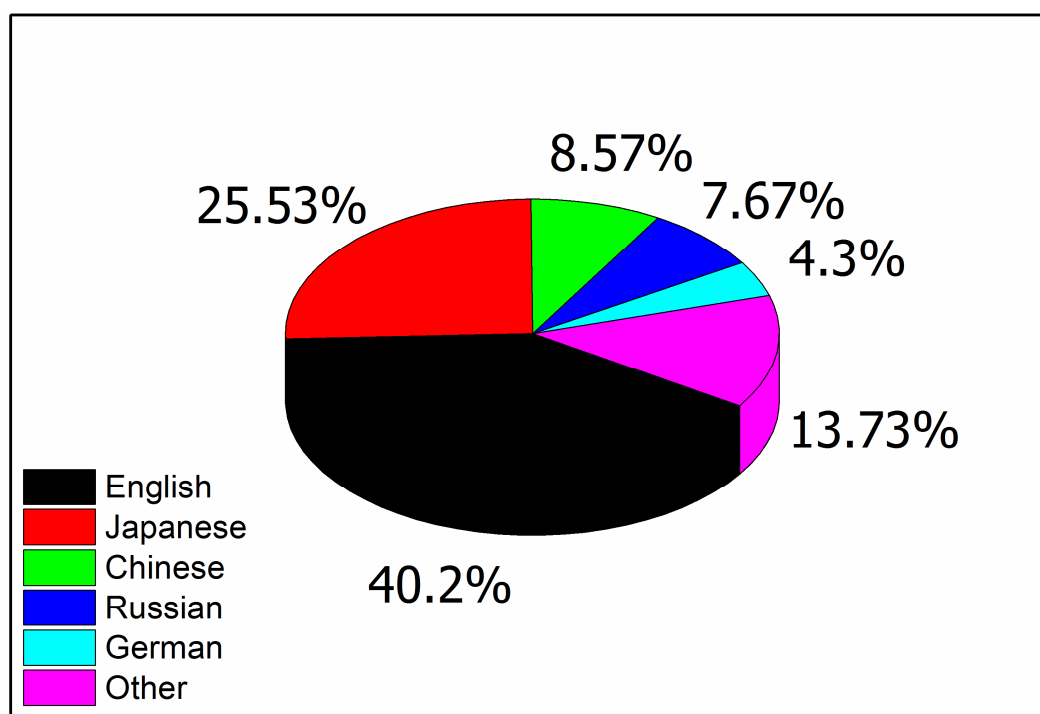


Figure 2: *Number of publications per language category relating to tetrafluoroethylene homo- and heteropolymerisation (compiled via the Sci-Finder database).*

2.2 Synthesis of TFE and concomitant safety aspects

Tetrafluoroethylene (CAS No: 116-14-3) is an odourless, colourless, and flammable gas with a density greater than air. TFE is highly unstable under certain conditions, and the monomer may undergo autodecomposition to carbon and CF_4 if heated to above $380\text{ }^\circ\text{C}$ [41] and may self-polymerize under pressure or under adiabatic compression [15]. The salient physical and chemical properties of tetrafluoroethylene are presented in Table 1.

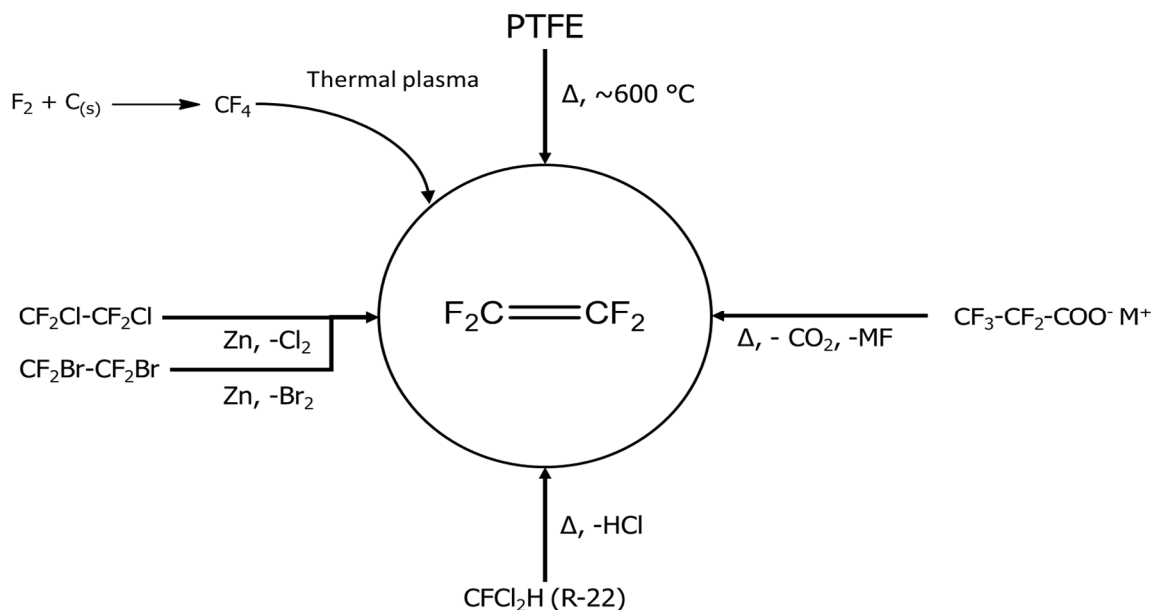
Table 1: *The physical and chemical properties of tetrafluoroethylene (CAS No: 116-14-3).*

Property		Unit and value	Reference
Molecular weight	(Da)	100.016	
Heat of formation	($\text{MJ}\cdot\text{mol}^{-1}$)	-63.31	[42]
Heat of combustion	($\text{kJ}\cdot\text{mol}^{-1}$)	-674	[42]
Heat of polymerisation	($\text{kJ}\cdot\text{mol}^{-1}$)	-196	[43]
Melting point	($^\circ\text{C}$)	-142.5	[44]
Boiling point	($^\circ\text{C}$)	[101.325 kPa] -76.3	[44]
Triple point	($^\circ\text{C}$)	-131.2	[45]
Solid density	($\text{g}\cdot\text{cm}^{-3}$)	[-173.15 $^\circ\text{C}$] 2.1	[46]
Liquid density	($\text{g}\cdot\text{cm}^{-3}$)	[-76.3 $^\circ\text{C}$] 1.519	[47]
		[-142.5 $^\circ\text{C}$] 1793	[47]
Critical temperature	($^\circ\text{C}$)	33.3	[48]
Critical pressure	(bar)	39.44	[48]
Critical density	($\text{g}\cdot\text{cm}^{-3}$)	0.5815	[48]
Acentric factor		0.226	[48]
Solubility		Water at $25\text{ }^\circ\text{C}$ 153 $\text{mg}\cdot\text{L}^{-1}$	[49, 50]

Tetrafluoroethylene cannot be obtained easily from commercial sources, although small quantities can be purchased from speciality chemical suppliers. Transport legislation varies by country and, in the continental USA, bulk transport of the stabilised liquid is permitted. However, most commercially-produced TFE is generated at the usage site, mainly due to safety and regulatory considerations, but also due to the cost of transport. Stabilised TFE has the UN number 1081 and falls in transport class 2 with a classification of 2F.

There are numerous methods to produce TFE with the most salient examples being ultra-fast pyrolysis of chlorodifluoromethane, ultra-fast, plasma pyrolysis of tetrafluoromethane [51, 52], dechlorination of $\text{CF}_2\text{Cl}\text{-CF}_2\text{Cl}$, or the debromination of $\text{CF}_2\text{Br}\text{-CF}_2\text{Br}$, pyrolysis of trifluoroacetic acid [53] or the alkali salts of perfluoropropanoic acid [54], and the pyrolysis of polytetrafluoroethylene under vacuum [1]. These methods have been extensively reviewed

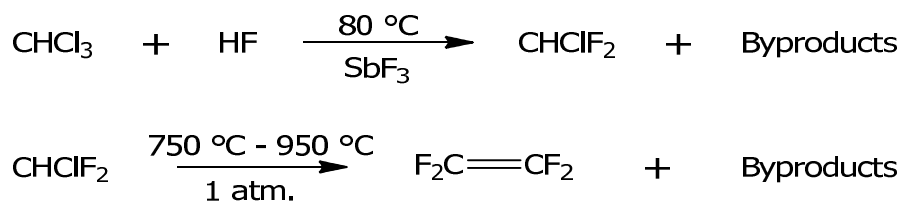
elsewhere [55] and are summarised in Scheme 1; the following discussion is a brief overview of the synthetic routes for TFE production.



Scheme 1: Common synthetic routes for the production of tetrafluoroethylene.

2.2.1 Ultra-fast pyrolysis of CF_2ClH

The industrial synthesis of tetrafluoroethylene follows the chlorodifluoromethane route, as depicted in Scheme 2 [56, 57]. Variations of this method substitute the CF_2ClH for trifluoromethane.



Scheme 2: The route for the industrial synthesis of tetrafluoroethylene via the ultra-fast pyrolysis of chlorodifluoromethane (R-22).

The major drawback of this, and most other routes is the production of byproducts such as HF, HCl, fluorocarbon, and chlorofluorocarbon side products (such as HFP, PFIB, *etc.*) that must be scrubbed or cryogenically distilled from the tetrafluoroethylene. Besides being dirty, such processes require costly equipment and are difficult to operate in batch. Therefore, the ultra-fast methods are not readily usable on a laboratory scale. In contrast, pyrolysis of R-22 is the preferred industrial method. A continuous process can be optimised to be relatively clean due to HF and HCl recycling, and economy-of-scale makes the process financially attractive.

2.2.2 Dehalogenation of halofluorocarbons

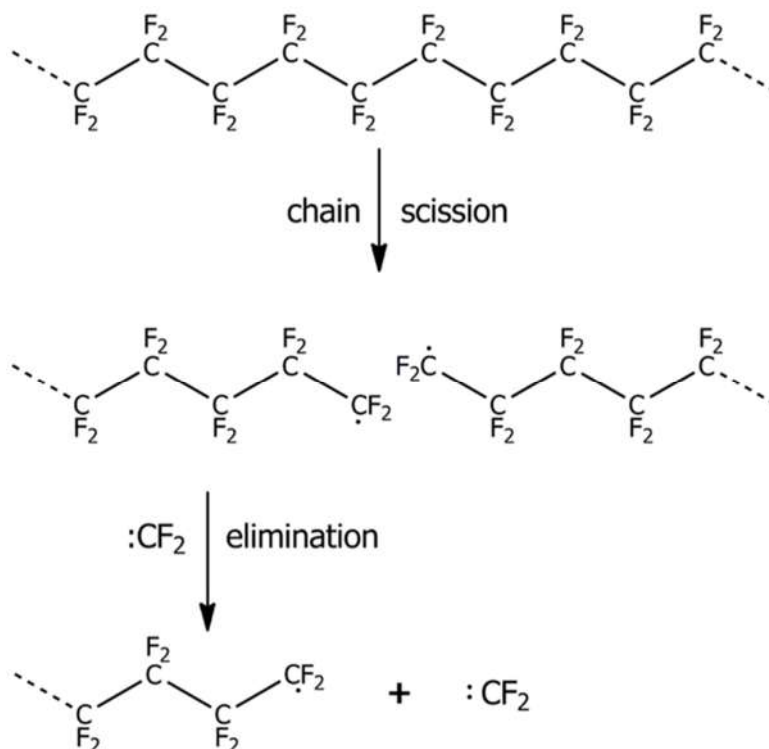
The first reasonable option for laboratory scale synthesis of TFE is the dechlorination of $\text{CF}_2\text{Cl}-\text{CF}_2\text{Cl}$ with zinc [58, 59]. The method is facile and safe, calling for the batch reaction of the symmetric chlorofluorocarbon with high surface area zinc dust using methanol as solvent. The reaction takes place from 70 °C and good yields are obtained in reasonable time scales (~5 hours), with non-condensable product consisting of ~ 95 % to 98 % TFE. Availability of the starting material is the only major technical drawback to employing this method as most of the starting materials are banned under the Montreal Protocol [60] due to their ozone depleting potential. A variant of this method includes the debromination of $\text{CF}_2\text{Br}-\text{CF}_2\text{Br}$ [61].

2.2.3 Pyrolysis of perfluoropropionic acid salts

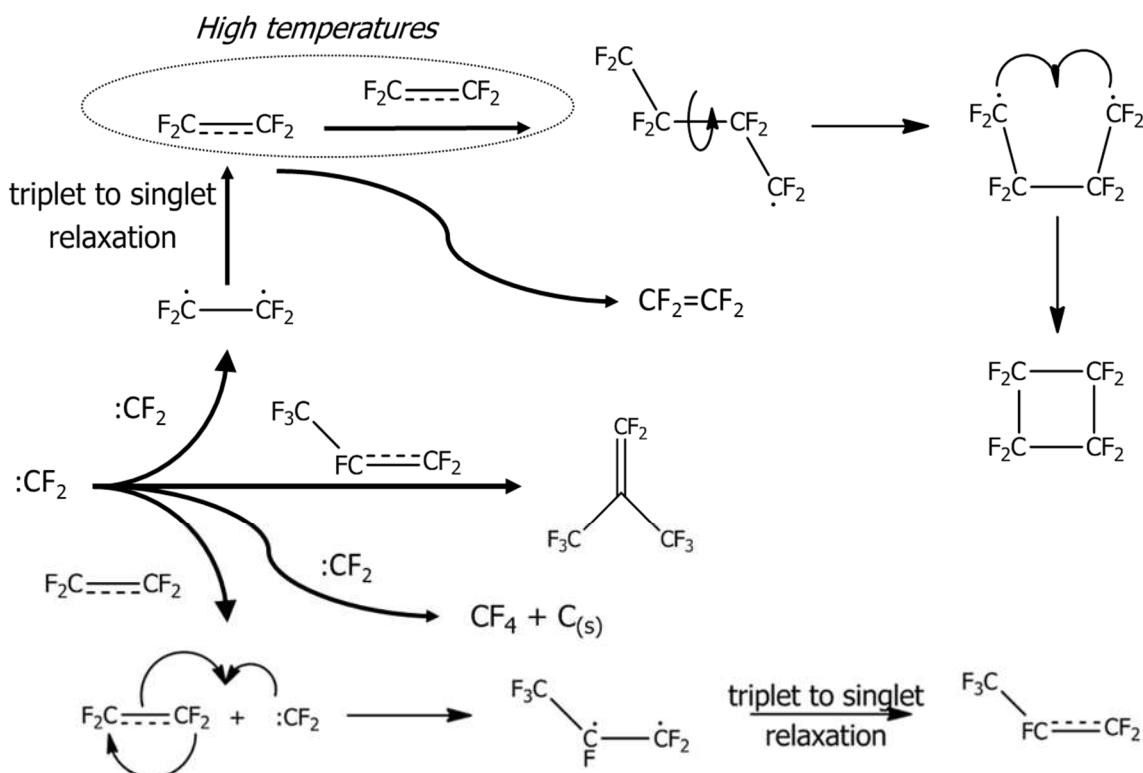
A second option for TFE production is the alkali salt pyrolysis route, which produces CO_2 and TFE in a 1:1 ratio as well as a metal fluoride [54]. This method is facile and safe, but generation of completely pure TFE requires the removal of CO_2 from the gas mixture. This method is not exceptionally expensive, provided one has ready access to commercial entities that can supply the acids. This is the only method of synthesis employed by the Thrasher Group at Clemson University [54].

2.2.4 Pyrolysis of PTFE under vacuum

The remaining option for TFE generation on a laboratory scale is the vacuum pyrolysis of polytetrafluoroethylene. This option has already been pursued to a great extent in the Fluoro-Materials Group at the University of Pretoria and in the research group at the University of Ottawa. The literature on the pyrolysis of PTFE has already been reviewed [12, 62-64]. In short: PTFE may be pyrolysed under vacuum of around 1 Pa and at 600 °C to yield nearly pure (99.5 %) tetrafluoroethylene, with minor amounts of HFP, OFCB, and the perfluorobutene isomers. The pyrolysis reactions are summarised in Scheme 3 and Scheme 4. This method is facile and does not require any expensive reagents or very expensive and complex process equipment. The kilogram-scale PTFE pyrolysis reactor built at the University of Pretoria is shown in Figure 3.



Scheme 3: Mechanism of PTFE breakdown by thermal chain scission to eliminate difluorocarbene.



Scheme 4: Gaseous radical reactions occurring during PTFE pyrolysis that leads to the formation of TFE and fluorocarbon by-products.

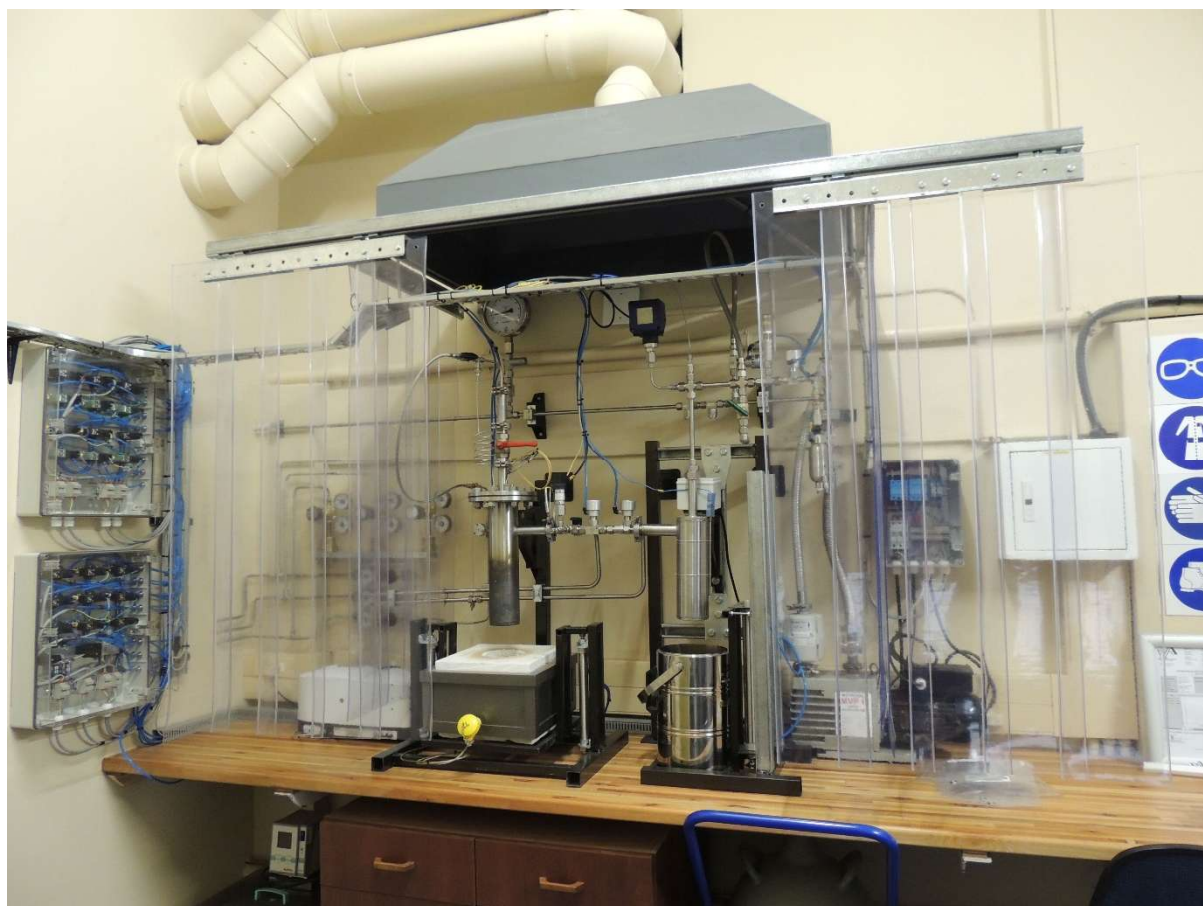


Figure 3: *The kilogram-scale PTFE pyrolysis reactor built at the University of Pretoria.*

Extreme care must be taken with the pyrolysis of PTFE as improper pyrolysis conditions will lead to the production of large quantities of perfluorobutene compounds [64]. The effects of temperature and pressure on the composition of the pyrolysis stream has been documented in detail by Bezuidenhoudt *et al.* [64].

Among these, perfluoroisobutene is the most dangerous. This species, existing as a gas at ambient conditions, is classed as a schedule 2 chemical weapon, and its production is banned by treaty [65]. Upper limits on the lethal concentrations for rats of 0.5 ppm in air [66] have been reported and lower limits for the toxicity have been reported in the 150 ppb range [67, 68]. The compound primarily attacks the lungs, causing pulmonary oedema [69, 70].

Proper containment and analysis of the pyrolysis gas before use in polymerisation is paramount, as is the destruction of the leftover gas or any pyrolysis gas that contains too high a level of these toxic perfluorobutenes.

2.2.5 Tetrafluoroethylene process safety

Safety is paramount when considering working with tetrafluoroethylene and it can, and due to lack of caution on the part of research or production staff, often does deflagrate. While 1- or 2-g quantities may burst a tube or a cylinder, larger amounts tend to do significant damage to infrastructure and at the 10 or 20 g scale, the detonating power of enclosed TFE is something to give pause to even the most reckless experimenters.

The companies and public entities who engage in working with TFE have developed facilities and expertise through long years of trial and error, many times at the cost of human life. The Thrasher group at Clemson University has spent years developing academic barricades to permit the safe use of large quantities of TFE in their facilities, and their recent publication on the topic is well worth the read [71].

The safety aspects detailed here are meant to guide and inform, but are no substitutes for experience. All work done with TFE should first be carried out in sub-gram quantities before being scaled up to any size.

2.2.5.1 Autogenic decomposition of tetrafluoroethylene

Tetrafluoroethylene is dangerous to work with and care must be taken to avoid subjecting TFE to conditions where it may autopolymerise or decompose. The mechanism of decomposition has been reported in detail [12, 41, 72-76]. In summary:

TFE does not exist in ethylenic form *per se*; that is, electronic and steric factors perturb the electron distribution in the π -orbital to such an extent that the molecule exists as a biradicaloid and not as a canonical ethylenic species [77]. This in turn translates to a molecule that can very easily undergo addition reactions, and TFE may easily undergo self-addition to form cyclo-octafluorobutane ($\Delta H_R = -103 \text{ kJ/mol}$) [78]. From the heat provided by this reaction, other addition and rearrangement reactions, and ultimately, rearrangement to form CF_4 and carbon ($\Delta H_R = -257 \text{ kJ}\cdot\text{mol}^{-1}$) may occur.

The kinetics of these reactions are strong functions of pressure and temperature, and they occur very slowly, if at all, at room temperature; but, if the pressure and temperature at any point in the gas are such that sufficient internal energy is available for the TFE to undergo cyclisation, local “hotspots” may occur that precipitate runaway decomposition reactions that lead to tremendous pressure spikes and the concomitant explosion of the containing vessel. There have been studies on the thermal decomposition of TFE in both small (1-L) and large volume (100-L) vessels, the

results of which indicate that the autodecomposition temperature decreases with pressure and decreases with reactor volume [41, 72].

The effect of volume is inferred to be related to an increase in internal vessel surface area. The rearrangement reaction to form CF_4 and carbon may occur in the gas phase, but requires high temperatures (which may also be induced by rapid changes in pressure). Provision of a metal surface on which the gas may rearrange greatly increases the reaction rate and contributes to a lower decomposition temperature. There is some evidence that the nickel and chromium in stainless steels and other alloys used in the fluorochemical industry act as catalysts for this rearrangement [62, 63, 79].

Institutions working with TFE have all developed their own rules for handling TFE. Three rules of thumb can be extracted from the literature:

- 1) Do not heat TFE above 100 °C when the gas is under a pressure of greater than 15 bar.
- 2) Furthermore, as seen in the case studies [75, 80] of the explosions of TFE-polymerisation plants, pressure shockwaves and other large fluctuations in pressure within the gas also have the potential to cause decomposition *via* adiabatic heating of the compressed gas to deflagration temperatures. Therefore, do not subject TFE to large pressure changes at any temperature. A technical implication of this rule is that TFE should not be subjected to sudden, drastic changes in flowpath diameter. That is, tubing should be of a consistent size throughout and any valves employed should have internal diameters of size similar to the tubing employed. In a similar vein, the flow of TFE through a valve should be sufficiently slow to ensure that there is little frictional heating of the gas.
- 3) Finally, oxygen may act as both inhibitor and initiator to polymerisation [81]. In the case of TFE, the presence of oxygen will not only inhibit polymerisation, but will also worsen any decomposition reaction [76]. Indeed, if sufficient oxygen is present alongside TFE, it may initiate a spontaneous decomposition under pressure. Molecular oxygen caps the PTFE macroradical, forming unstable peroxides [82]. Therefore, rigorously scrub free oxygen from any closed system containing TFE.

2.2.5.2 Storage of tetrafluoroethylene

Prolonged storage at pressures greater than about 2.2 bar is not recommended without addition of a radical scavenger. Various amine-based stabilisers [83] are employed in industry and small amounts of limonene, or other monoterpenes may also be used to stabilise TFE for indefinite storage [84]. The patent literature indicates that the monoterpenes form gum-like deposits on

prolonged storage due to their reaction with the minute amounts of oxygen, as well as with any other radical forming species, present in the tetrafluoroethylene gas. Therefore, the monoterpenes have been superseded by alpha-methyl-vinyl-toluene [85], which permits high pressure transport of the gas without gumming up pipes and valves, *etc.* Typically 0.5 mol % (TFE basis) of the vinyl toluene should be used, but this value may increase depending on the amount of oxygen introduced into the tetrafluoroethylene by back diffusion through system leaks during transfer operations. Usually, such contamination falls in the low-single-digit ppm range.

Another strategy employed in the stabilisation of TFE involves the use of CO₂ [86]. When contacted with CO₂, TFE shows an apparent increase in stability, and may be stored at very high pressures (up to 11 MPa) and moderately high temperatures for prolonged periods without decomposition. Ideally, a 1:1 molar ratio of TFE and CO₂ should be used.

2.2.5.3 Heat removal during polymerisation

The polymerisation reaction itself is also highly exothermic ($\Delta H_R = -196$ kJ/mol TFE) [43], and care must be taken to ensure that the heat generated be quickly removed. Therefore, jacketed reactors are not recommended as the thermal lag in a jacketed system is sufficiently large to permit the system to reach deflagration temperatures. Rather, an immersed cooling coil should be used, or preferably, a jacket and coil system should be used to ensure that the reaction medium is cool and that there are no severe thermal gradients in the polymerisation kettle.

The use of additives also plays a role in the removal of the heat of reaction, as in large polymerisation kettles there is a noticeable improvement in heat transfer within the reactor if emulsion polymerisation is employed (as compared to suspension polymerisation) [87].

As described in Section 2.5.2, solvents other than water may be used as reaction medium. Although TFE is only sparingly soluble in water, it is easily solubilised in fluorinated and partially fluorinated solvents. A danger exists here in that if the concentration of the TFE in the solvent is sufficiently high, local hotspots may develop even in the presence of proper cooling, leading to runaway reactions and explosions.

Our experience shows that performing batch polymerisation reactions (20 g of TFE in a 330-mL autoclave) using perfluorodecalin as solvent always leads to runaway reactions and explosions.

For this reason, use of solvents other than water should be avoided when performing batch reactions, and when solvents in which TFE is highly soluble are employed, it should rather be

done in a continuous monomer- and initiator-dosing mode, with strict control over the amount of TFE present in the kettle at any given time.

2.2.6 Conclusions

There are a variety of methods by which TFE may be prepared, not all of them suited to a laboratory setting, and while some synthesis routes are facile and inexpensive, the use of tetrafluoroethylene brings with it significant risk to the researcher. Importantly, care should be exercised regarding selection and sizing of gas handling equipment as well as the amount of TFE stored and its storage location, with a make-and-use strategy being preferred over make-and-store.

2.3 Polymerisation process and equipment

Tetrafluoroethylene is gaseous at standard conditions and is sparingly soluble in water. Thus high pressure equipment must be employed in the polymerisation process. Laboratory-scale work may take place in thick glass ampoules or in stainless-steel autoclaves; however, industrial-scale polymerisation primarily takes place in large, high-pressure, stirred-tank reactors.

Tetrafluoroethylene polymerisation can be performed by two distinctly different procedures in aqueous media:

- 1) The first procedure, called suspension polymerisation, involves contacting tetrafluoroethylene with an aqueous medium containing an initiator and, possibly, small amounts of additives such as pH buffers while stirring the mixture vigorously, obtaining a coarse, stringy or granular product.
- 2) The second procedure, called dispersion or emulsion polymerisation involves contacting tetrafluoroethylene with an aqueous medium containing an initiator, a dispersion agent, an anti-coagulant, and possibly some additives such as pH buffers and chain-transfer agents, usually obtaining a fine suspension of polymer.

Ordinary suspension polymerisation is not generally employed in industry as the properties of the product polymer cannot meet the current product specifications. All polymerisation used to date are some form of dispersion polymerisation, but with granular PTFE grades produced by a process bordering on the suspension precipitation method, as only a tiny amount (2 to 200 ppm) of dispersion agent is employed.

Furthermore, many of the polymerisation processes, as practiced, do not produce true TFE homopolymer, but rather a “modified PTFE”. This entails adding a small amount (≤ 0.6 mol %)

of a fluorinated comonomer, such as perfluoromethyl vinyl ether, to produce a TFE high polymer containing small amounts of modifier, just sufficient to impart the mechanical properties required for the moulding process [88].

The granular grades are employed in powder moulding-processes whereas the fine suspensions are employed in dispersion coating of metals and other substrates, impregnation of textiles and fibres, the preparation of films, porous sheeting resin (*i.e.*, Gore-Tex) and varnish, as well as paste-extrusion fabrication processes.

Other polymerisation procedures, such as bulk-phase polymerisation and supercritical-CO₂ polymerisation are possible, but are not known to be of commercial importance at present.

2.3.1 Polymerisation procedures

In theory, polymerisation of TFE may be carried out under a continuous regime, but for the most part it occurs either as a batch or as a semi-batch process, with semi-batch processes being industrially preferred. For the sake of clarity: a semi-batch process as contemplated here is defined in the literature [89] as a batch-like process in which reagents are fed into the reactor vessel while the reaction is taking place, but without removing any material from the reactor for the duration of the operation.

2.3.1.1 Batch and semi-batch polymerisation

The semi-batch process entails multiple possible dosing regimens, with the continuous dosing of TFE being the most common. Other dosing schemes include the continuous dosing of initiator, continuous dosing of chain-transfer agent and continuous dosing of dispersing agent [90], usually in conjunction with the continuous dosing of tetrafluoroethylene. Examples exist in the literature of stepped dosing as well [91, 92]. In most commercial cases, however, the continuous dosing of TFE into the semi-batch reactor is the order of the day, with all the other additives and the initiator being loaded beforehand. Variations on this theme include the loading and dosing of a mixture of TFE and some inert gas, such as N₂ or Ar, with the intent of decreasing the partial pressure of TFE as the reaction proceeds in order to control the molecular-weight distribution of the polymer [88].

The dosing of tetrafluoroethylene typically continues until the reactor contains 30 % to 35 % polymer solids. Examples exist in the literature for polymerisation being carried out to solids contents in the range of 15 % to 40 % by mass of the mixture [93]. This is not a hard limit, but a best practice adhered to in order to prevent excessive agglomeration of polymer particles in the

reactor. Herisson [94] from the Kuhlmann company indicates that dispersions in water of up to 50 % can be made if a continuous temperature ramp program is used.

It must also be noted that isothermal polymerisation is the rule in the greater majority of industrial operations, although there will be a non-isothermal temperature ramp up period, the length of which is dependent on the size of the reactor as well as safety considerations.

The polymerisation process, as practiced by DuPont/Chemours, consists of loading a reactor with the required amount of solvent, initiator, dispersing agent, anti-coagulant, *etc.* and pressuring the reactor with TFE to the desired reaction pressure. Heating is commenced, and the pressure is monitored to determine the start of reaction (evidenced by a pressure drop), after which TFE is dosed into the reactor to maintain a constant pressure while monitoring the mass of TFE dosed into the reactor. When the desired mass of TFE has been dosed into the reactor, the TFE line is shut, and the remaining TFE is allowed to react away before the reactor is cooled and opened.

Importantly, under ordinary process conditions, the monomer is gaseous, and at no point in the reaction does the monomer form a liquid phase in the polymerisation kettle. The Gore company has disclosed a liquid-phase polymerisation process that results in polymer morphologies substantially different from that obtained *via* the usual polymerisation methods [95].

2.3.1.2 *Post-polymerisation processing*

In the case of suspension polymerisation, the aftercare entails washing the granular polymer with water to remove any initiator residues as well as any remaining additives. After washing, the polymer may be mechanically processed by grinding to reduce the particle size. The final step involves the drying of the polymer, typically in large air driers.

In the case of dispersion polymerisation, product ear-marked to be sold as fine powder is coagulated under low-shear conditions and subjected to washing and drying. The washing step for dispersion polymerisation requires special attention as all the waste water must be treated before being disposed of in order to remove any perfluorinated surfactants and initiators.

2.3.2 Polymerisation equipment

Free-radical polymerisation may be carried out in glass, glass-lined reactors (enamelled), platinum- or silver-lined reactors, or directly in stainless steel reactors. Industrial polymerisation is carried out with reactors that are baffled and with stirrers that maximize the liquid-to-gas surface area, whereas one will come on any number of configurations in a laboratory setting with

baffled and unbaffled systems being equally common. Examples of bench-top and industrial-scale systems are presented in Figure 4 and Figure 5, respectively.

Typically, pitched-blade stirrers are used, with multi-blade arrangements being common in commercial-scale polymerisations. Other configurations reported include unbaffled reactors with anchor-type agitators [92]. Kim *et al.* [50] investigated the efficacy of various stirrer types for TFE polymerisation and found that vortex formation and the maximization of gas-to-liquid surface area are the most important criteria to look at when selecting a stirrer. They recommend the use of an anchor type stirrer with a baffled tank.

Heating of the vessel is carried out *via* a steam-fed heating jacket and internal vessel cooling is supplied in the form of chilled water circulated through pipes immersed in the reaction medium.

One major difficulty encountered during free-radical precipitation polymerisation of TFE is the propensity for polymer to adhere to the walls of the reactor. This seems to occur irrespective of the material of construction. This issue may be overcome by adding a chain-transfer agent to the polymerisation reactor.



Figure 4: *Examples of 1-L bench-top type autoclaves (both glass and stainless steel) suited to the polymerisation of TFE (Images courtesy of AMAR Equipments PVT. Ltd.).*



Figure 5: *Head section of an industrial 40-kL polymerisation reactor (Images courtesy of International Process Plants).*

2.3.3 Reaction mechanisms and kinetics

In the absence of chain-transfer agents or other materials, which may prematurely terminate the growing macroradical, the only kinetic parameters are initiation (k_i), propagation (k_p), and mutual termination (k_{td}). The mechanisms and kinetics are dependent on the specific polymerisation system (*i.e.*, free-radical, electrochemical, or coordination). The mechanisms for the electrochemical and coordination homopolymerisation of TFE have not been described, and the publically accessible literature contains limited information on the free-radical process.

2.3.3.1 *Suspension free-radical polymerisation kinetics*

Owing to the insolubility of even relatively short PTFE chains, the kinetics of TFE suspension homopolymerisation bears a heterogeneous character [82]. The fundamental homopolymerisation mechanism is characterised by the linear addition of TFE to the growing macroradical and no radical rearrangement or backbiting can occur within the polymer chain to produce branched structures. The macroradicals are essentially immobile (their thermal motion is limited by the rigid nature of the PTFE chain), and termination of the chain can occur only by recombination or the abstraction of a hydrogen from some non-fluorinated species that happens to pass by the macroradical.

Recombination itself is also not a clear-cut phenomenon: If mobile radical fragments (such as initiator radicals) find the radical chain end, recombination may take place, but, observation of the rate of depletion of active chain ends by EPR shows that chain recombination occurs slowly in the post-initiation phase (when all initiator radicals have been depleted), exhibits monomer concentration dependence (as opposed to chain end concentration dependence), and recombination stops entirely after a certain molecular weight has been achieved [82, 96]. The current understanding is that, in the post-initiation phase, the macroradical extends by monomer addition until two macroradicals are in close enough proximity to terminate. If no suitable macroradical is found, termination does not occur.

The use of Tobolsky's equation [97, 98] in describing TFE homopolymerisation is flawed as the polymerisation is not homogenous. A proper, fundamental kinetic expression for the homopolymerisation of TFE must differentiate between termination due to fortuitous termination (by initiator fragments, *etc.*) and termination due to mutual recombination of the PTFE macroradicals. Markevich *et al.* [82] have made some progress in this matter, and their kinetic expression for the apparent rate constant of mutual termination is presented in Equation (1),

$$\kappa = k_p[M]\lambda a \left(1 + \frac{4\pi\lambda r}{a}\right) \quad (1)$$

Here, κ is the apparent rate constant for mutual termination, k_p is the propagation constant, λ is the distance traveled for a macroradical with each monomer addition (twice the C-C bond length in PTFE), a is the cross-section of the TFE repeat unit in the polymer, and r is the radius of the cage around the macroradical in which a mutual recombination reaction can occur.

The implication of Equation (1) is that, for mutual recombination, there is no independent termination constant and the effective termination constant is a function of the propagation constant, as well as the monomer concentration.

Measurement of the propagation and termination parameters are somewhat difficult, but there are scattered reports in the literature. Plyusnin and Chirkov [99] estimated the elementary rate constants for free-radical suspension polymerisation in water at 40 °C by measuring the active chain-end concentrations using 2,2,6,6-tetramethyl-4-piperidinol and found the rates of propagation and dead-end termination (k_p and k_t) to be 7400 and 74 L·mol⁻¹·s⁻¹, respectively. Markevich *et al.* [82] determined an activation energy of 39 kJ·mol⁻¹ for the propagation constant (k_p) between 0 and 100 °C. They also found that the mutual recombination cage radius for a PTFE macroradical varied from 1 to 5 Å over the range from 0 to 100 °C.

2.3.3.2 Dispersion free-radical polymerisation kinetics

The intrinsic kinetics of dispersion polymerisation is the same as for suspension polymerisation, and the polymerisation still bears a heterogenous character. Kim *et al.* [50] published an investigation into the effects of the polymerisation conditions on the molecular weight of PTFE produced by dispersion polymerisation under a continuous TFE dosing regime. The observed kinetics of dispersive TFE homopolymerisation is closely tied with the mechanism of polymer-particle formation (discussed in Section 2.7.2.4) and is divided into a nucleation phase and a particle growth phase:

The nucleation phase is observed as an induction period, which may last as long as 40 minutes (though normally it lasts around 5 minutes) and is dependent on the shear rate and free surface area in the reactor (which in turn is dependent on the agitation speed). During this induction period, the rate of polymerisation increases to a plateau value, which is determined by the reaction conditions and the hydrodynamics of the reactor. The plateau area is reached essentially when the formation of polymer nuclei is halted (whether due to initiator depletion or due to depletion of the surfactant). The particle growth phase is noticed as a steady, plateaued rate of polymerisation, which continues until either monomer diffusion to the macroradical becomes the rate-limiting step, or the mass of polymer in the reactor reaches the threshold where agglomeration takes place. Particle consolidation results in a decreased reaction-surface area, which concomitantly, causes a drop in reaction rate. Kim *et al.* [50, 100] demonstrated that, for dispersion polymerisation under non-agglomerating conditions, at least two different kinetic regimes are at play, *viz.* gas-liquid- and gas-solid diffusion controlled reactions, and that the rate of polymerisation is a strong function of the number of nuclear polymer particles.

Punderson [90] reports that for dispersion polymerisation, the space-time yields are a strong function of both the surfactant concentration and the surfactant dosing regimen. For dispersion polymerisation using a single initial dose, the typical space-time yields are around $355 \text{ g}\cdot\text{L}^{-1}\cdot\text{h}^{-1}$ and when using a delayed dosing regimen, the typical space-time yields are below $200 \text{ g}\cdot\text{L}^{-1}\cdot\text{h}^{-1}$.

2.3.3.3 Supercritical CO_2 mediated free-radical polymerisation kinetics

Xu *et al.* [101] reported that the rates of polymerisation of TFE in a supercritical CO_2 medium conforms to the behaviour expected from homogenous polymerisation (that is, it follows Tobolsky's law [97, 98]). They found TFE polymerisation takes place homogeneously within the supercritical fluid and termination by mutual recombination occurs readily, resulting in precipitation of the polymer from the fluid. Xu *et al.* found apparent $k_p \cdot k_t^{-0.5}$ values of 0.38 (at 35

°C) for the homopolymerisation of TFE in supercritical CO₂. These values are markedly lower than the $k_p \cdot k_t^{-0.5}$ values for aqueous polymerisation (*ca.* 860).

2.3.3.4 *Gamma radiation induced free-radical polymerisation*

Tabata and coworkers extensively investigated the radiation induced polymerisation kinetics of TFE in solution [102], bulk liquid and in the solid state (*i.e.*, polymerisation in frozen TFE). They found that in-source polymerisation in bulk liquid and solution proceeds without any noticeable termination step in the initial stages of reaction, with the conversion being a strong function of dose rate. The propagation constants for post-polymerisation is a strong function of temperature with the activation energy for post-polymerisation being 4 times higher than the in-source activation energy.

2.3.4 Conclusion

Tetrafluoroethylene may be polymerised by either suspension-, emulsion-, or supercritical CO₂ mode polymerisation, and the procedure may be conducted either batch, semi-batch or continuously, with semi-batch using continuous dosing of TFE as the preferred industrial method.

Essentially, in any real-solvent mediated TFE polymerisation, the kinetics are governed by the diffusion of the monomer, either into the reaction medium, or through the reaction medium to the PTFE macroradical. Some reaction kinetics have been reported, but there remains a dearth of information on the temperature dependence of the propagation and termination rates.

No articles could be found in the literature that sets down reactor independent correlations for the polymerisation rate in terms of fundamental polymerisation constants of TFE. The polymerisation rates reported by Kim *et al.*, Xu *et al.*, Lai *et al.* [50, 101, 103], *etc.*, as well as all the patent literature, are lumped terms that include reactor hydrodynamics- as well as diffusion effects.

Significant research scope exists for determining the kinetics of polymerisation and, in particular, the effects of temperature and pressure on the molecular-weight distribution of PTFE.

2.4 Polymerisation initiators

The initiators used in TFE polymerisation are all-important as the polymer stability, colour, and molecular weight are all, to some extent, functions of the initiator chemistry.

The Brubaker patent [16] indicates that the use of peroxy compounds as initiators is preferred for free radical polymerisation, and in particular, the use of alkali or ammonium persulfate, using thermal activation, is preferred. Redox activation may also be used, but this method tends to contaminate the polymer with metal. However, the redox system does result in a more controlled reaction, and a polymer with a higher M_n [30]. As will be discussed in Section 2.7.3.3, persulfate initiators introduce discoloration into the polymer and have therefore been superseded by other organic peroxides, such as disuccinic acid peroxide, and, in particular, by perfluorinated peroxide initiators, such as HFPO dimer peroxide (di(perfluoro-2-methyl-3-oxahexanoyl) peroxide) [23, 104]. Some of the initiators reported to have been used with TFE are summarised in Table 2, and the individual classes of initiators are discussed hereafter.

2.4.1 Inorganic free-radical generating initiators

The most common inorganic free-radical generating initiators employed with tetrafluoroethylene are the various persulfate initiators, with sodium, potassium, and ammonium persulfate being the most common. Ammonium persulfate is preferred as any residual initiator not washed out of the polymer is decomposed and evaporated during the sintering steps for PTFE, leaving no residual inorganic contamination in the polymer. Typical concentrations of persulfate initiators required to produce high polymers fall in the range of 2 to 500 ppm. Polymerisation is typically continued until the reactor contains ~30 % solids [93].

Joyce and others [17, 21] indicated that molecular oxygen could also be used to polymerise TFE, but this contradicts other reports [30, 81, 105]. Oxygen is known to act as an inhibitor to polymerisation and must be rigorously excluded from the polymerisation system if any appreciable polymer yield is to be had. Oxygen difluoride may be used as an initiator, and the polymerisation occurs readily and rapidly at temperatures ranging from 25 °C down to -100 °C [106]. Ozone has also been cited as a possible initiator.

Furthermore, fluorine radicals may be generated by heating certain metal fluorides like CrF_3 and AgF_2 in the presence of tetrafluoroethylene, and polymerisation may be initiated in this manner to produce a high polymer [107]. At the opposite end of the spectrum, XeF_2 initiates the polymerisation of TFE at 25 °C *via* low temperature release of $\text{F}\cdot$ [108].

2.4.2 Organic free-radical-generating initiators

Organic free-radical generating initiators have been the mainstay initiators for commercial PTFE products, and the most common types are of the peroxide class. Since nearly all PTFE

production occurs in aqueous medium, those compounds that can dissolve well in water are most preferred, with disuccinic acid peroxide and diglutaric acid peroxide being the most cited initiators. Water insoluble compounds such as benzoyl peroxide can be used, but their application is limited to situations where organic solvents or water/organic biphasic systems are employed.

The selection of initiator is based primarily on solubility and half-life, but there are limitations on the chemistry and size of the initiators owing to the possibility of atom transfer from the initiator to the fluoromacroradicals. Lauroyl peroxide is an example of an organic initiator that will also act as a chain-transfer agent.

Importantly, azo-initiators have been found to not be very effective in initiating TFE polymerisation, with azobisisobutyronitrile (AIBN) and similar initiators producing no polymer at all, irrespective of concentration or reaction temperature.

Normally, organic peroxydicarbonates, such as bis(*tert*-butylcyclohexyl) peroxydicarbonate (Perkadox 16) do not initiate the polymerisation of tetrafluoroethylene, but Scoggins and Mahan [109] demonstrated that organic peroxydicarbonates, specifically di(saturated hydrocarbyl)s with carbon atom counts of 1 to 4, can initiate the polymerisation of tetrafluoroethylene, either carried on finely divided PTFE powder or as neat powders with no solvent. In the cases of diisopropyl and di(*sec*-butyl) peroxydicarbonates, TFE high polymer was obtained.

2.4.3 Free-radical generating redox initiators

Myers [30] indicated that when using a redox initiator with TFE systems, a redox system comprising an organic peroxide, a divalent metal promoter, and a reducing agent gives the best results. While nickel, copper, cobalt, manganese, and iron may be used, iron compounds are the most preferred promoters [110]. Although, most inorganic metal salts may be used, organic salts and chelates with the ability to dissolve well in the polymerisation medium, as well as the monomer, are preferred. Therefore metal compounds of perfluorocarboxylic acids are preferred. Any of a number of reducing agents may be employed, with bisulfites being most preferred [111]. Other reducing agents include hydrazine, dithionite, or diimines.

Other systems also reported include ammonium persulfate/sodium bisulfite with a copper-based accelerator (promoter) such as copper sulfate [111]. Interestingly, Halliwell also mentioned that an excessive amount of copper acts as an inhibitor, so the optimum amount of copper falls between 0.02 and 2 ppm as calculated on the liquid medium. Cobalt and iron show a much more

pronounced rate acceleration than silver when silver is used as sole promoter. A copper accelerator is far superior to all three.

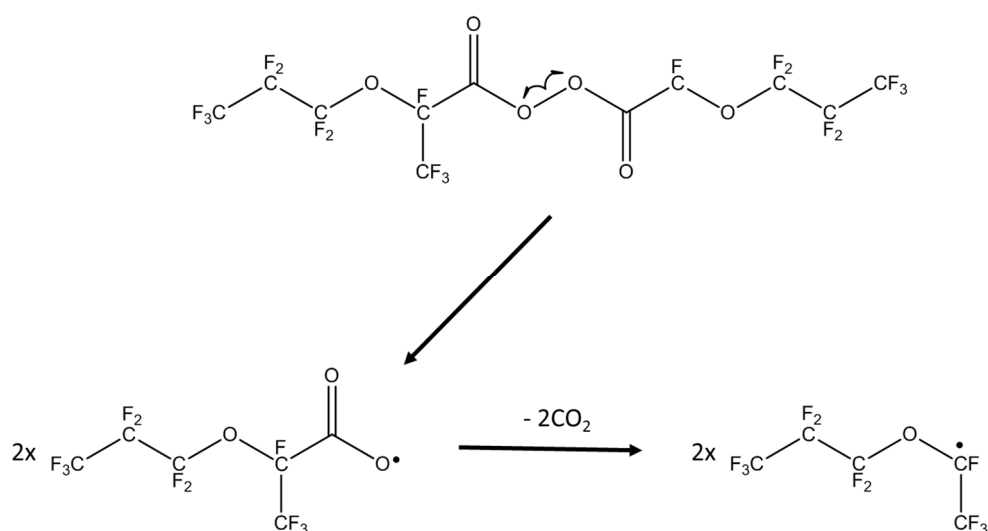
A variation on this theme includes the additional inclusion of silver ions to the bisulfite, which increase the reactivity of the radicals generated by the divalent metal/bisulfite mixtures towards the polymerisation of tetrafluoroethylene and tetrafluoroethylene/chlorotrifluoroethylene mixtures [112].

Redox initiated polymerisation exhibits one noticeable drawback, *viz.*, discoloration of the polymer due to metal inclusion in the final product powders.

2.4.4 Fluorinated free-radical generating initiators

Fluorinated dialkyl and diacyl peroxide initiators may be produced beforehand and added into the polymerisation reaction in the usual way, but many of these initiators are not thermally stable, even at 25 °C. It has been claimed in the patent literature [113] that fluorinated diacyl peroxide initiators may be produced *in situ* during polymerisation by introducing the anhydrides of perfluorinated carboxylic acids along with concentrated (~90 %) H₂O₂, although less concentrated H₂O₂ may be used as well. Other fluorinated initiators include (NaOC(CF₃)₂)-COO [114]. The commercially preferred class of fluorinated initiators are the poly(hexafluoropropylene oxide) peroxides [23, 104], such as bis(perfluoro-2-n-propoxypropionyl) peroxide [101, 115].

The mechanism of initiation for poly(hexafluoropropylene oxide) peroxide is rather complicated, as the initiator may undergo decarboxylation as well as internal radical re-arrangement to afford a number of different radical species [115, 116]. This is shown in Scheme 5.



Scheme 5: Thermal decomposition mechanisms of poly(hexafluoropropylene oxide) peroxide to yield two fluorinated radical species that may initiate polymerisation.

Di(perfluoroacyl) peroxide initiators have a tendency to hydrolyse when used in systems containing water, reducing the initiator efficiency and slowing the polymerisation rate [32]. The hydrolysed initiators may also result in unstable end-groups. The use of more sterically hindered initiators tends to overcome this problem. In the example from Nakagawa's patent [32], $(\text{ClCF}_2\text{-CF}_2)_2\text{-COO}$, is the preferred initiator. Di(perfluoroacyl) peroxide initiators are employed extensively in industry because they generate stable end-groups, thus reducing the need to treat the polymer with fluorine in the post-processing step. The claimed instability of di(perfluoroacyl) does not seem to be much of an issue in industry.

Fluorinated disulfides and thio mercury compounds have been reported [117], with bis(trifluoromethyl)-disulfide and bis(trifluoromethylthio)mercury being preferred, achieving high molecular-weight at faster polymerisation rates than that of the fluorinated peroxides.

2.4.5 Miscellaneous free-radical generating initiators

Convery [118] indicated that tetravalent lead salts of the perfluorinated or omega-hydrofluorinated carboxylic acids (with carbon count 11 or less) may be used as free-radical initiators in the polymerisation of tetrafluoroethylene.

2.4.6 Photoinitiators

UV irradiation has been employed *directly* as an initiation mechanism for tetrafluoroethylene and other perfluoromonomers in batch polymerisation systems [119]. Gamma radiation, from ^{60}Co , has also been employed *directly* to effect the polymerisation of tetrafluoroethylene, both in batch [120], and in a continuous reactor system [121], nominally producing a high-molecular-weight polymer.

More commonly, photoinitiation of TFE involves some photoactive species acting as initiator under the influence of UV, or other non-ionising radiation sources, with elemental mercury being the first example [122]. There has also been a report concerning the use of fluorinated azoalkanes like perfluoroazoethane as photoinitiators [123]. Most compounds that produce free-radicals by UV induce bond cleavage may be used as photoinitiators, with salient examples being Cl_2 , F_2 , SF_5Cl [124], N_2O [125], and short-chain acyl halides [126].

Typically, UV C radiation (280 – 100 nm) and lower energy UV B (300 – 280 nm) radiation is employed, with monochromatic light at 253.7 nm as the wavelength of choice. For gamma irradiation, dose rates of $2.6 \text{ kGy}\cdot\text{h}^{-1}$ have been reported, with total dosages usually of the order of 700 kGy [120].

Gamma radiation can be used to initiate TFE polymerisation in the gas, liquid, or in the solid state, with polymerisation temperatures as low as $-196\text{ }^{\circ}\text{C}$ being feasible [120].

2.4.7 Other initiators

DuPont/Chemours has published data concerning the use of active silica as initiator, prepared from silica gels heated to $400\text{ }^{\circ}\text{C}$, whereby TFE is polymerised at 1 bar and $25\text{ }^{\circ}\text{C}$, under anhydrous conditions to yield silica particles coated with a high homopolymer chemically bound to the particle *via* a carbon-silicon, or more likely a carbon-oxygen-silicon linkage [127]. The mechanism is not discussed, but the assumption is that oxygen moieties exist on the reconstructed silica surface, which possesses an unpaired electron that can add to TFE and initiate polymerisation. The rate of polymerisation was reported to drop sharply when the ratio of TFE polymer-to-filler reaches 3:1.

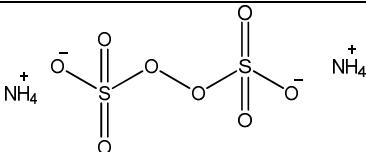
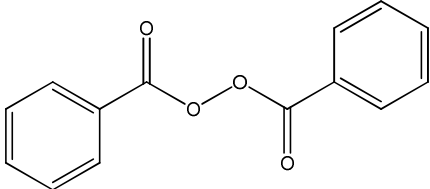
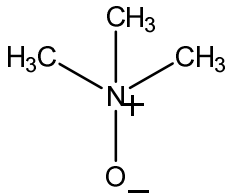
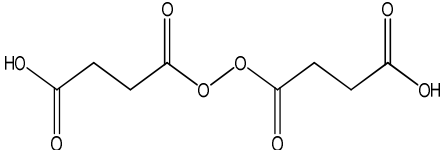
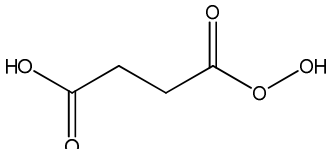
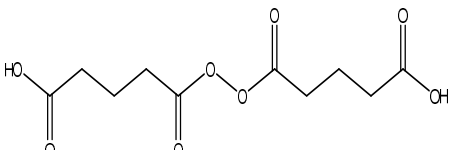
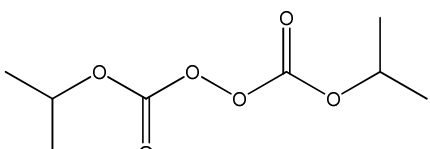
Similar claims have been made by the Allied Chemical Corporation [128] regarding activated alumina supported on silica particles, with the Fuhrmann and Jerolamon indicating the addition of small quantities of metal salts of hexavalent chromic acid (such as magnesium chromate) to the alumina ensure that the polymerisation reaction continues at good speed well past the 3:1 TFE to filler ratio limit. The rate of polymerisation on activated silica is reported to be 0.07 g of TFE per gram of catalyst per hour and the rate on chromium doped materials as 0.42 g of TFE per gram of catalyst per hour.

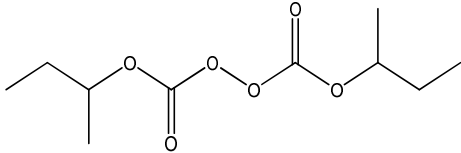
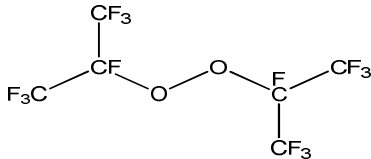
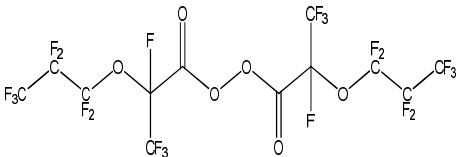
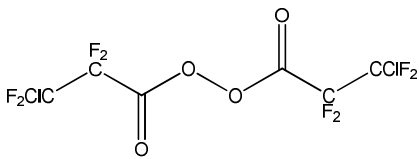
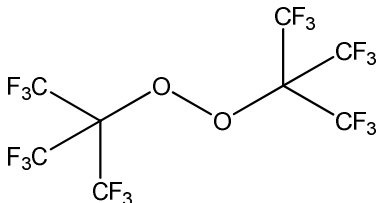
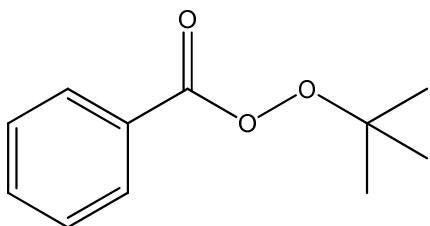
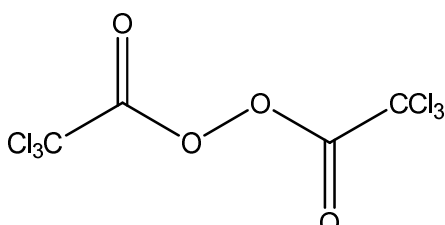
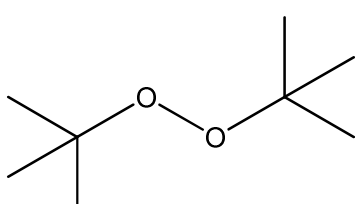
Furthermore, strong oxidizers, such as KMnO_4 in water [88, 129] have also been cited as initiators for the low temperature ($10\text{--}50\text{ }^{\circ}\text{C}$) polymerisation of tetrafluoroethylene, both in ordinary- and emulsion polymerisation, giving high-molecular-weight polymers. The claim was made that any of the salts of permanganic, manganic, and manganous acid can be used in this fashion.

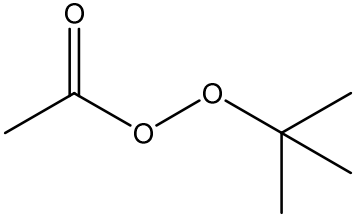
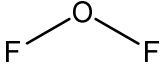
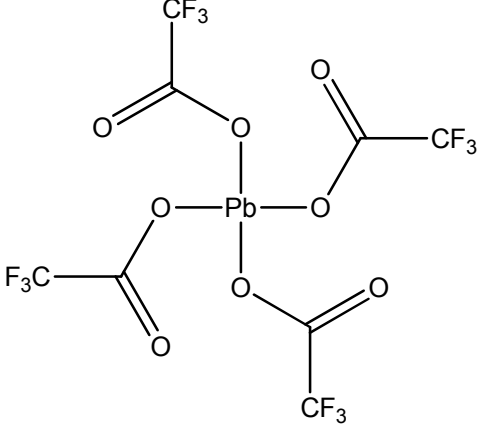
Other inorganic initiators include neat, anhydrous CsF [130] in contact with tetrafluoroethylene gas at temperatures in the region of $150\text{ }^{\circ}\text{C}$. This reaction can produce both polytetrafluoroethylene waxes and high polymer with properties comparable to high polymers obtained by free-radical mechanisms.

Electron-beam irradiation has also been used to directly initiate the homopolymerisation of TFE.

Table 2: *Radical generating initiators used in the polymerisation of tetrafluoroethylene.*

Initiator	Structure	CAS No:	Reference
Ammonium persulfate		7727-54-0	[16-18, 27-29, 33, 50, 103, 105]
Sodium bisulfite / FeSO ₄	NaHSO ₃ / FeSO ₄	7631-90-5	[27, 29, 103]
Potassium persulfate / FeSO ₄	K ₂ S ₂ O ₈ / FeSO ₄		[131]
Hydrogen peroxide	HO-OH	7722-84-1	[16-18]
Benzoyl peroxide		94-36-0	[19]
Trimethylamine oxide		1184-78-7	[20]
Disuccinic acid peroxide		123-23-9	[22, 28, 96]
Monosuccinic acid peroxide		3504-13-0	[22]
Diglutaric acid peroxide		10195-54-7	[22]
Diisopropyl peroxydicarbonate		105-64-6	[109]

Di(<i>sec</i> -butyl) peroxydicarbonate		19910-65-7	[109]
Perfluorodipropionyl peroxide		356-45-6	[24]
Di(perfluoro-2-methyl-3-oxahexanoyl) peroxide		56347-79-6	[23, 104]
bis(3-chloro-2,2,3,3-tetrafluoro-1-oxopropyl) peroxide		88505-66-2	[32]
Bis(trifluoromethyl)peroxide		927-84-4	[132]
<i>t</i> -butyl peroxybenzoate		614-45-9	[30]
Bis-trichloroacetyl peroxide		2629-78-9	[133, 134]
Di- <i>tert</i> -butyl peroxide		110-05-4	[105]

<i>Tert</i> -butyl peracetate		107-71-1	[105]
Oxygen difluoride		7783-41-7	[106]
Pb (IV) tetrakis(trifluoroacetate)			[118]
SF ₅ Cl			[124]
KMnO ₄		7722-64-7	[129]
CsF		13400-13-0	[130]
AgF ₂			[107]
CrF ₃			[107]
PbF ₄			[107]

2.4.8 Ziegler-Natta catalysts

There are also reports in the patent literature [34, 135] concerning the co-ordination polymerisation of tetrafluoroethylene and other perfluorinated monomers using tri-isobutyl aluminium ($5 \text{ mmol}\cdot\text{L}^{-1}$) and titanium tetrachloride ($10 \text{ mmol}\cdot\text{L}^{-1}$) in iso-octane.

2.4.9 Conclusions

Tetrafluoroethylene may be polymerised *via* free-radical, electrochemical, and coordination methods. Free-radical polymerisation may be initiated with well-known substances such as persulfates and organic acylperoxides as well as azo-based initiators in special instances. In particular, numerous water soluble organic peroxides, such as disuccinic acid peroxide, have been developed. Fluorinated organic initiators have been specially developed by commercial entities for use with TFE, permitting polymerisation in fluorinated solvents, *etc.* Photochemical initiation

as well as a variety of special inorganic initiators have also been investigated for use with tetrafluoroethylene. Initiator chemistry is all important for the thermal and chemical stability of the endgroups, which in turn, to a large extent determines the thermal and chemical stability of PTFE. Coordination polymerisation is under-represented in the literature and presents an interesting avenue for further research.

2.5 Reaction conditions

2.5.1 Monomer purity

Tetrafluoroethylene used in polymerisation should be as pure as possible, with a 99.99 % pure material classified as “polymerisation grade”. In industry TFE is routinely purified to 99.99 % and higher to ensure no telogenic species are present in the gas stream. Impurities usually come from the production process, with substances such as CF_4 , HFP, $\text{C}_2\text{F}_3\text{H}_3$, $\text{C}_2\text{F}_2\text{H}_4$, and C_2F_6 being the typical contaminants. The contaminants affect the solubility of TFE in the reaction medium, the reactivity of TFE or act as chain-transfer agents. These have deleterious effects on the reaction rate, product yield, molecular weight, and thermal stability of the final product. Specifically in the case of HFP, the contaminant may co-polymerise with TFE. However, the reaction rate is so low that most of the HFP simply remains unreacted, crowding the TFE out of the reaction medium and blanketing the gas-liquid interface, thereby forming an additional layer through which TFE must diffuse before it reaches the actual reaction zone, *etc.*

As tetrafluoroethylene is usually stored in the presence of a radical scavenger, the TFE must be cleaned before it can be used in polymerisation. In a laboratory setting, the stabiliser can be removed simply by slowly passing the gas stream through a silica gel column [136].

Furrow [137] discloses an industrial 3-step method for the scrubbing of impurities from TFE, in which TFE is first contacted with 98 % sulfuric acid (*via* bubbling or a counter-current gas scrubber), then with molecular sieves having an 8 Å pore size, and finally with pyrophoric copper to remove any trace oxygen from the gas stream.

2.5.2 Solvent environment

Tetrafluoroethylene may be polymerised either in the gas- or liquid phase, both autogenously [105], or in the presence of a suitable radical source, but as this bulk reaction cannot be easily controlled, it is preferred to polymerise TFE in the presence of a liquid carrier. As pointed out by Brubaker [16], the choice of solvent depends on the initiator used, heat transfer

considerations, and inertness to the polymerisation process as well as the solubility of the monomer. These criteria are repeated in nearly every polymer chemistry textbook in circulation today [138-146].

The term carrier, rather than solvent, should be used as the high polymer of TFE does not dissolve in anything, including hot fluorinated solvents [44]. The polymerisation process is classed as precipitation polymerisation [147] owing to the fact that even relatively short PTFE chains crash out of the solvent [148]. Naturally, if a non-fluorinated comonomer is used, it becomes possible to solubilise the polymer, depending on the amount of comonomer incorporated in the final polymer [149].

Discussions in the literature regarding the selection of polymerisation solvents are centred on monomer solubility and chain-transfer properties. In the case of TFE, and all fully fluorinated monomers, the largest criterion for a solvent is its atom transfer ability.

While it has been mentioned that perhalogenated monomers can be polymerised in bulk *a la* ethylene or styrene, the low temperatures and rather high pressures required make it an uneconomical process. Besides this, control of the polymerisation reaction in bulk medium is challenging at best and process safety cannot be guaranteed [113]. Hence, to the best of our knowledge, bulk polymerisation of fluorinated monomers is not employed in industry today.

Solvents may be completely avoided if gaseous photoinitiators are used in conjunction with UV light, but, as with bulk free radical polymerisation, removal of the heat of reaction is an issue that limits the commercial feasibility.

It is a given that the solvent should be a fluid at polymerisation conditions, but the solvent need not be a liquid at ambient conditions, as is the case with CO₂. More importantly, the solvent should not exhibit excessive vapour pressure at polymerisation conditions lest it contribute to the process equipment cost, and it should not boil at such a high temperature that it cannot be readily removed from the product polymer. The polymerisation of TFE, as practiced by DuPont/Chemours, prefers the use of solvents with a boiling point no higher than 150 °C, but preferably no higher than 100 °C, and no lower than 20 °C [104].

2.5.2.1 Solvents for free-radical polymerisation of TFE

Radical telomerisation and polymerisation of fluorinated monomers have been extensively reviewed by Ameduri and Boutevin [150], and they indicate a large number of solvents may be employed. However, owing to the electron-withdrawing effects of fluorine, the radical chain ends of the fluoromacroradical are highly electrophilic and proton transfer occurs readily

between the macroradical and conventional polymerisation solvents [96]. Therefore, hydrocarbon solvents cannot be used for the synthesis of perfluorinated high polymers by free radical mechanism.

Of the conventional solvents employed in polymer synthesis, only water seems to be completely inert toward the radicals of fully fluorinated monomers.

Other solvents that are inert toward fluorinated monomers include various liquid perfluorocompounds, such as perfluorohexane, perfluorocyclohexane and perfluorodecalin as well as various chlorofluorocarbons (specifically chlorofluoroalkanes of 1 to 2 carbons in length). The most preferred chlorofluorocarbon solvent is $\text{Cl}_2\text{FC}-\text{CClF}_2$ (Freon 113) [24].

Hydrofluorocarbons or hydrochlorofluorocarbons may also be employed, and hydrofluoroethers [23], hydrofluoropolyethers [151], and perfluoropolyethers are currently being investigated as polymerisation media for fluoromonomers.

Another option to be considered is the use of biphasic systems of fluorinated solvent (such as R113) and water (done in conjunction with emulsion polymerisation using fluorinated surfactants). In particular, the use of fluoropolyethers with hydrogenated end-groups as the hydrophobic solvent has been reported [151]. The Ausimont company has also indicated that highly-branched, short-chain hydrocarbons such as 2,2,4-trimethylpentane will not act as a CTA if used in a biphasic system with water [152]; however, the examples given in the patent are not sufficiently convincing.

Other fluorinated solvents, which may be used by themselves, or as part of a biphasic system, include perfluorinated cyclic tri-substituted amines without any N-F bonds, such as perfluoro-N-methylmorpholine [153], and linear and cyclic perfluoroalkyl sulphides [104].

Furthermore, it is possible to use liquid inorganic fluorides in their lower oxidation state as solvents for the polymerisation reactions [107], with arsenic trifluoride and anhydrous HF being the most prominent. It goes without saying that such solvents are neither environmentally friendly, nor economical and are not used anywhere in commercial production of fluoropolymers.

DuPont/Chemours has published extensively on the solvents used in the polymerisation of fluoromonomers [23, 24]. These reports indicate that in order to avoid the transfer of protons to the fluorinated macroradical from a hydrofluorocarbon, the solvent structure should not contain:

- Methyl groups ($-\text{CH}_3$), except as part of a fluoroether group (*i.e.* $\text{CF}_2\text{-O-CH}_3$) [23];
- More than two adjacent CH_2 groups (*i.e.* $-\text{CH}_2\text{-CH}_2-$);

- Hydrogens on a carbon adjacent to two CH₂ groups (*i.e.* CH₂-CH₂-CHF-);
- Not more than two hydrogens adjacent to ether oxygens apart from a methyl group (*i.e.* CH₂-O-CF₂, or CHF-O-CHF, but not CH₂-O-CHF, *etc.*); and
- Oxygen may be present in the solvent only as an ether or an alcohol unit.

It is preferred, though, that the solvent compound contains no more than one hydrogen and that this hydrogen be on the difluoromethyl group (*i.e.* -CF₂H) [24].

A recent development in fluorocarbon polymerisation is the use of supercritical CO₂ as solvent [25, 26, 101, 115]. The optimal (1:1) ratio of tetrafluoroethylene to CO₂ can be directly generated *via* the vacuum pyrolysis of alkali metal salts of perfluoropropanoic acid [54], so the supercritical CO₂ method has been facile in a laboratory setting for some time already. TFE is fully miscible in sc-CO₂, but PTFE is not, so the polymer will precipitate as the reaction continues, generating two distinct phases.

As was mentioned in Section 2.2.5, the use of solvents other than water is not generally recommended due to safety considerations. Besides safety, the commercial use of chlorofluorocarbons and hydrochlorofluorocarbons has been banned under the Montreal Protocol [60], and CO₂ and hydrofluorocarbons as well as their derivatives are coming under increasingly strict control from the Kyoto Protocol. Subsequently, the use of these compounds as solvents for the commercial synthesis of fluoropolymers is no longer possible. Even in a laboratory setting, the use of these compounds is being phased out, and it may not be possible to employ these compounds for solvents in any setting in the near future. Prior to the implementation of the Montreal Protocol, fluorinated solvents superseded water as the solvent of choice for free radical polymerisation of perfluorinated monomers, but were rarely used commercially due to cost.

Currently, water is the only environmentally benign solvent suitable for the synthesis of high-molecular-weight PTFE by free radical polymerisation.

Brubaker mentions that the polymerisation can be performed in either acidic, neutral or alkaline aqueous environments, but that alkaline conditions are preferred as acidic environments could leach metals from the reactor into the polymer, causing discolorations. This claim has been repeated by a number of other authors [17-19, 21, 22]. The Brubaker patent indicates the use of borax as the most desirable buffer, but other alkaline compounds such as sodium phosphate and NaOH may also be employed. Other literature indicates that acid environments are preferred for obtaining TFE high polymers [30], with the pH being preferably between 3.5 and 4.5. The pH of the solvent is seen to be immaterial to the actual polymerisation reaction, and pH only plays a

role with respect to the stability of the initiator, additives, reactor apparatus, and any comonomers.

It is vital that any solvent employed in the polymerisation of tetrafluoroethylene be rigorously deoxygenated (into the sub-ppm levels) as oxygen will inhibit the polymerisation reaction and may form an explosive mixture with tetrafluoroethylene. Some of the solvents thus far employed in the polymerisation of tetrafluoroethylene are summarised in Table 3.

2.5.2.2 Solvents for coordination polymerisation of tetrafluoroethylene

The coordination polymerisation of tetrafluoroethylene may be carried out in any non-aromatic hydrocarbon solvent, with iso-octane being preferred [34].

2.5.2.3 Solvents for electrochemical polymerisation of tetrafluoroethylene

Electrochemical polymerisation may be carried out in the liquid monomer, in anhydrous HF or in a mixture of fluorinated carboxylic acids, or in hexafluorodimethylcarbonate [35, 36].

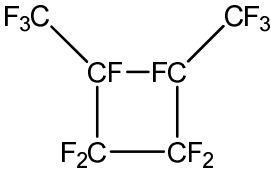
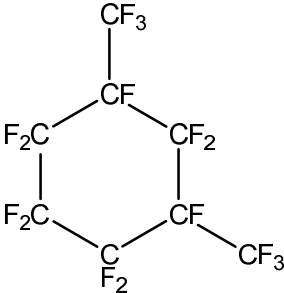
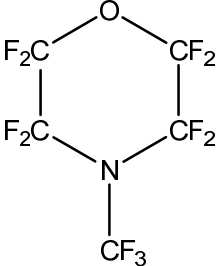
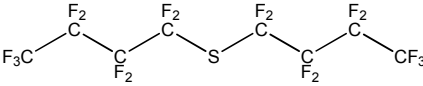
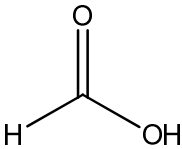
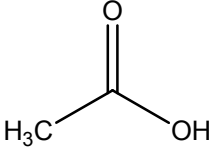
2.5.2.4 Solvent pre-treatment

As stated previously, the polymerisation process is sensitive to the presence of oxygen, so care must be taken to remove oxygen from the solvent as well as the monomer.

Typically in industry, large reservoirs of demineralised water are sparged with nitrogen (with or without stirring) to liberate the dissolved oxygen, ensuring the reservoir remains under a slight positive pressure to frustrate any oxygen back diffusion into the reservoir.

On a lab scale, the same method may be employed, but nitrogen, argon or even TFE itself may be used to sparge. Alternatively, the unsparged water may be charged into the reactor, and the entire reactor de-oxygenated *via* the freeze-thaw method.

Table 3: *Solvents employed in the free-radical polymerisation of tetrafluoroethylene.*

Solvent	Structure	CAS No.:	Reference
Water	H ₂ O	7732-18-5	[16]
HF, anhydrous	H-F	7664-39-3	[107]
CF ₂ ClH	CF ₂ ClH	75-45-6	[102]
Perfluoro-1,2-dimethylcyclobutane		28677-00-1	[113]
Perfluoro-1,3-dimethylcyclohexane		335-27-3	[107]
Perfluoro-N-methylmorpholine		382-28-5	[153]
Bis(perfluoro-n-butyl) sulfide			[104]
Formic acid		64-18-6	[154] ^a
Acetic acid		64-19-7	[154] ^a
Sulfuric acid (97 %)	H ₂ SO ₄	7664-93-9	[154] ^a
AsF ₃	AsF ₃	7784-35-2	[107]

^aSee the section on chain-transfer agents for more details.

2.5.3 Temperature and pressure

The temperature and pressure conditions inside the polymerisation kettle are of utmost importance, as they determine kinetics of reaction, and thus, polymer yield and molecular weights. Furthermore, operating temperature and pressure need to be taken into account when designing the reactor system in order to ensure the process operates within safety limits.

2.5.3.1 Pressure

In general, the concentration of TFE in the reaction medium is determined by the partial pressure of the gas and the reaction pressure has little direct effect on the properties of the final polymer other than those which may be influenced by concentration. The operating pressure is determined by the equipment employed, but, as discussed in Section 2.2.5, TFE may spontaneously decompose under pressure, resulting in a pressure spike in the reactor and possibly an explosion. The upper pressure limit is determined by temperature and the vessel size, but is generally set at 90 bar.

TFE will polymerise even at low pressures, but, in the case of gas-phase polymerisation (*i.e.* photoinitiation by UV and SF₅Cl [124]), the kinetics and, therefore, the molecular weight of the PTFE obtained, as well as the yield, is determined by the partial pressure of TFE. The higher the pressure, the greater the yield and molecular weight.

2.5.3.2 Temperature

In free-radical polymerisation the operating temperature is selected based primarily on the decomposition kinetics of the initiator, but other factors, such as solvent boiling point and kinetic considerations also influence the choice of temperature. Generally, the polymerisation temperatures do not exceed 150 °C. For example, Brubaker [16] reports that, for optimal results, free-radical polymerisation should be carried out at 20 bar TFE or higher and at temperatures around 80 °C to give yields in the range of 80 to 100 %.

The patent literature indicates that proton transfer is a strong function of temperature and by lowering the polymerisation temperature to between -40 °C and 0 °C, a TFE high polymer may be obtained even in the presence of significant amounts (≥ 10 %) of chain-transfer agents [154].

Polymerisation may be performed at ambient temperatures using photoinitiation methods such gamma or UV light, with the temperature of a UV-photoinitiated polymerisation reaction being determined by the temperature required to keep the initiator and other additives in the gas phase. For coordination polymerisation the recommended reaction temperature falls between 30 °C and

40 °C [34], and for electrochemical polymerisation the temperatures fall in the range of -80 °C to ambient.

The greater majority of polymerisation operations are isothermal in nature, with the reactors starting at some ambient temperature, being ramped up to the reaction temperature and then maintained at this temperature for the duration of the operation. The Kuhlmann company has disclosed a dispersion polymerisation process [94] that entails the continuous increase of the temperature during the operation in order to maintain the stability of the emulsion, which in turn permits a higher final solids loading to be achieved. The temperature ramp rate (defined here as $\Delta T/\Delta t$) should not be less than $1/6 \text{ }^\circ\text{C}\cdot\text{min}^{-1}$ and they place an upper limit of 120 °C on the reaction temperature. This scheme does not appear to be followed in any commercial setting.

2.5.4 Agitation

Importantly, the shear rate plays a role in determining the size of the PTFE particle agglomerates in dispersion polymerisation, so there is an optimum shear rate that must be maintained if a fine dispersion is to be produced. The literature indicates that a power number to discharge coefficient ratio of greater than 1.4, but preferably 3.4, should be used and that the power input of the stirrer should be in the region of 0.0004 to $0.002 \text{ kg}\cdot\text{m}\cdot\text{s}^{-1}\cdot\text{mL}^{-1}$, preferably around $0.001 \text{ kg}\cdot\text{m}\cdot\text{s}^{-1}\cdot\text{mL}^{-1}$ [155]. In supercritical CO_2 mediated polymerisation, the agitation plays a major role in determining the particle size distribution [101].

2.5.5 Polymerisation additives

Brubaker [16] mentions that filler materials, such as glass, carbon black, copper and bronze may be added to the polymerisation kettle to produce “filled” PTFE in-situ. More common additives include pH controlling agents, dispersants, anti-coagulants, and chain-transfer agents.

2.5.5.1 Buffering agents

As previously stated, pH controllers include borax [16, 111], NaOH, HCl, acetic acid, K_2CO_3 , NH_4CO_3 [129], or buffer mixtures. The role of the pH controller is primarily to ensure that the aqueous polymerisation medium does not adversely affect the initiator performance and that metals from the materials of construction are not leached into the reaction mixture, with typical pH values ranging from 7 to 11 [114]. In non-aqueous media, buffering agents are not required.

The choice of buffering agent must be carefully considered as it not only adds to the cost of the polymer, but may contaminate the polymer and cause problems in the end application, and using

buffering agents that may undergo proton transfer lead to premature termination and low-molecular-weights.

2.5.5.2 *Dispersants for emulsion polymerisation*

In aqueous polymerisation, production of fine PTFE powder requires the use of a dispersing agent (*i.e.* a surfactant). This process is commonly referred to as emulsion polymerisation. It should be noted here that when using fluorinated solvents or supercritical CO₂, a dispersing agent is not required.

Initially, alkaline buffers, which may act as detergents (such as borax), were employed. Longer chain hydrocarbon peroxides (such as diglutaric and disuccinic acid peroxide) [22] as well as long-chain saturated hydrocarbons (such as tetradecane, cetane, paraffin wax, and heavy mineral oil) [28] were also used to disperse the polymer. In the abovementioned, the peroxides acted as both initiator and dispersing agents.

The primary problem with using hydrocarbon dispersants (surfactants) is the probability of the formation of low-molecular-weight polymers due to hydrogen abstraction by the growing fluoromacroradical [33, 90]. Furthermore, the affinity of hydrocarbons for tetrafluoroethylene and its polymers is limited, so the dispersive effects of hydrocarbon agents are not good. However, Bankoff [28] states that hydrocarbons may be used as dispersive agents in aqueous polymerisation without significant chain transfer, provided the hydrocarbon is greater than 12 carbons in length. The rationale for this is the extremely low solubility of the hydrocarbon in water as well as the low solubility of TFE, initiator, or macroradical in the hydrocarbon, thus limiting the contact between the hydrocarbon and the macroradical. The implication here is that the active polymerisation occurs in the aqueous phase. Examples in the literature exist for the use of “paraffin” as a dispersant [156].

Instability of the dispersion is a further disadvantage of hydrocarbon-based dispersants. It is exceedingly difficult to obtain a dispersion of a perfluorinated polymer that may be stored for prolonged periods using such dispersants. Also, the dispersion particle size is, in general, undesirably large when using a hydrocarbon dispersant with perfluoropolymers.

Imperial Chemical Industries (ICI) reported that the difficulty of chain transfer between tetrafluoroethylene macroradicals and hydrocarbon surfactants (in particular, aliphatic sulfonic acids and derivatives, *i.e.* sodium lauryl sulfate) may be overcome if said dispersant is introduced to the reaction mixture after polymerisation has started, but before the mass of polymer produced exceeds 7 % of the total mass of the reaction mixture (polymer + everything else),

with the addition occurring as either a batch- or a staged addition [157]. However, it appears this method has not been taken up by other commercial manufacturers of PTFE as this method does not provide sufficient control over the particle size distribution. Punderson [90] reported a refinement of the ICI method, where a low initial dose of surfactant is used (as little as 0.015 mass %) followed by a continuous addition of surfactant until the reactor reached 35 mass % solids content. This method provides particle size distributions substantially similar to those obtained from fluorinated surfactants.

Berry [29] introduced the use of fluorinated species as dispersive agents, employing perfluorodimethylcyclohexane as dispersing agent. Chlorofluorocarbons and perfluorinated oils may also be used as dispersing agents. However, perfluorinated monocarboxylic acids, or their salts [93, 105, 110, 111, 136] have traditionally been the best and most widely used dispersant. Typical concentrations of dispersing agent range from 2 to 200 ppm based on the mass of water.

Prior to Berry, attempts were made by Benning to modify existing anionic surfactants for use with fluoropolymers, employing fluorinated aliphatic phosphate surfactants [33]. Similar work was carried out by ICI, with various perfluorosulfonic acids and their salts [158]. Other compounds employed as dispersive agents included keto acids and their derivatives (particularly the metal salts) [119], hexachlorobicyclo-5-heptene-2,3-dicarboxylic acid (chlorendic acid) and its salts [159], tertiary perfluoroalkoxide [91], and perfluoropolyether-based carboxylic acid salts [92]. The patent literature also claims that tertiary perfluoroalkoxide provide an increase in instantaneous polymerisation rates over the ordinary monocarboxylic acid salts. It is evidenced from the patent literature (*e.g.* [91, 94, 95, 160]) that the preferred method for emulsion polymerisation of PTFE consists of water as solvent, perfluorooctanoic acid as dispersant, and a water-insoluble aliphatic hydrocarbon as anti-coagulant (as opposed to using the hydrocarbon by itself as the dispersant). Some of the compounds used as dispersive agents in the aqueous emulsion polymerisation of tetrafluoroethylene are summarised in Table 4.

The fluorinated surfactants are not a “renewable” resource within the reactor and the concentration of free surfactant decreases with polymer yield (that is, reaction time). Depending on the starting concentration, an initial, rapid drop in concentration to below the critical micellar concentration (CMC) is seen to occur, followed by a nearly linear decrease of concentration with time. This behaviour is illustrated for the lithium salts of carboxylic acids in Figure 6. This behaviour is primarily due to the sequestering of the surfactant *via* incorporation into the developing polymer particles [90].

The CMC values for ammonium perfluorooctanoate ($C_7F_{15}COONH_4$) have been reported as 0.5 to 1.422 %, depending on the measurement technique and the temperature [100, 161-163]. Kissa [162] provides a comprehensive summary of the CMC values for number of fluorinated surfactants.

The long-chain perfluorocarboxylic are being phased out due to health- [164] and environmental concerns, with 3M having ceased production of PFCAs and its phosphonate and sulfonate analogues. W.L. Gore & Associates have stopped using PFCAs altogether. DuPont/Chemours has also stopped using PFCAs and, in 2017, they reached a settlement regarding a class action lawsuit resulting from the use of perfluorocarboxylic acids in the polymerisation process.

In recent years considerable effort has gone into developing safer and more environmentally benign surfactants [165].

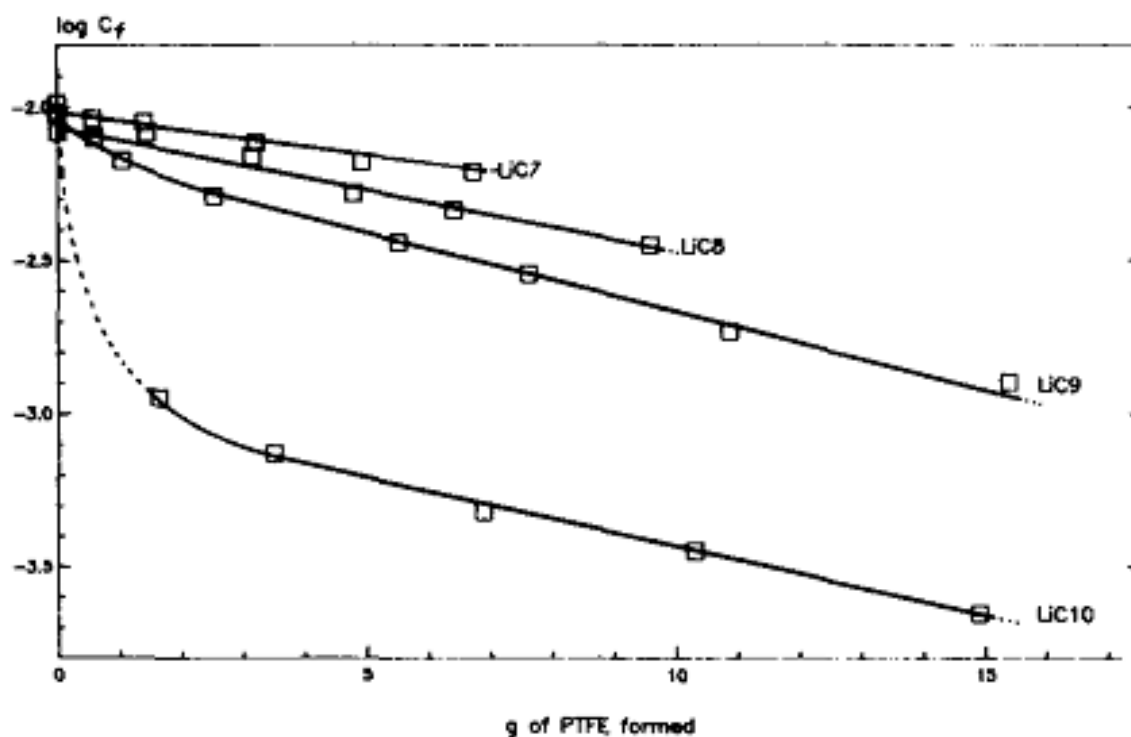


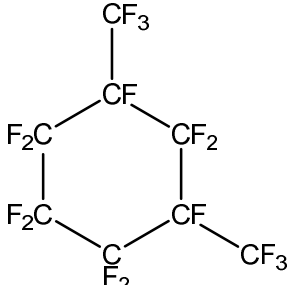
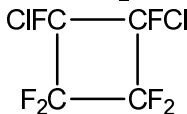
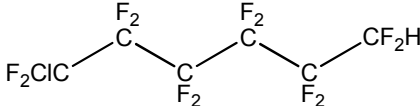
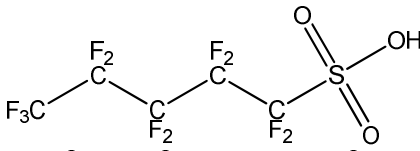
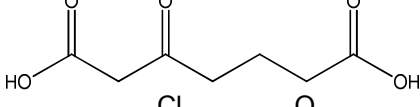
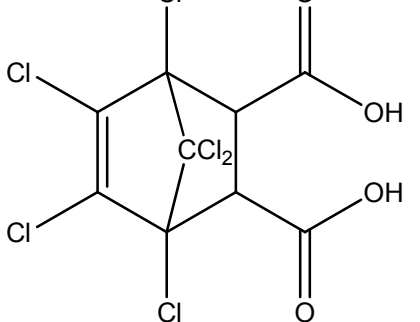
Figure 6: Free surfactant concentration (in $mol \cdot L^{-1}$) of the lithium salts of the homologous series of perfluorinated carboxylic acids from 7 to 10 carbons in length [136].

2.5.5.3 Stabilisers

While hydrocarbons are undesirable as surfactants, they have found use as stabilisers in the dispersion polymerisation of TFE. Long-chain aliphatic hydrocarbons are added to the dispersion to prevent the premature agglomeration of the dispersed particles. Mixtures of

hydrocarbon compounds under the generic name of “paraffin” have been employed, as have pure hydrocarbon compounds such as n-hexadecane [29, 50, 100, 156].

Table 4: *Dispersive agents used in the aqueous emulsion polymerisation of tetrafluoroethylene.*

Surfactant	Structure	CAS No:	Reference
Perfluorodimethylcyclohexane		355-02-2	[29]
1,2 - Dichlorohexafluorocyclobutane		356-18-3	[29]
1-Chloro-6-hydroperfluorohexane		307-22-2	[29]
1,2 - Dichlorotetrafluoroethane	$\text{ClF}_2\text{C}-\text{CF}_2\text{Cl}$	76-14-2	[29]
Perfluorokerosene			[29]
Perfluorocarboxylic acids and salts			[31, 50, 96, 103, 105, 111, 136, 156, 166]
Chlorofluorocarboxylic acids			[167]
Perfluoropolyether-based carboxylic acids			[92]
Perfluoro-n-pentane sulfonic acid			[158]
3-Keto pimelic acid			[119]
Chlorendic acid		115-28-6	[159]

2.5.5.4 Chain-transfer agents in tetrafluoroethylene polymerisation

Chain-transfer agents are generally undesirable in tetrafluoroethylene polymerisation as the electrophilic fluoromacroradicals will do its utmost to abstract any atom it can (hydrogen most particularly) to terminate the chain, which may result in a low-molecular-weight polymer *sans* the thermal- or mechanical properties of a TFE high polymer. Ameduri and Boutevin [150] provide some transfer constants for various fluoromonomers to methanol and to dialkyl phosphite, but the works cited do not determine transfer-constants for tetrafluoroethylene.

However, the patent literature [96] indicates that, if tetrafluoroethylene is permitted to polymerise to very high-molecular-weights ($\sim 10^7$ - 10^8 Da), a significant portion of the macroradicals may become entrapped in the polymer matrix and be immobilised such that they cannot terminate by mutual recombination. As discussed in Section 2.7.3.2 this results in lower polymer thermal stability, *etc.* To overcome this, addition of H₂, methane, ethane, *etc.* may be added to the polymerisation kettle in order to “cap” the growing macroradical before it reaches too high a molecular weight. The addition of a chain-transfer agent may be continuous, or may be done batchwise, with the available literature indicating batch addition to be preferable owing to more accurate concentration control.

CTAs are also employed to reduce the adhesion of PTFE to the walls of the reactor and the stirrer mechanism. Examples of such CTAs include citric acid. The CTAs used with tetrafluoroethylene and their typical quantities (based on TFE) are summarised in Table 5.

Table 5: *Chain-transfer agents employed in aqueous free-radical polymerisation of tetrafluoroethylene.*

Chain-transfer agent	CAS No:	Monomer relative quantities (mol %)	Reference
H ₂	1333-74-0	0.01 – 2.5	[96]
CH ₄	74-82-8	0.0008 – 0.4	[96]
CH ₂ F ₂	75-10-5	0.01 – 2.5	[96]
CHF ₃	75-46-7	0.01 – 10	[96]
CH ₃ -CHF ₂	75-37-6	0.01 – 0.5	[96]
C ₂ H ₆	74-84-0	0.01 – 0.05	[96]
CH ₃ OH	67-56-1	0.01	[166]
CH ₃ CH ₂ COOH	79-09-4	0.05	[166]
Citric acid	77-92-9	0.01	[93]

As would be expected, the addition of a CTA to a tetrafluoroethylene polymerisation strongly affects the rate of polymerisation, with an addition of just 0.15 mol % of H₂ resulting in a 20 % reaction rate decrease [96].

The patent literature indicates that the kinetics of chain transfer are strong functions of temperature, and chain transfer may be suppressed completely for aliphatic carboxylic acids such as formic acid, acetic acid, as well as for sulfuric acid, if the temperature is brought to between -40 °C and 0 °C [154].

It is important to mention that there is a vast body of literature [3, 150] on the telomerisation and oligomerisation of tetrafluoroethylene and other fluoromonomers, and these processes extensively employ chain-transfer agents. The chain-transfer agents mentioned here are those that are employed specifically in the processes, which result in polymers of tetrafluoroethylene and do not amount to the whole gamut of CTAs used with fluoromonomers.

2.5.6 Conclusions

Tetrafluoroethylene may be polymerised *via* free-radical, electrochemical, and coordination methods. The PTFE-synthesis process is highly sensitive to factors such as monomer purity and the presence of chain-transfer agents and one is restricted to a narrow range of solvents. For any kind of polymerisation, perfluorinated liquids are the solvent of choice, with water following after them as the most stable solvent. The future of PTFE production may reside in supercritical carbon dioxide as this solvent negates much of the problems associated with perfluorinated surfactants as well as the concerns over water wastage.

Perfluorooctanoic acid and its sodium salts are the premier dispersing agent for emulsion polymerisation if aqueous systems are used, although there are numerous other surfactants available. Research into more environmentally benign surfactants, such as partially fluorinated polyethers, is being conducted, but it remains to be seen if there will be any implementation of these surfactants in industry.

2.6 Telomerisation and reversible-deactivation radical polymerisation of TFE

2.6.1 Telomerisation of TFE

The preceding discussion focused on the conventional free radical polymerisation of TFE to produce high-molecular-weight PTFE. The telomerisation of TFE is not strictly related to the production of high-molecular-weight PTFE, but the radical chemistry for both processes are

nearly identical, and an understanding of telomerisation may aid in elucidating the reaction mechanisms of PTFE polymerisation.

Ameduri and Boutevin [150] have reviewed the telomerisation of fluorinated monomers. Telomerisation of TFE has been extensively studied in the context of the initiation pathways, *viz.*, redox-, photochemical-, thermal-, electron beam-, and free radical initiation; the last one being the most used by far.

Many CTAs, or telogens, have been employed and 1-iodoperfluoroalkanes (such as CF_3I [168, 169], $\text{C}_2\text{F}_5\text{I}$ and $\text{IC}_2\text{F}_4\text{I}$) were the primary telogens for TFE telomerisation. Other halogenated telogens include HBr , CH_2Cl_2 [170], CHCl_3 [171, 172], CCl_4 [173], and $\text{CF}_2\text{Cl-CFClI}$ [174]. In the last case, the reaction was initiated by ^{60}Co gamma rays, while when $\text{CF}_3\text{CCl}_2\text{I}$ [175] was employed, thermal activation was preferred. For radical telomerisations involving alcohols as CTAs, the chain-transfer constants for methanol, ethanol, and isopropanol were determined as 0.036, 0.085, and 0.17, respectively [176].

The telomerisation of TFE may be improved by the use of a suitable catalyst. Fielding [177] obtained TFE telomers containing more than ten TFE units using CCl_4 as CTA in the presence of tetraethylammonium fluoride catalyst. This evidenced a lower chain-transfer constants (*ca.* 10^{-2}) than either 1-iodoperfluoroalkanes or HBr . The catalytic redox telomerization of TFE with carbon tetrachloride was reported by Boutevin *et al.* using FeCl_3 /benzoin catalytic complex. They evaluated the K_1 constant of the reaction rate between the telogen and the metal at its lowest oxidation state, as well as the structure of low-molecular-weight telomers by mass spectrometry. Hanford [178] utilized $\text{C}_2\text{H}_5\text{SH}$ to telomerize TFE using a peroxide initiation pathway and claimed to have obtained $\text{H}-(\text{CF}_2\text{CF}_2)_n-\text{C}_2\text{H}_4\text{SH}$ telomers. However, the real structures were $\text{H}-(\text{CF}_2\text{CF}_2)_n-\text{SC}_2\text{H}_5$. When disulfides such as $\text{H}_3\text{CS-SCH}_3$ were used, the resulting telomers exhibited $\text{H}_3\text{C-S}-(\text{CF}_2-\text{CF}_2)_n-\text{S-CH}_3$ structure, showing that hydrogen atoms were not leaving groups.

The low chain-transfer constants mentioned above obviously led to rather high-molecular-weight telomers. However, by redox catalysis, lower-molecular-weight chains were produced. Telomerisation of C_2F_4 using CCl_4 catalysed by CuCl_2 , copper powder [179] and by $\text{Fe}(\text{CO})_5$ [180] was also reported. Telomers obtained by these processes always exhibited a $\text{Cl}_3\text{C}-(\text{C}_2\text{F}_4)_n-\text{Cl}$ structure with yields for the mono-, di-, tri-, and quaternary adducts being 11, 16.6, 15, and 6.5 %, respectively. The yield of telomers with n greater than 4 was reported as 41 %. Battais *et al.* [181] reported that redox telomerisation led to low molar mass-telomers since the transfer

occurred on the catalytic complex exclusively. An example of the product mixtures obtained from telomerisation of TFE is shown in Figure 7.

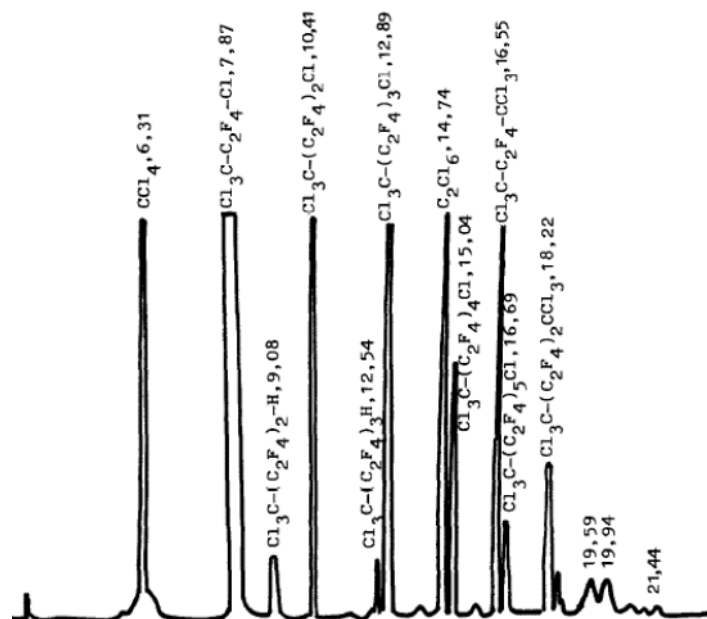


Figure 7: Gas chromatogram of the total product mixture from the redox telomerisation of TFE with CCl_4

2.6.2 Reversible-deactivation radical polymerisation of TFE

Controlled-radical (or, reversible-deactivation radical polymerisation) of TFE is underreported in the literature. The publically accessible literature contains reports on the iodine transfer polymerisation (ITP) of TFE only. The ITP polymerisation of TFE is closely related to the telomerisation of TFE where 1-iodoperfluoroalkanes are employed as CTAs. These two techniques differ mostly in the target molecular weight of the polymer. The work on ITP of TFE was pioneered by Tatemoto at Daikin [182-185], with later contributions from Ausimont [186-188]. Techniques such as RAFT/MADIX have been applied to the homo- and copolymerisation of VDF [189-191], CTFE [192], and HFP [193], but not to TFE.

2.7 Properties of PTFE

Polytetrafluoroethylene (CAS No: 9002-84-0) is a white, hydrophobic solid, whose properties depend strongly on its molecular weight. High-molecular-weight PTFE is chemically inert and insoluble in all known solvents, including hot fluorinated liquids. The polymer also exhibits an exceptionally low frictional coefficient and superb thermal stability. The salient properties of PTFE are summarised in Table 6.

These properties are divided into two broad categories, *viz.*, properties of the as-polymerised or “virgin” PTFE, and properties of the processed PTFE. The molecular weight, polymer morphology as well as the chemical, electrical, and thermal properties are dependent on the chemistry of the polymer and count among the properties of as-polymerised PTFE, whereas the mechanical and tribological properties can only be studied with processed PTFE and are, to a large extent, a function of the processing condition; therefore they count among the properties of processed PTFE.

The polymerisation process is highly sensitive to the purities of the monomer and the additives, the level of oxygen in the system as well as the fluctuations of pressure in the reactor. Hence, the polymerisation process is difficult to reproduce exactly and no two batches of product will have the exact same properties in terms of yield, molecular weight, and particle size. Nevertheless, the polymer properties will fall in a narrow range and some properties, such as thermal stability, will vary so minutely between batches as to be undetectable.

This section discusses the properties of PTFE in relation to the polymerisation conditions. Some of the properties covered here, such as the mechanical properties, have received detailed discussion in the literature [4, 6, 7] and will be touched on only briefly.

Table 6: *Physical and chemical properties of PTFE.*

Property	Value			Measurement standard	Reference
As-polymerised PTFE					
Melting point	335	(°C)		D3418	[194]
Glass transition	-103	(°C)		-	[195]
Decomposition point	590	(°C)		-	[62, 63, 196]
Phase transition	19	(°C)		-	[197]
Processed PTFE					
Theoretical density	at 23 °C	2.16	(g·cm ⁻³)	ASTM D4895	[198]
Tensile strength	at 23 °C	31	(MPa)	ASTM D4894	[198]
Compressive strength	at 23 °C	4.4	(MPa)	ASTM D695	[198]
Hardness		55	(Shore D)	ASTM D2240	[198]

2.7.1 Molecular weight

Aqueous free-radical polymerisation (both precipitation and emulsion) may yield molecular weights anywhere from 300 Da to 10^7 Da, depending on the initiator concentration, temperature and reaction pressure. Higher TFE partial pressures, low initiator concentrations and low temperatures generally result in higher molecular weights. Commercial PTFE is marketed with a reported number-average molecular weight range of 10^6 – 10^7 Da. Table 7 compares the number-average molecular weight reported in the literature for the various techniques.

Table 7: *Comparison of the molecular weights obtained for commercial PTFE resins by various techniques.*

Number-average molecular weight (Da)	Technique	PTFE grade	Reference
1.10×10^7	End-group analysis	Teflon® 6	[199]
1.27×10^7	Rheology	Teflon® 6	[199]
9.60×10^6	Standard Specific Gravity	Not stated	[194]
4.55×10^6	DSC (Suwa equation)	Not stated	[194]

Liquid medium photoinitiation usually produces a waxy, low-molecular-weight polymer; however, the Ausimont corporation has indicated that high polymers with thermal and mechanical properties similar to those produced by conventional free-radical methods can be obtained at low temperatures ($\sim 15^\circ\text{C}$) when combining photoinitiation of peroxide initiators with emulsion polymerisation techniques [87]. Provided the heat of reaction can be removed sufficiently quickly, gaseous photoinitiators (*i.e.* SF_5Cl) can be used to initiate polymerisation in the gas phase (that is, *sans* any solvent or liquid carrier in the polymerisation vessel), with the resulting polymer exhibiting a range of molecular weights ranging from telomeric liquids to waxes to high polymers with thermal and mechanical properties indistinguishable from polymers prepared by conventional techniques.

Claims have been made in the patent literature [166] that, when polymerising TFE in the presence of a dispersing agent, the number-average molecular weight of the polymer comprising the spherical particles varies with the radius of the particle, having a lower molecular weight in the core than on the surface of the shell. Furthermore, proper choice of chain-transfer agent added to the polymerisation mixture permits tailoring of the ratio of the shell and core molecular weights as well as affecting the particle size distribution [92] (see Section 2.6.2.1 for the

mechanism). This core/shell structure may be continuous, or may be discrete, depending on the monomer, initiator and chain-transfer agent dosing regimen [92]. Noda *et al.* claims a shell molecular weight ranging from 10 k to 800 kDa [92].

Little is known in the literature about the weight-average molecular weight (M_w) of PTFE. Wu [199] reports the M_w of commercial and specially synthesised PTFE determined using rheological methods, indicating that Teflon® 6 and 7 resins, both having a M_n of $\sim 10^7$ Da, exhibit a polydispersity of 3.58 and 2.76, respectively. Tuminello *et al.* [200] reports M_w values for specially synthesized PTFE, but does not give details of the synthesis method, so a comparison of molecular-weight distributions as a function of polymerisation conditions cannot be made.

Bernd *et al.* [88] indicates that the molecular-weight distribution of PTFE may be controlled to a certain extent by playing with the partial pressure of TFE during the polymerisation reaction and by decreasing the partial pressure during the run, the molecular-weight distribution may be broadened significantly. As stated in Section 2.3.3, there is a dearth of literature on the reaction kinetics and the effects of temperature and pressure on the molecular-weight distribution of PTFE. Figure 8 compares the differential-molecular-weight-distribution curves obtained from rheology for commercial PTFEs.

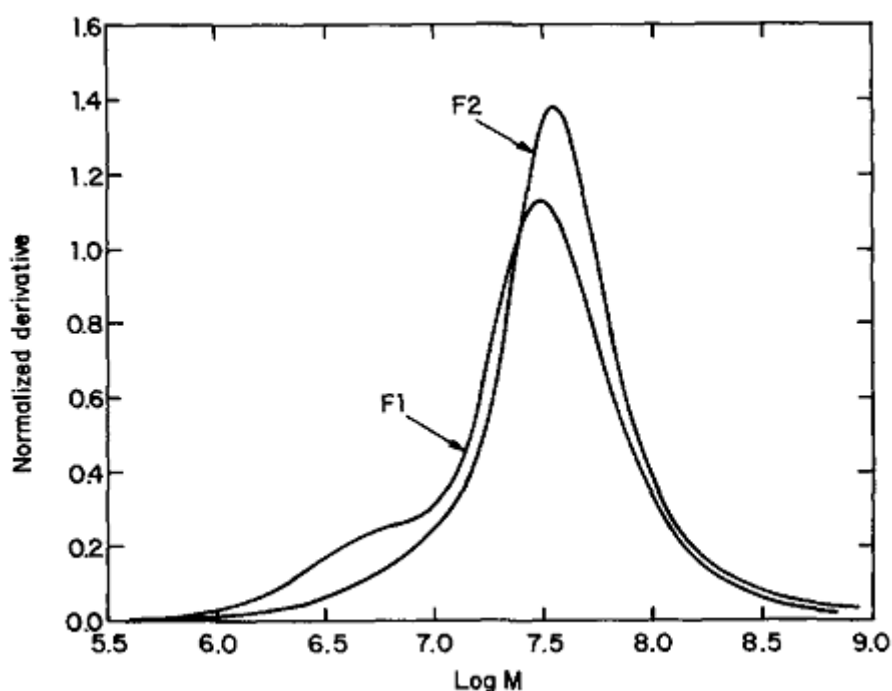


Figure 8: *Differential-molecular-weight-distribution curves for Teflon® 6 and 7A, obtained by viscoelastic spectroscopy [199].*

2.7.2 Morphology

The discussion here summarises the structure of PTFE as polymerised in terms of the chain arrangements, the microparticle structure, and the structure of bulk particles. The micro- and macrostructure of PTFE post-sintering and post-shaping, that is, the morphology of bulk articles, has already been discussed in several reviews [4, 7, 201], particularly relating to the effects thereof on the mechanical properties of PTFE.

2.7.2.1 Microstructure of PTFE

Polytetrafluoroethylene synthesised *via* free radical polymerisation is always obtained as a linear chain. There are no branches and no loop structures as backbiting cannot occur with a fully fluorinated polymer backbone [18, 148]. The PTFE chain adopts a helical structure (shown in Figure 9), and the polymer crystallizes in a hexagonal crystal arrangement. The helical structure itself is due to lone pair – lone pair repulsion between the fluorine atoms on adjacent CF_2 units. The helical conformations seem to not be a function of polymerisation conditions, but rather a function of the temperature and pressure under which the polymer is studied [4, 202].

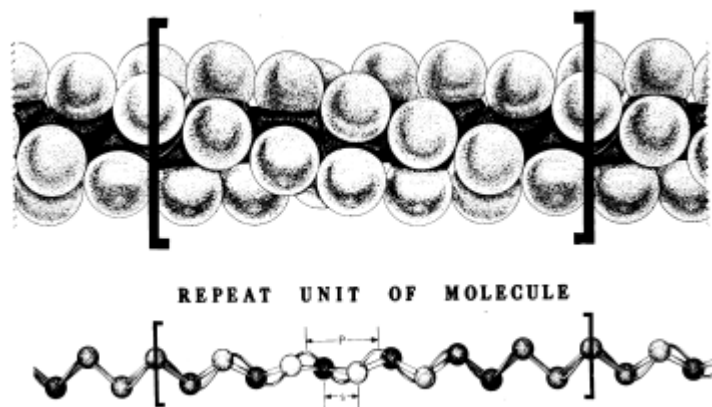


Figure 9: *Helical chain structure of PTFE in phase II crystal form [202].*

Polytetrafluoroethylene may exist in one of four crystal phases (the phase diagram is shown in Figure 10), with phase I being the most common, followed by phase IV and then phase II. In phase I, the PTFE helix adopts a 13/6 conformation (this means 13 CF_2 units taking part in 6 full rotations about the carbon axis to return the fluorine atoms to the starting coordinates), and it adopts a 15/7 conformation in phase IV. Phases I and IV are the commonly observed crystal phases for PTFE as they occur at atmospheric pressure and ambient temperatures. Phase II is encountered usually at sub-ambient temperatures, while phase III is encountered only at high pressures.

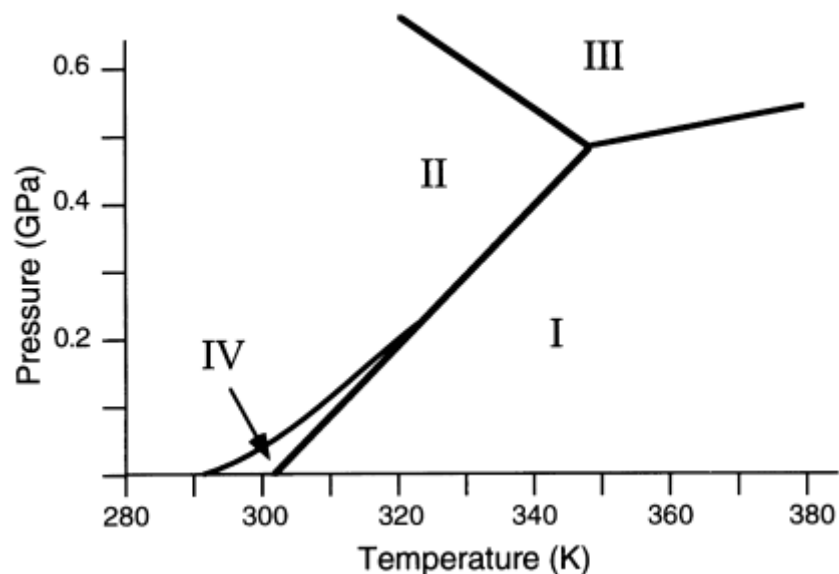


Figure 10: *Pressure-temperature phase diagram for the crystal structure of PTFE [202].*

Importantly, the helical structure imparts a stiff, rod-like character to the polymer chain, and, as a result, the polymer crystallites are expected to consist of an assemblage of large regions of long, straight, and ordered chain packing. Diffraction studies have shown that this is indeed the case, and that all PTFE crystallites adopt this arrangement [203]. This is the chief reason for the high crystallinity observed in both virgin and sintered PTFE. Polytetrafluoroethylene produced by other methods of initiation may differ in microstructure, with PTFE synthesised *via* gamma radiation initiation of TFE in the solid state exhibiting branching similar to what is observed in electron-beam irradiated PTFE [120, 204-207].

2.7.2.2 Mesostructure of PTFE

Polytetrafluoroethylene exhibits an unusual particle structure in that the polymer is composed of microparticles in the form of both spherical- (or cobblestone shaped) and rod-like structures, with the rod-like structures consisting of long ranged, highly ordered, directionally oriented crystallite packing (being virtual single crystals), and the spherical structures appear to consist of more randomly oriented, smaller crystallites [136, 208]. Ribbon-like structures [203, 209] and hexagonal platelets [210] have also been observed.

These features were first reported by Berry [156], and they are present in both suspension and dispersion polymerisation products. Berry also indicated that the ratio of rod-like- to spherical particles can be tailored by adjusting the concentration of dispersant and initiator, with higher concentrations of surfactant delivering a higher percentage of rod-like particles. Furthermore, Punderson [90] indicated that the charging regime for the surfactant strongly affects the ratio of

rod-like- to spherical particles, with a polymerisation carried out using only a total initial charge of surfactant producing more rod-like particles than spherical particles, whereas the continual dosing of surfactant produces a higher proportion of spherical particles.

Kim *et al.* [100] shed some light on the exact effect the surfactant has on the microparticle morphology, indicating that spherical particles predominate when the surfactant is present in concentrations below the CMC and that the morphology gradually shifts to predominantly rod-like particles as the surfactant concentration approaches the CMC. Rod-like particles form the vast majority of the polymer at surfactant concentrations above the CMC.

Micrographs detailing the particle- and chain structure for the rod-like particles are shown in Figure 11, for the spherical particles in Figure 12, and for the ribbon structures in Figure 13. Examples of the hexagonal platelets are given in Figure 16. Polytetrafluoroethylene formed from the monomer in the solid state (by gamma irradiation [120]) exhibits an irregular, flaky morphology.

The rod-like structures exhibit an approximately triangular cross-section [211] made up of closely packed elementary fibrils with an approximate diameter of 6 nm [212]. Using the chain diameter of 0.49 nm obtained by Chanzy *et al.* [208], the fibrils are seen to be made up of approximately 12, closely packed, PTFE chains. The preceding arrangements are shown in Figure 14. Luhmann *et al.* [136] reports that the length-to-width ratio of the rods can vary from unity to well over 100:1, with the ratio generally increasing with increasing surfactant concentration.

The ribbon like structures range in length and width, but appear to be 6 nm in thickness, exhibiting an average length of 500 nm and an average width of 250 nm [203]. The thickness seems to be invariant of the source of the polymer (*i.e.* the manufacturer). The implication is that, if the rod structures are considered as 1D structures or as lines, the ribbon structures are 2D extensions, in essence a stacking of rods. The work by Rahl *et al.*, Luhmann *et al.*[136] and the electron micrographs of Chanzy *et al.* (Figure 12) indicate that the spherical particles are nothing more than folded ribbon structures rolled up in a ball. This is illustrated in Figure 15, as first theorised by Rahl *et al.* [203].

The hexagonal platelets are observed only in PTFE with very low-molecular-weight or early on in emulsion polymerisation, but virtually never in suspension polymerisation, and they are completely different from the other structures observed in PTFE as the polymer chains are arranged perpendicular to the basal plane of the platelet. In essence, the hexagons are merely oversized rod structures that have been permitted to expand radially by addition of more chains as opposed to the lengthwise expansion *via* growth of the chain [136].

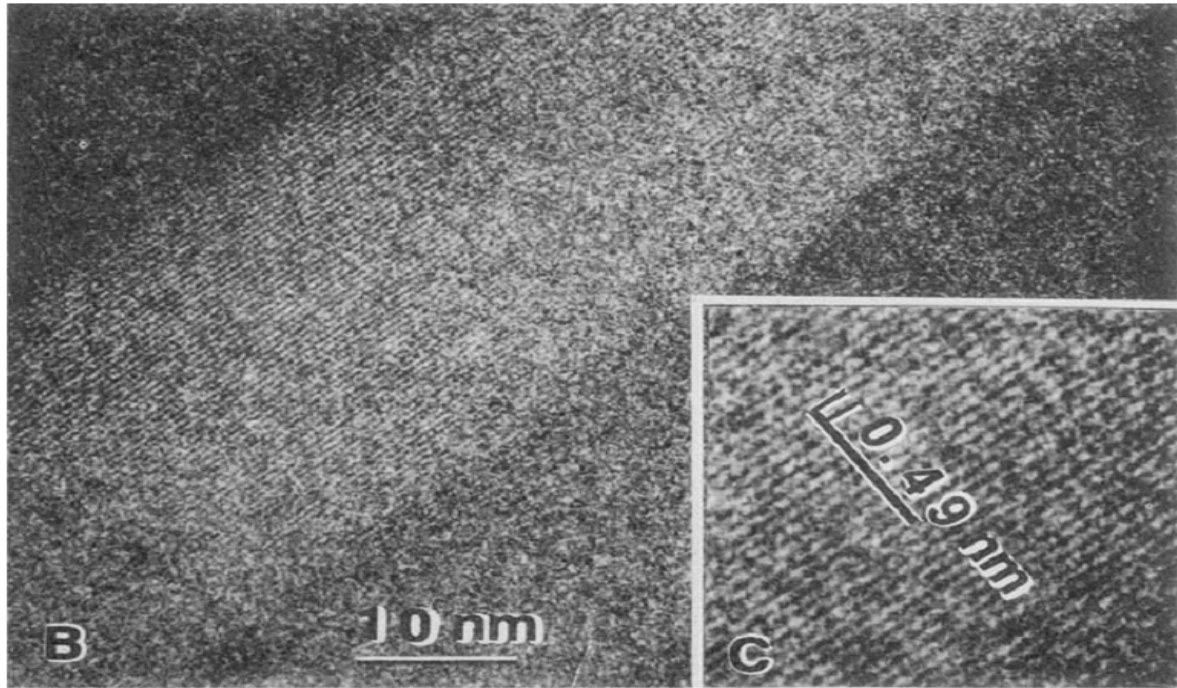


Figure 11: *Low dose, high resolution, negative contrast electron micrograph of rod-like PTFE particles showing the linear nature of the PTFE chains and their ordered long distance packing [208] (reprinted with permission from John Wiley and Sons).*

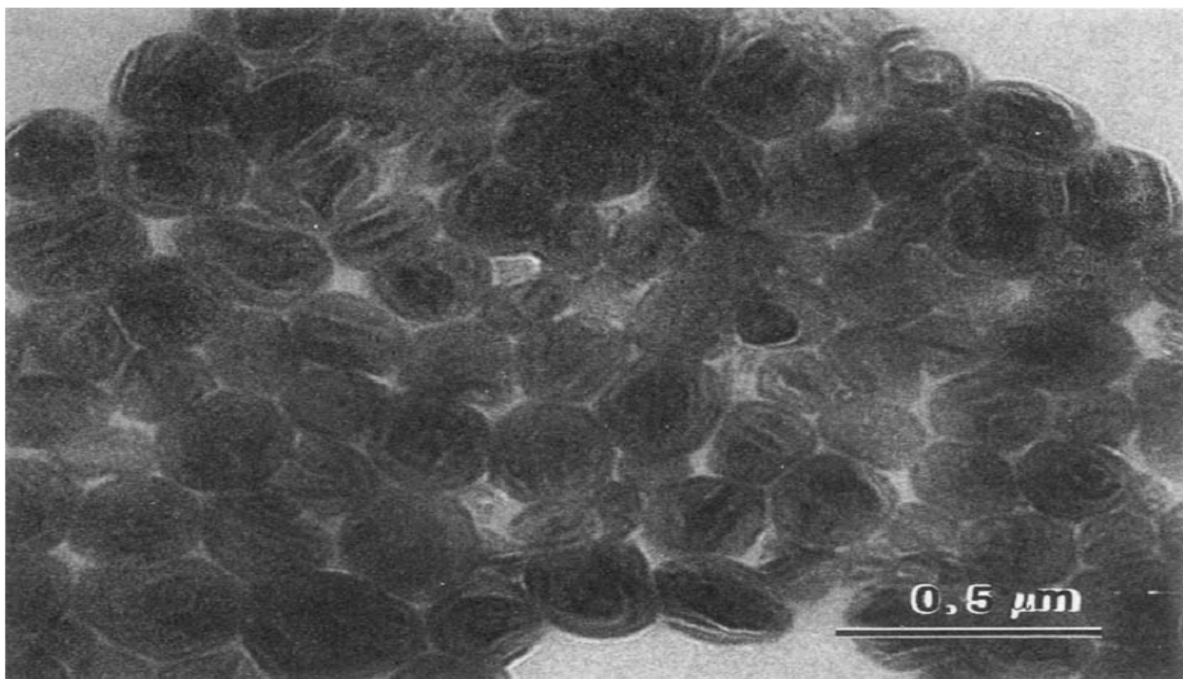


Figure 12: *Transmission electron micrograph of spherical PTFE particles that has been beam etched at 200 keV with a cumulative dose of 40 electrons.Å² [208] (reprinted with permission from John Wiley and Sons).*

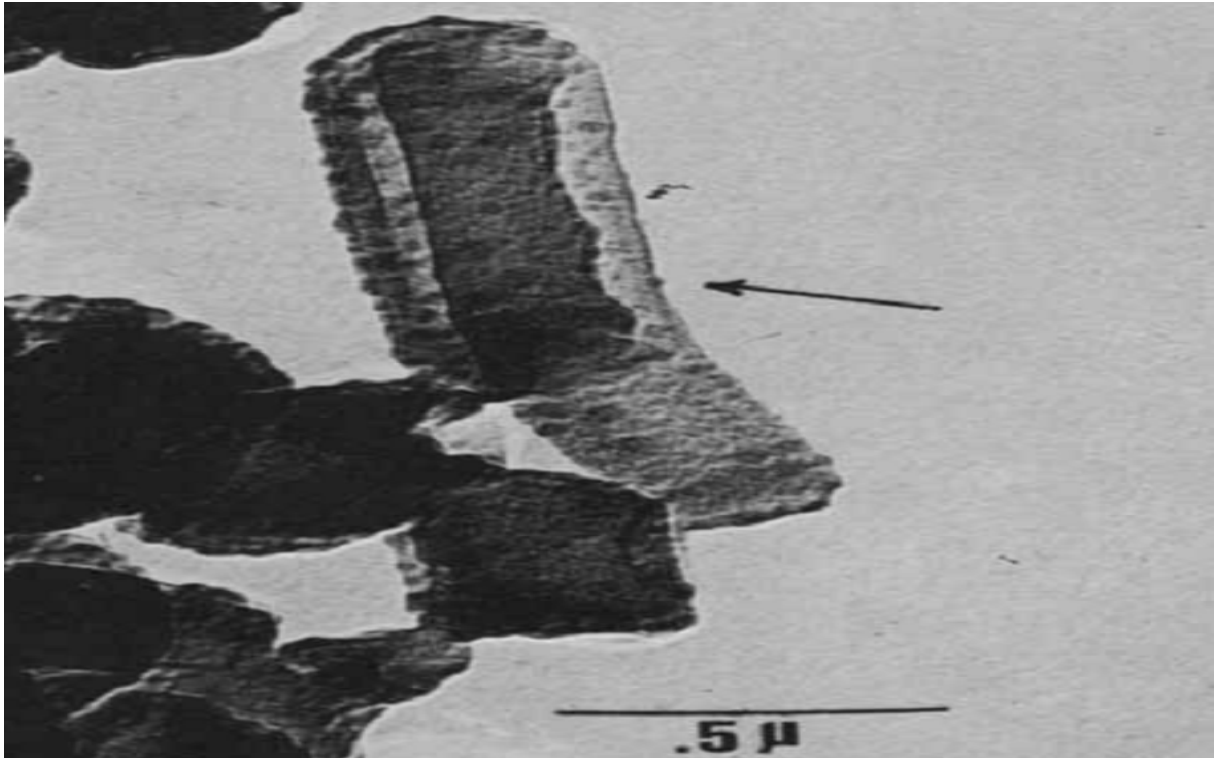


Figure 13: *Transmission electron micrograph of a PTFE ribbon taken from a batch of emulsion polymerised PTFE [203] (reprinted with permission from John Wiley and Sons).*

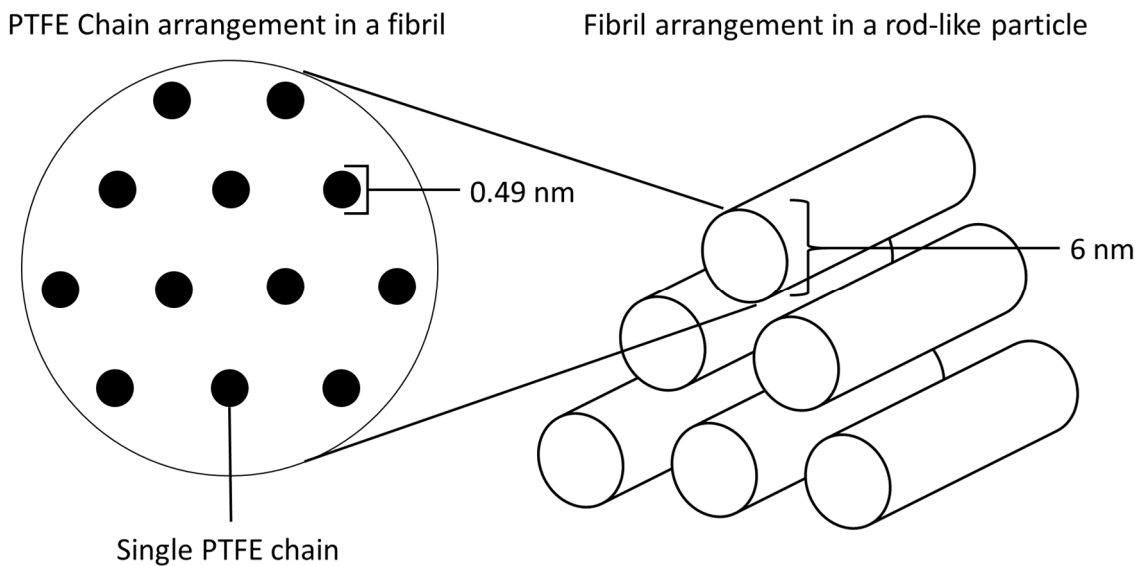


Figure 14: *Chain arrangements of PTFE in an elementary fibril and fibril arrangement in a rod-like particle for PTFE in phase II crystal form.*

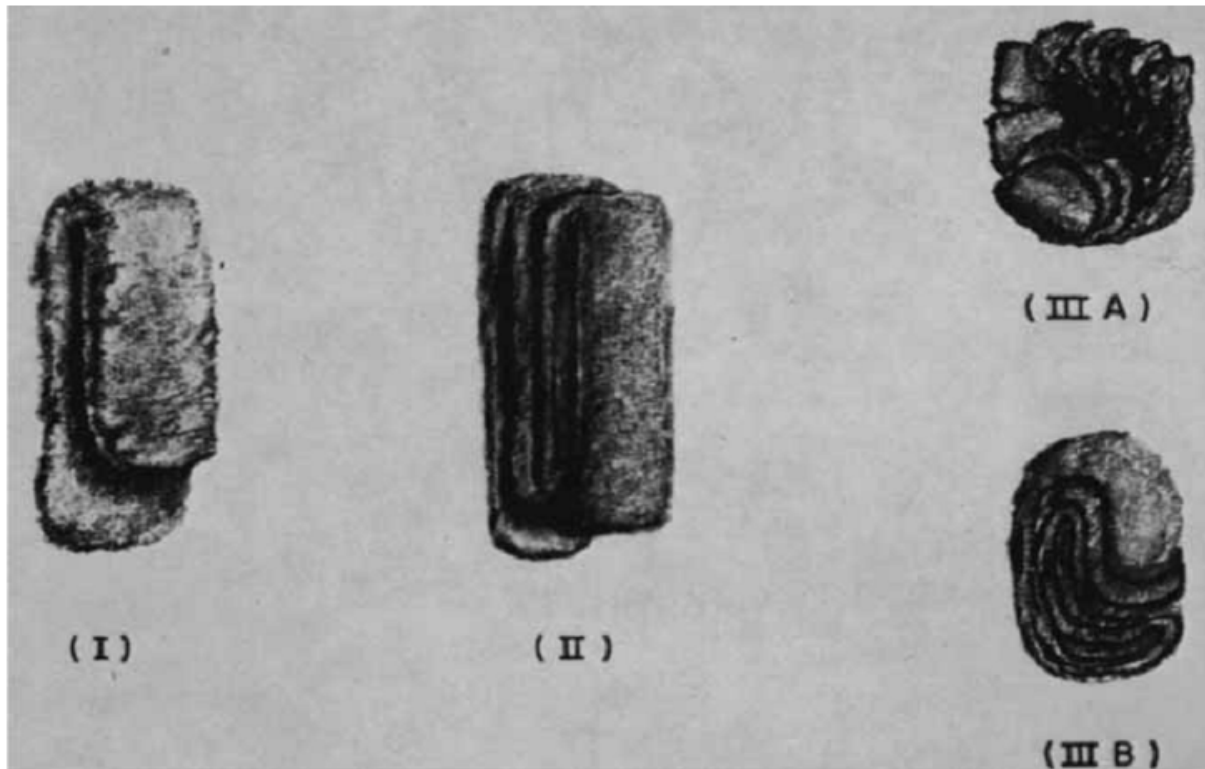


Figure 15: *Spherical PTFE particle formation by roll-up of a PTFE ribbon structure [203] (reprinted with permission from John Wiley and Sons).*

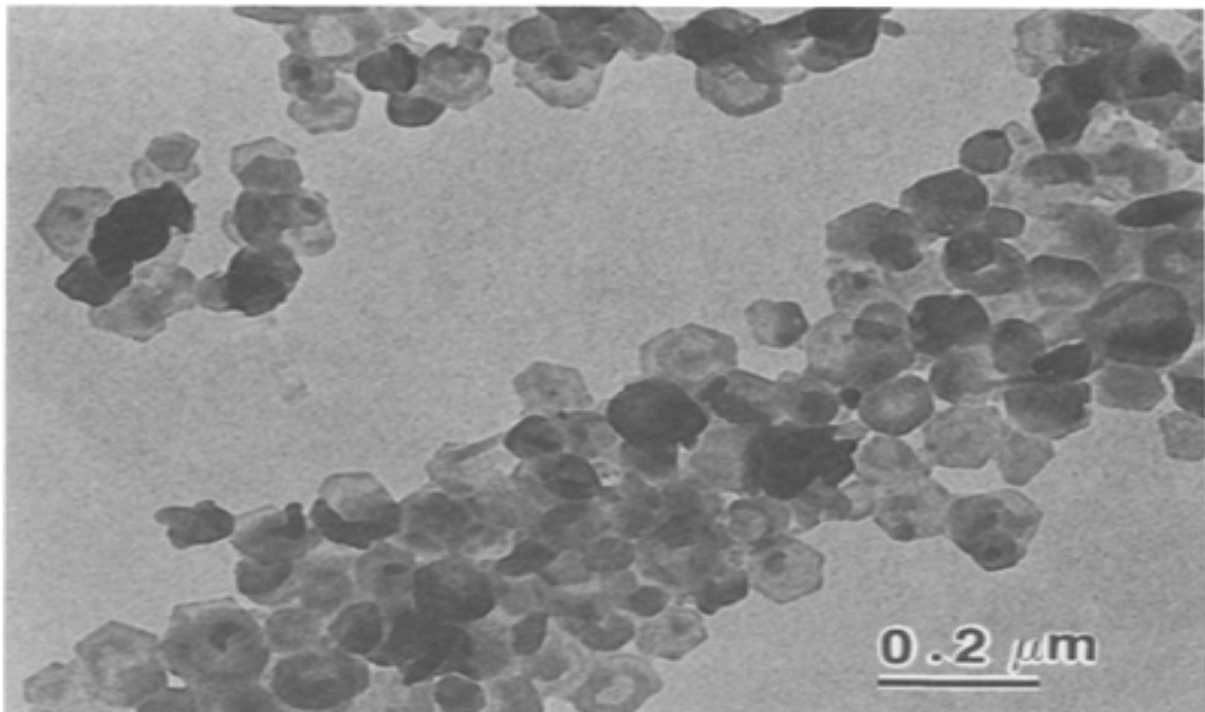


Figure 16: *Hexagonal platelets typically observed dispersion polymerised oligomeric PTFE [210].*

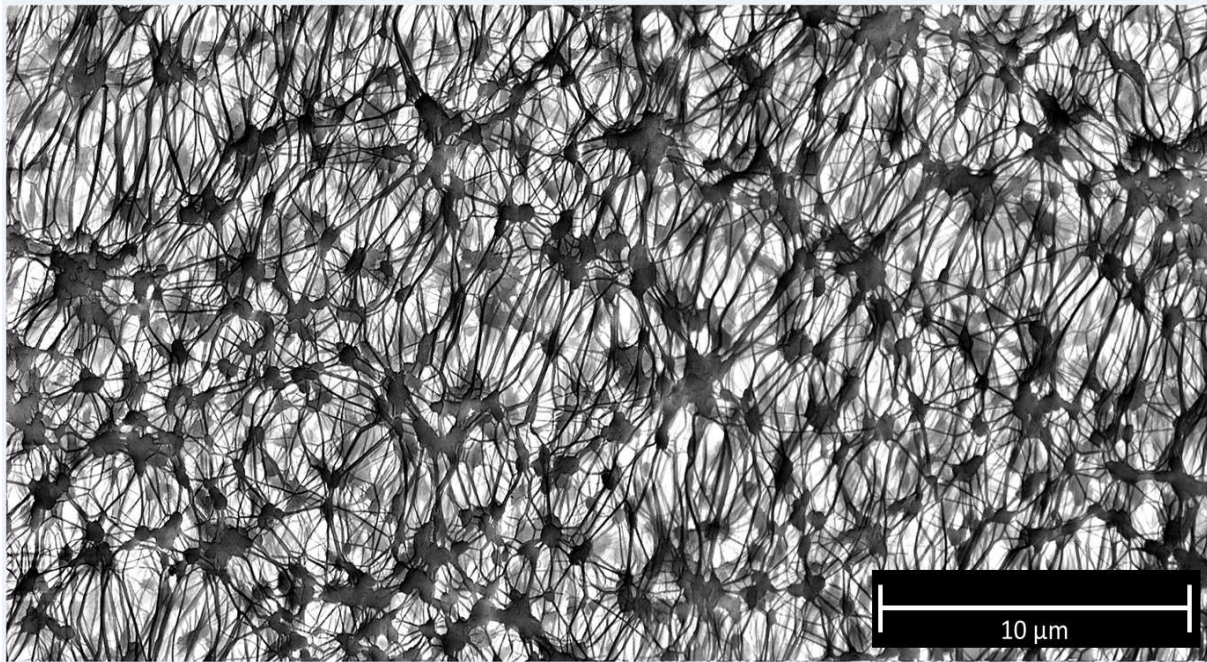


Figure 17: *Mesostructure of expanded PTFE showing the elementary fibrils (courtesy of W.L. Gore & Associates).*

When PTFE is subjected to a sudden tension while at temperatures near its melting point, PTFE elongates rather than breaks. This elongation results in a microporous PTFE commonly known as expanded PTFE (or ePTFE). The mesostructural morphology of ePTFE is shown in Figure 17. Essentially, the expanded polymer mesostructure is composed of partitioned elementary fibrils [7].

2.7.2.3 Macrostructure of PTFE

In aqueous, free-radical suspension polymerisation, the polymer is usually isolated from the reactor as clumps of coarse, compacted, granular material of irregular shape or as stringy particles, with the degree of clumping and the size of granules depending on the vigorousness of the agitation in the reactor [100], as well as the molecular weight of the polymer and the level of solids reached in the reactor, but not on the temperature or the pressure [88, 111, 155]. If a dispersing agent is employed, the polymer is isolated as a fine powder when coagulated under low-shear conditions. Uncoagulated dispersions of PTFE in water are also commercially available.

The mesoscale structures (rods, spheres, ribbons) tend to both grow and consolidate during polymerisation, giving rise to the large particle structures observed for the bulk polymer, similar in shape to their constituents, but ranging into the micrometer scales for the rod-like structures.

In ordinary suspension polymerisation, the spherical particle size can vary drastically with agglomerate d_{50} particle sizes in excess of 1.5 mm [88], but in the case of PTFE high polymer ($M_n \sim 10^6$ Da) prepared with a dispersing agent, spherical particle size ranges from 0.05 to 0.5 μm , and a d_{50} ranging from 0.12 to 0.35 μm has been reported [166]. Still other literature reports an average d_{50} of 0.1 μm [92, 157]. If the dispersions are coagulated and dried, the agglomerates exhibit a particle size between 100 and 1000 μm [92]. The use of the continuous TFE partial pressure drop method in ordinary suspension polymerisation results in a decrease of agglomerate d_{50} particle sizes to the sub-millimetre range [88].

When the polymerisation process is carried out using liquid-phase TFE, the bulk morphology and microstructure differ substantially from the norm, with the polymer isolated from the reaction vessel as a foam or as a clear to slightly opaque, stable dispersion that does not coagulate under shear stress [95]. This material, when dried, becomes a sponge-like PTFE consisting of layers of polymer sheets. This material exhibits a continuous, randomly oriented three-dimensional fibril microstructure with the fibrils having a sub-micron diameter. In some instances, the microstructure consists of platelets of highly crystalline PTFE.

The flaky microparticles isolated from solid-state polymerisation usually range from 2 to 5 μm and form irregular clumps with no definitive size [120].

If water is not the reaction medium, the morphology may vary considerably, depending on the molecular weight obtained and type of termination reaction, with the polymer isolated as granular powder, finely dispersed powder, or gummy goo.

In the case of supercritical CO_2 , the polymer is isolated as a fine, free-flowing powder with particle sizes dependent on the agitation within the reactor. Xu *et al.* [101] indicated the particle size distribution of PTFE from an unstirred polymerisation ranges from 400 μm to well over 2 mm, with a d_{50} of 240 μm , and a stirred particle size distribution ranging from 20 to 800 μm , with a d_{50} of 135 μm .

Besides the aforementioned bulk morphologies, PTFE may also be deposited onto a substrate *via* admicellar polymerisation [103]. This produces a thin films of PTFE coating on the surface of whatever substrate was employed with examples from the literature including alumina chips and alumina powders[103].

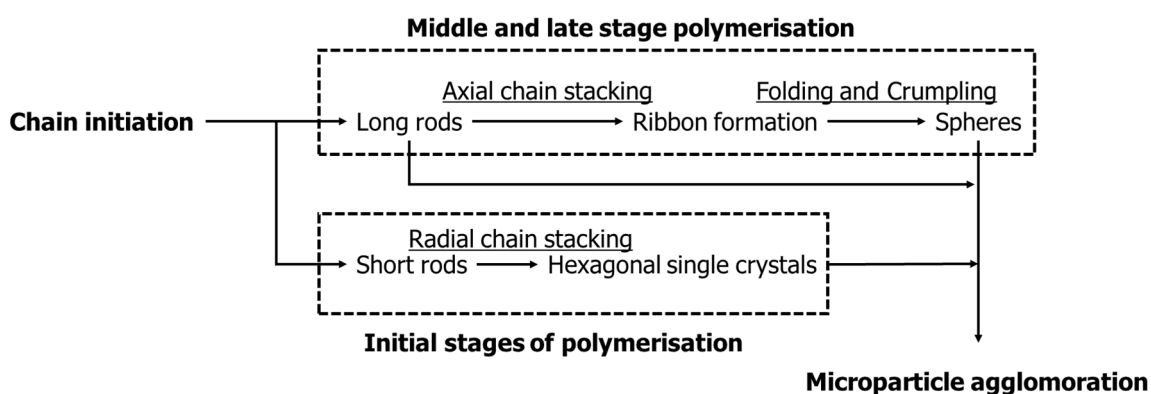
2.7.2.4 Mechanisms of particle growth

Suspension polymerisation and emulsion polymerisation are differentiated in terms of particle growth by the mechanism of particle nucleation: In suspension polymerisation, particle

nucleation occurs homogeneously, throughout the liquid phase, with short-chain, elementary fibril crystallites containing active end-groups crashing out of “solution” to form microscopic, local fluorine-rich phases within the solvent [148]. Polymerisation continues in this fluorine-rich region to form the initial rod structures, some of which aggregate to form ribbons and finally spherical particles.

The available literature [50, 90, 100, 136, 155, 166, 213] indicates that, during emulsion polymerisation, the initial stage of polymerisation is dominated by nucleation in micelles according to the same mechanism found in suspension polymerisation, followed by the formation of small, water-wetted polymer particles composed of a mixture of microparticle geometries and sizes, which depend strongly on surfactant chemistry and concentration. The processes of chain growth and agglomeration into particles is summarised in Scheme 6.

During the course of the reaction, the particles grow until they cannot be wetted any longer and become a distinct, hydrophobic bulk phase in the reactor. At this point, fluoromacroradicals are deposited from the aqueous medium onto the solid particles and come into direct contact with the gaseous tetrafluoroethylene, which results in a great increase in reaction rate with the concomitant generation of high-molecular-weight polymers.



Scheme 6: *The formation of the various microparticle types found within PTFE produced by dispersion polymerisation.*

If the agitation in the reactor is such that these growing particles collide and consolidate into larger particles, then the gas-contacted polymerisation occurs both on the surface and in the interstices of the consolidate particles. The increased rate of reaction on the particles surface draws TFE away from the liquid medium, resulting in a decrease in the number of new “nucleation particles” with the concomitant increase in particle size, but narrowing in particle size distribution.

Hence, the particle size and the particle size distribution can be controlled by altering the agitation regime to ensure low-shear mixing, which promotes the formation of new nuclei over the consolidation of existing particles, or by adding chain-transfer agents to cap any fluoromacro radicals at a certain molecular weight (and thus chain length) to prevent particle growth due to gas-contacted polymerisation. However, the use of a CTA leads to lower molecular weights and is not ordinarily preferred. Changing the monomer concentration in the liquid phase or the concentration of initiator will not promote the formation of new nuclei as the number of particles and the particle size is seen to be nearly independent of initiator [100].

It is possible to seed the polymerisation medium with small particles (specific surface area greater than $9 \text{ m}^2\cdot\text{g}^{-1}$ is preferred), but this contaminates the polymer with residues, so altering the shear rate to ensure *in situ* PTFE nuclei production is the preferred method by which the particle size is controlled. Also, the higher the shear rate, the stringier the particle agglomerates tend to be.

The aforementioned nucleation stage cannot last forever as the dispersing agent is slowly incorporated into the growing polymer particles and optimisation of the shear rates will only prevent the premature termination of the nucleation phase. Under optimal shear conditions, polymerisation carried out with a batch loading of dispersing agent will transition smoothly from a nucleation dominated regime to a particle growth dominated regime when the polymer solids content of the reactor has reacted 4 to 10 mass % [90], depending on the initial concentration of the dispersing agent.

2.7.3 Chemical and thermal properties

2.7.3.1 *Chemical stability*

The chemical stability of high-molecular-weight PTFE is ostensibly due to the strength of the C-F bond ($\sim 441 \text{ kJ/mol}$) [214]. Polytetrafluoroethylene is attacked by neither acids nor bases. In particular, PTFE is inert in boiling sulfuric, nitric, hydrofluoric, and hydrochloric acid, and in boiling solutions of aqueous bases [4, 44]. Polytetrafluoroethylene does not dissolve in any solvent and is not swollen by any solvent.

Only nascent alkali- and alkali earth metals, as well as a small selection of other metals and metal oxides are known to attack PTFE below its thermal decomposition temperature, generating the metal fluoride and carbon. Aluminium and magnesium mixtures with PTFE are the most salient examples of reactive mixtures [215]. Steam may also attack very finely divided PTFE, generating HF and CO_2 .

Oxygen attacks PTFE by forming CF_2O from the radical degradation products of PTFE thermal decomposition, and not by any intrinsic mechanism of attack. This CF_2O then undergoes further reaction to CO_2 , CO , and CF_4 , or to HF if there is moisture present.

2.7.3.2 Thermal stability

Polytetrafluoroethylene also exhibits excellent thermal stability, being inert to over $400\text{ }^\circ\text{C}$ even under pure oxygen. Pure PTFE will exhibit nearly the same degradation temperature under air and nitrogen, while modified and filled PTFE will generally exhibit a lower oxidative stability due to catalytic effects. The mechanism of tetrafluoroethylene polymer breakdown has been discussed in detail [12]. In summary:

A tetrafluoroethylene macroradical may unzip, that is, depolymerise, giving back the monomer species. Ordinarily, the forward polymerisation reaction dominates at low temperatures and in an excess of TFE. As the temperature increases, or the partial pressure of TFE decreases, the depolymerisation reaction starts to dominate. The fully terminated PTFE polymer chain may decompose by undergoing chain scission at temperatures in excess of $590\text{ }^\circ\text{C}$, followed by unzipping of the new radically terminated chain segment. This chain scission is intrinsic to the polymer structure and cannot be improved upon by simple tweaking of the polymerisation conditions. Alternatively, the fully terminated chain may unzip from the end-group and the more prone the end-group toward elimination, the less thermally stable the polymer becomes. The mechanism of breakdown is presented schematically in Scheme 3.

In the particular case of PTFE initiated by persulfate, the sulfate group is hydrolysed to OH in the aqueous polymerisation medium [27, 216]. The unstable 1,1-difluorocarbon end-group reacts to form carboxyl groups, so ultimately, PTFE produced from persulfate initiators ends up terminated by fluorocarboxyl end-groups. These end-groups may eliminate CO_2 and HF , even at moderate temperatures, to form unsaturated end-group structures, which being much less stable than the PTFE backbone, are eliminated first at elevated temperatures, followed by the unzipping of the chain from the end. Furthermore, the presence of unsaturated chain ends produces a discoloration of the polymer. Initiation using sodium bisulfite does not produce hydrolysable end-groups, with the chain being terminated by a more stable bisulfite end-group and, concomitantly, the chain is more thermally stable [27].

One caveat should be kept in mind: While the intrinsic thermal stability of PTFE is determined by the end-group or the CF_2 backbone, any real TFE homopolymer exhibits a pseudo-thermal stability. Low-molecular-weight PTFE or PTFE with a large polydispersity tends to evaporate

off the low-molecular-weight chains from 300 °C to the bulk breakdown temperature. In these cases, thermogravimetric experiments may show total polymer mass loss before the bulk breakdown temperature, even though no chain breakage has occurred.

In aqueous or fluorinated solvents, TFE polymerisation is terminated by recombination; however, if a TFE high polymer is produced, it has been noticed that the polymer may undergo thermal breakdown quicker than a lower-molecular-weight PTFE. This has been attributed to the existence of unterminated macroradicals in the bulk polymer [96]. Essentially, the macroradicals become so large that the chain ends become immobile and polymerisation is conducted by diffusion of monomer into the bulk polymer; but when the polymerisation is completed, these chain ends are not at liberty to terminate by recombination, remaining as macroradicals until contacted with air, producing unstable peroxide end-groups. This difficulty is overcome by adding minute quantities of specific chain-transfer agents to the polymerisation that permit the radical to be capped by a hydrogen, and so ensuring the stability of the polymer chain towards unzipping from the unterminated macroradical chain end [96].

2.7.3.3 *End-groups in PTFE*

It is generally accepted that end-groups have no significant effect on the macroscopic properties of most polymers. This is because of their negligible weight when compared to the whole mass of polymer and because energy values for the bonds in end-groups and those in the constitutive units are practically equal [217]. However, this is not true for perfluoropolymers where hydrogen-containing end-groups (produced by, *e.g.* persulfate initiators) do have definite influences on the performance and stability, ascribed to the difference in bond strength of C-H and C-F (410 and 460 kJ·mol⁻¹).

With hydrogen- and fluorine-containing polymers, such as PVDF, it has been shown that thermal stability and fire resistance are influenced by the end-groups generated in the presence of different initiators. In this case the relative strength of C-H to C-F bonds cannot be the determining factor. This unexpected behaviour was attributed to different degradation mechanisms induced by the nature of the end-groups [218]. In addition to the thermal stability, other properties such as fluidity and electrical conductivity have been demonstrated to be significantly influenced by end-groups.

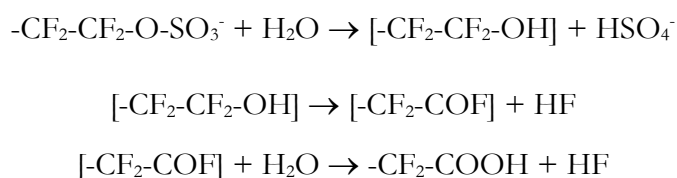
Knowledge of the type and number of chain end units can reveal information about the mechanisms and relative rates of chain transfer and termination processes [219]. End-groups can

also determine the crystallisation kinetics from the melt of thermoplastic fluoropolymers, and hence the processing and end-use properties.

There is a dearth of literature on the subject of end-groups in PTFE, or more specifically, the end-groups produced by different initiators. Madorskaya and co-workers reported the end-groups and subsequent effects on properties of the polymer for PVDF [218], but a similar, rigorous treatment of the end-groups in PTFE has not been published. Pianca *et al.* [217] gives an overview of some of the end-groups present in fluoropolymers as well as their mechanisms of elimination, with the most studied initiator type being the ammonium and metal persulfates [216] and bisulfites [27]. The end-groups produced by these initiators include: (C=O)OH, (C=O)NH₂, C≡N, CF₂H, (C=O)F, CF=CF₂, S(=O)₂OH and (C=O)O⁻ X⁺, where X is a metal (such as Na, K, Li) or an ammonium group [217]. Of these, the amide, carboxylic acid, carboxylates, and sulfonates are the primary end-groups. Xu *et al.* treat the end-groups generated by perfluorinated initiators [101, 115].

Little has been said in the literature regarding the mechanisms by which the end-groups form from the initiator. Sometimes the mechanisms are similar to those observed in non-fluorinated polymers, but for the case of PTFE, the end-groups differ significantly from hydrocarbon polymers.

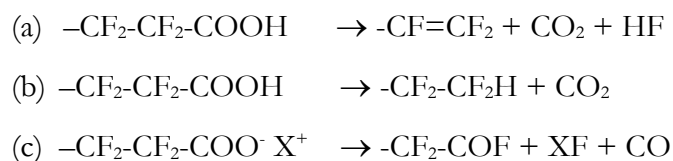
The reported mechanism by which a persulfate forms a carboxylic acid end-group is shown in Scheme 7.



Scheme 7: *Mechanism of carboxylic acid end-group formation by persulfate initiators.*

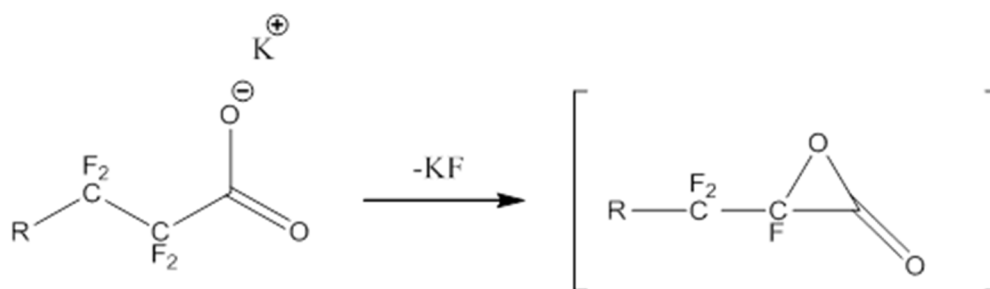
The primary end-groups may decompose *in situ* during polymerisation or under post-polymerisation thermal treatment, leading to mixtures of end-group functionalities in the final polymer. For a carboxylic acid and carboxylic acid salt terminated PTFE chain, the reported elimination reactions are summarised in Scheme 8. Path (a) is observed when the sample is treated at 380 °C and delivers perfluorovinyl end-groups as well as carbon dioxide and hydrogen fluoride. Path (b) occurs when the polymer is treated with water at 210 to 250 °C. This mechanism gives rise to difluoromethyl groups and carbon dioxide. Path (c) is observed during industrial extrusion of perfluoropolymers manufactured by aqueous emulsion polymerisation

with potassium persulfate as initiator and causes acyl fluoride groups, as well as hydrogen fluoride and carbon monoxide to be formed.



Scheme 8: *Decomposition pathways of carboxylic acid end-groups in PTFE to produce various secondary end-groups.*

The proposed mechanism for the formation of an acyl fluoride is a carboxylate thermolysis with carbon monoxide elimination similar to the method described by Pellerite [220] and is shown in Scheme 9. The cyclic zwitterionic intermediate loses CO upon heating to form the acyl fluoride group. This acyl fluoride will hydrolyse on contact with atmospheric moisture to return a carboxylic acid.



Scheme 9: *Unimolecular reaction mechanism proposed for formation of zwitterionic intermediate that leads to formation of acyl fluoride groups.*

The elimination reactions of the other end-groups have not been reported in literature. In particular, how a nitrile group could form from an amide group is not discussed. Furthermore, PTFE synthesised with persulfates tend to undergo discoloration during thermal treatment, but the proposed mechanisms do not elucidate how a conjugated end-group of sufficient size to effect the aforementioned discoloration can be generated.

Markevich *et al.* [82] indicated that, if the PTFE macroradical is not terminated by mutual recombination with some other radical fragment or capped *via* abstraction, then the PTFE macroradicals may persist indefinitely and that, in practice, the PTFE macroradicals persist for days if kept at temperatures below 100 °C. Upon exposure to atmospheric oxygen, these macroradicals form peroxides, which are stable at ambient conditions, but are prone to easy elimination upon heating (see Section 2.7.3.1).

2.7.3.4 Melting point and glass transition

Polytetrafluoroethylene does not exhibit a melt phase like PE does. Rather, the high polymers have a transition point at ~ 335 °C where the chains move more freely. Polytetrafluoroethylene composites manufactured by powder processing techniques are “sintered” at or slightly above this temperature in order to coalesce the agglomerate particle. This melting point is a strong function of the molecular weight and the crystallinity of the polymer, with the melting point usually falling in the range 300 to 330 °C, depending on the initial crystallinity of the polymer.

Polytetrafluoroethylene produce *via* solid-state polymerisation [120] exhibits a strong drop in melt temperature with increasing radiation dose as the crystallinity decreases, with the initial, highly crystalline material exhibiting a melting point in the region of 335 °C.

The glass-transition temperature is a lot trickier to understand than the melting point. There are numerous contradictions in the literature regarding the transition temperature, with some results indicating a low T_g and others indicating a high T_g , the various reported values for the glass transition are summarised in Table 8. More recent investigations using mechanical analysis [195] indicates that PTFE exhibits two transitions, one relating to the mobile amorphous regions and the other to the rigid amorphous regions (detailed in Figure 18), with the “true” glass transition being at -103 °C.

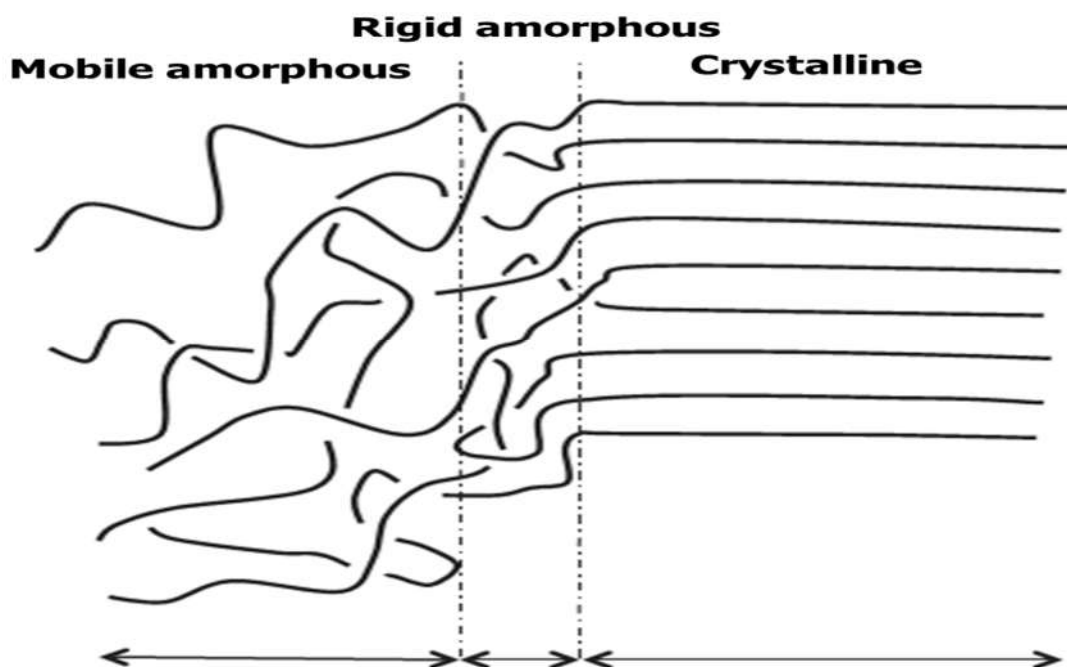


Figure 18: *Polymer chain arrangements in PTFE at the amorphous to crystalline transition, showing the different types of amorphous region [195].*

2.7.4 Mechanical properties

Polytetrafluoroethylene chains have little propensity for polarisation and ionisation and do not engage in hydrogen bonding. This results in a minimisation of the polar and non-polar forces between PTFE chains and between PTFE chains and other molecules. Besides this, and, as already discussed, PTFE adopts a ridged, linear chain conformation. Consequently, the PTFE chains can slip easily past each other, rendering the polymer soft and ductile.

The mechanical properties of PTFE (such as tensile and compressive strength, flexural modulus, hardness, and impact toughness) have been extensively investigated under a variety of temperatures and loading conditions and numerous summaries exist [198, 221-228]. Both the tensile and compressive properties are strong functions of the temperature and the strain rate, but are weak functions of crystallinity. The modes of failure of PTFE articles differ significantly, depending on whether PTFE is above or below its glass-transition temperature [228].

Table 8: *The reported glass-transition temperatures for PTFE, indicating the scope of the controversies regarding this property of PTFE.*

Technique	T _g (°C)	Reference
Positive glass-transition temperatures		
Dynamic mechanical analysis	+130	[229, 230]
	+116	[195]
Rheometry	+110	[231, 232]
Dilatometry	+123	[233]
Thermally stimulated currents	+130	[234]
Negative glass-transition temperatures		
Dynamic mechanical analysis	-110	[235]
	-103	[195]
Various mechanical measurements	-110	[222]
Calorimetry	-110	[236]
	-50	[237]
Calculational methods	-75	[238]

In general, the mechanical properties of finished PTFE articles are strongly affected by the processing conditions, with air inclusions being the most common moulding defect.

The molecular weight of the PTFE also plays an important role in its mechanical properties. The long chains of high-molecular-weight PTFE are to some extent prevented from moving. If shorter chains are present, they may act as lubricants for the long chains, increasing the rate of chain slippage. Hence, the higher the number-average molecular weight and the lower the polydispersity of the polymer, the stronger the final moulded article will be in tension environments, and vice versa.

For the aforementioned reasons, PTFE is also highly susceptible to cold flow (creep) and exhibits a large elongation-to-break, with 300 to 500 % elongation being common. Numerous manufacturers of finished and semi-finished PTFE articles have taken to incorporating filler materials into PTFE in order to combat the polymer's propensity for cold flow. These filler materials include glass fibres, silica, brass, amorphous carbon, graphite, MoS₂, and a host of metal- and metal oxide powders [239, 240]. These fillers also affect the hardness of PTFE resin.

To date, there have been no rigorous studies published on the mechanical properties of PTFE as a function of the molecular-weight distribution as PTFE cannot be subjected to the usual methods employed to determine the molecular-weight distribution. Each manufacturer of PTFE resin provides the mechanical properties of their polymers under standard testing conditions (*i.e.* Section 2.8), and these properties may vary greatly between grades.

2.7.5 Hydrophobicity and surface properties

Articles made from pure PTFE are hydrophobic and non-adhesive. Hydrophobic polymers are characterised by a static water contact angle of $>90^\circ$ and smooth PTFE surfaces exhibit a contact angle of 108 to 114 ° [241], going up to 118 ° if the polymer is unmodified [242]. Zhang *et al.* [242] indicated that PTFE articles could be made superhydrophobic by extension (pulling) of the substrate, with contact angles of up to 165° possible. The hydrophobicity of smooth PTFE is due to the lack of polarisability of the PTFE chain, which stymies the interaction of water with the surface of the polymer by hydrogen bonding.

Recent studies on the wettability of non-polar surfaces have shown that smooth, clean PTFE surfaces may be wetted to a significant extent by water if the interfacial surface tension is lowered with a surfactant [243-257] and contact angle values as low as 8 ° have been reported [251]. Non-ionic (TX100, TX165), cationic (CTAB, PCyB), anionic (SDS), and zwitterionic surfactants have all been investigated (this includes both hydrocarbon and fluorocarbon

compounds). The extent to which surfactant containing water can be made to wet PTFE is dependent on the surfactant chemistry, but for the first three classes of surfactants the effect is noticeable only up to the CMC and there is very little increase in the wetting of aqueous solutions of these surfactants beyond the CMC. The CMC acts as a turning point: Initially there is little change in the contact angle between the water and PTFE, but as the surfactant concentration approaches the CMC, the contact angle drops rapidly with concentration until a plateau is reached, where the contact angle is invariant of surfactant concentration. The same effect is observed with zwitterionic surfactants, but the point where there is a drop in the contact angle is found at surfactant concentrations far in excess of the CMC.

The use of static water contact angle measurements to determine hydrophobicity has been called into question, with Gao and McCarthy [258] indicating that advancing and receding contact angle hysteresis provides a much clearer picture of hydrophobicity and hydrophilicity. Their experiments show that a PTFE thin film will wrap itself around any water droplet placed on its surface; essentially PTFE shows a strong affinity for water. Based on this, PTFE should be considered a hydrophilic material, as opposed to a hydrophobic material. However, their definitions have not received much consideration in the surface science community, and PTFE is still considered a hydrophobic material.

The lack of any significant van der Waals interactions between PTFE and other molecules negates the climbing ability of species like ants and geckos, which make use of van der Waals interactions in their feet [259]. This lack of interaction is also the reason why adhesives do not stick to PTFE.

The surface properties of PTFE may be altered by including small amounts of modifier monomers or by treatment of the PTFE surface by electron beam- [260-265], UV-radiation- [266], glow discharge- [267-271], jet plasma- [272-275], wet chemical- [276-278], and grafting techniques [279].

The surface properties of PTFE are not known to be a function of the molecular weight or the as-polymerised polymer microstructure, and therefore, of the polymerisation conditions. Nearly all surface property tests are conducted on a sintered sheet or a film of PTFE and under these testing conditions, imperfections in the shaping of the film or sheet play a much larger role in the measured surface property than the as-polymerised microstructure or molecular weight. However, there have been no rigorous investigations into the effects of the ratio of rod-like to spherical particles or the molecular-weight distribution on the surface properties.

2.7.6 Tribology and friction coefficients

The dynamic coefficient of friction ranges from 0.05 to 0.1 [198]. The dynamic friction coefficient and the static coefficient are both nearly independent of operating temperature up to the melting point of PTFE. The coefficient of friction is also dependent on the pressure, with the coefficient decreasing with increasing pressure, as well as the filler material and filler loading [4, 7, 239, 240, 252]. Polytetrafluoroethylene will undergo rapid mass loss under abrasive conditions if the PV value is exceeded [252].

Polytetrafluoroethylene exhibits interesting self-lubricating behaviour: When rubbed against metal surfaces the PTFE chain undergoes scission to produce various radical fragments, some of which form metal-carbon bonds with the surface of the metal substrate. These surface-bonded radical fragments form a continuous PTFE-like transfer film, which effectively results in the PTFE on the metal mimicking a PTFE on PTFE system [252]. The lack of significant interaction between PTFE chains results in an extremely low coefficient of friction, and hence the exceptional tribological properties.

Depending on the metal substrate, the formation of a layer of metal fluoride on the metal surface due to abstraction of fluorine from any nascent metal sites may also occur. The surface fluorination competes with the formation of a transfer layer, resulting in an increase in wear between the polymer and the metal surface. Iron and aluminium are particularly susceptible to the formation of metal fluorine, whereas copper is less susceptible. Hence, PTFE exhibits much less wear when rubbed against copper than aluminium or iron [280, 281].

The effects of PTFE wear due to surface fluorination cannot be mitigated by simple oxide layer passivation as the conditions at the polymer metal interface are such that PTFE will strip oxygen from the metal surface [280]. Hence, control of PTFE wear requires a detailed control of the surface chemistry of the underlying substrate.

As with the mechanical properties, there has been no rigorous investigation of the tribological properties of PTFE as a function of the molecular-weight distribution.

2.7.7 Electrical properties

Polytetrafluoroethylene is non-conductive and possesses an excellent dielectric strength due to the non-polarisability of the polymer chains. The dielectric strength remains nearly constant with frequency up to 10 MHz and remains nearly constant with temperature as well [4, 6]. Weathering has minimal effect on the dielectric strength of PTFE.

2.7.8 Conclusions

Polytetrafluoroethylene exhibits a range of useful properties, many of which are strong functions of temperature and molecular weight. The molecular weight is dependent on both the initiator chemistry, the reaction temperature as well as the chemistry of additives present in the reaction. The polymerisation process is sensitive to impurities and any materials that can donate a proton will result in a reduced molecular weight

Polytetrafluoroethylene may exist as rods, spheres, ribbons, or hexagons. The polymer morphology is highly dependent on the method used to polymerise the monomer, with dispersion polymerisation producing more spherical particles with smaller d_{50} and suspension polymerisation producing more rodlike particles with larger particle d_{50} , but with severe agglomeration.

Thermal and chemical stability of the initiator is a determining factor in the stability of the PTFE chain, and the more prone the endgroup is to elimination, the lower the chemical and thermal stability of the polymer. Currently, the use of sterically hindered, perfluorinated peroxide initiators is preferred as it imparts an increased stability to the polymer.

The mechanical- and tribological properties are dependent on the molecular weight, the crystallinity and the size of the particle agglomerates in addition to the testing temperature. Imperfection, such as voids, contribute greatly to premature mechanical failure of PTFE finished articles.

Polytetrafluoroethylene is superhydrophobic and exhibits a low coefficient of friction, but suffers from low mechanical strength and is severely susceptible to creep and to abrasion.

The determination of the molecular-weight distribution of PTFE is onerous and a rigorous treatment of the mechanical properties of PTFE in relation to the molecular-weight distribution is lacking in the literature. The use of rheological techniques [199, 282] to characterise the molecular-weight distribution and compare the mechanical behaviour of PTFE with differing polydispersities presents an interesting avenue for further research.

2.8 Polymer analysis techniques

The physical properties most important for the characterisation of PTFE include thermal stability, melting point, chemical purity, crystallinity, molecular weight, and polydispersity index [1, 4]. As PTFE is not soluble in any solvent, gel-permeation chromatography and osmotic pressure methods cannot be used for determination of the number-average molecular weight or

the molecular-weight distribution of the polymer. Non-solubility also implies that conventional light scattering techniques cannot be employed to determine the M_w of the polymer.

2.8.1 Spectroscopic techniques

2.8.1.1 *Gamma-ray spectrometry*

Berry *et al.* determined the M_n of PTFE for the first time using radioactive end-group analysis [27]. Berry and Peterson used ^{36}S containing potassium persulfate and sodium bisulfite, with the ^{36}S obtained from Oak Ridge National Laboratory. The technique involved direct measurement of the radiodecay of the end-groups using a Geiger counter.

2.8.1.2 *Infrared*

End-group analysis, either by FTIR [283] or UV/Vis or by NMR spectroscopy, permits the determination of M_n . For FTIR analysis, the ratio of the end-group to the CF_2 units is correlated to the film thickness and the absorbance at wave numbers specific to the expected end-group (the relation is shown in Equation (2)).

$$\frac{[\text{CF}_2]}{[\text{End Groups}]} = \frac{A \cdot \delta}{d \cdot 10^{-6}} \quad (2)$$

Here A is the absorbance, δ is the end-group specific correction factor and d is the film thickness of the sample.

For this correlation, the end-groups COF , $\text{COOH}^{\text{free}}$ and $\text{COOH}^{\text{bound}}$ are used (1883 cm^{-1} , 1815 cm^{-1} and 1809 cm^{-1} , 1777 cm^{-1}). The calibration factor δ differs for each end-group, being 406 for COF , 335 for CO_2H (free), and 320 for CO_2H (bound) [284]. See also the article by Pianca *et al.* [217] for a detailed description of the end-groups and their IR absorbance bands.

2.8.1.3 *Nuclear magnetic resonance*

Chemical purity is determined by solid-state NMR spectroscopy, using MAS to record the ^{19}F and ^1H spectra for the polymer. For pure high-molecular-weight PTFE, only the $-\text{CF}_2-\mathbf{CF}_2-\text{CF}_2-$ signal should be seen (found at $\sim -122 \text{ ppm}$) and no signals should be seen in the proton spectrum [101]. In reality, some minor signals attributable to end-groups will be present in the spectra and typical ^{19}F NMR side signals include CF at $\sim -143 \text{ ppm}$ and CF_3 at $\sim -80 \text{ ppm}$. A sample SS NMR spectrum of PTFE synthesised in sc-CO_2 with a fluorinated initiator is presented in Figure 19.

It is important to mention here that liquid-state NMR spectroscopy is not possible for PTFE as even low-molecular-weight PTFE waxes are not soluble in any solvent, including solvents commonly used for recalcitrant samples in NMR spectroscopy (*e.g.* deuterated DMF and deuterated DMSO). Chemical analysis of PTFE or other perfluoropolymers must rely solely on solid-state MAS NMR spectroscopy. Several textbooks and articles on the solid-state NMR spectroscopic analysis of polymers are in circulation [285-290] that discuss the available methods for solid-state NMR spectroscopy of fluoropolymers, such as MAS and CRAMPS, both with and without decoupling. For perfluoropolymers, high-speed MAS is used, with 50 kHz spin rates giving good results.

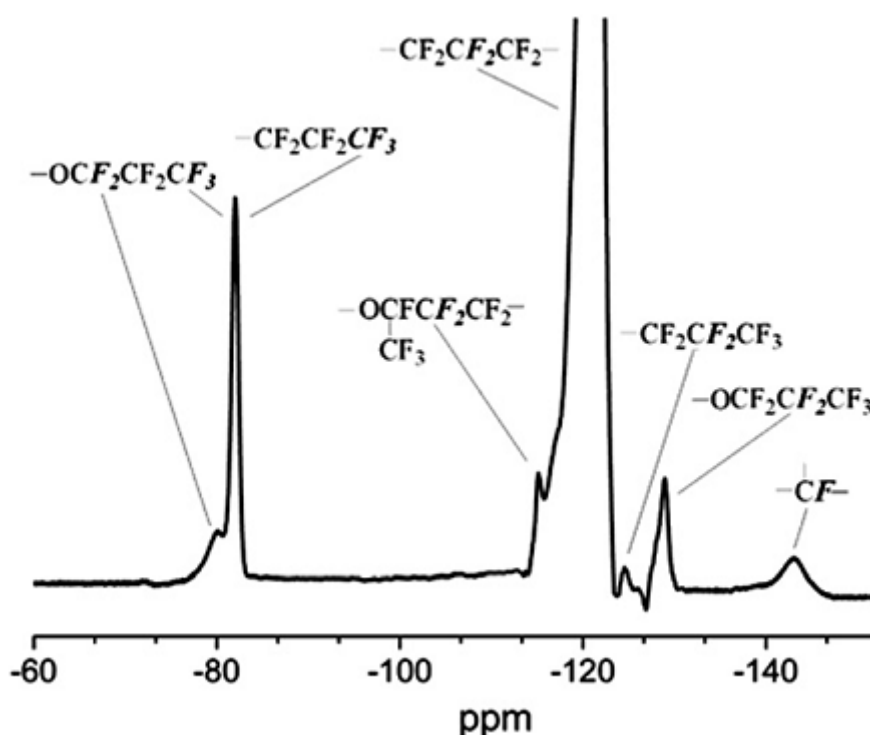


Figure 19: ^{19}F SS NMR spectrum of PTFE synthesised in $sc\text{-CO}_2$ using bis(perfluoro-2-n-propoxypropionyl) peroxide as initiator [101].

As an example of collection parameters: Lappan *et al.* [283] collected ^{19}F NMR spectra using a CRAMPS probe with 2.5 mm MAS rotor. Single pulse excitations were performed with a MAS spin rate of 32 kHz and a $\pi/2$ (90°) pulse duration of 3 μs , accumulating 1024 scans for each spectrum.

Note: Solid-state NMR spectroscopy is not a ubiquitous technique, and those research groups who do own such an instrument often do not have a MAS rotor capable of 50 kHz spin rates.

Compared to the data available for PVDF (*cf.* [189-191, 291, 292]), data for the homopolymers of highly fluorinated monomers (such as CTFE and TFE) are sparse.

2.8.2 Microscopy and particle analysis

The ratio of spheroidal to rod-like micro-particles, the average spheroidal micro-particle diameter, and the distribution of micro-particle diameters may be accomplished by direct inspection of SEM micrographs of the polymer. However, care should be taken when using an electron microscope as PTFE is highly susceptible to electron-beam-induced chain scission [204-208, 260-263, 293-303].

Sample preparation for PTFE dispersions require dilution to approximately ~ 0.02 mass % in demineralised water and dripped onto a metal grid suitable for SEM or TEM analysis. To ensure the PTFE is conductive, the polymer can be stained with phosphotungstic acid (PTA) and this is best effected by adding 1 mol % of PTA to the diluent water [136]. Non-dispersed polymers can simply be immobilized on some conductive adhesive film and then sputter coated using gold or carbon [101].

The distribution of agglomerate particle diameters may be determined by sieve tray analysis, but depending on the size of the agglomerates, readings will vary considerably due to electrostatic effects causing the particles to adhere to the sieves. The average particle diameter may also be determined *via* Mie-light scattering analysis of a dilute dispersion (~ 0.02 mass% solids in water) with 550 nm light as well as by a sedigraph, using an ultra-centrifuge technique [166]. Particle surface areas per mass of sample are determined by the BET method [93].

2.8.3 Diffraction and light scattering

2.8.3.1 X-ray diffraction

Crystallinity of the polymer is usually determined by powder X-ray diffraction (XRD), but other methods, such as FTIR and DSC can also be used [304-306]. The most reliable methods is XRD, and fractional crystallinity is determined by dividing the peak area under the crystalline peaks by the total peak area of the spectrum. Numerous software packages are capable of performing the integration and crystallinity calculations, with TOPAS [307] being the most salient example.

2.8.3.2 *Light scattering*

Chu *et al.* [308] managed to perform high-temperature light scattering on low-molecular-weight PTFE using oligomers of CTFE as a “solvent” at temperatures above the melting point of the polymer (~ 330 °C), using specialised equipment. They determined, among other properties, the M_w and the radius of gyration of a PTFE chain.

2.8.4 Rheology

In the late 1980s, Wu, Tuminello *et al.*, and Starkweather *et al.* developed a method to characterise PTFE by rheology, employing the viscoelastic spectroscopy technique [199, 200, 282]. In the case of “low-molecular-weight” PTFE, the dynamic modulus is used, whereas for “high- molecular-weight” PTFE, the stress relaxation modulus is used.

They claimed to be able to extract a molecular-weight distribution for PTFE from the rheological data. Wu [199] indicated that the M_n values obtained by rheology do not significantly differ from the M_n values obtained by end-group analysis. For example, with commercial Teflon® 6 resin he found a M_n of 1.1×10^7 Da by end-group analysis and a M_n of 1.27×10^7 Da by rheology.

The accuracy of the molecular-weight distribution determined by rheological techniques is not dependent on the accuracy with which the molecular weights of a series of calibration compounds are known. Viscoelastic spectroscopy provides an assessment of the molecular weights of PTFE independent of the calorimetric and standard specific gravity methods, which are reliant on the accuracy of the end-group analysis technique. However, there is a paucity of literature on the application of viscoelastic spectroscopy in research on the synthesis of PTFE.

2.8.5 Thermal analysis

2.8.5.1 *Thermogravimetric analysis*

The intrinsic thermal stability of PTFE is measured *via* thermogravimetric analysis (TGA) [12], using the standard ASTM method for polymer analysis, which follows a heating program from ambient (~ 25 °C) to 850 °C at a rate of 10 °C \cdot min $^{-1}$ under a nitrogen atmosphere flowing at 50 mL \cdot min $^{-1}$. Oxidative thermal stability follows the same method, substituting oxygen or air for nitrogen. Typically, 25 mg of polymer is used in the analysis and α -alumina crucibles are employed, although, platinum or any other high-temperature material may be specified as crucible material. Depending on the reaction conditions in the instrument, mixtures of PTFE

with certain metals may undergo runaway reaction and care must be taken to ensure that these compositions do not destroy the instrument [215].

2.8.5.2 Differential scanning calorimetry

Melting point is determined using either a DTA or a DSC, running approximately 5 mg of polymer at $10\text{ }^{\circ}\text{C}\cdot\text{min}^{-1}$ from ambient to $400\text{ }^{\circ}\text{C}$ and back again under a nitrogen atmosphere flowing a $50\text{ mL}\cdot\text{min}^{-1}$ [120]. Typically, aluminium or platinum pans are used for the melting point determination. Accuracy requires that the polymer be cycled through at least one, but preferably two thermal cycles to remove any thermal history, with the melting point determined from the data of the third thermal cycle.

Heat of crystallisation (determined by DSC) has been correlated to M_n by Suwa *et al.* [194] and by Weigel *et al.* These correlations are presented in Equation (3) and Equation (4), respectively, with ΔH_c in $\text{cal}\cdot\text{g}^{-1}$. Re-examination of the literature [283] indicates that the equation of Weigel is preferred over Suwa's correlation. It must be noted that these correlations can be trusted only if the calculated M_n falls between 10^5 and 10^7 Da.

$$\bar{M}_n = 2.1 \times 10^{10} \times \Delta H_c^{-5.16} \quad (3)$$

$$\bar{M}_n = 3.5 \times 10^{11} \times \Delta H_c^{-5.16} \quad (4)$$

Typical collection parameters require the use of a closed lid aluminium pan and ~ 5 mg of polymer sample. The heat of crystallisation is, as far as is known, independent of heating rate (at least between heating rates of 5 to $35\text{ }^{\circ}\text{C}\cdot\text{min}^{-1}$).

Suwa *et al.* [194] used custom-synthesised PTFE as standards. The number-average molecular weight of these polymers were determined by standard specific gravity techniques based on the methods presented by Sperati *et al.* [309, 310].

2.8.6 Standard specific gravity techniques

Specific gravity measurements have also been used to determine the number-average molecular weight [309, 310], but this method is not generally used as defects generated during sample preparation, such as voids and gas bubbles, can seriously affect the accuracy measurement. For high-molecular-weight PTFE, or TFE polymers where a simple chain-transfer agent was employed (*i.e.* no branching or pendant groups), the standard specific gravity (SSG) is correlated to the number-average molecular weight by Equation (5) [166]. Variations on this equation have

been published in subsequent literature [50, 92], and the equation used by Kim *et al.* is given in Equation (6).

$$SSG = 2.612 - 0.582 \log_{10} \bar{M}_n \quad (5)$$

$$\log_{10} M_n = 31.83 - 11.58 \times SSG \quad (6)$$

The SSG was correlated to the number-average molecular weight using end-group analysis [27, 216, 309, 310] and this method is only as accurate as the end-group analysis. The SSG is defined by the ratio of the mass of a sample plate to the mass of water, at 23 °C, of an equal volume of pure water. Sample plates are typically prepared by moulding 3.5 g of polymer in a 1-” diameter cylindrical die *via* gradually increasing the pressure (minimum time is 30 s) to $\sim 352 \text{ kg.cm}^{-2}$ and held there for ~ 2 minutes to permit stress equalisation. The preform is sintered at 380 °C, typically for 30 minutes, before being slow cooled ($\sim 1 \text{ }^\circ\text{C.min}^{-1}$) to 300 °C. The plate should be conditioned at 23 °C for 3 hours after removal from the furnace to ensure that the entire volume is isothermal.

2.8.7 Conclusions

Polytetrafluoroethylene may be subjected to a range of analyses techniques. The structure of PTFE is typically studied using infrared spectroscopy while the molecular weight is usually determined *via* calorimetric means. However, owing to the complete insolubility of PTFE, it cannot be subjected to the critically important analyses such as gel-permeation chromatography (GPC). Furthermore, the solid-state NMR spectroscopic analysis of PTFE is non-trivial and can be challenging even to the best equipped of laboratories.

The routine methods (DSC and SSG) employed in the determination of the molecular weight of PTFE are all ultimately calibrated against data obtained from end-group analysis. The accuracy of this data is questionable by today’s standards and the values obtained for number-average molecular weight from Suwa’s equation and the SSG correlations are subjective. In particular, Suwa’s equation should be used with extreme caution, as the heat of crystallisation is a function of the entire molecular-weight distribution, not just the number-average molecular weight. Using Suwa’s equation with PTFE sample having polydispersities significantly different from the calibrant samples may result in gross errors in M_n values.

There is significant scope for the re-investigation of the DSC correlations for molecular weight using well defined polymers whose molecular weights are corroborated independently by techniques such as NMR spectroscopy and rheology.

2.9 Applications of PTFE

Polytetrafluoroethylene finds use in a vast number of technical fields, with applications ranging from electrical- to medical equipment, clothing, and even pyrotechnics. The information provided here is not meant to be an exhaustive catalogue of all the current and past application fields of PTFE, but rather to illustrate the contemporary importance of PTFE as well as the recent trends in the utilisation of PTFE.

2.9.1 Electrical and electronic applications

Since its first appearance on the market, PTFE has been employed in the electrical industry as cable insulation and as dielectric in capacitors. The electrical and electronic applications are made possible by the high dielectric strength and the invariance of the dielectric constant over a wide frequency range. In particular, PTFE is applied as insulator in radio and microwave frequency communication cabling (co-axial cables, *etc.*), insulator in Wi-Fi antennas and medical instrument cables [311]. Polytetrafluoroethylene is especially employed in the military-, automotive-, and aerospace electronics sector [312] where electrical insulation material is required to perform under extreme temperatures. Polytetrafluoroethylene insulation is also employed in cable coatings in the oil and gas industry, particularly in deep well settings owing to the excellent chemical resistance, low permeability, and thermal stability. Figure 20 and Figure 21 show examples of electrical products made with PTFE.



Figure 20: *Polytetrafluoroethylene insulated co-axial cable (image courtesy of Bhupal Cables Company).*



Figure 21: *Cut-open film capacitor showing the PTFE dielectric roll (image courtesy of RuTubes Audio Components Company).*

2.9.2 Pipes, tubing, gaskets, seals, filters, and machined parts

Polytetrafluoroethylene may be ram extruded to form pipes and tubes, which find application in the fine chemical, petrochemical, nuclear, and food processing industries. Numerous types of connectors, nozzles, valves, and filter membranes are produced for chemical industry and laboratory applications are produced the world over (*cf.* [313-316]). Figure 22 provides an example of filter cartridges made with PTFE membranes.

Polytetrafluoroethylene has also been used as gasket material [317, 318], as O-rings and other seals (such as plumber's tape) as well as valve seats in ball valves and needle valves (*cf.* [319]). Polytetrafluoroethylene sealing tape is probably the most ubiquitous application of PTFE in daily life. Industrially, the most commonly encountered PTFE are PTFE valve seats and gaskets.

It is a historical fact that PTFE's first major uses were in the nuclear industry, where it was employed as gasket- and pipe liner material in the uranium enrichment plant operating during World War II.



Figure 22: *Polytetrafluoroethylene filter cartridges showing the PTFE membranes (image courtesy of the American Melt Blown & Filtration Company).*

2.9.3 Tribological applications

Polytetrafluoroethylene is employed as a dry lubricant and as a release agent, with the most common household applications being the lubrication of bicycle and motorcycle sprockets and chains as well as door and window hinges [320] (PTFE dry lubricant is most well-known under the brand name WD-40 [321]). Polytetrafluoroethylene is also employed as the contact surface in slider bearings (such as the structural bearings in bridges and expansion sliders for piping systems [322]). The low-friction properties of PTFE was used to good effect during the construction of the Millau viaduct in France [323], where PTFE slider bearings were used to jack the pre-assembled roadway across the pylons. Figure 23 provides a detailed cutaway of a PTFE slider bearing.

Lai *et al.* [103] have indicated that PTFE surface coatings could be used as a non-magnetic dry lubricant for high-speed magnetic storage devices used in the electronics industry (such as hard disk drives).

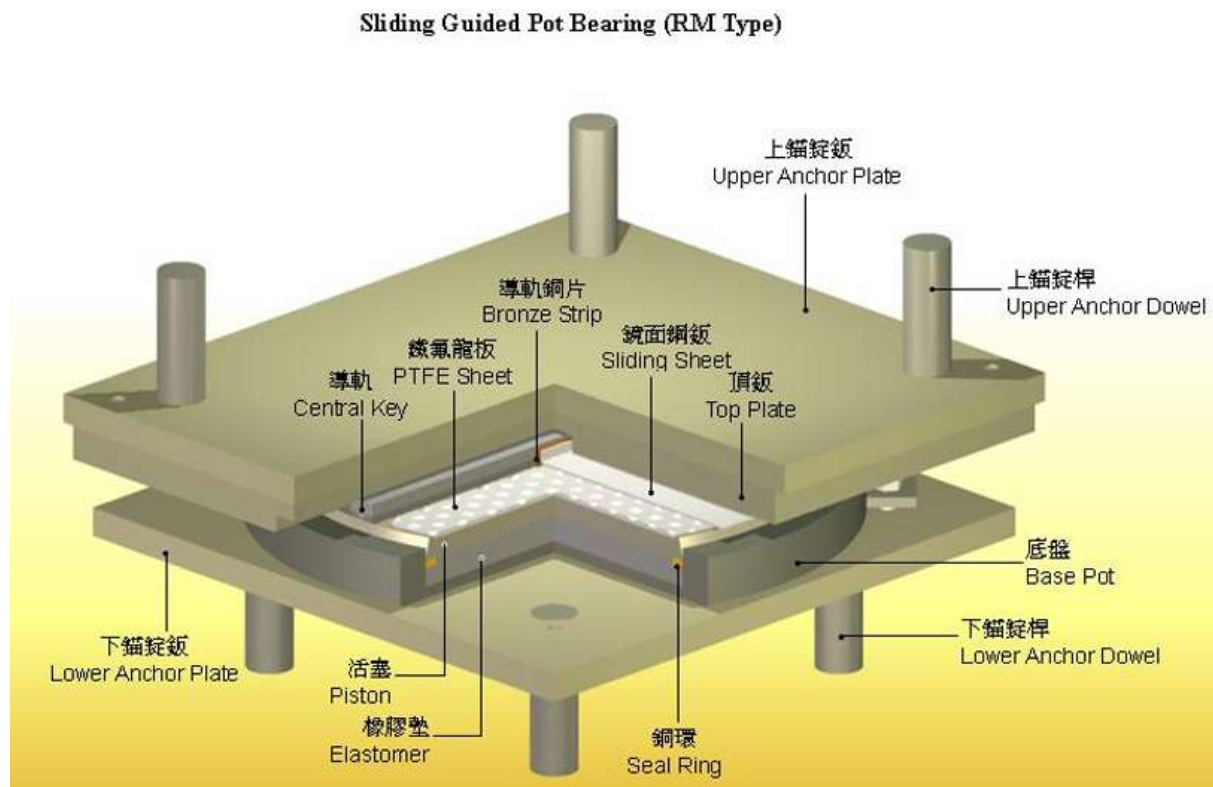


Figure 23: Diagram of a PTFE sliding expansion bearing for road bridge applications (image courtesy of Nippon Pillar Singapore).

2.9.4 Chemically resistant, hydrophobic coatings and textiles

Polytetrafluoroethylene is most widely recognised as the non-stick coating on frying pans and PTFE has been employed as a non-stick, easy-cleaning, chemically inert coating in the food industry for many years [324]. Other uses of PTFE coatings include release coatings on moulds, pipe liners (example shown in Figure 24), vessel- and thermocouple coatings in the pharmaceutical and chemical industries [314, 325] (including pipe liners in acid plants, non-fouling coatings in heat exchangers *etc.*) as well as anti-corrosion coatings for machinery housings [312]. One cannot enter a chemistry laboratory without finding, at minimum, PTFE coated magnetic stirring bars.

Polytetrafluoroethylene is also used to coat textiles for water proofing [326]. In particular, expanded PTFE has been used as water proof, breathable membranes in clothing (known commercially as Gore-Tex [327]).



Figure 24: *Polytetrafluoroethylene lined pipe reducer (image courtesy of JCS Line Piping Products).*

2.9.5 Medical applications

Medical applications of PTFE (used mainly as expanded PTFE) include vascular grafts [328-330] and as surgical meshes, catheters, scaffolds for ligament and tendon repair, and facial augmentation material in plastic surgery [331]. Polytetrafluoroethylene was also used in early replacement heart valves. The medical uses for PTFE primarily exploit the chemical inertness and hydrophobicity of the polymer and, in addition to the above-mentioned *in vivo* uses, are also used to coat various medical devices and tools. Figure 25 shows an example of ePTFE vascular grafts.



Figure 25: *Example of an ePTFE vascular graft (image courtesy of the Terumo Corporation).*

2.9.6 Pyrotechnic applications

Polytetrafluoroethylene finds a niche use as the fuel in some metal/fluorocarbon pyrotechnic formulations. Polytetrafluoroethylene mixed with various metals, such as magnesium, aluminium, calcium, and silicon are used in missile counter measures, thermal lances, and signal flares [215].

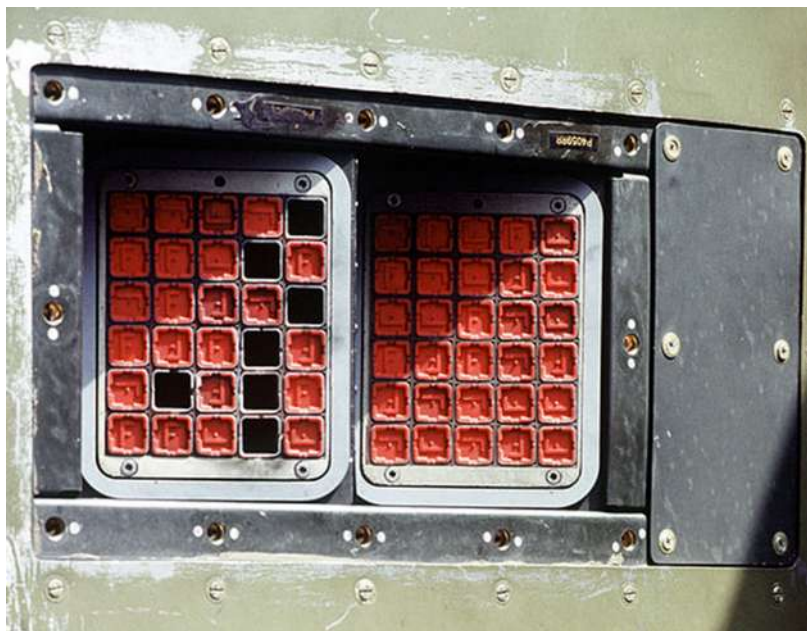


Figure 26: *Magnesium/Teflon/Viton (MTV) countermeasure flare cartridges mounted in a C-130 Hercules.*

2.9.7 Conclusions

Polytetrafluoroethylene has found application in numerous fields, ranging from electrical insulation and pipe liners to coated fabrics and vascular grafts. A combination of exceptional chemical and thermal stability, as well as hydrophobicity, sets PTFE at the top of the list of extreme polymers.

2.10 Perspectives

The bulk fluoropolymer trade is estimated to grow to 94 ktons in 2018. Figure 27 details the bulk fluoropolymer market valuation for the period 1998 to 2018. Even through the economic downturn of 2008 and the years thereafter, growth has been steady. The fluoropolymer type distribution, Figure 28, indicates that PTFE remains the predominant product amongst the vast array of fluoropolymers in use.

Recently, there has been global shift towards using sustainable materials, such as bio-sourced polymers, in order to reduce the impact of the plastics industry has on the environment. Commodity plastics such as high density polyethylene and polypropylene are being replaced with bio-derived polymers made from corn starch, and similar feedstock. Despite the global drive

towards bio-derived plastics, the exceptional properties of fluoropolymers ensure that they cannot be replaced with more benign materials in high-tech applications. However, the fluorochemical industry, and by extension, the fluoropolymer industry, arguably has a poor environmental track record. The lack of innovation on the environmental aspects by large industry players has resulted in class-action lawsuits and significant reputational damage to these enterprises. Indeed, DuPont has recently spun off their fluoropolymers division into a separate company, Chemours, to mitigate any legal and public relations fallout over the environmental pollution generated by their fluoropolymer related activities.

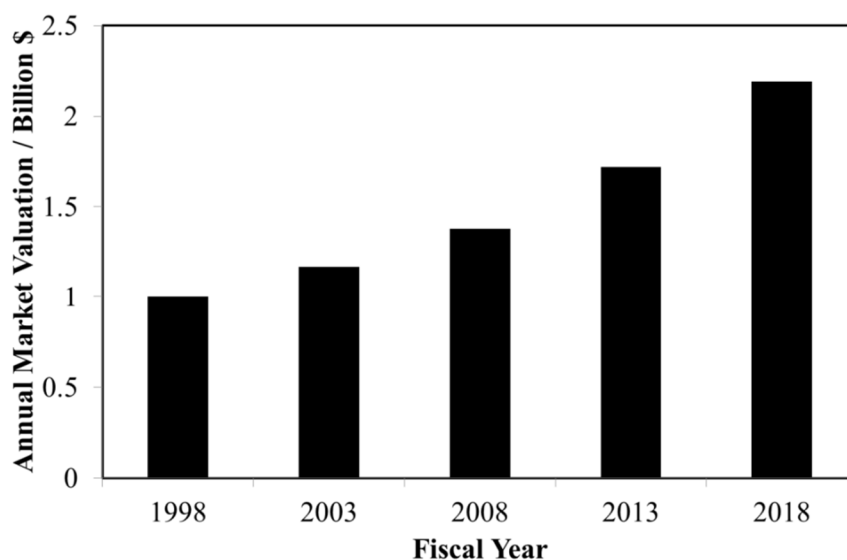


Figure 27: Bulk fluoropolymer market value for the period 1998 to 2018 (the 2018 value is an estimate).

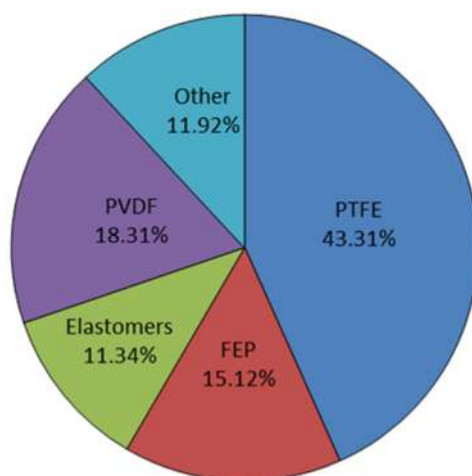


Figure 28: *Distribution of fluoropolymer market share by polymer type in 2013.*

There clearly are economic opportunities in this market. Some of these may lie in the recent phase-out of perfluorinated surfactants. DuPont/Chemours stopped using PFOA in 2013, and the rest of the industrial industry had followed suit by 2015. Evidently the replacements have been short-chain, partially fluorinated acids. Proven, but dormant, technologies such as supercritical-CO₂ synthesis may have to be resuscitated.

The full characterisation of PTFE molecular-weight distribution and the effects of the molecular-weight distribution on the physical properties of PTFE are aspects that appear underexploited. Significant research scope exists for the evaluation of these properties as a function of the molecular-weight distribution, and incorporation of these relationships into new product development. Control of the molecular-weight distribution will enable primary producers to better tailor their PTFEs to the applications, reducing material wastage and the concomitant negative environmental impact.

Spent PTFE cannot be recovered by the ordinary methods used for plastics recycling and the material ends up on landfills or other disposal sites where it persists nearly indefinitely. Vacuum pyrolysis is one of the few methods available to recover the fluorine content in PTFE. When properly executed, tetrafluoroethylene may be recovered from waste PTFE in high yields and good purity, adopting a cradle-to-cradle approach. Dyneon seems to be the only large PTFE producer doing this; undoubtedly other producers will follow in time, with increasing pressure on them to commit to higher degrees of environmental accountability.

2.11 References

- [1] Drobny, J.G., 2014, *Technology of Fluoropolymers*, CRC Press, Boca Raton, Florida.
- [2] Ameduri, B., "From vinylidene fluoride (VDF) to the applications of VDF-containing polymers and copolymers: Recent developments and future trends", *Chemical Reviews*, 2009, 109 (12), 6632-6686.
- [3] Boschet, F. and Ameduri, B., "(Co)polymers of chlorotrifluoroethylene: synthesis, properties, and applications", *Chemical Reviews*, 2013, 114 (2), 927-980.
- [4] Ebnesajjad, S., 2000, *Fluoroplastics, Volume 1: Non-melt Processible Fluoroplastics*, Elsevier Science, Norwich, New York.
- [5] Ebnesajjad, S., 2002, *Fluoroplastics, Volume 2: Melt Processible Fluoroplastics: The Definitive User's Guide*, Elsevier Science, Norwich, New York.
- [6] Ebnesajjad, S., 2000, "Homofluoropolymer polymerization and finishing", in (eds.), *Non-Melt Processible Fluoroplastics*, William Andrew Publishing, Norwich, NY.
- [7] Ebnesajjad, S., 2016, *Expanded PTFE Applications Handbook: Technology, Manufacturing and Applications*, Elsevier Science, Norwich, New York.
- [8] Gardiner, J., "Fluoropolymers: Origin, production, and industrial and commercial applications", *Australian Journal of Chemistry*, 2015, 68 (1), 13-22.
- [9] Hercules, D.A., Parrish, C.A., and Thrasher, J.S., 2017, "Research and Non-major Commercial Co- and Terpolymers of Tetrafluoroethylene", in B. Ameduri and Sawada, H. (eds.), *Fluorinated Polymers: Volume 2: Applications*, The Royal Society of Chemistry, Croydon, United Kingdom.
- [10] Gangal, S.V. and Brothers, P.D., 2002, "Perfluorinated polymers, polytetrafluoroethylene", in (eds.), *Encyclopedia of Polymer Science and Technology*, John Wiley & Sons, Inc., New York.
- [11] Hougham, G., Cassidy, P.E., Johns, K., and Davidson, T., 1999, *Fluoropolymers 1*, Springer US, New York.
- [12] Smith, D.W., Iacono, S.T., and Iyer, S.S., 2014, *Handbook of Fluoropolymer Science and Technology*, Wiley, Hoboken, New Jersey.
- [13] Hyatt, T. "Chemical Economics Handbook: Fluoropolymers", **2016**.
- [14] Wood, L. "Global Fluoropolymers Products, Technologies and Applications Market Report 2016 - Research and Markets", **2016**, 588.
- [15] Plunkett, R.J., (Kinetic Chemicals, Inc.) 1941, *Tetrafluoroethylene polymers*, US2230654.
- [16] Brubaker, M.M., (E.I. du Pont de Nemours and Company) 1946, *Process for polymerizing tetrafluoroethylene*, US2393967.
- [17] Joyce, J.R.M., (E.I. du Pont de Nemours and Company) 1946, *Process for polymerizing tetrafluoroethylene*, US2394243.
- [18] Hanford, W.E. and Joyce, R.M., "Polytetrafluoroethylene", *Journal of the American Chemical Society*, 1946, 68 (10), 2082-2085.
- [19] Harmon, J. and Joyce, R.M., (E.I. du Pont de Nemours and Company) 1946, *Sulfur-dioxide modified tetrafluoroethylene polymer*, US2411722.
- [20] Dorough, G.L., (E.I. du Pont de Nemours and Company) 1946, *Catalytic polymerization of monoolefinic organic compounds*, US2398926.
- [21] E.I. du Pont de Nemours and Company, (E.I. du Pont de Nemours and Company) 1946, *Improvements in or relating to the polymerisation of tetrafluoroethylene*, GB574688(A).
- [22] Renfrew, M.M., (E.I. du Pont de Nemours) 1950, *Polymerization of tetrafluoroethylene with dibasic acid peroxide catalysts*, US2534058.
- [23] Feiring, A.E., Krespan, C.G., Resnick, P.R., Smart, B.E., Treat, T.A., and Wheland, R.C., (E.I. du Pont de Nemours and Company) 1993, *Hydrofluorocarbon solvents for fluoromonomer polymerization*, US5182342.

- [24] Carlson, D.P., (E.I. du Pont de Nemours and Company) 1972, *Tough stable tetrafluoroethylene-fluoroalkyl perfluorovinyl ether copolymers*, US3642742.
- [25] DeSimone, J.M. and Romack, T., (University of North Carolina) 1997, *Nonaqueous polymerization of fluoromonomers*, US5674957.
- [26] Du, L., Kelly, J.Y., Roberts, G.W., and DeSimone, J.M., "Fluoropolymer synthesis in supercritical carbon dioxide", *The Journal of Supercritical Fluids*, 2009, 47 (3), 447-457.
- [27] Berry, K.L. and Peterson, J.H., "Tracer studies of oxidation—Reduction polymerization and molecular weight of “Teflon” tetrafluoroethylene resin", *Journal of the American Chemical Society*, 1951, 73 (11), 5195-5197.
- [28] Bankoff, G.S., (E.I. du Pont de Nemours) 1952, *Polymeric tetrafluoroethylene dispersions*, US2612484.
- [29] Berry, K.L., (E.I. du Pont de Nemours and Company) 1953, *Process for obtaining dispersions of polyfluorethylenes*, US2662065.
- [30] Myers, R.L., (General Electric Company) 1952, *Method for polymerizing tetrafluoroethylene*, US2613203.
- [31] Robb, E.L. and Lontz, F.J., (E.I. du Pont de Nemours and Company) 1952, *Process for producing tetrafluoroethylene polymer compositions*, US2593582.
- [32] Nakagawa, S., Nakagawa, T., Yamaguchi, S., Ihara, K., Amano, T., Omori, M., and Asano, K., (Daikin Kogyo Company Ltd.) 1985, *Process for preparing tetrafluoroethylene/fluoro(alkyl vinyl ether) copolymer*, US4499249.
- [33] Benning, A.F., (E.I. du Pont de Nemours) 1951, *Fluorinated aliphatic phosphates as emulsifying agents for aqueous polymerizations*, US2559749.
- [34] Duck, E.W., (Petrochemicals Limited) 1960, *Improvements in or relating to the preparation of fluorine-containing polymeric materials by the catalytic polymerisation of fluorine-containing unsaturated compounds and the resulting polymeric materials*, GB853355.
- [35] Goerrig, D., Jonas, H., and Moschel, W., (Farbenfabriken Bayer) 1955, *Process for the polymerisation of low-molecular-mass aliphatic halogenated olefins, Part 1*, D935867.
- [36] Goerrig, D. and Jonas, H., (Farbenfabriken Bayer) 1956, *Process for the polymerisation of low-molecular-mass aliphatic halogenated olefins, Part 2* D937919.
- [37] Weisz, P.B. and Goodwin, R.D., (Socony-Vacuum Oil Company) 1954, *Gaseous polymerization by electrical discharge*, US2676145.
- [38] Golub, M.A., Wydeven, T., and Finney, L.S., "Plasma homo- and copolymerizations of tetrafluoroethylene and chlorotrifluoroethylene", *Plasmas and Polymers*, 1996, 1 (2), 173-194.
- [39] Golub, M.A. and Wydeven, T., "Relative rates for plasma homo- and copolymerizations of a homologous series of fluorinated ethylenes", *Plasmas and Polymers*, 1998, 3 (1), 35-42.
- [40] Golub, M.A., Wydeven, T., and Johnson, A.L., "Similarity of plasma-polymerized tetrafluoroethylene and fluoropolymer films deposited by RF sputtering of poly(tetrafluoroethylene)", *Langmuir*, 1998, 14 (8), 2217-2220.
- [41] Ferrero, F., Beckmann-Kluge, M., Spoomaker, T., and Schröder, V., "On the minimum ignition temperature for the explosive decomposition of tetrafluoroethylene on hot walls: Experiments and calculations", *Journal of Loss Prevention in the Process Industries*, 2012, 25 (2), 293-301.
- [42] Duus, H.C., "Thermochemical studies on fluorocarbons - heat of formation of CF₄, C₂F₄, C₃F₆, C₂F₄ dimer, and C₂F₄ polymer", *Industrial & Engineering Chemistry*, 1955, 47 (7), 1445-1449.
- [43] Patrick, C.R., "Thermal Stability of Polytetrafluoroethylene", *Nature*, 1958, 181 (4610), 698-698.
- [44] Renfrew, M.M. and Lewis, E.E., "Polytetrafluoroethylene. Heat Resistant, Chemically Inert Plastic", *Industrial & Engineering Chemistry*, 1946, 38 (9), 870-877.

- [45] Furukawa, G.T., McCoskey, R.E., and Reilly, M.L., "Heat capacity, heats of fusion and vaporization, and vapour pressure of tetrafluoroethylene", *Journal of Research of the National Bureau of Standards, Section A: Physics and Chemistry*, 1953, 51 (2), 69-72.
- [46] Lentz, D., Bach, A., Buschmann, J., Luger, P., and Messerschmidt, M., "Crystal and Molecular Structures and Experimentally Determined Charge Densities of Fluorinated Ethenes", *Chemistry – A European Journal*, 2004, 10 (20), 5059-5066.
- [47] Ruff, O. and Bretschneider, O., "Die Bildung von Hexafluoräthan und Tetrafluoräthylen aus Tetrafluorkohlenstoff", *Zeitschrift für Anorganische und Allgemeine Chemie*, 1933, 210 (2), 173-183.
- [48] Yaws, C.L., 2003, *Yaws' Handbook of Thermodynamic and Physical Properties of Chemical Compounds: Physical, Thermodynamic and Transport Properties for 5,000 Organic Chemical Compounds*, McGraw-Hill, New York.
- [49] Veretennikof, N.V., Reshetova, L.I., and Fil'chakova, T.A., "Solubility of different fluorine-containing compounds in water and aqueous solutions of fluoro-organic surfactants", *Fizika Khimiya*, 1984, 1984 (4), 112-114.
- [50] Kim, C.U., Lee, J.M., and Ihm, S.K., "Emulsion polymerization of tetrafluoroethylene: effects of reaction conditions on the polymerization rate and polymer molecular weight", *Journal of Applied Polymer Science*, 1999, 73 (5), 777-793.
- [51] Von Tress, W.R., (Dow Chemical Company) 1964, *Preparation of Tetrafluoroethylene*, US3113871.
- [52] Farlow, M.W., (E. I. du Pont de Nemours and Company) 1963, *Method for the preparation of tetrafluoroethylene*, US3081245.
- [53] M. Jollie, D. and G. Harrison, P., "An in situ IR study of the thermal decomposition of trifluoroacetic acid", *Journal of the Chemical Society, Perkin Transactions 2*, 1997 (8), 1571-1576.
- [54] Hercules, D.A., Parrish, C.A., Sayler, T.S., Tice, K.T., Williams, S.M., Lowery, L.E., Brady, M.E., Coward, R.B., Murphy, J.A., Hey, T.A., Scavuzzo, A.R., Rummel, L.M., Burns, E.G., Matsnev, A.V., Fernandez, R.E., McMillen, C.D., and Thrasher, J.S., "Preparation of tetrafluoroethylene from the pyrolysis of pentafluoropropionate salts", *Journal of Fluorine Chemistry*, 2017, 196, 107-116.
- [55] Siegemund, G., Schwertfeger, W., Feiring, A., Smart, B., Behr, F., Vogel, H., McKusick, B., and Kirsch, P., 2000, "Fluorine compounds, organic", in (eds.), *Ullmann's Encyclopedia of Industrial Chemistry*, Wiley-VCH Verlag GmbH & Co. KGaA, Weinheim, Germany.
- [56] Chinoy, P.B. and Sunavala, P.D., "Thermodynamics and kinetics for the manufacture of tetrafluoroethylene by the pyrolysis of chlorodifluoromethane", *Industrial & Engineering Chemistry Research*, 1987, 26 (7), 1340-1344.
- [57] Henne, A.L., "Fluorinated Derivatives of Methane", *Journal of the American Chemical Society*, 1937, 59 (7), 1400-1401.
- [58] Benning, A.F. and Plunkett, R.J., (Kinetic Chemicals, Inc.) 1946, *Preparation of tetrafluoroethylene*, US2401897.
- [59] Mantell, R.M., (The M. W. Kellogg Company) 1954, *Dehalogenation of fluorocarbons*, US2697124.
- [60] Lang, W., Rummel-Bulska, I., and Tolba, M.K., "Montreal Protocol on Substances that Deplete the Ozone Layer", *United Nations Treaty Series*, 1989, 1522, 28-111.
- [61] Locke, E.G., Brode, W.R., and Henne, A.L., "Fluorochloroethanes and Fluorochloroethylenes", *Journal of the American Chemical Society*, 1934, 56 (8), 1726-1728.
- [62] Puts, G.J. and Crouse, P.L., "The influence of inorganic materials on the pyrolysis of polytetrafluoroethylene. Part 1: The sulfates and fluorides of Al, Zn, Cu, Ni, Co, Fe and Mn", *Journal of Fluorine Chemistry*, 2014, 168, 260-267.

- [63] Puts, G.J. and Crouse, P.L., "The influence of inorganic materials on the pyrolysis of polytetrafluoroethylene. Part 2: The common oxides of Al, Ga, In, Zn, Cu, Ni, Co, Fe, Mn, Cr, V, Zr and La", *Journal of Fluorine Chemistry*, 2014, 168, 9-15.
- [64] Bezuidenhout, A., Sonnendecker, P.W., and Crouse, P.L., "Temperature and pressure effects on the product distribution of PTFE pyrolysis by means of qualitative, in-line FTIR analysis", *Polymer Degradation and Stability*, 2017, 142 (Supplement C), 79-88.
- [65] "Convention on the prohibition of the development, production, stockpiling and use of chemical weapons and on their destruction", *United Nations Treaty Series*, 1997, 1974, 317-481.
- [66] Smith, L.W., Gardner, R.J., and Kennedy, G.L., "Short-Term Inhalation Toxicity of Perfluoroisobutylene", *Drug and Chemical Toxicology*, 1982, 5 (3), 295-303.
- [67] Wang, H., Ding, R., Ruan, J., Yuan, B., Sun, X., Zhang, X., Yu, S., and Qu, W., "Perfluoroisobutylene-Induced Acute Lung Injury and Mortality are Heralded by Neutrophil Sequestration and Accumulation", *Journal of Occupational Health*, 2001, 43 (6), 331-338.
- [68] Gad, S.C., 2014, "Perfluoroisobutylene", in (eds.), *Encyclopedia of Toxicology* Academic Press, Oxford, United Kingdom.
- [69] Timperley, C.M., "Fluoroalkene chemistry: Part 1. Highly-toxic fluorobutenes and their mode of toxicity: reactions of perfluoroisobutene and polyfluorinated cyclobutenes with thiols", *Journal of Fluorine Chemistry*, 2004, 125 (5), 685-693.
- [70] Lailey, A.F., "Oral N-acetylcysteine protects against perfluoroisobutene toxicity in rats", *Human & Experimental Toxicology*, 1997, 16 (4), 212-216.
- [71] Hercules, D.A., DesMarteau, D.D., Fernandez, R.E., Clark, J.L., and Thrasher, J.S., 2014, "Evolution of academic barricades for the use of tetrafluoroethylene (TFE) in the preparation of fluoropolymers", in D.W. Smith, Iacono, S.T., and Iyer, S.S. (eds.), *Handbook of Fluoropolymer Science and Technology*, John Wiley & Sons, Inc., Hoboken, New Jersey.
- [72] Ferrero, F., Zeps, R., Beckmann-Kluge, M., Schröder, V., and Spoormaker, T., "Analysis of the self-heating process of tetrafluoroethylene in a 100-dm³-reactor", *Journal of Loss Prevention in the Process Industries*, 2012, 25 (6), 1010-1017.
- [73] Babenko, Y.I., Lisochkin, Y.A., and Poznyak, V.I., "Explosion of tetrafluoroethylene during nonisothermal polymerization", *Combustion, Explosion and Shock Waves*, 1993, 29 (5), 603-609.
- [74] Lacher, J.R., Tompkin, G.W., and Park, J.D., "The Kinetics of the Vapor Phase Dimerization of Tetrafluoroethylene and Trifluorochloroethylene¹", *Journal of the American Chemical Society*, 1952, 74 (7), 1693-1696.
- [75] Ferrero, F., Meyer, R., Kluge, M., Schröder, V., and Spoormaker, T., "Self-ignition of tetrafluoroethylene induced by rapid valve opening in small diameter pipes", *Journal of Loss Prevention in the Process Industries*, 2013, 26 (1), 177-185.
- [76] Ferrero, F., Meyer, R., Kluge, M., Schröder, V., and Spoormaker, T., "Study of the spontaneous ignition of stoichiometric tetrafluoroethylene-air mixtures at elevated pressures", *Journal of Loss Prevention in the Process Industries*, 2013, 26 (4), 759-765.
- [77] Wang, S.Y. and Borden, W.T., "Why is the .pi. bond in tetrafluoroethylene weaker than that in ethylene? An ab initio investigation", *Journal of the American Chemical Society*, 1989, 111 (18), 7282-7283.
- [78] Atkinson, B. and Atkinson, V.A., "The thermal decomposition of tetrafluoroethylene", *Journal of the Chemical Society (Resumed)*, 1957 (0), 2086-2094.
- [79] Miller, W., 1951, "Preparation of fluorocarbons by polymerization of olefins", in C. Slessor and Schram, S.R. (eds.), *Preparation, Properties, and Technology of Fluorine and Organic Fluoro Compounds.*, McGraw-Hill, New York.

- [80] Reza, A. and Christiansen, E., "A case study of a TFE explosion in a PTFE manufacturing facility", *Process Safety Progress*, 2007, 26 (1), 77-82.
- [81] Bhanu, V.A. and Kishore, K., "Role of oxygen in polymerization reactions", *Chemical Reviews*, 1991, 91 (2), 99-117.
- [82] Markevich, A.M., Volokhonovich, I.Y., Kleimenov, N.A., Nosov, E.F., Mel'nikov, V.P., and Berlin, A.A., "The heterogeneous polymerization of tetrafluoroethylene", *Polymer Science U.S.S.R.*, 1975, 17 (11), 2909-2915.
- [83] Hanford, W.E., (E.I. du Pont de Nemours and Company) 1946, *Stabilization of tetrafluoroethylene*, US2407419.
- [84] Dietrich, M.A. and Joyce, R.M., (E.I. du Pont de Nemours and Company) 1946, *Stabilization of tetrafluoroethylene*, US2407405.
- [85] Marks, B.M. and Thompson, J.B., (E.I. du Pont de Nemours and Company) 1956, *Inhibition of tetrafluoroethylene polymerisation*, US2737533.
- [86] Van Bramer, D.J., Shiflett, M.B., and Yokozeki, A., (E.I. du Pont de Nemours and Company) 1994, *Safe handling of tetrafluoroethylene*, US5345013.
- [87] Abusleme, J.A., (Ausimont S.p.A.) 1995, *(Co)Polymerisation process of fluorinated olefinic monomers in aqueous emulsion*, EU0650982A1.
- [88] Felix, B., Lohr, G., and Hengel, R., (Hoechst Aktiengesellschaft) 1992, *Process for the preparation of tetrafluoroethylene polymer in aqueous suspension*, US5153285.
- [89] Rudin, A., 1999, *The Elements of Polymer Science and Engineering*, Academic Press, San Diego, California.
- [90] Punderson, J.O., (E.I. du Pont de Nemours and Company) 1968, *Polymerization Process*, US3391099.
- [91] Beresniewicz, A., (E.I. du Pont de Nemours and Company) 1986, *Tertiary perfluoroalkoxides as surfactants in PTFE dispersion polymerisation*, US4564661.
- [92] Noda, Y., Hosokawa, K., Mizuno, T., Ihara, K., and Shimizu, T., (Daikin Industries) 1994, *Polytetrafluoroethylene Particles and Powder*, US5324785.
- [93] Cavanaugh, R.J., (E.I. du Pont de Nemours and Company) 1985, *Process for the suspension polymerization of tetrafluoroethylene*, US4529781.
- [94] Herisson, J.-L., (Produits Chimiques Ugine Kuhlmann) 1984, *Process for the Polymerization of Tetrafluoroethylene in Aqueous Dispersion*, US4481343.
- [95] Hazlebeck, D.E., (W. L. Gore & Associates, Inc.) 1995, *Polymerisation of Liquid Tetrafluoroethylene in Aqueous Dispersion*, US5399640.
- [96] Brinker, K.C. and Bro, M.I., (E.I. du Pont de Nemours and Company) 1958, *Process for polymerizing perfluorinated monomers*, GB805115.
- [97] Tobolsky, A.V., "Dead-end Radical Polymerization", *Journal of the American Chemical Society*, 1958, 80 (22), 5927-5929.
- [98] Tobolsky, A.V., Rogers, C.E., and Brickman, R.D., "Dead-end Radical Polymerization. II", *Journal of the American Chemical Society*, 1960, 82 (6), 1277-1280.
- [99] Plyusnin, A.N. and Chirkov, N.M., "Use of stable radicals for the determination of rate constants of elementary processes", *Theoretical and Experimental Chemistry*, 1966, 2 (6), 563-566.
- [100] Kim, C.U., Lee, J.M., and K. Ihm, S., "Emulsion polymerization of tetrafluoroethylene: effects of reaction conditions on particle formation", *Journal of Fluorine Chemistry*, 1999, 96 (1), 11-21.
- [101] Xu, A., Yuan, W.Z., Zhang, H., Wang, L., Li, H., and Zhang, Y., "Low-molecular-weight polytetrafluoroethylene bearing thermally stable perfluoroalkyl end-groups prepared in supercritical carbon dioxide", *Polymer International*, 2012, 61 (6), 901-908.

- [102] Tabata, Y., Ito, W., Oshima, K., and Takaci, J., "Radiation-Induced Polymerization of Tetrafluoroethylene in Solution", *Journal of Macromolecular Science: Part A - Chemistry*, 1970, 4 (4), 815-824.
- [103] Lai, C.-L., Harwell, J.H., O'Rear, E.A., Komatsuzaki, S., Arai, J., Nakakawaji, T., and Ito, Y., "Formation of Poly(tetrafluoroethylene) Thin Films on Alumina by Admicellar Polymerization", *Langmuir*, 1995, 11 (3), 905-911.
- [104] Krespan, C.G., (E.I. du Pont de Nemours and Company) 1994, *Perfluoroalkyl Sulfide Polymer Solvents for Fluoromonomer Polymerisation*, US5286822.
- [105] Kroll, A.E. and Nelson, D.A., (E.I. du Pont de Nemours and Company) 1956, *Polymerization of tetrafluoroethylene with tertiary butyl peroxide or peracetate*, US2753329.
- [106] Cook, N.C., (General Electric Company) 1956, *Preparation of fluorinated polymers with oxygen difluoride catalyst*, US2757167.
- [107] Krespan, C.G., (E.I. du Pont de Nemours and Company) 1960, *Polymerization of tetrafluoroethylene with selected metal fluorides*, US2938889.
- [108] Engelhardt, V.A., (E.I. du Pont de Nemours) 1967, *Addition polymerisation of polymerizable unsaturated compounds with xenon fluorides as initiators*, US3326874.
- [109] Scoggins, L.E. and Mahan, J.E., (Phillips Petroleum Company) 1971, *Polymerization of Tetrafluoroethylene*, US3592802.
- [110] Kroll, A.E., (E.I. du Pont de Nemours and Company) 1956, *Dispersion polymerisation process for tetrafluoroethylene*, US2750350.
- [111] Halliwell, R.H., (E.I. du Pont de Nemours and Company) 1963, *Low Pressure Tetrafluoroethylene Polymerization Process*, US3110704.
- [112] Hamilton, J.M., (E.I. du Pont de Nemours and Company) 1951, *Polymerization of trifluorochloroethylene in the presence of silver ion, bisulfate ion and persulfate*, US2569524.
- [113] Bro, M.I., Convery, R.J., and Schreyer, R.C., (E. I. du Pont de Nemours and Company) 1961, *Polymerization of fluorine containing monomers*, US2988542.
- [114] Anderson, L.R., Fox, W.B., and Gefri, F.J., (Allied chemical Corporation) 1974, *Fluorinated peroxides*, US3839462.
- [115] Xu, A., Li, H., Yuan, W.Z., Geng, B., Zhang, S., Zhang, H., Wang, L., and Zhang, Y., "Radical homopolymerization of tetrafluoroethylene initiated by perfluorodiacyl peroxide in supercritical carbon dioxide: Reaction mechanism and initiation kinetics", *European Polymer Journal*, 2012, 48 (8), 1431-1438.
- [116] Zhao, C., Zhou, R., Pan, H., Jin, X., Qu, Y., Wu, C., and Jiang, X., "Thermal decomposition of some perfluoro- and polyfluorodiacyl peroxides", *The Journal of Organic Chemistry*, 1982, 47 (11), 2009-2013.
- [117] Bro, M.I., (E.I. du Pont de Nemours and Company) 1962, *Polymerization of perfluoroolefin mixtures*, US3023196.
- [118] Convery, R.J., (E.I. du Pont de Nemours and Company) 1961, *Polymerization catalysts*, US2985673.
- [119] Carlson, N.G., (Minnesota Mining and Manufacturing Company) 1959, *Polymerization of fluoroethylene monomers*, US2912373.
- [120] Ikeda, S., Tabata, Y., Suzuki, H., Miyoshi, T., and Katsumura, Y., "Formation of crosslinked PTFE by radiation-induced solid-state polymerization of tetrafluoroethylene at low temperatures", *Radiation Physics and Chemistry*, 2008, 77 (4), 401-408.
- [121] Dumas, A.C., (The Dow Chemical Company) 1967, *Process for polymerizing tetrafluoroethylene in continuous manner using high energy ionizing radiation*, US3342899.
- [122] Atkinson, B., "The mercury-photosensitised reactions of tetrafluoroethylene", *Journal of the Chemical Society (Resumed)*, 1952 (0), 2684-2694.
- [123] Coffman, D.D., (E.I. du Pont de Nemours and Company) 1962, *Polymerization process using polyfluoroalkanes as initiators*, US3047553.

- [124] Roberts, H.L., (Imperial Chemical Industries) 1962, *Process for Polymerizing Tetrafluoroethylene with Sulfur Chloride Pentafluoride and Ultraviolet Radiation*, US3063922.
- [125] Vogh, J.W., (The Dow Chemical Company) 1966, *Process for Polymerizing Tetrafluoroethylene*, US3228865.
- [126] Clocker, E.T., (Ashland Oil & Refining Company) 1969, *Preparation of halogenated olefin polymers using gaseous phase polymerization in the presence of a carbonyl Initiator*, US3475306.
- [127] Wheeler, A., (E.I. du Pont de Nemours and Company) 1958, *Improvements in or relating to the polymerisation of tetrafluoroethylene*, GB793217.
- [128] Fuhrmann, R. and Jerolamon, D., (Allied Chemical Corporation) 1967, *Gas phase polymerisation of tetrafluoroethylene*, US3304293.
- [129] Felix, B., Hintzer, K., and Lohr, G., (Hoechst Aktiengesellschaft) 1996, *Preparation of a modified polytetrafluoroethylene and use thereof*, US5530078.
- [130] Teumac, F.N., (Fred N. Teumac) 1965, *Polymerization of Tetrafluoroethylene and preparation of Fluorocarbon Waxes*, US3223739.
- [131] Bjornson, G., (Phillips Petroleum Company) 1971, *Isolation of chemical reactants*, US3560466.
- [132] Darby, R.A. and Ellingboe, E.K., (E.I. du Pont de Nemours and Company) 1962, *Polymerization of ethylenically unsaturated compounds with bis(trifluoromethyl)peroxide as polymerization initiator*, US3069404.
- [133] Miller, W.T., (United States Atomic Energy Commission) 1952, *Copolymers of perfluoropropene and tetrafluoroethylene and method of making same*, US2598283.
- [134] Miller, W.T., (W.T. Miller) 1953, *Process for copolymerizing $CF_2=CF_2$ with $CF_2=CFCl$* , US2662072.
- [135] MacKenzie, J.C. and Orzechowski, A., (Cabot Corporation) 1966, *Process for the Polymerization and Copolymerization of Halogenated Mono- and Di-olefins* US3285898.
- [136] Luhmann, B. and Feiring, A.E., "Surfactant effects in polytetrafluoroethylene dispersion polymerization", *Polymer*, 1989, 30 (9), 1723-1732.
- [137] Furrow, C.L., (Phillips Petroleum Company) 1974, *Isolation of polymerisation grade tetrafluoroethylene*, US3804910.
- [138] Carraher, C.E., 2012, *Introduction to Polymer Chemistry*, CRC Press, Boca Raton, Florida.
- [139] Cowie, J.M.G., 1991, *Polymers: Chemistry and Physics of Modern Materials*, Taylor & Francis, Abingdon, United Kingdom.
- [140] Flory, P.J., 1953, *Principles of Polymer Chemistry*, Cornell University Press, Ithaca, New York.
- [141] Misra, G.S., 1993, *Introductory Polymer Chemistry*, J. Wiley & Sons, New York.
- [142] Nicholson, J.W., 2012, *The Chemistry of Polymers*, Royal Society of Chemistry, London, United Kingdom.
- [143] Ravve, A., 2013, *Principles of Polymer Chemistry*, Springer US, New York.
- [144] Stevens, M.P., 1999, *Polymer Chemistry: An Introduction*, Oxford University Press, Oxford, United Kingdom.
- [145] Teegarden, D.M., 2004, *Polymer Chemistry: Introduction to an Indispensable Science*, NSTA Press, National Science Teachers Association, Arlington, Virginia.
- [146] Brandrup, J., Immergut, E.H., and Grulke, E.A., 2003, *Polymer Handbook*, Wiley, New York.
- [147] Slomkowski, S., Alemán José, V., Gilbert Robert, G., Hess, M., Horie, K., Jones Richard, G., Kubisa, P., Meisel, I., Mormann, W., Penczek, S., and Stepto Robert, F.T. "Terminology of polymers and polymerization processes in dispersed systems (IUPAC Recommendations 2011)", *Pure and Applied Chemistry*, 2011, 83 (12), 2229.
- [148] Bunn, C.W., Cobbold, A.J., and Palmer, R.P., "The fine structure of polytetrafluoroethylene", *Journal of Polymer Science*, 1958, 28 (117), 365-376.

- [149] Martin, E.L., (E.I. du Pont de Nemours and Company) 1946, *Polymeric materials*, US2409948.
- [150] Ameduri, B. and Boutevin, B., 2004, *Well-architected Fluoropolymers: Synthesis, Properties and Applications*, Elsevier Science, Amsterdam, The Netherlands.
- [151] Abusleme, J.A. and Maccone, P., (Ausimont S.p.A.) 1995, *Radical (co)polymerization process of fluorinated olefinic monomers in aqueous emulsion*, US5428122.
- [152] Abusleme, J.A. and Gregorio, G., (Ausimont S.p.A.) 1995, *Radical (co)polymerisation process of fluorinated olefinic monomers*, US5434229.
- [153] Treat, T.A., (E.I. du Pont de Nemours and Company) 1994, *Process for synthesizing Fluoropolymers*, US5310836.
- [154] Bro, M.I. and Schreyer, R.C., (E.I. du Pont de Nemours and Company) 1962, *Polymerization of tetrafluoroethylene*, US3032543.
- [155] Anderson, R.F., Edens, W.L., and Larsen, H.A., (E.I. du Pont de Nemours and Company) 1966, *Polytetrafluoroethylene molding powder and its preparation*, US3245972.
- [156] Berry, K.L., (E.I. du Pont de Nemours and Company) 1951, *Aqueous colloidal dispersions of polytetrafluoroethylene and the formation of shaped structures therefrom*, US2559750.
- [157] Duddington, J.E. and Sherratt, S., (Imperial Chemical Industries) 1959, *Improvements in polymerisation processes*, GB821353.
- [158] Smith, R.P., (Imperial Chemical Industries) 1960, *Improved Polymerisation Process*, GB836741.
- [159] Brinker, K.C. and Ross, R.M., (E.I. du Pont de Nemours and Company) 1957, *Process of polymerizing a fluoroethylene in water containing a chloroendic acid compound*, US2816082.
- [160] Brinker, K.C. and Bro, M.I., (E.I. du Pont de Nemours and Company) 1962, *Process for polymerizing tetrafluoroethylene*, US3066122.
- [161] Suwa, T., Takehisa, M., and Machi, S., "Radiation-induced emulsion polymerization of tetrafluoroethylene", *Journal of Applied Polymer Science*, 1974, 18 (8), 2249-2259.
- [162] Kissa, E., 2001, *Fluorinated Surfactants and Repellents*, Taylor & Francis, Abingdon, United Kingdom.
- [163] Matsuda, O., Okamoto, J., Suzuki, N., Ito, M., and Danno, A., "Radiation-induced emulsion copolymerization of tetrafluoroethylene with propylene. IV. Effects of emulsifier concentration and dose rate", *Journal of Polymer Science: Polymer Chemistry Edition*, 1974, 12 (9), 1871-1880.
- [164] Nicole, W., "PFOA and Cancer in a Highly Exposed Community: New Findings from the C8 Science Panel", *Environmental Health Perspectives*, 2013, 121 (11-12), A340-A340.
- [165] Lehmler, H.-J., "Synthesis of environmentally relevant fluorinated surfactants—a review", *Chemosphere*, 2005, 58 (11), 1471-1496.
- [166] Cardinal, A.J., Van Dyk, J.W., and Edens, W.L., (E.I. du Pont de Nemours and Company) 1961, *Novel tetrafluoroethylene resins and their preparation*, GB885809.
- [167] Kellogg, M.W., (M.W. Kellogg Company) 1958, *Improvements in or relating to polymerisation process.*, GB795513.
- [168] Haszeldine, R.N., "473. The addition of free radicals to unsaturated systems. Part I. The direction of radical addition to 3 : 3 : 3-trifluoropropene", *Journal of the Chemical Society (Resumed)*, 1952 (0), 2504-2513.
- [169] Jaeger, H., (Ciba ltd) 1971, *Process for the manufacture of perfluoroalkyl iodides*, US3557224.
- [170] Moore, L.O., "Radical reactions of highly polar molecules. Reactivities in atom abstractions from chloroalkanes by fluoroalkyl radicals", *The Journal of Physical Chemistry*, 1971, 75 (14), 2075-2079.
- [171] Hanford, W.E. and Joyce, R.M., (E.I. du Pont de Nemours and Company) 1951, *Fluorinated compounds*, US2562547.
- [172] Miller, W.T., (W.T. Miller) 1955, *Halocarbon polymers*, US2700661.

- [173] Krespan, C.G., Harder, R.J., and Drysdale, J.J., "Bis-(polyfluoroalkyl)-acetylenes. I. Synthesis of Bis-(polyfluoroalkyl)-acetylenes", *Journal of the American Chemical Society*, 1961, 83 (16), 3424-3427.
- [174] Fearn, J.E., "Synthesis of fluorodienes", *Journal of Research of the National Bureau of Standards, Section A: Physics and Chemistry*, 1971, 75 (1), 41-56.
- [175] Braid, M. and Hauptschein, M., (Pennsalt Chemicals Corporation) 1965, *Method for the preparation of telomer iodides*, US3219712.
- [176] Joyce, R.M., (E.I. du Pont de Nemours and Company) 1951, *Fluorine-containing alcohols and process for preparing the same*, US2559628.
- [177] Fielding, H.C., (Imperial Chemical Industries) 1968, *Adducts of tetrafluoroethylene*, GB1127045.
- [178] Hanford, W.E., (E.I. du Pont de Nemours and Company) 1948, *Organic fluorine-containing sulfur compounds and methods for their preparation*, US2443003.
- [179] Tittle, B. and Platt, A.E., (Imperial Chemical Industries) 1965, *Preparation of tetrafluoroethylene telomers*, GB1007542.
- [180] Platt, A.E. and Tittle, B., "The reaction of chlorofluoroalkanes with triethyl phosphite", *Journal of the Chemical Society C: Organic*, 1967 (0), 1150-1152.
- [181] Battais, A., Boutevin, B., Pietrasanta, Y., Bertocchio, R., and Lantz, A., "Telomerisation du tetrafluoroethylene avec le tetrachlorure de carbone par catalyse redox", *Journal of Fluorine Chemistry*, 1989, 42 (2), 215-232.
- [182] Tatemoto, M. and Nakagawa, T., (Daikin Kogyo Company) 1979, *Segmented polymers containing fluorine and iodine and their production*, US4158678.
- [183] Tatemoto, M., 15-16 February, 1979, presented at the The First Regular Meeting of Soviet-Japanese Fluorine Chemists, Tokyo, Japan.
- [184] Tatemoto, M., (Daikin Industries) 1990, *Fluorine containign elastormer composition*, EP0399543.
- [185] Tatemoto, M., "Development of Iodine Transfer Polymerization and Its Applications to Telechelically Reactive Polymers", *KOBUNSHI RONBUNSHU*, 1992, 49 (10), 765-783.
- [186] Arcella, V., Brinati, G., Albano, M., and Tortelli, V., (Ausimont S.p.A.) 1997, *Fluorinated thermoplastic elastomers having superior mechanical and elastic properties, and the preparation process thereof*, US5612419.
- [187] Arcella, V., Brinati, G., Albano, M., and Tortelli, V., (Ausimont S.p.A.) 1997, *New fluorinated thermoplastic elastomers having superior mechanical and elastic properties, and preparation process thereof*, US5605971.
- [188] Apostolo, M., Arcella, V., Storti, G., and Morbidelli, M., "Free radical controlled polymerization of fluorinated copolymers produced in microemulsion", *Macromolecules*, 2002, 35 (16), 6154-6166.
- [189] Guerre, M., Campagne, B., Gimello, O., Parra, K., Ameduri, B., and Ladmiral, V., "Deeper Insight into the MADIX Polymerization of Vinylidene Fluoride", *Macromolecules*, 2015, 48 (21), 7810-7822.
- [190] Guerre, M., Rahaman, S.M.W., Améduri, B., Poli, R., and Ladmiral, V., "Limits of Vinylidene Fluoride RAFT Polymerization", *Macromolecules*, 2016, 49 (15), 5386-5396.
- [191] Guerre, M., Lopez, G., Soulestin, T., Totée, C., Améduri, B., Silly, G., and Ladmiral, V., "A Journey into the Microstructure of PVDF Made by RAFT", *Macromolecular Chemistry and Physics*, 2016, 217 (20), 2275-2285.
- [192] Liu, L., Lu, D., Wang, H., Dong, Q., Wang, P., and Bai, R., "Living/controlled free radical copolymerization of chlorotrifluoroethene and butyl vinyl ether under ⁶⁰Co [gamma]-ray irradiation in the presence of S-benzyl O-ethyl dithiocarbonate", *Chemical Communications*, 2011, 47 (27), 7839-7841.

- [193] Wang, P., Dai, J., Liu, L., Dong, Q., Jin, B., and Bai, R., "Xanthate-mediated living/controlled radical copolymerization of hexafluoropropylene and butyl vinyl ether under ^{60}Co [gamma]-ray irradiation and preparation of fluorinated polymers end-capped with a fluoroalkyl sulfonic acid group", *Polymer Chemistry*, 2013, 4 (6), 1760-1764.
- [194] Suwa, T., Takehisa, M., and Machi, S., "Melting and crystallization behavior of poly(tetrafluoroethylene). New method for molecular weight measurement of poly(tetrafluoroethylene) using a differential scanning calorimeter", *Journal of Applied Polymer Science*, 1973, 17 (11), 3253-3257.
- [195] Calleja, G., Jourdan, A., Ameduri, B., and Habas, J.-P., "Where is the glass transition temperature of poly(tetrafluoroethylene)? A new approach by dynamic rheometry and mechanical tests", *European Polymer Journal*, 2013, 49 (8), 2214-2222.
- [196] Puts, G., Crouse, P., and Ameduri, B., 2014, "Thermal degradation and pyrolysis of polytetrafluoroethylene", in D.W. Smith, Iacono, S.T., and Iyer, S.S. (eds.), *Handbook of Fluoropolymer Science and Technology*, John Wiley & Sons, Inc., New York.
- [197] Brown, E.N. and Dattelbaum, D.M., "The role of crystalline phase on fracture and microstructure evolution of polytetrafluoroethylene (PTFE)", *Polymer*, 2005, 46 (9), 3056-3068.
- [198] Company, E.I.d.P.d.N.a., *PTFE Handbook*, E.I. du Pont de Nemours and Company, Wilmington, Delaware.
- [199] Wu, S., "Characterization of polymer molecular weight distribution by transient viscoelasticity: Polytetrafluoroethylenes", *Polymer Engineering & Science*, 1988, 28 (8), 538-543.
- [200] Tuminello, W.H., Treat, T.A., and English, A.D., "Poly(tetrafluoroethylene): molecular weight distributions and chain stiffness", *Macromolecules*, 1988, 21 (8), 2606-2610.
- [201] Davidson, T., Gounder, R.N., Weber, D.K., and Wecker, S.M., 1999, "A Perspective on solid state microstructure in polytetrafluoroethylene", in G. Hougham, Cassidy, P.E., Johns, K., and Davidson, T. (eds.), *Fluoropolymers 2: Properties*, Springer US, Boston, Massachusetts.
- [202] Clark, E.S., "The molecular conformations of polytetrafluoroethylene: forms II and IV", *Polymer*, 1999, 40 (16), 4659-4665.
- [203] Rahl, F.J., Evanco, M.A., Fredericks, R.J., and Reimschuessel, A.C., "Studies of the morphology of emulsion-grade polytetrafluoroethylene", *Journal of Polymer Science Part A-2: Polymer Physics*, 1972, 10 (7), 1337-1349.
- [204] Oshima, A., Ikeda, S., Seguchi, T., and Tabata, Y., "Change of molecular motion of polytetrafluoroethylene (PTFE) by radiation induced crosslinking", *Radiation Physics and Chemistry*, 1997, 49 (5), 581-588.
- [205] Oshima, A., Ikeda, S., Katoh, E., and Tabata, Y., "Chemical structure and physical properties of radiation-induced crosslinking of polytetrafluoroethylene", *Radiation Physics and Chemistry*, 2001, 62 (1), 39-45.
- [206] Oshima, A., Ikeda, S., Seguchi, T., and Tabata, Y., "Improvement of radiation resistance for polytetrafluoroethylene (PTFE) by radiation crosslinking", *Radiation Physics and Chemistry*, 1997, 49 (2), 279-284.
- [207] Oshima, A., Ikeda, S., Kudoh, H., Seguchi, T., and Tabata, Y., "Temperature effects on radiation induced phenomena in polytetrafluoroethylene (PTFE)—Change of G-value", *Radiation Physics and Chemistry*, 1997, 50 (6), 611-615.
- [208] Chanzy, H.D., Smith, P., and Revol, J.-F., "High-resolution electron microscopy of virgin poly(tetrafluoroethylene)", *Journal of Polymer Science Part C: Polymer Letters*, 1986, 24 (11), 557-563.
- [209] Khatipov, S.A., Serov, S.A., Sadovskaya, N.V., and Konova, E.M., "Morphology of irradiated polytetrafluoroethylene", *Polymer Science Series A*, 2012, 54 (9), 684-692.

- [210] Chanzy, H., Folda, T., Smith, P., Gardner, K., and Revol, J.-F., "Lattice imaging in polytetrafluoroethylene single crystals", *Journal of Materials Science Letters*, 1986, 5 (10), 1045-1047.
- [211] Yamaguchi, S. and Shimizu, T., "Morphology of Electron Beam-Irradiated Polytetrafluoroethylene Emulsion Particles", *KOBUNSHI RONBUNSHU*, 1982, 39 (5), 339-344.
- [212] Yamaguchi, S., Tatemoto, M., and Tsuji, M., "Fine Structures in As-Polymerized and Sintered Poly (tetrafluoroethylene)", *Sen'i Gakkaishi*, 1996, 52 (12), 657-659.
- [213] Uhlund, K.L., (E.I. du Pont de Nemours and Company) 1963, *Process for the Preparation of Improved Polytetrafluoroethylene Extrusion Powder*, US3088941.
- [214] O'Hagan, D., "Understanding organofluorine chemistry. An introduction to the C-F bond", *Chemical Society Reviews*, 2008, 37 (2), 308-319.
- [215] Koch, E.C., 2012, *Metal-Fluorocarbon Based Energetic Materials*, Wiley, New York.
- [216] Bro, M.I. and Sperati, C.A., "Endgroups in tetrafluoroethylene polymers", *Journal of Polymer Science*, 1959, 38 (134), 289-295.
- [217] Pianca, M., Barchiesi, E., Esposto, G., and Radice, S., "End groups in fluoropolymers", *Journal of Fluorine Chemistry*, 1999, 95 (1-2), 71-84.
- [218] Madorskaya, L.Y., Loginova, N.N., Panshin, Y.A., and Lobanov, A.M., "Role of end groups in polyvinylidene fluoride", *Polymer Science U.S.S.R.*, 1983, 25 (10), 2490-2496.
- [219] Li, L., Twum, E.B., Li, X., McCord, E.F., Fox, P.A., Lyons, D.F., and Rinaldi, P.L., "NMR Study of the Chain End and Branching Units in Poly(vinylidene fluoride-co-tetrafluoroethylene)", *Macromolecules*, 2013, 46 (18), 7146-7157.
- [220] Pellerite, M.J., "Unusual reaction chemistry in thermal decomposition of alkali metal 2-alkoxy-2,3,3,3-tetrafluoropropionate salts", *Journal of Fluorine Chemistry*, 1990, 49 (1), 43-66.
- [221] Company, A.G.C., *Physical Properties of Fluon Unfilled and Filled PTFE: Technical Service Note F12/13*, Asahi Glass Chemicals Company, Tokyo, Japan.
- [222] Rae, P.J. and Dattelbaum, D.M., "The properties of poly(tetrafluoroethylene) (PTFE) in compression", *Polymer*, 2004, 45 (22), 7615-7625.
- [223] Rae, P.J. and Brown, E.N., "The properties of poly(tetrafluoroethylene) (PTFE) in tension", *Polymer*, 2005, 46 (19), 8128-8140.
- [224] Zheng, X., Wen, X., Wang, W., Gao, J., Lin, W., Ma, L., and Yu, J., "Creep-ratcheting behavior of PTFE gaskets under various temperatures", *Polymer Testing*, 2017, 60, 229-235.
- [225] Zheng, X., Wen, X., Gao, J., Yu, J., Lin, W., and Xu, J., "Temperature-dependent ratcheting of PTFE gaskets under cyclic compressive loads with small stress amplitude", *Polymer Testing*, 2017, 57, 296-301.
- [226] Zhang, Z. and Chen, X., "Multiaxial ratcheting behavior of PTFE at room temperature", *Polymer Testing*, 2009, 28 (3), 288-295.
- [227] Zhang, Z., Chen, X., and Wang, Y., "Uniaxial ratcheting behavior of polytetrafluoroethylene at elevated temperature", *Polymer Testing*, 2010, 29 (3), 352-357.
- [228] Speerschneider, C.J. and Li, C.H., "A Correlation of Mechanical Properties and Microstructure of Polytetrafluoroethylene at Various Temperatures", *Journal of Applied Physics*, 1963, 34 (10), 3004-3007.
- [229] Starkweather, H.W., "The effect of absorbed chemicals on the internal motions in poly(tetrafluoroethylene)", *Macromolecules*, 1984, 17 (6), 1178-1180.
- [230] Wortmann, F.J., "Analysing the relaxation behaviour of poly(tetrafluoroethylene) in the α -transition region by applying a two-component model", *Polymer*, 1996, 37 (12), 2471-2476.

- [231] Tobolsky, A.V., Katz, D., and Takahashi, M., "Rheology of polytetrafluoroethylene", *Journal of Polymer Science Part A: General Papers*, 1963, 1 (1), 483-489.
- [232] Araki, Y., "Stress relaxation of polytetrafluoroethylene in the vicinity of its glass transition temperature at about 130°C", *Journal of Applied Polymer Science*, 1965, 9 (4), 1515-1524.
- [233] Araki, Y., "Thermal expansion coefficient of polytetrafluoroethylene in the vicinity of its glass transition at about 400°K", *Journal of Applied Polymer Science*, 1965, 9 (2), 421-427.
- [234] Sauer, B.B., Avakian, P., and Starkweather, H.W., "Cooperative relaxations in semicrystalline fluoropolymers studied by thermally stimulated currents and ac dielectric", *Journal of Polymer Science Part B: Polymer Physics*, 1996, 34 (3), 517-526.
- [235] McCrum, N.G., "An internal friction study of polytetrafluoroethylene", *Journal of Polymer Science*, 1959, 34 (127), 355-369.
- [236] Fai Lau, S., Suzuki, H., and Wunderlich, B., "The thermodynamic properties of polytetrafluoroethylene", *Journal of Polymer Science: Polymer Physics Edition*, 1984, 22 (3), 379-405.
- [237] Durrell, W.S., Stump, E.C., and Schuman, P.D., "The glass transition temperature of polytetrafluoroethylene", *Journal of Polymer Science Part B: Polymer Letters*, 1965, 3 (10), 831-833.
- [238] Marchionni, G., Ajroldi, G., Righetti, M.C., and Pezzin, G., "Molecular interactions in perfluorinated and hydrogenated compounds: linear paraffins and ethers", *Macromolecules*, 1993, 26 (7), 1751-1757.
- [239] Unal, H., Mimaroglu, A., Kadioglu, U., and Ekiz, H., "Sliding friction and wear behaviour of polytetrafluoroethylene and its composites under dry conditions", *Materials & Design*, 2004, 25 (3), 239-245.
- [240] Goyal, R.K. and Yadav, M., "The wear and friction behavior of novel polytetrafluoroethylene/expanded graphite nanocomposites for tribology application", *Journal of Tribology*, 2013, 136 (2), 021601-021601-5.
- [241] Bernett, M.K. and Zisman, W.A., "Relation of wettability by aqueous solutions to the surface constitution of low-energy solids", *The Journal of Physical Chemistry*, 1959, 63 (8), 1241-1246.
- [242] Zhang, J., Li, J., and Han, Y., "Superhydrophobic PTFE Surfaces by Extension", *Macromolecular Rapid Communications*, 2004, 25 (11), 1105-1108.
- [243] Szymczyk, K. and Jańczuk, B., "The wettability of polytetrafluoroethylene by aqueous solution of cetyltrimethylammonium bromide and Triton X-100 mixtures", *Journal of Colloid and Interface Science*, 2006, 303 (1), 319-325.
- [244] Szymczyk, K., Zdziennicka, A., Jańczuk, B., and Wójcik, W., "The wettability of polytetrafluoroethylene and polymethyl methacrylate by aqueous solution of two cationic surfactants mixture", *Journal of Colloid and Interface Science*, 2006, 293 (1), 172-180.
- [245] Szymczyk, K. and Jańczuk, B., "Wettability of a Polytetrafluoroethylene Surface by an Aqueous Solution of Two Nonionic Surfactant Mixtures", *Langmuir*, 2007, 23 (17), 8740-8746.
- [246] Szymczyk, K. and Jańczuk, B., "Wetting Behavior of Aqueous Solutions of Binary Surfactant Mixtures to Poly(tetrafluoroethylene)", *Journal of Adhesion Science and Technology*, 2008, 22 (10-11), 1145-1157.
- [247] Szymczyk, K. and Jańczuk, B., "The wettability of poly(tetrafluoroethylene) by aqueous solutions of ternary surfactant mixtures", *Applied Surface Science*, 2010, 256 (24), 7478-7483.
- [248] Szymczyk, K. and Jańczuk, B., "Wettability of Polymeric Solids by Aqueous Solutions of Anionic and Nonionic Surfactant Mixtures", *Journal of Adhesion Science and Technology*, 2011, 25 (19), 2641-2657.

- [249] Szymczyk, K. and Jańczuk, B., "Surface Tension of Polytetrafluoroethylene and Polymethyl Methacrylate under the Influence of the Fluorocarbon Surfactant Film", *Industrial & Engineering Chemistry Research*, 2012, 51 (43), 14076-14083.
- [250] Szymczyk, K., Zdziennicka, A., Krawczyk, J., and Jańczuk, B., "Correlation between wetting, adhesion and adsorption in the polymer–aqueous solutions of ternary surfactant mixtures–air systems", *Applied Surface Science*, 2014, 288, 488-496.
- [251] Szymczyk, K., González-Martín, M.L., Bruque, J.M., and Jańczuk, B., "Effect of two hydrocarbon and one fluorocarbon surfactant mixtures on the surface tension and wettability of polymers", *Journal of Colloid and Interface Science*, 2014, 417, 180-187.
- [252] Biswas, S.K. and Vijayan, K., "Friction and wear of PTFE — a review", *Wear*, 1992, 158 (1), 193-211.
- [253] Biswal, N.R. and Paria, S., "Effect of electrolyte solutions on the adsorption of surfactants at PTFE–Water interface", *Industrial & Engineering Chemistry Research*, 2010, 49 (15), 7060-7067.
- [254] Biswal, N.R. and Paria, S., "Wetting of PTFE and glass surfaces by aqueous solutions of cationic and anionic double-chain surfactants", *Industrial & Engineering Chemistry Research*, 2012, 51 (30), 10172-10178.
- [255] Yuan, F.Q., Liu, D.D., Guo, L.L., Zhu, Y.W., Xu, Z.C., Huang, J.B., Zhang, L., and Zhang, L., "Effect of branched cationic and betaine surfactants on the wettability of a poly(tetrafluoroethylene) surface", *Wuli Huaxue Xuebao/ Acta Physico - Chimica Sinica*, 2015, 31 (4), 715-721.
- [256] Liu, D.-D., Xu, Z.-C., Zhang, L., Luo, L., Zhang, L., Wei, T.-X., and Zhao, S., "Adsorption Behaviors of Cationic Surfactants and Wettability in Polytetrafluoroethylene–Solution–Air Systems", *Langmuir*, 2012, 28 (49), 16845-16854.
- [257] Zhou, Z.-H., Zhang, Q., Wang, H.-Z., Xu, Z.-C., Zhang, L., Liu, D.-D., and Zhang, L., "Wettability of a PTFE surface by aqueous solutions of zwitterionic surfactants: Effect of molecular structure", *Colloids and Surfaces A: Physicochemical and Engineering Aspects*, 2016, 489, 370-377.
- [258] Gao, L. and McCarthy, T.J., "Teflon is hydrophilic. Comments on definitions of hydrophobic, shear versus tensile hydrophobicity, and wettability characterization", *Langmuir*, 2008, 24 (17), 9183-9188.
- [259] Autumn, K. and Peattie, A.M., "Mechanisms of adhesion in geckos", *Integrative and Comparative Biology*, 2002, 42 (6), 1081-1090.
- [260] Pugmire, D.L., Wetteland, C.J., Duncan, W.S., Lakis, R.E., and Schwartz, D.S., "Cross-linking of polytetrafluoroethylene during room-temperature irradiation", *Polymer Degradation and Stability*, 2009, 94 (9), 1533-1541.
- [261] Dorschner, H., Lappan, U., and Lunkwitz, K., "Electron beam facility in polymer research: Radiation induced functionalization of polytetrafluoroethylene", *Nuclear Instruments and Methods in Physics Research, Section B: Beam Interactions with Materials and Atoms*, 1998, 139 (1-4), 495-501.
- [262] Lappan, U., Geißler, U., and Lunkwitz, K., "Modification of polytetrafluoroethylene by electron beam irradiation in various atmospheres", *Nuclear Instruments and Methods in Physics Research, Section B: Beam Interactions with Materials and Atoms*, 1999, 151 (1-4), 222-226.
- [263] Lappan, U., Geißler, U., and Lunkwitz, K., "Changes in the chemical structure of polytetrafluoroethylene induced by electron beam irradiation in the molten state", *Radiation Physics and Chemistry*, 2000, 59 (3), 317-322.
- [264] Lappan, U. and Geißler, U., "PTFE micropowder functionalized with carboxylic acid groups", *Macromolecular Materials and Engineering*, 2008, 293 (6), 538-542.

- [265] Lunkwitz, K., Bürger, W., Lappan, U., Brink, H.J., and Ferse, A., "Surface modification of fluoropolymers", *Journal of Adhesion Science and Technology*, 1995, 9 (3), 297-310.
- [266] Hopp, B., Geretovszky, Z., Bertóti, I., and Boyd, I.W., "Comparative tensile strength study of the adhesion improvement of PTFE by UV photon assisted surface processing", *Applied Surface Science*, 2002, 186 (1), 80-84.
- [267] Baumgärtner, K.M., Schneider, J., Schulz, A., Feichtinger, J., and Walker, M., "Short-time plasma pre-treatment of polytetrafluoroethylene for improved adhesion", *Surface and Coatings Technology*, 2001, 142 (Supplement C), 501-506.
- [268] Xu, H., Hu, Z., Wu, S., and Chen, Y., "Surface modification of polytetrafluoroethylene by microwave plasma treatment of H₂O/Ar mixture at low pressure", *Materials Chemistry and Physics*, 2003, 80 (1), 278-282.
- [269] Shi, T., Shao, M., Zhang, H., Yang, Q., and Shen, X., "Surface modification of porous poly(tetrafluoroethylene) film via cold plasma treatment", *Applied Surface Science*, 2011, 258 (4), 1474-1479.
- [270] Kolská, Z., Řezníčková, A., Hnatowicz, V., and Švorčík, V., "PTFE surface modification by Ar plasma and its characterization", *Vacuum*, 2012, 86 (6), 643-647.
- [271] Gilman, A., Piskarev, M., Yablokov, M., Kechek'yan, A., and Kuznetsov, A., "Adhesive properties of PTFE modified by DC discharge", *Journal of Physics: Conference Series*, 2014, 516 (1), 012012.
- [272] Sarani, A., De Geyter, N., Nikiforov, A.Y., Morent, R., Leys, C., Hubert, J., and Reniers, F., "Surface modification of PTFE using an atmospheric pressure plasma jet in argon and argon+CO₂", *Surface and Coatings Technology*, 2012, 206 (8), 2226-2232.
- [273] Wang, C., Chen, J.-r., and Li, R., "Studies on surface modification of poly(tetrafluoroethylene) film by remote and direct Ar plasma", *Applied Surface Science*, 2008, 254 (9), 2882-2888.
- [274] Encinas, N., Pantoja, M., Torres-Remiro, M., and Martínez, M.A., "Approaches to poly(tetrafluoroethylene) adhesive bonding", *The Journal of Adhesion*, 2011, 87 (7-8), 709-719.
- [275] Dufour, T., Hubert, J., Viville, P., Duluard, C.Y., Desbief, S., Lazzaroni, R., and Reniers, F., "PTFE surface etching in the post-discharge of a scanning RF plasma torch: Evidence of ejected fluorinated species", *Plasma Processes and Polymers*, 2012, 9 (8), 820-829.
- [276] Badey, J.P., Espuche, E., Jugnet, Y., Chabert, B., and Duct, T.M., "Influence of chemical and plasma treatments on the adhesive properties of PTFE with an epoxy resin", *International Journal of Adhesion and Adhesives*, 1996, 16 (3), 173-178.
- [277] Kaplan, S.L., Lopata, E.S., and Smith, J., "Plasma processes and adhesive bonding of polytetrafluoroethylene", *Surface and Interface Analysis*, 1993, 20 (5), 331-336.
- [278] Fu, C., Liu, S., Gong, T., Gu, A., and Yu, Z., "Investigation on surface structure of potassium permanganate/nitric acid treated poly(tetrafluoroethylene)", *Applied Surface Science*, 2014, 317 (Supplement C), 771-775.
- [279] Wang, C. and Chen, J.-R., "Studies on surface graft polymerization of acrylic acid onto PTFE film by remote argon plasma initiation", *Applied Surface Science*, 2007, 253 (10), 4599-4606.
- [280] Onodera, T., Kawasaki, K., Nakakawaji, T., Higuchi, Y., Ozawa, N., Kurihara, K., and Kubo, M., "Chemical Reaction Mechanism of Polytetrafluoroethylene on Aluminum Surface under Friction Condition", *The Journal of Physical Chemistry C*, 2014, 118 (10), 5390-5396.
- [281] Onodera, T., Nakakawaji, T., Adachi, K., Kurihara, K., and Kubo, M., "Tribochemical Degradation of Polytetrafluoroethylene Catalyzed by Copper and Aluminum Surfaces", *The Journal of Physical Chemistry C*, 2016, 120 (20), 10857-10865.

- [282] Starkweather, H.W. and Wu, S., "Molecular weight distribution in polymers of tetrafluoroethylene", *Polymer*, 1989, 30 (9), 1669-1674.
- [283] Lappan, U., Geißler, U., Häußler, L., Pompe, G., and Scheler, U., "The Estimation of the Molecular Weight of Polytetrafluoroethylene Based on the Heat of Crystallisation. A Comment on Suwa's Equation", *Macromolecular Materials and Engineering*, 2004, 289 (5), 420-425.
- [284] Buckmaster, M.D., Foss, R.V., and Morgan, R.A., (E.I. du Pont de Nemours and Company) 1992, *Melt-processible tetrafluoroethylene/perfluoroolefin copolymers and processes for preparing them*, EP0222945B1.
- [285] Bovey, F.A. and Mirau, P.A., 1996, *NMR of Polymers*, Elsevier Science, Amsterdam, The Netherlands.
- [286] Asakura, T. and Ando, I., 1998, *Solid state NMR of Polymers*, Elsevier Science, Amsterdam, The Netherlands.
- [287] Duer, M.J., 2008, *Solid State NMR Spectroscopy: Principles and Applications*, Wiley, New York.
- [288] Reinsberg, S.A., Ando, S., and Harris, R.K., "Fluorine-19 NMR investigation of poly(trifluoroethylene)", *Polymer*, 2000, 41 (10), 3729-3736.
- [289] Aimi, K., Ando, S., Avalle, P., and Harris, R.K., "Solid-state ^{19}F MAS and $^1\text{H}\rightarrow^{19}\text{F}$ CP/MAS NMR study of the phase transition behavior of vinylidene fluoride-trifluoroethylene copolymers: 1. Uniaxially drawn films of VDF 75% copolymer", *Polymer*, 2004, 45 (7), 2281-2290.
- [290] Aimi, K. and Ando, S., "Solid-state ^{19}F MAS and $^1\text{H}\rightarrow^{19}\text{F}$ CP/MAS NMR study of the phase-transition behavior of vinylidene fluoride-trifluoroethylene copolymers: 2. semi-crystalline films of VDF 75% copolymer", *Polymer Journal*, 2012, 44 (8), 786-794.
- [291] Boyer, C., Valade, D., Sauguet, L., Ameduri, B., and Boutevin, B., "Iodine transfer polymerization (ITP) of vinylidene fluoride (VDF). Influence of the defect of VDF chaining on the control of ITP", *Macromolecules*, 2005, 38 (25), 10353-10362.
- [292] Guerre, M., Wahidur Rahaman, S.M., Ameduri, B., Poli, R., and Ladmiral, V., "RAFT synthesis of well-defined PVDF-b-PVAc block copolymers", *Polymer Chemistry*, 2016, 7 (45), 6918-6933.
- [293] Oshima, A., Tabata, Y., Kudoh, H., and Seguchi, T., "Radiation induced crosslinking of polytetrafluoroethylene", *Radiation Physics and Chemistry*, 1995, 45 (2), 269-273.
- [294] Oshima, A., Seguchi, T., and Tabata, Y., "ESR study on free radicals trapped in crosslinked polytetrafluoroethylene (PTFE)", *Radiation Physics and Chemistry*, 1997, 50 (6), 601-606.
- [295] Oshima, A., Seguchi, T., and Tabata, Y., "ESR study on free radicals trapped in crosslinked polytetrafluoroethylene(PTFE)—II radical formation and reactivity", *Radiation Physics and Chemistry*, 1999, 55 (1), 61-71.
- [296] Lappan, U., Häußler, L., Pompe, G., and Lunkwitz, K., "Thermal stability of electron beam-irradiated polytetrafluoroethylene", *Journal of Applied Polymer Science*, 1997, 66 (12), 2287-2291.
- [297] Fischer, D., Lappan, U., Hopfe, I., Eichhorn, K.J., and Lunkwitz, K., "FTi.r. Spectroscopy on electron irradiated polytetrafluoroethylene", *Polymer*, 1998, 39 (3), 573-582.
- [298] Lappan, U., Geißler, U., and Lunkwitz, K., "Electron beam irradiation of polytetrafluoroethylene in vacuum at elevated temperature: an infrared spectroscopic study", *Journal of Applied Polymer Science*, 1999, 74 (6), 1571-1576.
- [299] Schierholz, K., Lappan, U., and Lunkwitz, K., "Electron beam irradiation of polytetrafluoroethylene in air: investigations on the thermal behaviour", *Nuclear Instruments and Methods in Physics Research, Section B: Beam Interactions with Materials and Atoms*, 1999, 151 (1-4), 232-237.

- [300] Fuchs, B., Lappan, U., Lunkwitz, K., and Scheler, U., "Radiochemical yields for cross-links and branches in radiation-modified poly(tetrafluoroethylene)", *Macromolecules*, 2002, 35 (24), 9079-9082.
- [301] Allayarov, S.R., Konovalikhin, S.V., Olkhov, Y.A., Jackson, V.E., Kispert, L.D., Dixon, D.A., Ila, D., and Lappan, U., "Degradation of γ -irradiated linear perfluoroalkanes at high dosage", *Journal of Fluorine Chemistry*, 2007, 128 (6), 575-586.
- [302] Lappan, U., Geißler, U., and Scheler, U., "The influence of the irradiation temperature on the ratio of chain scission to branching reactions in electron beam irradiated polytetrafluoroethylene (PTFE)", *Macromolecular Materials and Engineering*, 2007, 292 (5), 641-645.
- [303] Geißler, U. and Lappan, U., "Particle size distribution and carboxy group content of irradiated polytetrafluoroethylene (PTFE) micropowders", *Gummi, Fasern, Kunststoffe*, 2011, 64 (6), 351-353.
- [304] Perelygin, I.S., Peskova, M.Z., Zakirov, Z.Z., and Glinkin, I.M., "Determination of the crystallinity of polytetrafluoroethylene from infrared absorption spectra", *Journal of Applied Spectroscopy*, 24 (6), 732-734.
- [305] Bottenbruch, L., *Technische Thermoplaste*, Hanser, Munich, Germany.
- [306] Hu, T.-Y., "Characterization of the crystallinity of polytetrafluoroethylene by X-ray and IR spectroscopy, differential scanning calorimetry, viscoelastic spectroscopy and the use of a density gradient tube", *Wear*, 1982, 82 (3), 369-376.
- [307] Coelho, A. "TOPAS-Academic", **2016**, 6.
- [308] Chu, B., Wu, C., and Buck, W., "Light-scattering characterization of poly(tetrafluoroethylene)", *Macromolecules*, 1988, 21 (2), 397-402.
- [309] Sperati, C.A. and Starkweather, H.W., 1961, "Fluorine-containing polymers. II. Polytetrafluoroethylene", in (eds.), *Fortschritte Der Hochpolymeren-Forschung*, Springer Berlin Heidelberg, Berlin, Germany.
- [310] Doban, R.C., Knight, A.C., Peterson, J.H., and Sperati, C.A., 1956, "The molecular weight of polytetrafluoroethylene", presented at the Meeting of the American Chemical Society, Atlantic City, The American Chemical Society.
- [311] The Chemours Company, 2017, *Electronics cable applications*, retrieved on 13/09/2017 from https://www.chemours.com/Cabling_Solutions/en_US/uses_apps/electronics_cable.html
- [312] The Chemours Company, 2017, *How Teflon™ fluoroplastics enabled martian exploration*, retrieved on 13/09/2017 from https://www.chemours.com/Teflon_Industrial/en_US/uses_apps/case_studies/teflon-fluoroplastics-mars-exploration-rovers.html
- [313] Bola Company, 2017, *Bola PTFE products*, retrieved on 13/09/2017 from <http://www.bola.de/en/products.html>
- [314] The Chemours Company, 2017, *Pharmaceutical and biopharma manufacturing*, retrieved on 13/09/2017 from https://www.chemours.com/Teflon_Industrial/en_US/uses_apps/pharmaceutical/index.html
- [315] The Chemours Company, 2017, *Long-life valve withstands corrosive environments*, retrieved on 13/09/2017 from https://www.chemours.com/Teflon_Industrial/en_US/uses_apps/case_studies/teflon-next_casestudy.html
- [316] The Chemours Company, 2017, *Filtration membrane increases air flow, lowers operating costs*, retrieved on 13/09/2017 from https://www.chemours.com/Teflon_Industrial/en_US/uses_apps/case_studies/teflon-ptfe_app_profile.html

- [317] AccuTrex Products Incorporated, 2017, *Teflon® & PTFE gaskets*, retrieved on 13/09/2017 from <http://www.accutrex.com/ptfe-gaskets>
- [318] Henning Gasket & Seals Incorporated, 2017, *PTFE gaskets, seals & washers*, retrieved on 13/09/2017 from <http://www.henniggasket.com/ptfe>
- [319] Swagelok Company, 2017, *Ball valves*, retrieved on 13/09/2017 from <https://www.swagelok.com/en/product/Valves/Ball>
- [320] Miller-Stephenson Incorporated, 2017, *PTFE dry film lubricants*, retrieved on 13/09/2017 from <https://www.miller-stephenson.com/chemicals/lubricants/ptfe-dry-film-lubricants/>
- [321] WD-40 Company, 2017, *Dirt & dust resistant dry lube PTFE spray*, retrieved on 13/09/2017 from <https://www.wd40specialist.com/products/dry-lube/>
- [322] Fabreeca International Incorporated, 2017, *Fabreeca-PTFE bearing pad*, retrieved on 13/09/2017 from <https://www.fabreeca.com/products/fabreeca-ptfe-bearing-pad/>
- [323] Saxton, J.L., 2007, "Report on the Millau Viaduct", presented at the Proceedings of Bridge Engineering 2 Conference 2007, University of Bath, Bath, UK, University of Bath.
- [324] The Chemours Company, 2017, *Better food processing with Teflon™*, retrieved on 13/09/2017 from https://www.chemours.com/Teflon Industrial/en_US/uses_apps/food_processing/index.html
- [325] Toefco Engineered Coating Systems Incorporated, 2017, *PTFE industrial coating: History and common applications* retrieved on 13/09/2017 from <http://toefco.com/ptfe-history-and-common-applications/>
- [326] Green Belting Industries Limited, 2017, *PTFE and silicone performance coatings*, retrieved on 13/09/2017 from <http://www.greenbelting.com/about/ptfe-and-silicone-coatings.html>
- [327] W. L. Gore and Associates, 2017, *The GORE-TEX® membrane*, retrieved on 13/09/2017 from <https://www.gore-tex.com/technology/gore-tex-membrane>
- [328] Berardinelli, L., "Grafts and graft materials as vascular substitutes for haemodialysis access construction", *European Journal of Vascular and Endovascular Surgery*, 2006, 32 (2), 203-211.
- [329] Williams, M.R., Mikulin, T., Lemberger, J., Hopkinson, B.R., and Makin, G.S., "Five year experience using PTFE vascular grafts for lower limb ischaemia", *Annals of The Royal College of Surgeons of England*, 1985, 67 (3), 152-155.
- [330] MAQUET Holding GmbH & Co., 2017, *PTFE vascular grafts*, retrieved on 13/09/2017 from <http://www.atriummed.com/en/vascular/PTFEgrafts-peripheral.asp>
- [331] Maitz, M.F., "Applications of synthetic polymers in clinical medicine", *Biosurface and Biotribology*, 2015, 1 (3), 161-176.

Chapter 3

Tetrafluoroethylene generator and Carius tube manifold design

3.1 Introduction

Tetrafluoroethylene cannot be obtained easily from commercial sources, although small quantities can be purchased from speciality chemical suppliers. Transport legislation varies by country and, in the continental USA, bulk transport of the stabilised liquid is permitted; however, most commercially produced TFE is generated at the usage site, mainly due to safety and regulatory considerations, but also due to the cost of transport. Stabilised TFE has the UN number 1081 and falls in transport class 2 with a classification of 2F.

There are numerous methods to produce TFE with the most salient examples being ultra-fast pyrolysis of chlorodifluoromethane, ultra-fast, plasma pyrolysis of tetrafluoromethane [1, 2], dechlorination of $\text{CF}_2\text{Cl}-\text{CF}_2\text{Cl}$, or the debromination of $\text{CF}_2\text{Br}-\text{CF}_2\text{Br}$, pyrolysis of trifluoroacetic acid or the alkali salts of perfluoropropanoic acid [3], and the pyrolysis of polytetrafluoroethylene under vacuum [4]. These methods have been extensively reviewed elsewhere [5] and are mentioned in detail in Chapter 2. The following discussion is only a brief overview of the synthetic routes for TFE production.

The industrial synthesis of tetrafluoroethylene follows the chlorodifluoromethane route, in which chlorodifluoromethane is pyrolysed at temperatures between 750 °C and 950 °C. The major drawback of this, and most other routes is the production of byproducts such as HF, HCl, and chlorofluorocarbon side products that must be scrubbed or cryogenically distilled from the tetrafluoroethylene. Besides being dirty, such processes require costly equipment and are difficult to operate in batch. Therefore, these methods are not readily usable on laboratory scale.

A second option is the perfluoropropionate alkali metal salt pyrolysis route, which produces CO_2 and TFE in a 1:1 ratio as well as a metal fluoride. This method is facile and safe, but generation of completely pure TFE requires the removal of CO_2 from the gas mixture. This method is not exceptionally expensive, provided one has ready access to commercial entities that can supply the acids. The purchase and import of the acid in bulk is beyond the reach of the FMG's budget and we are not permitted to store bulk quantities of the acid at the University of Pretoria due to safety concerns regarding the potential bio-accumulation and carcinogenic effects of the acid. Therefore, this route was not viable at the University of Pretoria.

The remaining option for TFE generation was the vacuum pyrolysis of polytetrafluoroethylene. This option has already been pursued to a great extent in the Fluoro-Materials Group. However, the existing depolymerisation unit at the Fluoro-Materials Group was designed and built as a test reactor for a much larger system to be built at the Nuclear Energy Corporation of South Africa's

Pelchem subsidiary, and this system was not amenable to supplying the laboratory with TFE for polymerisation.

Consequently, a system for the pyrolysis of PTFE on the 10- to 100-g scale was designed and constructed. This system must be capable of being coupled to a Parr polymerisation autoclave or to a Carius tube manifold, providing a complete generation-to-polymerisation solution for the laboratory.

It must also be noted here that the use of an autoclave, or any large vessel, for TFE polymerisation, brings with it the potential for a violent explosion, should a novel polymerisation reaction result in runaway conditions, and for TFE deflagration. For this reason, a small volume reaction system was required when piloting novel reactions. Carius tubes are an obvious choice as reaction system, combining design simplicity, inertness to the reaction medium and, to a certain extent, inherent safety. However, a Carius tube facility was not available to the Fluoro-Materials Group. A further objective was to design and construct a Carius tube system for use with TFE. This chapter relates the design and construction of said systems.

3.2 Design philosophy

3.2.1 Depolymerisation reactor system

The flow diagram for the full process, as generally employed, is presented in Figure 29. In summary: from the depolymerisation reactor, the pyrolysis gas flows to a cold trap and remains there for the duration of the pyrolysis reaction. Upon completion of the pyrolysis reaction, the TFE batch may be recovered by gentle heating of the cold trap using an ice bath. Purifying the captured gas by cryogenic distillation is an optional step, as is long-term storage.

The limited facilities and laboratory space at the University of Pretoria placed some constraints on the design of the depolymerisation reactor system. The system was designed such that:

- The pyrolysis unit can be used with the existing systems in the laboratory (such as the gas manifolds and the available tube furnace);
- The pyrolysis unit is compact and transportable as well as storable; and
- The pyrolysis unit has safety features that prevent pressure buildup and/or explosion of the unit.

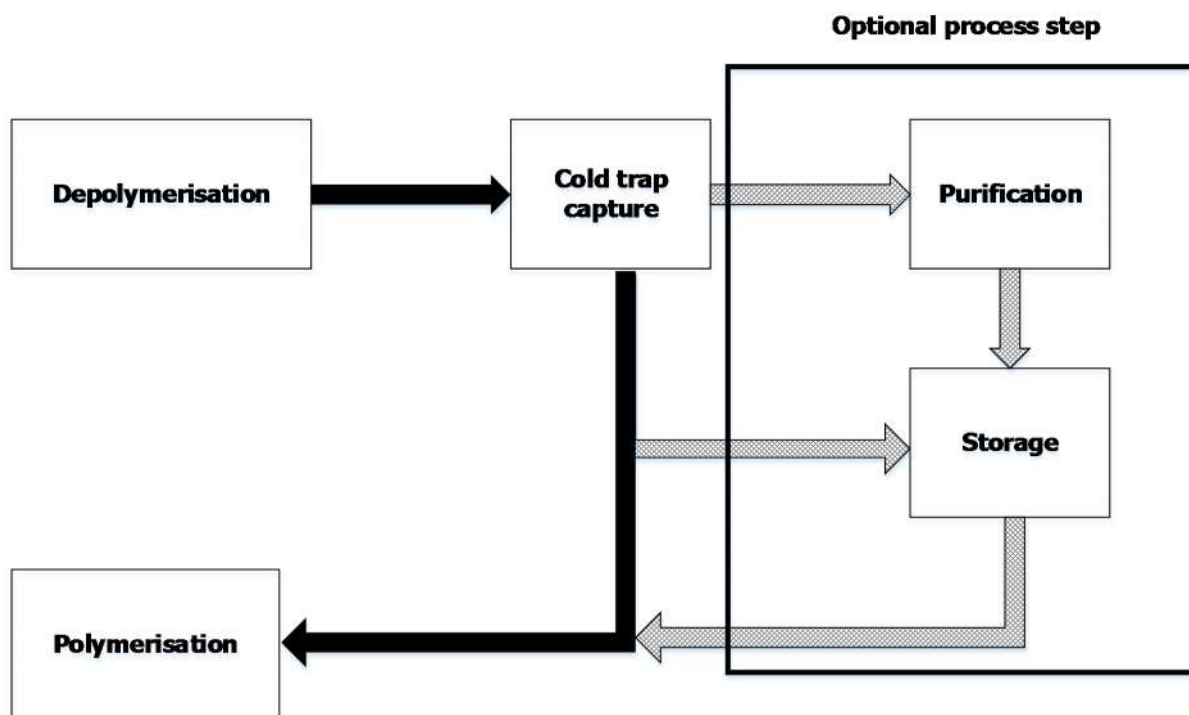


Figure 29: *Flow diagram detailing the general process from depolymerisation to polymer synthesis.*

To meet these requirements the pyrolysis system was constructed from off-the-shelf Swagelok components, keeping to a minimum the amount of custom manufacturing. Furthermore, the actual pyrolysis furnace chamber was made detachable from the cold trap and reactor coupling section of the depolymerisation system. Finally, the system was equipped with not only a pressure gauge, but also a blow-off valve to protect against overpressure.

As the long term storage of TFE comes with serious safety considerations, and as UP does not have bunkers for the storage of bulk explosives, the purification and storage steps were forgone and the system was built to be capable of being connected to the polymerisation rig immediately after completion of the depolymerisation procedure, using the cold trap as temporary TFE reservoir. It must be understood here that, although TFE can be stored safely when mixed with small amounts of monoterpenes, the legal requirements for TFE storage cannot be met with the current laboratory site.

Furthermore, in order to ensure some form of inherent safety in the design, the recommendation from the literature [6-8] regarding tube diameters was implemented. In summary: use ¼"-o.d. tubing for the TFE flow path wherever possible.

Additionally, excess TFE should, according to industry best practice and an environmentally sympathetic mind-set, be destroyed by burning. However, owing to the impracticality of this procedure on a lab scale, excess TFE need, in this case, not be destroyed, merely vented from

the lab in a safe manner. Therefore, the depolymerisation unit was equipped with valves for venting and inert gas purging of the system after use.

3.2.2 Carius tube system

The flow diagram for the process employed when using Carius tubes for polymerisation is depicted in Figure 30.

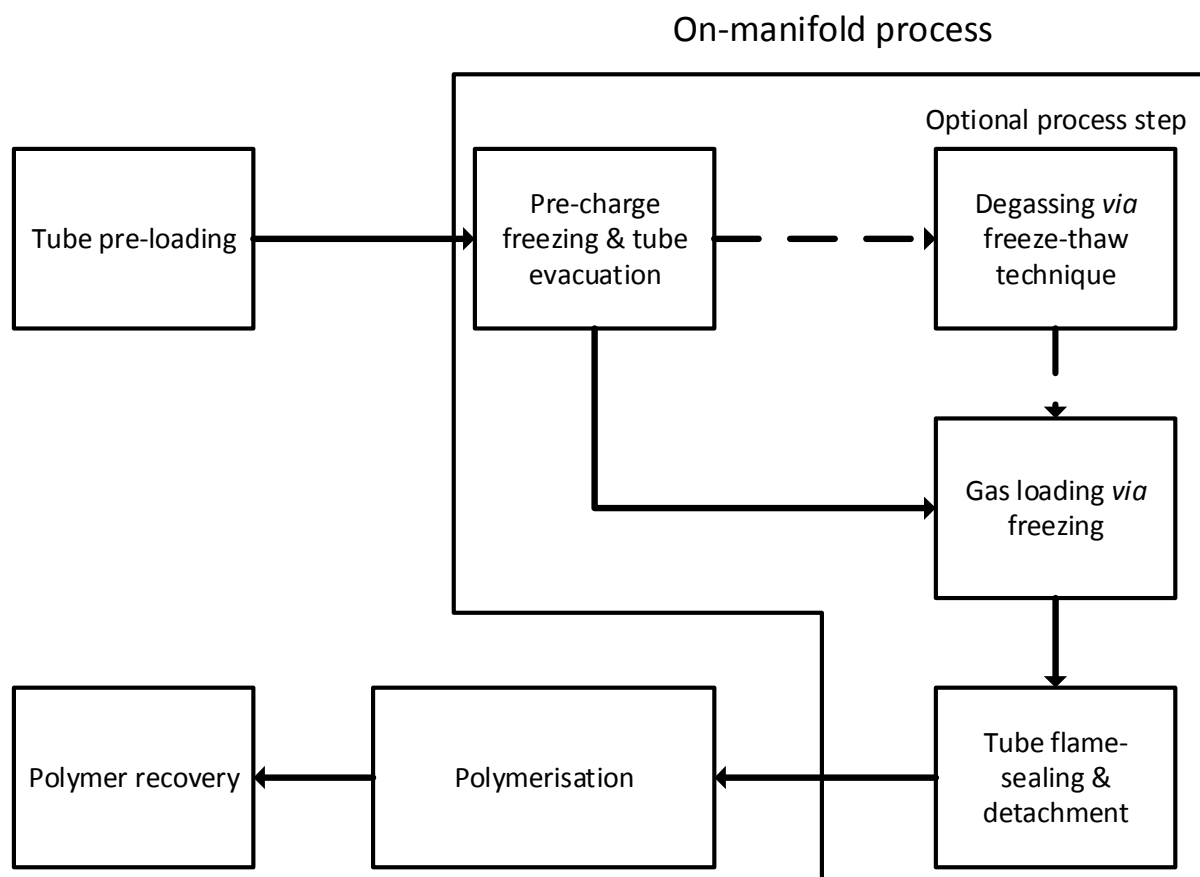


Figure 30: *Flow diagram detailing the general process for the use of Carius tubes in polymer synthesis.*

Owing to prior experience with-, and access to a working Carius tube manifold and tube shaker system during a pre-doctoral sabbatical at the Institute Charles Gerhardt in Montpellier, there was no need to undertake a careful design study for the construction of such a manifold; the Carius tube system in Montpellier was simply reproduced from memory. The addition of a fixed volume preloading chamber for accurate estimation of the mass of added monomer gas was the only notable alteration to the French design.

Since the safety aspects of the French design assumed the availability of a bunker for the tube shaker, the design also includes schematics for a blast-resistant chamber for the safe heating of Carius tubes.

3.3 Depolymerisation reactor design

3.3.1 Design overview

The depolymerisation system, detailed in Figure 31, was designed taking into account the design considerations mentioned in Section 3.2.1.

From the depolymerisation reactor to the cold trap, the line was specified as 1"-o.d., so as to minimise side reactions of the hot TFE, and all other lines were specified as ¼"-o.d., so as to minimise the surface area available for TFE decomposition. The valves were all specified to have the largest flow co-efficient of their class, so as to minimise frictional heating of the TFE under flow.

The mechanical design and sizing of the depolymerisation vessel as well as the sizing of the cold trap will be discussed in the subsequent sections.

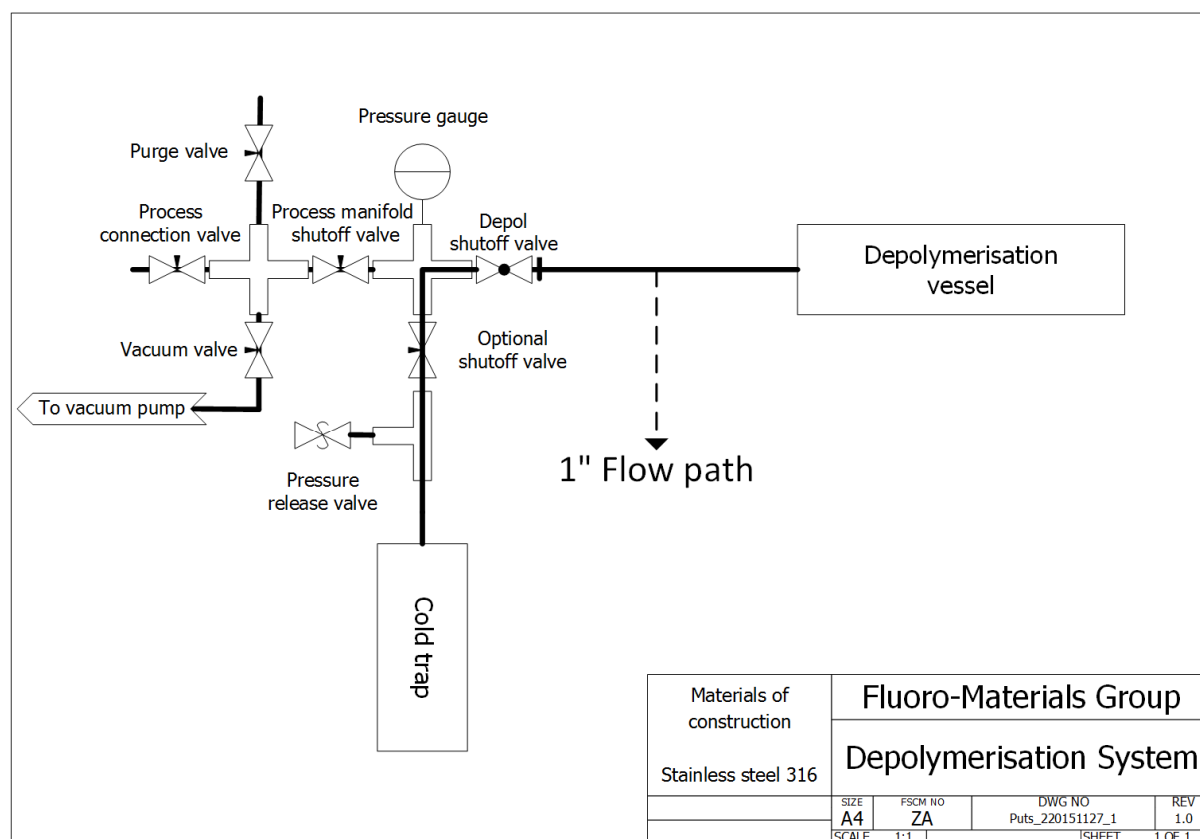


Figure 31: Piping diagram for the depolymerisation reactor system.

The bill of materials for the Swagelok fittings used in this design is presented in Table 9. The pressure gauge was supplied by Wika Instruments (Type 232.50, 100-mm dial size with ¼" MNPT lower back mount) specified for pressures from -1 to 30 bar (gauge pressure).

The cold trap was supplied by Hoke and specified as a 500-mL formed, single ended 304 stainless steel sample cylinder with a ¼"-o.d. FNPT inlet (Part No.: 4HS500). The inlet was initially specified as 1"-o.d. to maintain a single diameter flowpath, but, no supplier could be found that would supply a single ended pressure cylinder with a 1"-o.d. NPT inlet, hence the next largest size was specified. The cylinder is capable of handling up to 124 bar of gauge gas pressure. The weldable 1"-o.d. KF25 flange socket for the depolymerisation vessel was supplied by Pfeiffer Vacuum. Pfeiffer also supplied the sealing rings and KF25 clamps. The depolymerisation vessel was manufactured from locally sourced 316 stainless steel pipe offcuts and 4 mm metal sheet.

Table 9: *Bill of materials for the depolymerisation reactor.*

Quantity	Part description	Swagelok part number
1	3-Piece Ball Valve 1" FNPT	SS-65TF16
3	Short Hex Nipple 1" MNPT	SS-16-HN
1	Pipe Cross 1" FNPT	SS-16-CS
1	Pipe Tee 1" FNPT	SS-16-T
3	Reducing Bushing 1" FNPT to ¼" MNPT	SS-16-RB-4
1	Reducing Nipple 1" MNPT to ¼" MNPT	SS-16-HRN-4
1	Short Hex Nipple ¼" MNPT	SS-4-HN
1	Long Hex Nipple ¼" MNPT	SS-4-HLN-3
1	Pipe Cross ¼" FNPT	SS-4-CS
1	Street Elbow ¼" MNPT to ¼" FNPT	SS-4-SE
1	¼" MNPT to ¼" CP*	SS-400-1-4
1	Mud Dauber Fitting ¼" MNPT	SS-MD-4
4	Needle Valve ¼" FNPT to ¼" MNPT	SS-1RM4-F4
1	KF25 Flange to ¼" MNPT	JNWMPT2514
1	KF25 Flange to 1" MNPT	JNWMPT2510
1	Steel Braid Hose ¼" Fitting	SS-FM4TA4TA4-36
1	¼" CP to DESO Quick Connect	SS-QC4-S-400
1	High-Pressure Proportional Relief Valve	SS-4R3A5
1	Blue Spring Kit 3.4 to 24.1 bar	177-R3A-K1-A

* CP means "Compression fitting"

3.3.2 Depolymerisation vessel mechanical design

The design schematics for the depolymerisation vessel are presented in Figure 34 and Figure 35. As will be discussed hereafter, the depolymerisation vessel is built out of two sections, the large furnace insert vessel and the 1" exit tube. This design was chosen over a single diameter as the local availability of vacuum flanges was limited to type KF25, for which the maximum tube diameter is 1", and a trade-off was required between providing the maximum space for pyrolysis gas to expand into and being able to construct the system connections from locally sourced parts.

3.3.2.1 Furnace insert vessel sizing

The available tube furnace has an internal diameter of 75 mm. Therefore, the depolymerisation vessel furnace insert, under effects of thermal expansion, must not exceed this diameter, but must still be as large as possible to provide the maximum volume for the pyrolysis gases to expand into when exiting the molten PTFE mass, in order to minimise unwanted side reactions. The equation used to calculate annular thermal expansion is presented in Equation (7).

$$D_1 = D_0(\alpha \cdot \Delta T + 1) \quad (7)$$

Here, D is the external diameter of the tube, α is the thermal expansion of 316 stainless steel ($1.99 \times 10^{-5} \text{ m} \cdot \text{m}^{-1} \cdot \text{K}^{-1}$ [9]), and ΔT is the temperature difference (in this case $750 \text{ }^\circ\text{C} - 35 \text{ }^\circ\text{C}$, or $715 \text{ }^\circ\text{C}$). For the purposes of this application, $750 \text{ }^\circ\text{C}$ is considered the maximum operating temperature at which depolymerisation may take place.

The metal suppliers registered with the University of Pretoria carry various sizes of stainless steel pipes, but tubing only in sizes smaller than 1"-o.d., and no foundry or machine shop could be found that would cast a vessel to specific dimensions. For the sake of practicality and minimisation of costs, the depolymerisation vessel will have to be made from commonly available stainless steel pipes.

Stainless steel pipes and tubes come in specific nominal sizes (*viz.* 1", 1.5", 2", 2.5", 3", *etc.*) and Schedule 40 pipes are the most commonly available type of pipe. Table 10 gives the outer diameters of some schedule 40 pipes at ambient and $750 \text{ }^\circ\text{C}$. The data shows that 3" is too large and the clearance for a 2.5" pipe is less than 1 mm, smaller than what is considered prudent, so, therefore, the 2" Schedule 40 pipe is the most suitable for vessel construction.

Table 10: *Schedule 40 pipe outer diameters at ambient and maximum operation temperature.*

Nominal pipe size	OD (mm) at 25 °C	OD (mm) at 750 °C
1½ "	48.26	48.95
2"	60.33	61.18
2½ "	73.03	74.06
3"	88.90	90.16

The tube furnace hot zone is approximately 500 mm long, and the mullite working tube is approximately 1 m long. To ensure even temperature distribution throughout the polymer bed, the depolymerisation vessel should be shorter than 500 mm, and the vessel length was specified at 300 mm as a matter of convenience.

3.3.2.2 Exit tube sizing

As the best high-temperature seal supplied by Pfeiffer Vacuum (our local supplier of vacuum fittings and equipment) boasts a safe working temperature of only 250 °C, the exit tube from the depolymerisation-furnace insert should not only be longer than the remainder of the mullite working tube (~350 mm), but also be long enough that the temperature at the seal connection end be well below this safe working temperature.

The furnace operates at 30 A and 220 V single phase power when under maximum draw and under maximum load; 5.28 kW of real power is pushed by the elements. The furnace is temperature controlled, and the power input into the depolymerisation vessel is variable as the controller will always attempt to maintain the set temperature. Therefore, the section of the tube exiting the furnace can be modelled as if it were attached to a wall of constant temperature. It is assumed that all energy is lost *via* convective and radiative heat loss and no energy passes through the fluorocarbon seal. It is also assumed that, given the vacuum conditions in the depolymerisation vessel, the tetrafluoroethylene flowing through the tube has no impact on the heat transfer in the tube wall.

The aforementioned assumptions render the calculation similar to the classical case of heat loss *via* a fin attached to a heat sink; however, the radiative heat loss term makes the governing equations so non-linear that conventional analytical techniques cannot be used. McWilliams *et al.* [10] published the method for the numerical determination of the longitudinal temperature profile in a cylindrical rod attached to a wall of constant temperature. Their method was employed to approximate the longitudinal temperature profile in the exit tube. The method was

not modified to reflect the annular nature of the tube as the derivation of the governing equation is thereby rendered too complex.

The governing heat transfer equation is presented in Equation (8) and the transformed equations used to calculate the longitudinal temperature profile in the tube are presented in Equations (9) to (14).

$$\frac{d}{dz} \left(k \frac{dT}{dz} \right) = \left(\frac{2h}{R} \right) (T - T_a) + \left(\frac{2\alpha}{R} \right) (\epsilon T^4 - \sigma T_a^4) \quad (8)$$

$$\alpha^2 \frac{d^2\theta}{d\rho^2} = 2\beta(\theta - \theta_a) + 2\gamma(\theta^4 - \theta_a^4) \quad (9)$$

$$\frac{d\theta}{d\rho} = \int \left(\frac{d^2\theta}{d\rho^2} \right) d\rho + \left(\frac{d\theta}{d\rho} \right)_0 \quad (10)$$

$$\theta = \int \left(\frac{d\theta}{d\rho} \right) d\rho + \theta_0 \quad (11)$$

$$\alpha = \frac{R}{L} \quad (12)$$

$$\beta = R \frac{h_{avg}}{k_{avg}} \quad (13)$$

$$\gamma = \frac{\beta(\sigma\epsilon_{avg}T_w^3)}{h_{avg}} \quad (14)$$

Here T is the surface temperature of the tube at any position along its length, T_w is the temperature of the isothermal wall, T_a is the ambient temperature, L is the total length of the tube, z is the length of the tube, R is the radius of the tube, h is the convective heat transfer coefficient, k is the thermal conductivity of the tube, ϵ is the emissivity coefficient, and σ is the Stefan-Boltzmann constant. The transformation variables are defined as $\theta = \frac{T}{T_w}$, $\theta_a = \frac{T_a}{T_w}$ and $\rho = \frac{z}{L}$. The conductive- and convective heat transfer coefficients are a function of temperature, but simple correlations could not be found for them and they were approximated as constant over the temperature range in question. The values for h , k , and ϵ were taken as constant and equal to h_{avg} , k_{avg} , and ϵ_{avg} .

A schematic representation of the thermal geometry is given in Figure 32.

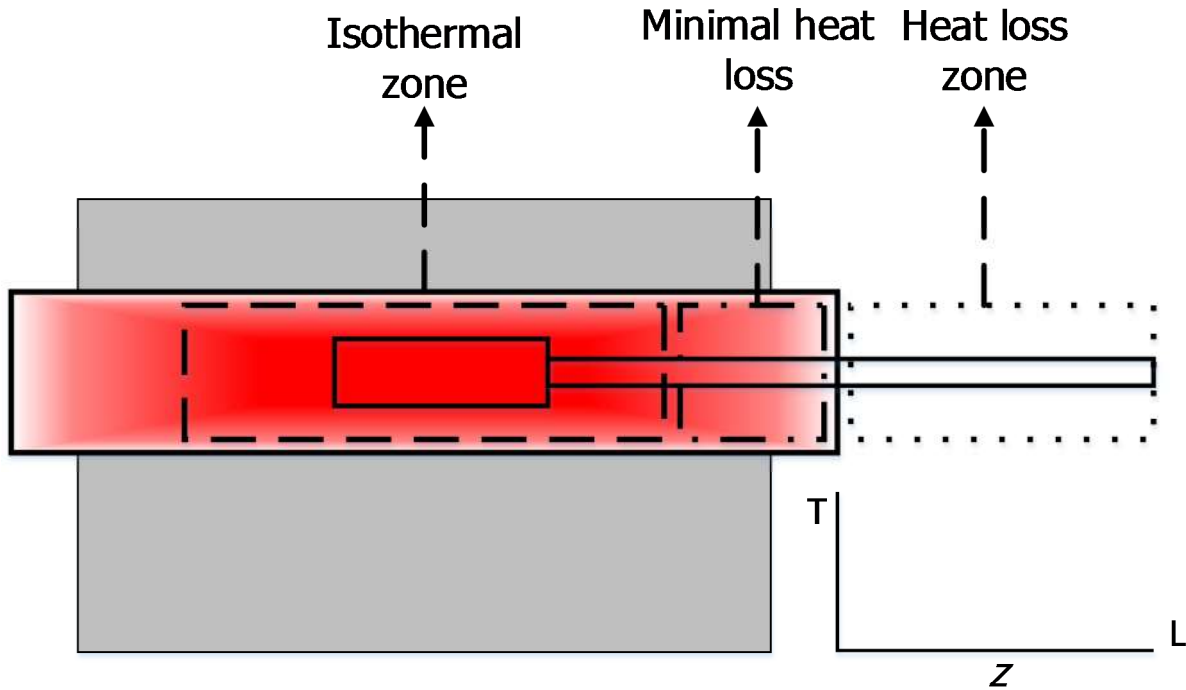


Figure 32: *Depolymerisation vessel thermal geometry detailing the various temperature zones.*

The calculations were performed in MS Excel, following the method stipulated in the literature and using an integration step size of 1 mm. The ambient temperature was taken as 30 °C, the emissivity of stainless steel taken as 0.56 [11], the thermal conductivity taken as $21.4 \text{ W}\cdot\text{m}^{-1}\cdot\text{K}^{-1}$ [9], and the convective heat transfer coefficient taken as $\sim 25 \text{ W}\cdot\text{m}^{-2}\cdot\text{K}^{-1}$ for natural- and $200 \text{ W}\cdot\text{m}^{-2}\cdot\text{K}^{-1}$ for forced air convection over the outside of the tube.

The approximated longitudinal temperature profile in the tube wall is presented in Figure 33 for both natural- and forced air convection. The temperature profile indicates that with a 30-cm section of tube protruding from the furnace, the temperature at the seal should be around 60 °C, assuming natural convection cooling, but that little improvement in the temperature is gained with longer sections, hence, the use of a 30-cm protrusion.

The total length of the exit tube comes to 650 mm, and the reactor vessel has a total length of 950 mm.

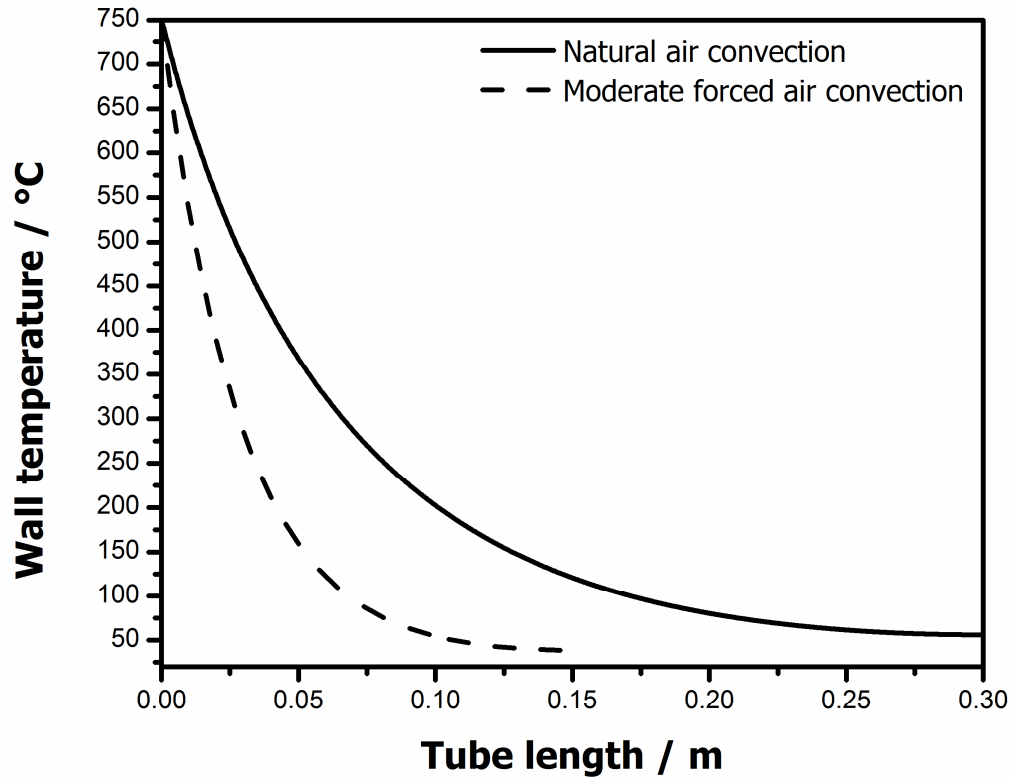


Figure 33: Longitudinal temperature profile in the tube wall for the section of exit tube protruding from the tube furnace.

3.3.2.3 Miscellaneous considerations

The mass of the depolymerisation vessel and the temperature of operation may result in serious deflection of the exit tube and must be taken into account to ensure no permanent deformation results in seal breakage under vacuum or renders the depolymerisation vessel unusable after the first run.

The methods used to calculate deflection of a cantilever beam with a load at one end are well-described in literature [12]. The formula for the deflection is presented in Equation (15)

$$\delta = \frac{Pl^3}{3EI} \quad (15)$$

Here δ is the deflection, P is the load in newton, l is the length of the tube, E is the elasticity modulus, and I is the area moment of inertia of the tube cross section. The loading on the exit tube due to the depolymerisation vessel mass was calculated as 60 N, while the second area

moment of inertia for the exit tube was calculated as $7.2729 \times 10^{-8} \text{ m}^4$. Young's modulus for 316 stainless steel was taken as 190 GPa at 25 °C [9] and as 125 GPa at 750 °C.

The deflection distance was calculated as being 0.0004 m at 25 °C and as 0.0006 m at 750 °C. The small size of these values indicate that there is no need to be concerned about the effects of deflection on the geometry of the depolymerisation vessel and no extra stiffening supports are necessary.

3.3.3 Cold trap sizing

The specification of the cold trap volume is based on both consideration of working pressure and availability of off-the-shelf items that are certified pressure vessels. While the depolymerisation vessel could be custom manufactured because it does not operate under super-atmospheric pressure, the cold trap will operate under pressure and must be certified as a pressure vessel in order to conform to South African law concerning pressurised equipment safety.

Depending on the mode of polymerisation (*i.e.* Carius tube or autoclave polymerisation), the pressure in the reactor may need to be as high as 25 bar. In the case of Carius tube work, the total pressure is not a concern, as the monomer gas is frozen into the tube. All that is required is that the pressure be high enough so that the preloading chamber is sufficiently pressurised in order to load the required mass of monomer. In the case of autoclave polymerisation, the reactor must be capable of delivering high pressure and ensure a minimum pressure drop over the course of the reaction (typically, this requires that a significant portion of the TFE exist as a saturated liquid within the cold trap).

3.3.3.1 Phase behaviour of tetrafluoroethylene

No reports on the phase behaviour of TFE exist in the open literature, and the two-phase envelope must be calculated from known thermodynamic properties before closed system pressure calculations can be performed. The Peng-Robinson equation of state is simple to use and is sufficiently accurate for the calculation of the phase behaviour of fluorinated gases [13]. The EOS is shown in Equation (16),

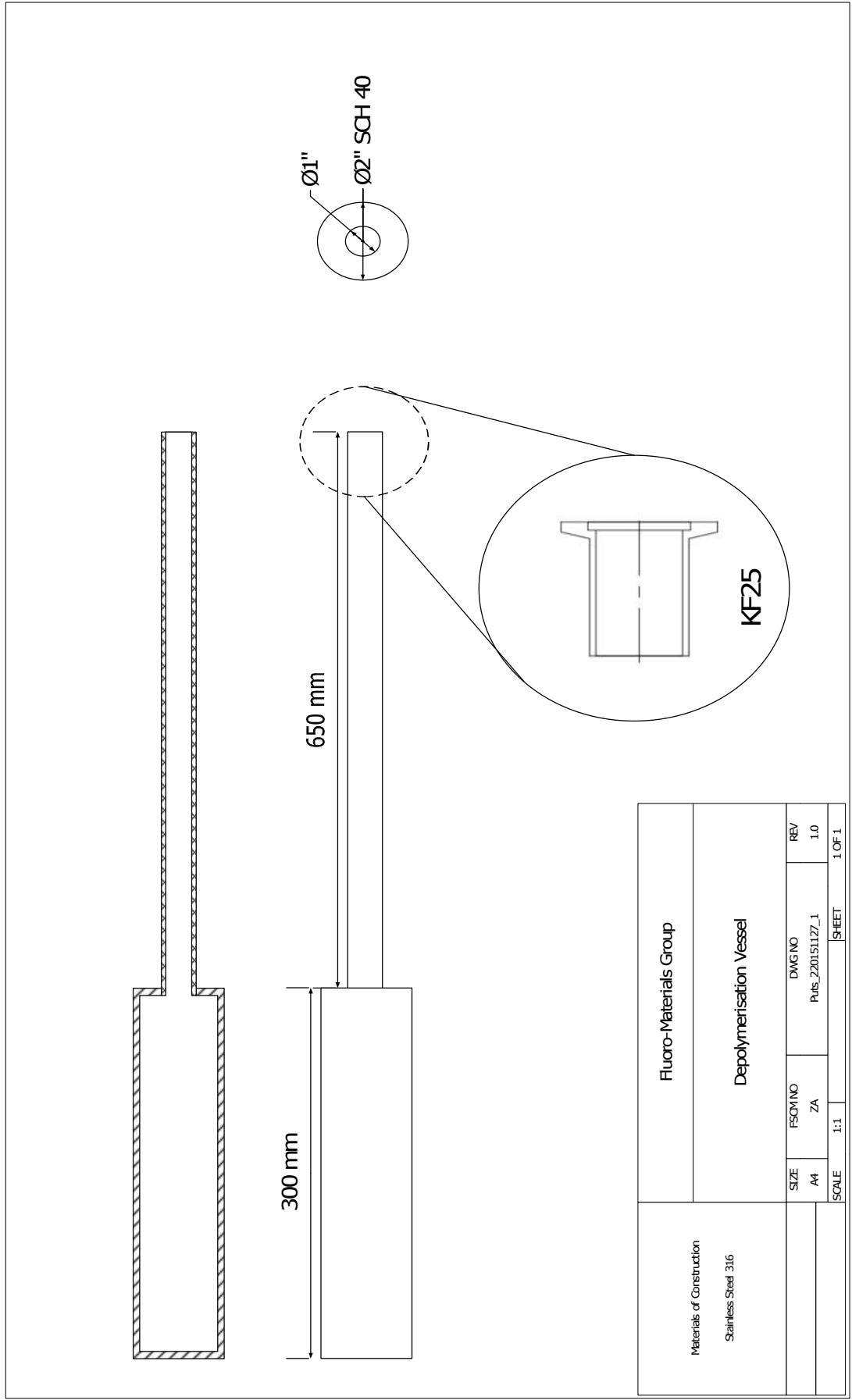


Figure 34: Mechanical overview of the depolymerisation vessel.

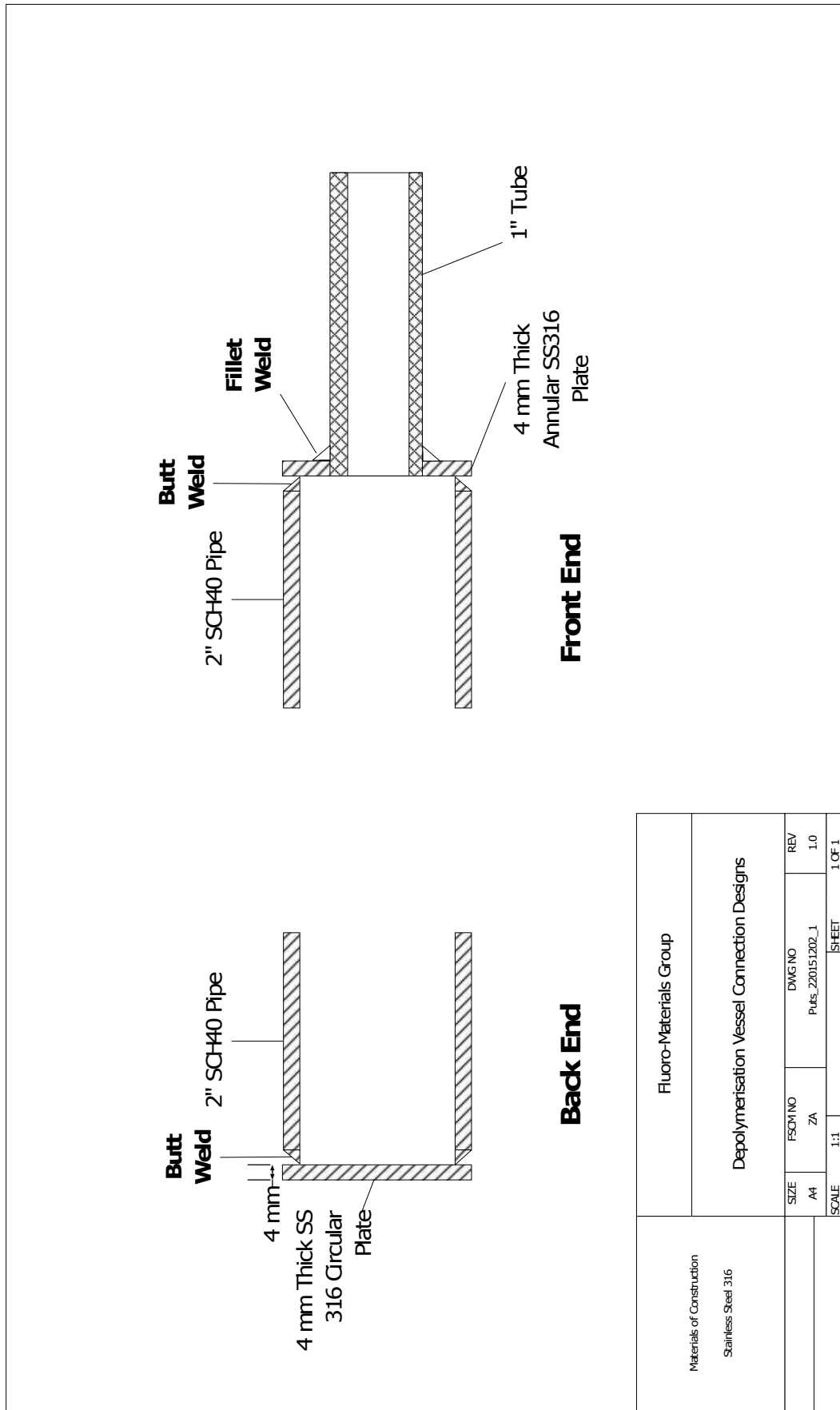


Figure 35: Detailed mechanical drawing of the depolymerisation vessel furnace insert.

$$P = \frac{RT}{V_m - b} - \frac{a\alpha(T)}{V_m^2 - 2bV_m - b^2} \quad (16)$$

Here P is the pressure, P_c is the critical pressure, V_m is the molar volume, R is the universal gas constant, T is the temperature, and T_c is the critical temperature. The lumped variables are defined as $a = 0.427R^2T_c^2$, $b = \frac{0.08664RT_c}{P_c}$, and $T_r = \frac{T}{T_c}$.

The Luo alpha function is presented in Equation (17),

$$\alpha(T) = 1 + (0.32877 + 1.1317\omega)(T_r^{-0.5} - T_r) \quad (17)$$

Here ω is the acentric factor and T_r is defined as above. The Luo alpha function was employed over the Twu or Mathias-Copeman as it is a little more accurate than the original alpha function, especially at conditions greater than the critical point, but does not require fitted parameters and does not excessively increase complexity of the calculations [14].

The method for calculating the two-phase region is well discussed in the literature [15], and involves optimising an objective function by minimizing the difference between the areas of the two lobes of the cubic EOS curve as a function of molar volume at fixed temperature and pressure. As these areas must be determined *via* numeric integration, the calculations are computationally intensive and, depending on chosen starting conditions for the integration, may result in nonsensical values (*i.e.* negative molar volumes or imaginary molar volumes close to the critical point).

There were repeated convergence failures in calculating the two-phase envelope of TFE by the standard method due to the severe non-ideality of the gas. The standard calculation method resulted in large negative molar volumes for the liquid phase. To overcome this, a new method was developed: By definition, the two-phase envelope occurs where the system exists at saturation, that is, at P^{sat} and T^{sat} . Since the saturation pressure and temperature for TFE is known at the saturated liquid molar volume (this is the vapour pressure curve), the volume polynomial form (shown in Equation (18), with ancillary definitions in Equation (19) to Equation (21)) of the Peng-Robinson EOS may be solved at vapour- pressure and temperature to extract both the liquid molar volumes and the vapour molar volumes that demarcate the two-phase envelope.

$$V^3 + AV^2 + BV + C = 0 \quad (18)$$

$$A = b - \frac{RT}{P} \quad (19)$$

$$B = \frac{a}{P} - 3b^2 + \frac{RT}{P} 2b \quad (20)$$

$$C = b^3 + \frac{RT}{P} b^2 - \frac{ab}{P} \quad (21)$$

Equation (18) has three roots. The largest root yields the vapour molar volume and the smallest yields the liquid molar volume. The intermediate root has no physical meaning and is discarded.

Provided a sufficient number of these points are available, logarithmic or spline interpolation between these points should be sufficiently accurate for determination of the two-phase envelope boundaries at arbitrary isotherms.

Python code was written to perform two-phase envelope- and pressure calculations according to the previously described method and the code executed using the IPython Notebook package within the Python(x,y) distribution.

Vapour pressure data for TFE were collated from various sources and are reproduced in Figure 36. The calculated volumes for the two phase envelope are compared to available experimental data in Figure 37 and Figure 38, while the calculated two-phase envelope is presented in Figure 39.

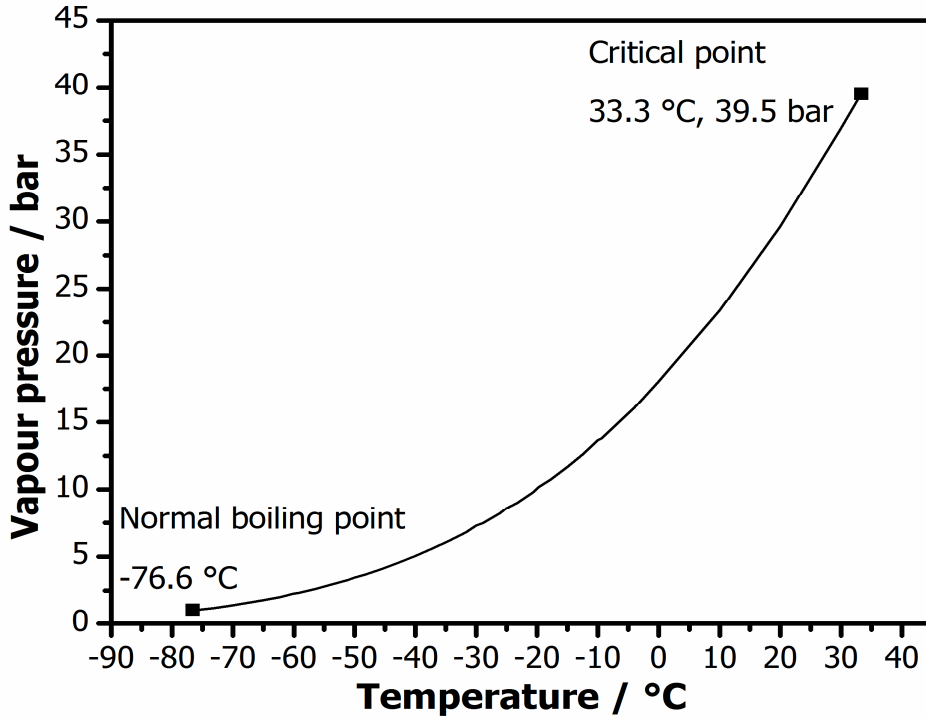


Figure 36: *Experimental vapour pressure curve for TFE between its normal boiling and critical points [16-20].*

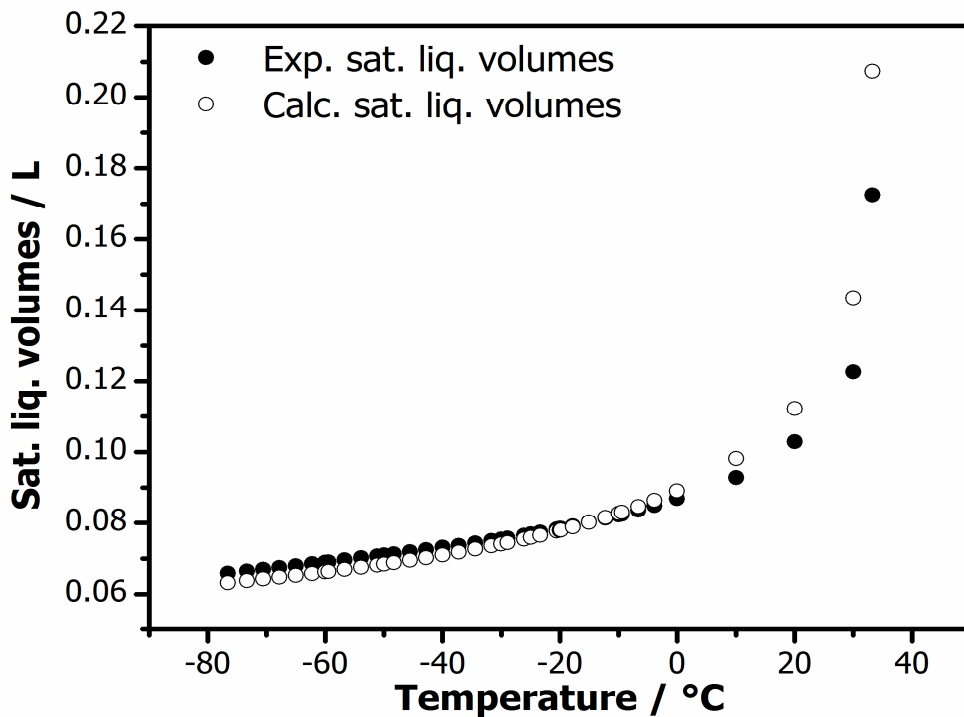


Figure 37: *Comparison between the experimental- and calculated saturated liquid volumes of TFE using the Peng-Robinson EOS.*

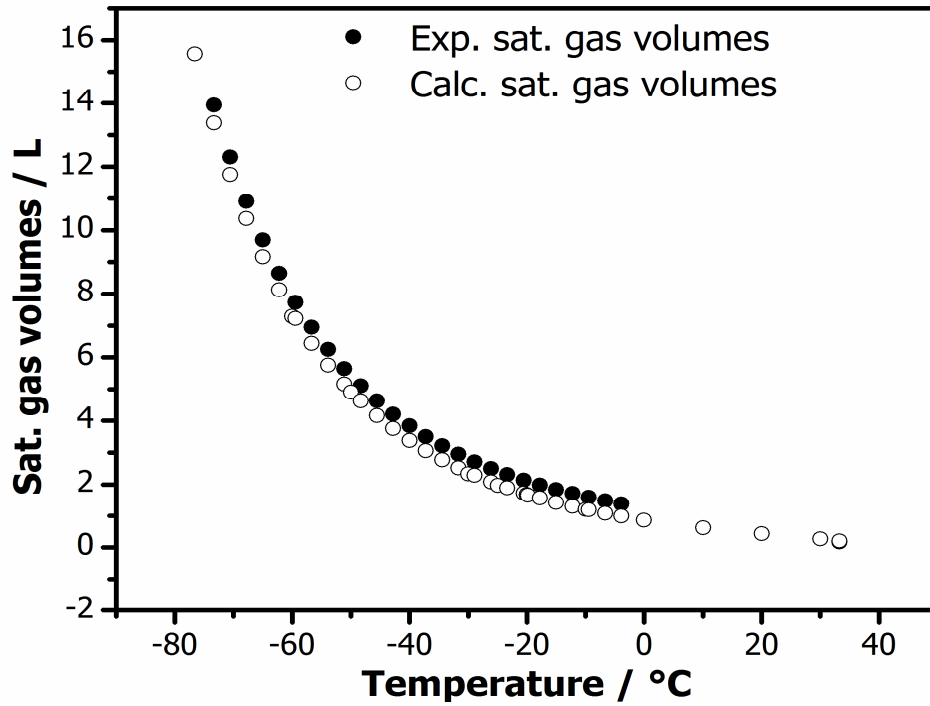


Figure 38: Comparison between the experimental- and calculated saturated gas volumes of TFE using the Peng-Robinson EOS.

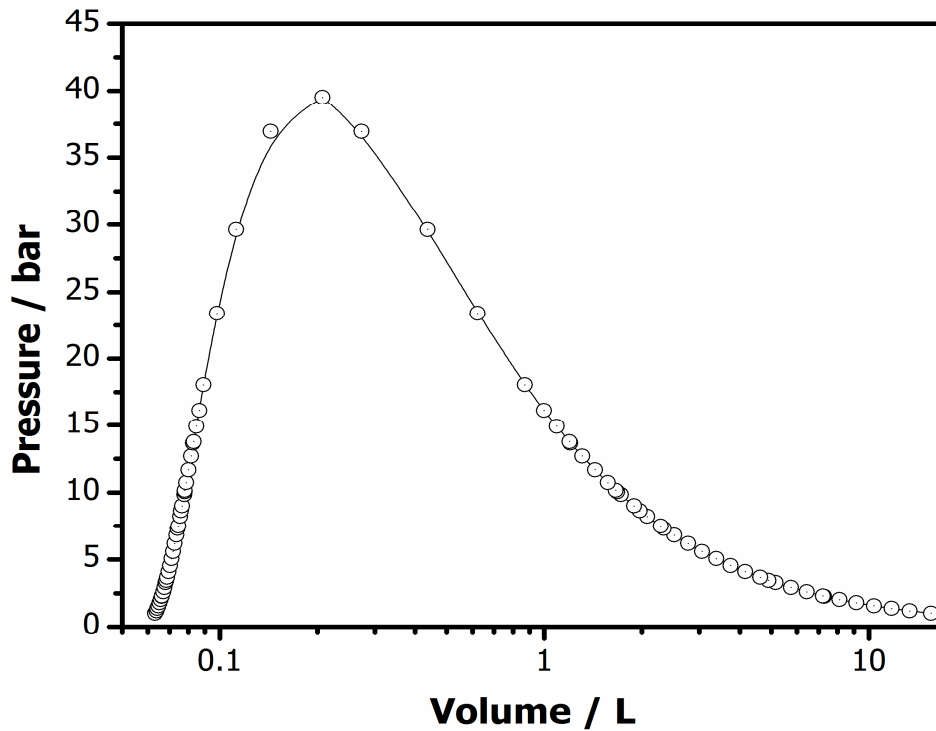


Figure 39: The calculated two-phase region for TFE using the Peng-Robinson EOS with a B-spline fitted to represent the continuous data.

3.3.3.2 Catch vessel pressure calculations

Water/methanol ice baths are the typical method of heating a cold trap from cryogenic temperatures to operating temperature and this same method is used to regulate the cold trap temperature throughout the autoclave polymerisation process.

Standard procedure at the Nuclear Energy Corporation of South Africa is to keep the TFE reservoir at around $-10\text{ }^{\circ}\text{C}$ in order to achieve a working pressure of 20 bar in a 300-mL catch vessel. These values were determined by trial and error and not *via* calculation, so it would be useful to determine the system pressure and liquid fraction TFE as a function of the vessel size and moles of TFE present for more than just this isotherm.

The system pressure as a function of molar amount of TFE in the system is presented at selected isotherms for a 250-mL catch vessel in Figure 40, a 500-mL catch vessel in Figure 41, and a 750-mL catch vessel in Figure 42. These same figures also show the liquid fraction of TFE as a function of the molar amount of TFE in the system. The volume of the 1" line leading from the shutoff valve to the catch vessel was measured as being 225 mL, and this volume was taken into account when performing the calculations.

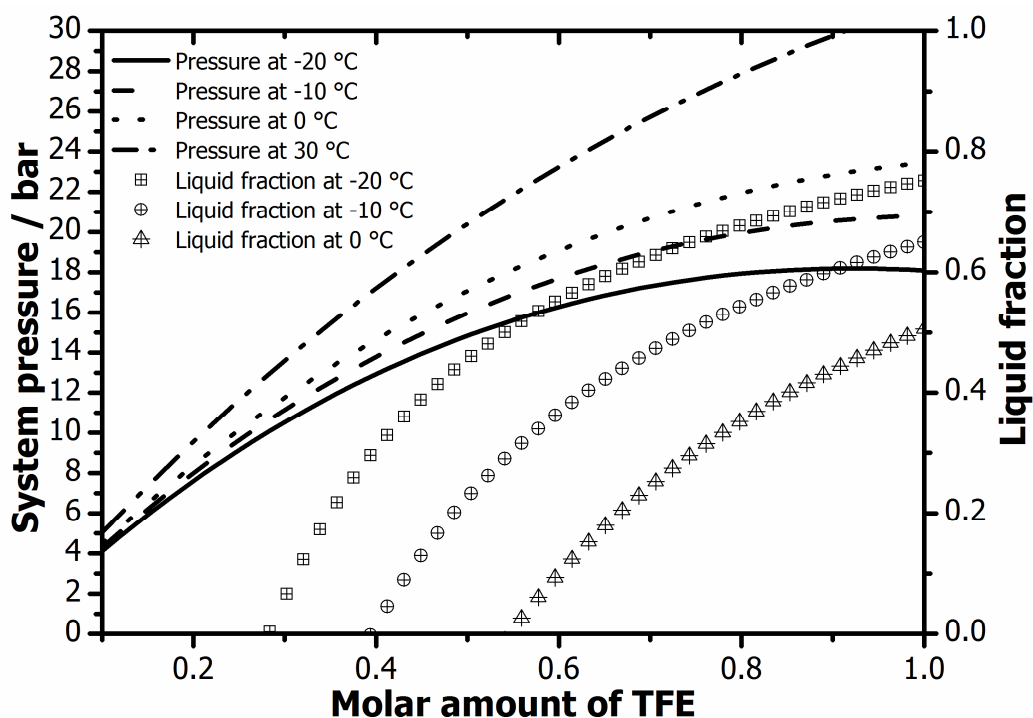


Figure 40: *Depolymerisation reactor system pressure as a function of the molar amount of TFE in the system at selected isotherms for a 250-mL catch vessel (475 mL total volume).*

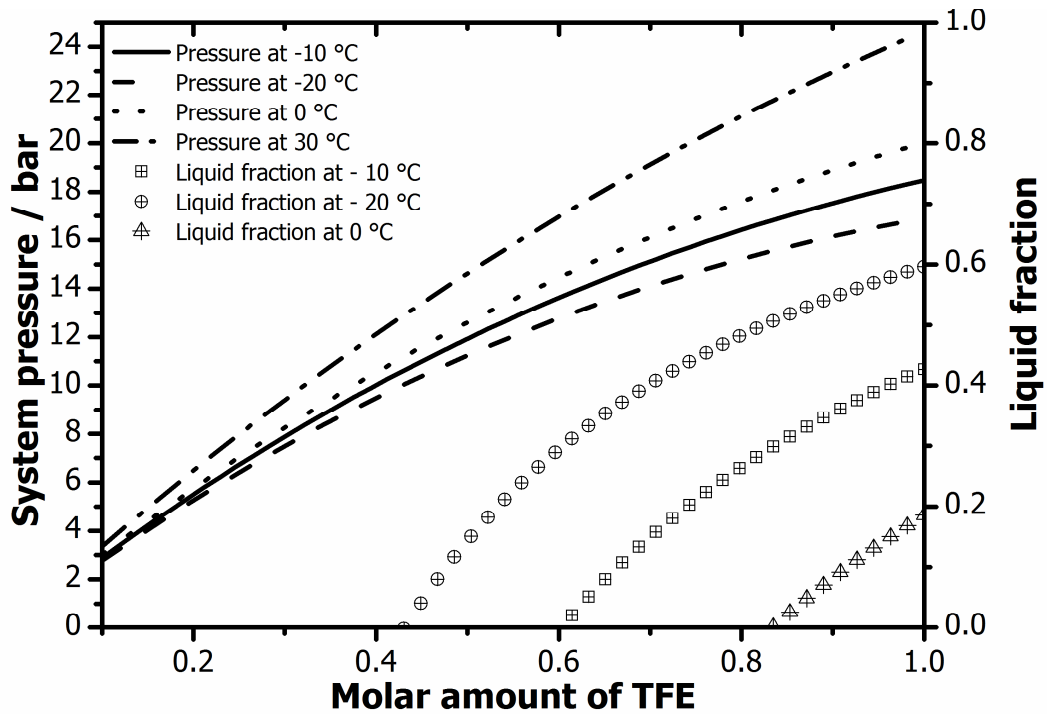


Figure 41: *Depolymerisation reactor system pressure as a function of the molar amount of TFE in the system at selected isotherms for a 500-mL catch vessel (775 mL total volume).*

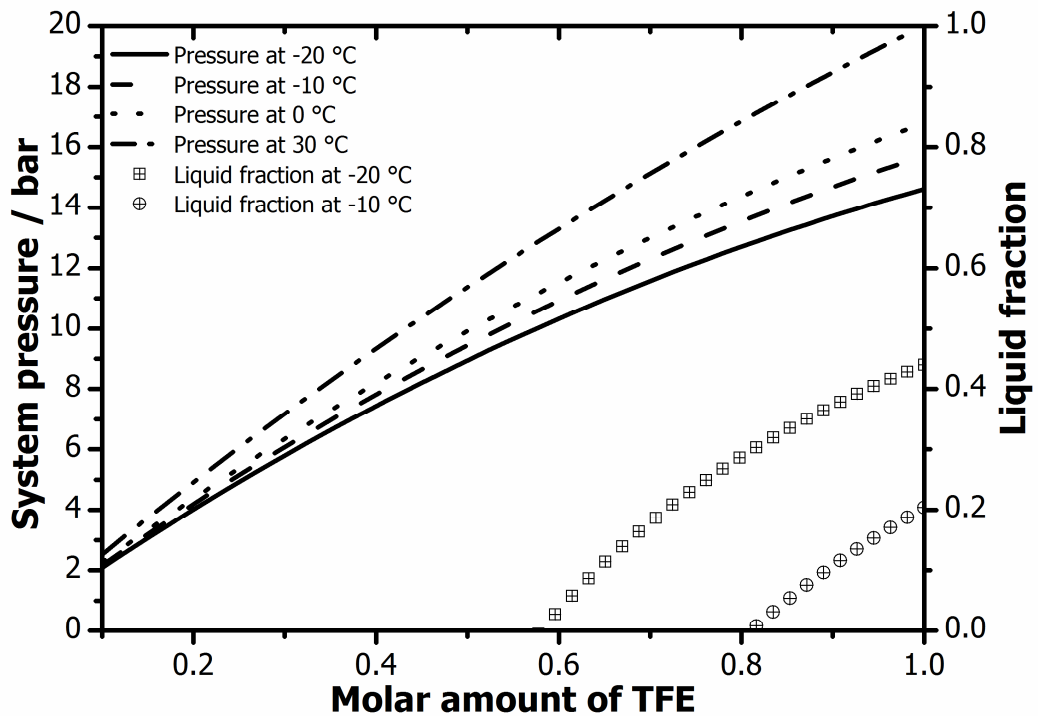


Figure 42: *Depolymerisation reactor system pressure as a function of the molar amount of TFE in the system at selected isotherms for a 750-mL catch vessel (975 mL total volume).*

The pressure curves reveal that, at 30 °C, the 250-mL vessel gives a TFE pressure well in excess of the 25 bar safety limit, while the 500-mL and 750-mL vessel are well below the safety limit.

The 250-mL vessel shows the most optimal pressure drop behaviour with the pressure drop at -20 and -10 °C being less than 1 bar for 0.4 mol.

The 750-mL vessel reaches a maximum pressure at -10 °C of only 15 bar, whereas the 500-mL vessel boasts a pressure of 18.47. Furthermore, the 750-mL vessel hardly has any liquid TFE at 0 °C and above, resulting in a relatively fast pressure drop (~5 bar for 0.4 mol at -10 °C), whereas the rate of pressure drop for the 500-mL vessel is slower.

Apart from the unacceptable pressure conditions in the event of cooling failure, the 250-mL vessel gives the best pressure behaviour; however, this vessel must be foregone in favour of the 500-mL vessel to avoid over pressure of the system in the event of cooling failure.

Using a methanol water icebath requires a mixture of 17 % methanol by volume to achieve a freezing point at -10 °C.

3.3.4 Safety calculations

Autodecompositional deflagration of TFE and the accompanying explosion of the depol system is the ultimate safety hazard. It is necessary to know what sort of pressures could be expected in the vessel during such an event, and if the design could withstand the explosion.

Working under the assumption that pure TFE is present in the reactor, the pressures at the adiabatic reaction temperature for the reaction where TFE goes to $\text{CF}_4(\text{g})$ and $\text{C}(\text{s})$ would be close to the maximum pressures experienced by the depol system during deflagration.

Assuming a constant volume scenario, the adiabatic temperature is calculated according to Equation (22),

$$H_{rxn}^{\circ} = \int_{298}^{T_{ad}} (C_{v, \text{CF}_4} + C_{v, \text{C}}) dT \quad (22)$$

Here H_{rxn}° is the standard heat of reaction, C_v is the constant volume heat capacity, and T is the temperature. H_{rxn}° was calculated from the standard enthalpies of formation [21, 22] as -269 $\text{kJ}\cdot\text{mol}^{-1}$. Since the C_v for graphite is approximately constant at around $8.314 \text{ kJ}\cdot\text{mol}^{-1}\cdot\text{K}^{-1}$, only the temperature dependence of the C_v for CF_4 needs to be calculated.

No experimental values for the C_v of CF_4 as a function of temperature could be found in the open literature. However, ideal gas C_v values were available in the open literature [23], and the

real C_p as a function of temperature and pressure was determined by adding the ideal gas values to the residual C_p values calculated from the Peng Robinson EOS [24]. The calculated pressures at the adiabatic reaction temperatures as a function of the moles of TFE in the catch vessel are presented in Figure 43 for the various vessel volumes.

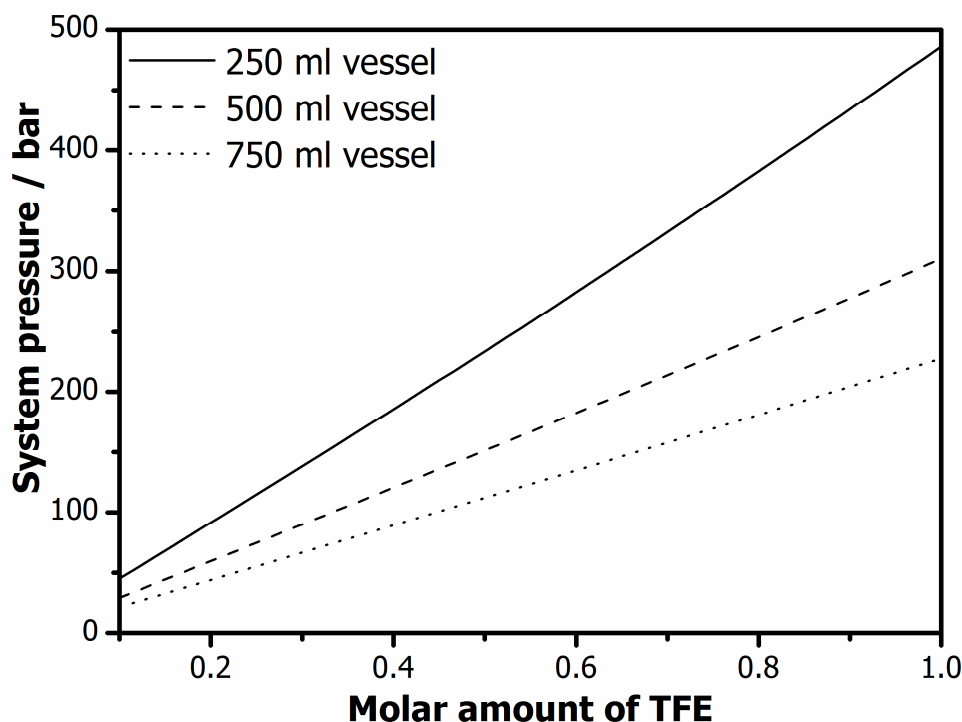


Figure 43: *Depol reactor system pressure as a function of the molar amount of TFE in the system at the adiabatic reaction temperature for a 250-, 500- and 750-mL catch vessel (475, 725 and 975 mL total volume).*

It is evident from the figure that, should a deflagration happen, the system would not be able to withstand the pressure build up. If the pressure release valve does not adequately release the pressure during deflagration, the pressure gauge and the sample cylinder would be the first to fail.

3.3.5 Mechanical support stand for the depolymerisation system

The depolymerisation apparatus cannot stand by itself and must be mounted onto a mobile frame if it is to be used. Furthermore, the tube furnace must be raised to the correct height in order to permit the furnace insert to be used. The frame and furnace height extender are both made from mild-steel square tubing welded together. The depolymerisation apparatus is attached to its frame by way of plastic 2" Swagelok tube support clamps (304-S6-PP-32T) bolted to the

frame. The fully assembled, mounted depolymerisation apparatus, and tube furnace are shown in Figure 44.

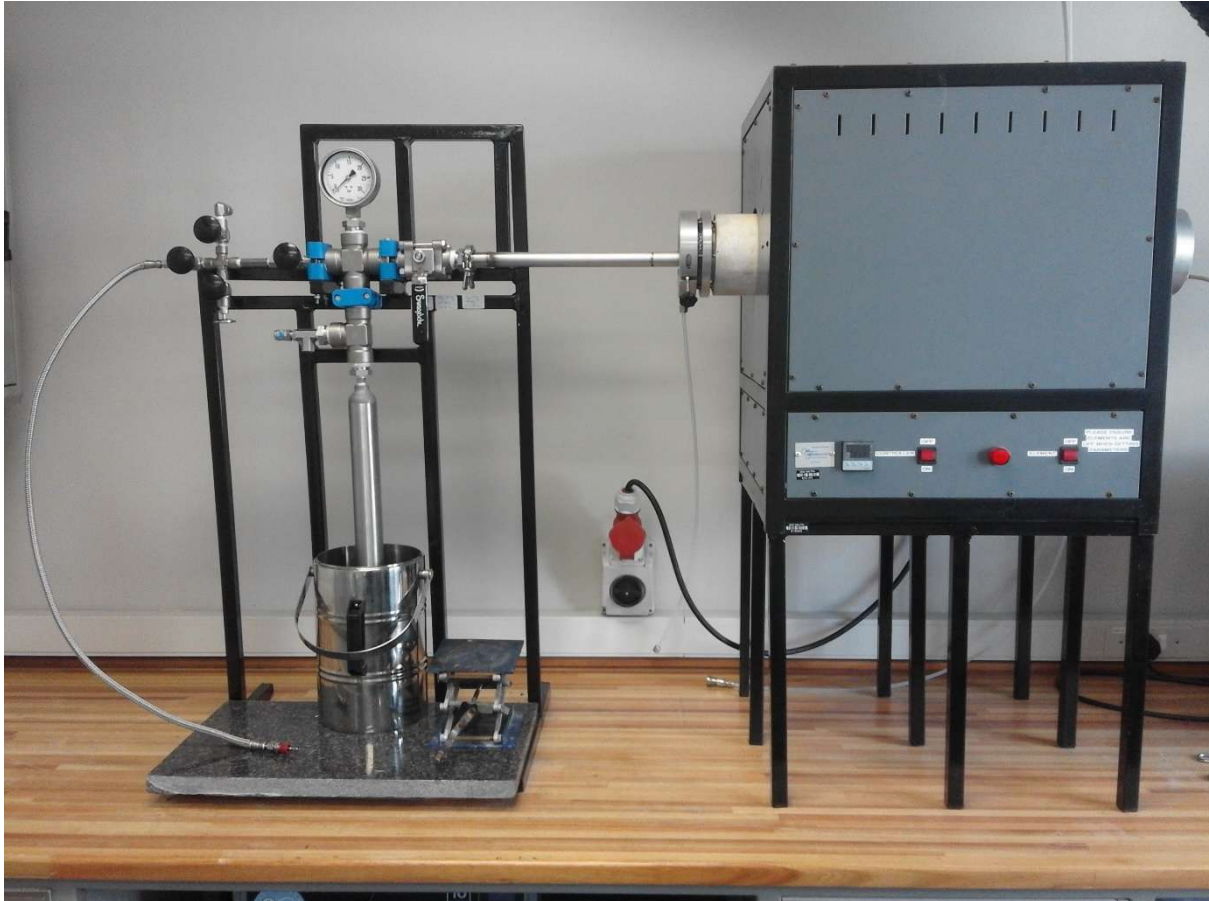


Figure 44: *Photograph of the fully assembled, mounted depolymerisation apparatus and tube furnace as installed in the FMG laboratory.*

3.4 Carius tube system design

3.4.1 Design overview

Taking into account the various points mentioned in Section 3.2.1, the design as detailed in the piping diagram in Figure 45 was developed. This design is similar to the unit used at the ENSCM in Montpellier, save for the addition of a loading vessel and being only a single tube loading unit.

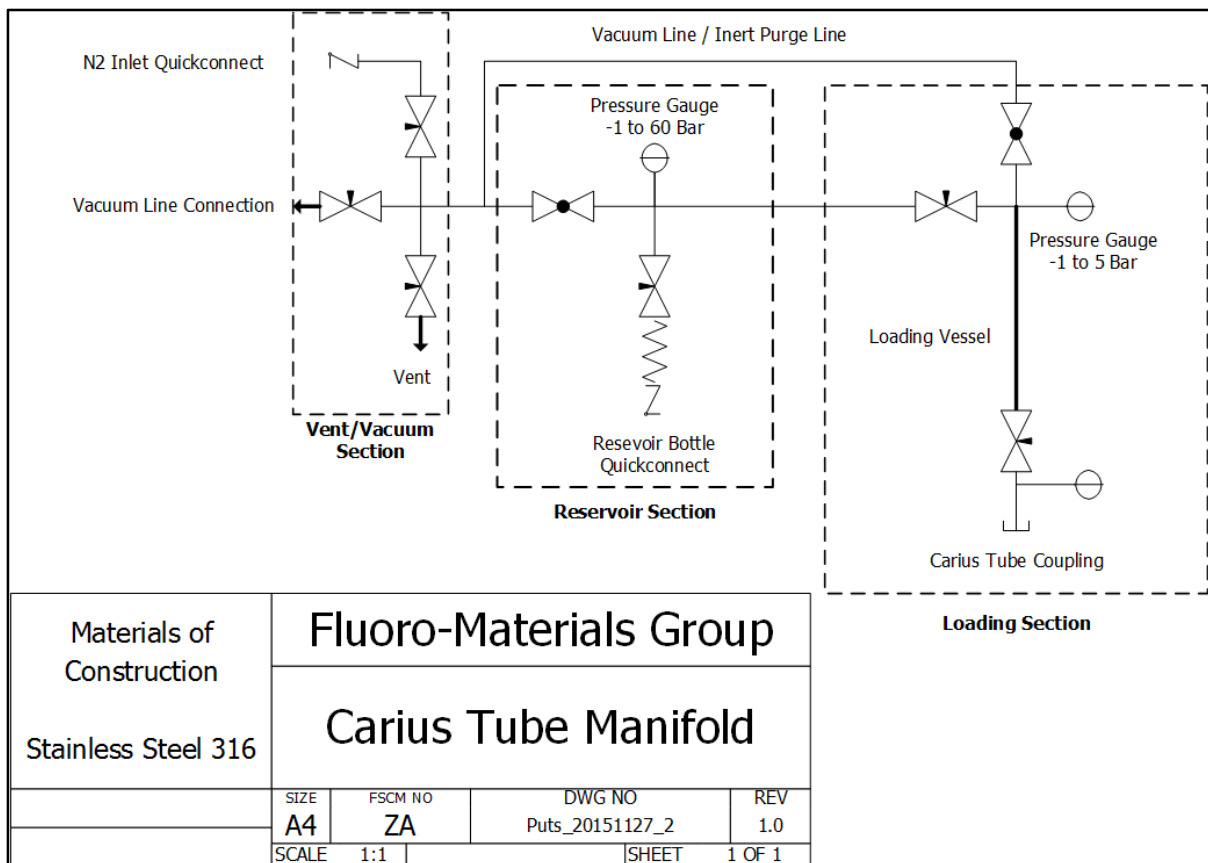


Figure 45: Piping diagram for the Carius tube manifold.

The bill of materials for the Swagelok components used in this design is presented in Table 11.

All lines are specified to be 1/4"-o.d., with the regulating valves specified as regulating stem, integral bonnet, needle valves and the shutoff valves as one piece instrumentation ball valves with PTFE seats with the quickconnect units being of the DESO type. The loading vessel was made from a 150-mL double-ended Swagelok sample cylinder fitted with female 1/4" NPT inlets. The Carius tube coupling is a 1/4"-o.d. compression fitting to 8-mm compression fitting union and the ferrules are 5/16" PTFE double compression type.

The pressure gauges and their mounting brackets were supplied by Wika Instruments (Type 232.50, 100-mm dial size with ¼" MNPT back mount). The pressure gauge on the reservoir section is specified for pressures from -1 to 60 bar (gauge pressure), while the gauges on the loading section are specified for -1 to 5 bar (gauge pressure).

Table 11: *Bill of materials for the Carius tube manifold.*

Quantity	Part description	Swagelok part number
5	Needle Valve ¼" CP*	SS-1RS4
3	2-Way Ball Valve ¼" CP	SS-42S4
2	Union ¼" CP to MNPT	SS-400-1-4
2	Tee ¼" CP	SS-400-3
3	Cross ¼" CP	SS-400-4
1	Female Quick Connect ¼" CP	SS-QC4-B-400
1	Male Quick Connect ¼" CP	SS-QC4-D-400
3	Elbow ¼" FNPT to CP	SS-400-8-4
1	Elbow ¼" FNPT to MNPT	SS-4-SE
2	Union ¼" CP to FNPT	SS-400-7-4
1	Mud Dauber Fitting ¼" MNPT	SS-MD-4
1	Short Hex Nipple ¼" MNPT	SS-4-HN
1	Union ¼" FNPT to FNPT	SS-4-HCG
1	150-mL Sampling Cylinder	304L-HDF4-300
1	Union ¼" to 8 mm CP	SS-8M0-6-4
1	KF 25 Vacuum Flange ¼" MNPT	JNWMPT2514
5	PTFE Ferrule Set 5/16"	T-500-SET

* CP means "Compression fitting"

3.4.2 Carius tube design

The design drawings for the French Carius Tubes are shown in Figure 46. The French Carius tube specification calls for an 8-mm leading tube and an 18-mm outer diameter main tube, which is not in line with the Fluoro-Materials Group's policy of using even fractionals of an inch for tube sizes. However, in attempting to redesign the tubes, it was found that the imperial tube sizes available to the FMG's glass blowers do not conform to the structural parameters necessary for

the tubes to admit flea type stirrer bars while still being flame sealable and able to resist pressure at reaction temperature. For this reason the French design was maintained, hence the use of a fractional-to-metric reducing union.

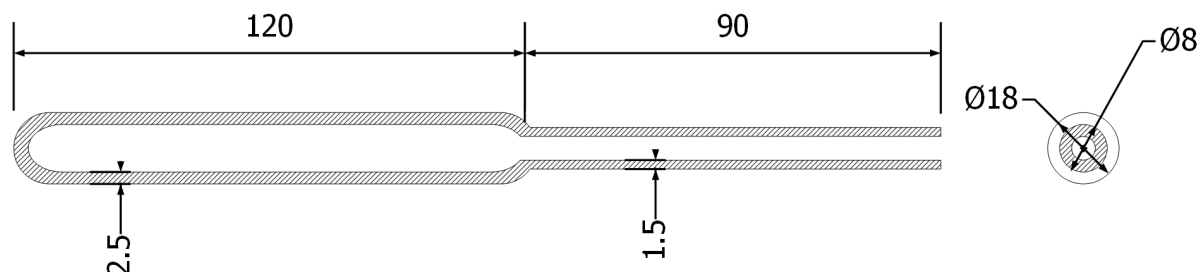


Figure 46: *Design schematic for the Carius tubes used at ENSCM in France.*

Polytetrafluoroethylene ferrules are employed here as the glass to metal union requires a soft, but chemically inert and temperature resistant material. As no ferrule supplier stocks, or manufactures, PTFE ferrules in 8-mm size, 5/16" (7.94 mm) ferrules were specified.

The dimensions reported in Figure 46 give an internal volume of ~15 mL. The correlation between tube dimensions and pressure are given in Equation (23),

$$P = \frac{20 \cdot W \cdot K}{OD - W} \quad (23)$$

Here P is the pressure, W is the wall thickness, K is the glass stress parameter, and OD is the outer diameter of the tube. For borosilicate 3.3 glass, the stress parameter was taken as 7 N.mm⁻², as per the DIN 1595 Standard. The maximum operational pressure for the glass tubing was calculated as 22.5 bar at all temperatures below 200 °C.

In reality, the various stresses and structural weaknesses introduced by the leading tube and the flame sealing will result in a lower pressure resistance, and therefore, to play it safe, a maximum working pressure of 15 bar is assumed.

3.4.3 Tube loading masses

Measuring the mass of TFE (or any other gas) loaded into the tube is difficult to do directly as the degassing and flame sealing will result in an indeterminate and variable mass loss from the tube. Therefore, precise calculation of the mass loaded into the tube as a function of pressure in the loading vessel is required. Using the Peng-Robinson EOS, the mass-pressure relations for

TFE, HFP, and VDF were calculated for the gases at 20 °C (the nominal laboratory temperature) assuming a working loading vessel volume of 160 mL (150 mL of the vessel plus 10 mL measured for the volume of the fittings and the dead space in the valves). These relations are presented graphically in Figure 49. The working pressure is the sum of the partial pressures of all components present in the tube. To avoid the tube bursting, no more than 2 g, but preferably, no more than 1 g of monomer gas should be added to a tube.

3.4.4 Mounted housing for the Carius tube system

The manifold system cannot stand by itself and must be mounted on a frame if it is to be used. Furthermore, prudence dictates that the “guts” of the manifold should be quarantined from the rest of the lab space by some form of cover plate so that, in case of an internal explosion, there is a second layer of protection that keeps any metal debris from flying all over the laboratory. The mounting itself is made from mild steel square tubing welded together and the faceplate is made from 4-mm thick 316 stainless steel sheet metal bent into the correct shape, with the seams welded up and holes cut out using a laser cutter to permit access to the valve handles and the gauge dials. The fully assembled, mounted Carius manifold is shown in Figure 47.



Figure 47: *Photograph of the fully assembled, mounted Carius manifold as installed in the FMG laboratory.*

3.4.5 Explosion containment system

The Carius tubes are made from brittle glass, and the flame sealing as well as the large temperature changes during degassing invariably induce stresses in the glass. If, for whatever reason, these stresses, in combination with the stress induced by gas pressure within the tube, exceed the maximum allowable stress, the tube will break, and, undoubtedly, the explosion will result in dangerous flying debris. It is prudent to have some system that will be able to effectively contain the shrapnel in the event of a blast, but said system should not interfere with the heat transfer to the tube from whatever heating method is employed. A metal shielding-tube design was developed that incorporates only off-the-shelf components, which will not hinder the heat transfer, and is able to withstand an explosion in the event of tube failure.

Utilising 22-mm o.d. copper plumbing pipe (i.d. 20-mm) with a copper end cap and a brass screw fitting, all brazed together, a multi-use shield tube is assembled, as depicted in Figure 48. The sealed Carius tube is placed into the shield tube along with a small amount of silicon oil, the galvanised mild steel cap is wrapped with plumbers tape and screwed into place. The shielded tube may then be placed in a heated shaking oven, oil-bath, rocker oven, or any other heating system without fear for an explosion. Five such shield tubes were constructed for use in this work, but more may be easily assembled.

The French Carius system also employs a form of shield tube, but these tubes are constructed of thick walled stainless steel, which hampers the heat transfer to the glass tube. With copper, there is no large thermal lag, and heat is transferred to the tube almost instantaneously. To prevent the glass tube from knocking against the metal during agitation, some tissue paper may be placed at the bottom of the shield tube and in the galvanised iron cap.



Figure 48: *Copper Carius shield tube for containment of "live" Carius tubes, assembled with off-the-shelf fittings.*

3.5 Summary

In summary, the equipment built for this project included the TFE generation system, the Carius tube manifold, their respective mechanical supports as well as an explosion containment system. The equipment has been in continuous use since commissioning, without mishap or incident.

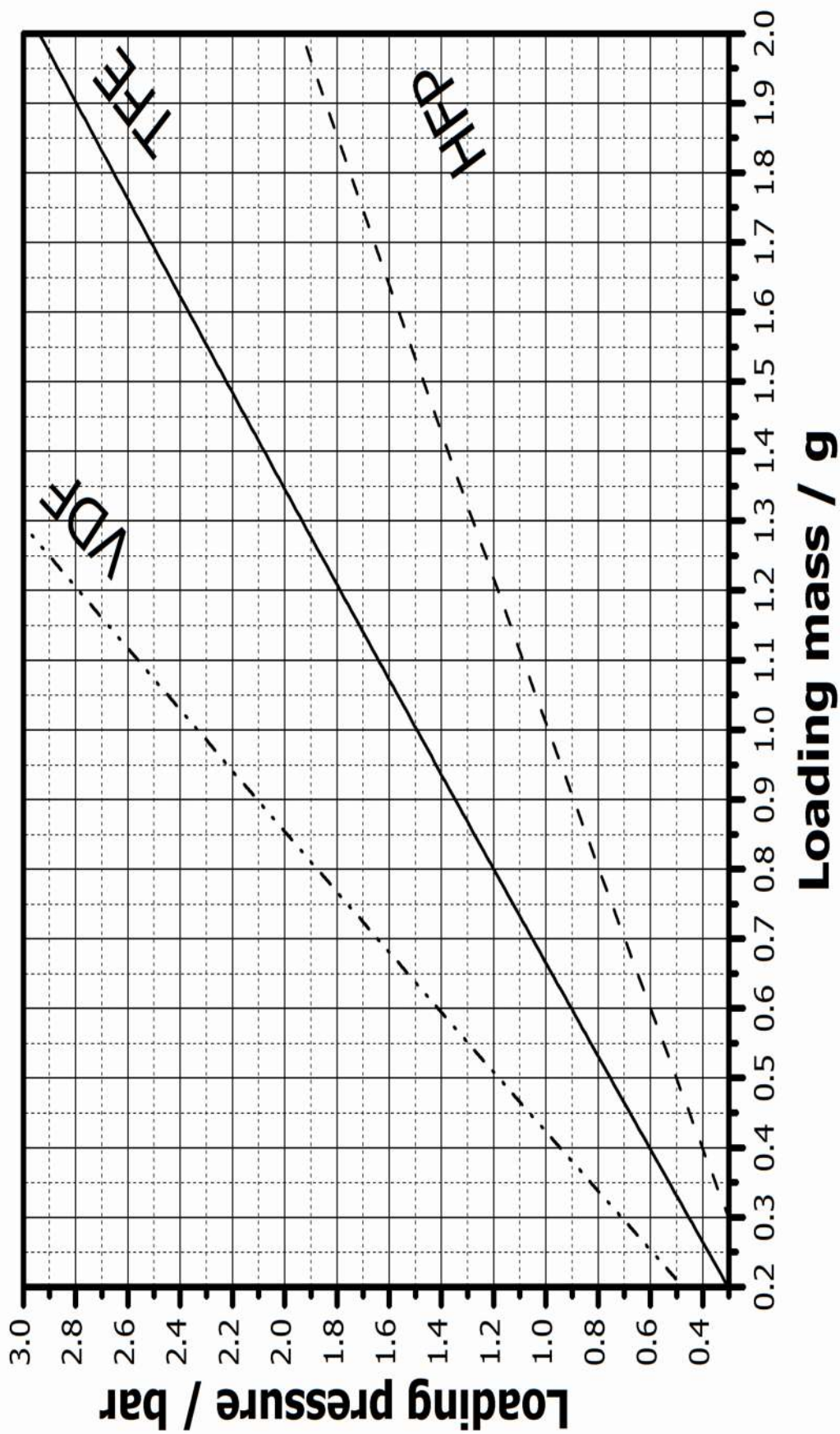


Figure 49: Mass-pressure relations at 20 °C for TFE, HFP and VDF, assuming a working loading vessel volume of 160 mL.

3.6 References

- [1] Von Tress, W.R., (Dow Chemical Company) 1964, *Preparation of Tetrafluoroethylene*, US3113871.
- [2] Farlow, M.W., (E. I. du Pont de Nemours and Company) 1963, *Method for the preparation of tetrafluoroethylene*, US3081245.
- [3] Hercules, D.A., Parrish, C.A., Sayler, T.S., Tice, K.T., Williams, S.M., Lowery, L.E., Brady, M.E., Coward, R.B., Murphy, J.A., Hey, T.A., Scavuzzo, A.R., Rummeler, L.M., Burns, E.G., Matsnev, A.V., Fernandez, R.E., McMillen, C.D., and Thrasher, J.S., "Preparation of tetrafluoroethylene from the pyrolysis of pentafluoropropionate salts", *Journal of Fluorine Chemistry*, 2017, 196, 107-116.
- [4] Drobny, J.G., 2014, *Technology of Fluoropolymers*, CRC Press, Boca Raton, Florida.
- [5] Siegemund, G., Schwertfeger, W., Feiring, A., Smart, B., Behr, F., Vogel, H., McKusick, B., and Kirsch, P., 2000, "Fluorine compounds, organic", in (eds.), *Ullmann's Encyclopedia of Industrial Chemistry*, Wiley-VCH Verlag GmbH & Co. KGaA, Weinheim, Germany.
- [6] Ferrero, F., Beckmann-Kluge, M., Spoomaker, T., and Schröder, V., "On the minimum ignition temperature for the explosive decomposition of tetrafluoroethylene on hot walls: Experiments and calculations", *Journal of Loss Prevention in the Process Industries*, 2012, 25 (2), 293-301.
- [7] Ferrero, F., Meyer, R., Kluge, M., Schröder, V., and Spoomaker, T., "Self-ignition of tetrafluoroethylene induced by rapid valve opening in small diameter pipes", *Journal of Loss Prevention in the Process Industries*, 2013, 26 (1), 177-185.
- [8] Ferrero, F., Zeps, R., Beckmann-Kluge, M., Schröder, V., and Spoomaker, T., "Analysis of the self-heating process of tetrafluoroethylene in a 100-dm³-reactor", *Journal of Loss Prevention in the Process Industries*, 2012, 25 (6), 1010-1017.
- [9] AK Steel. "Product Data Sheet 316/316L Stainless Steel", http://www.aksteel.com/pdf/markets_products/stainless/austenitic/316_316l_data_sheet.pdf, 2007.
- [10] McWilliams, M.L. and Nichols, D.G., "Heat Transfer in a Rod with Convective and Radiative Losses", *Proceedings of the West Virginia Academy of Science*, 1974, 46 (Engineering Section), 128-134.
- [11] Cverna, F. and Committee, A.S.M.I.M.P.D., 2002, *ASM Ready Reference: Thermal Properties of Metals*, ASM International, Russel, Ohio.
- [12] Hibbeler, R.C. and Sekar, K.S.V., 2013, *Mechanics of Materials*, Pearson Education Canada, Ontario, Canada.
- [13] Conradie, F.J., Crouse, P.L., Courtial, X., Nelson, W.M., van der Walt, I.J., and Ramjugernath, D., "Isothermal vapor-liquid equilibrium data for the 1,1,2,3,3,3-hexafluoroprop-1-ene +1,1,2,2,3,3,4,4-octafluorocyclobutane binary system: Measurement and modeling from (292 to 352) K and pressures up to 2.6 MPa", *Journal of Chemical & Engineering Data*, 2015, 60 (3), 966-969.
- [14] Luo, M., Hu, B., Jiang, T., Xia, S., and Ma, P., "Analysis and Comparison of the Alpha Functions of SRK Equation of State", *Chinese Journal of Chemical Engineering*, 2008, 16 (5), 766-771.
- [15] Nasri, Z. and Binous, H., "Application of the Peng-Robinson Equation of State using Matlab", *Chemical Engineering Education*, 2009, 42 (2), 1-10.
- [16] Furukawa, G.T., McCoskey, R.E., and Reilly, M.L., "Heat capacity, heats of fusion and vaporization, and vapour pressure of tetrafluoroethylene", *Journal of Research of the National Bureau of Standards, Section A: Physics and Chemistry*, 1953, 51 (2), 69-72.
- [17] Administration, N.O.a.A. "Tetrafluoroethylene", *CAMEO Chemicals Database*, 1999.
- [18] Lide, D.R. and Kehiaian, H.V., 1994, *CRC Handbook of Thermophysical and Thermochemical Data*, CRC Press, Boca Raton, Florida.

-
- [19] European Chemicals Agency. "Tetrafluoroethylene", *ECHA Chemicals Database*, **2015**.
- [20] Renfrew, M.M. and Lewis, E.E., "Polytetrafluoroethylene. Heat Resistant, Chemically Inert Plastic", *Industrial & Engineering Chemistry*, 1946, 38 (9), 870-877.
- [21] Walker, L.C., "The enthalpy of decomposition of $\text{CF}_3\text{NF}_2(\text{g})$ to $\text{CF}_4(\text{g})$, $\text{N}_2(\text{g})$, and $\text{F}_2(\text{g})$ ", *The Journal of Chemical Thermodynamics*, 1972, 4 (2), 219-223.
- [22] Kolesov, V.P., Zenkov, I.D., and Skuratov, S.M., "The standard enthalpy of formation of tetrafluoroethylene", *Russian Journal of Physical Chemistry (translation of Zhurnal Fizicheskoi Khimii)*, 1962, 36, 45-47.
- [23] Cheric. "Pure component properties of tetrafluoromethane", **2015**.
- [24] R.M., P., "Thermodynamic Properties Involving Derivatives using the Peng-Robinson Equation of State", *Chemical Engineering Education*, 2001, 35 (2), 112-115.

Chapter 4
Synthesis of low-molecular-weight
polytetrafluoroethylene waxes

4.1 Introduction

Besides the usual uses for perfluoropolymers (such as chemically-resistant coatings, low-friction materials in bearings, *etc.* [1, 2]), mixtures of perfluoropolymers with silicon, magnesium, or aluminium metal are used as high-energy pyrolants, finding application in missile-countermeasure flares, thermal lances, and as fuse material in demolitions time-delay elements [3]. These time-delay elements are employed extensively in the mining industry as part of the explosives packages used in the blasting process, both underground and in surface mining.

A difficulty faced by all manufacturers of metal-fluorocarbon-based pyrolant mixtures, is that the facile extrusion and molding methods for such mixtures are still non-existent, as non-melt-processable, high-molecular-weight PTFE is employed. The use of fluorocarbon waxes has been stymied by pre-ignition evaporation of the polymer, resulting in a reduced reaction temperature, variable burn times, or in extreme cases, total removal of the fluorocarbon and subsequent ignition failure.

It would be of immense commercial importance to the South African mining- and fluorochemical industries if a perfluoropolymer could be synthesised that would permit extrusion moulding while overcoming the difficulties encountered when using fluoropolymer waxes. A potential solution for these difficulties is the use of a PTFE wax, provided the molecular-weight distribution of the wax can be tailored such that low-temperature evaporation can be eliminated, but the wax remains amenable to the standard polymer compounding, extrusion, and moulding techniques.

Polytetrafluoroethylene waxes are not new products, and there are numerous companies that sell them (*cf.* Shamrock Technologies and Clariant). However, the PTFE wax grades sold commercially are not true waxes. Rather they are blends of PTFE microparticles with some wax-like carrier (usually, a hydrocarbon material).

The microparticles in these waxes are produced by micronisation of PTFE high polymer using jet mills or electron-beam radiation breakdown techniques [4]. Consequently, a PTFE wax may comprise an ultra-fine dispersion of PTFE high polymer, or a fine dispersion of low-molecular-weight PTFE powder. The feed material rarely comprises virgin PTFE, and the vast majority of waxes are made from waste PTFE. Typically, the micronised particle sizes range from 2 to 200 μm . These waxes are employed in many fields, most notably in the lubrication and coatings industry, but they may also be found as additives in elastomers, inks, and personal care products.

Commercial PTFE wax blends cannot be employed in pyrotechnics as inclusion of hydrocarbon material results in the generation of HF, which decreases the reaction heat for the metal fluorine exchange reaction and may smother the reaction entirely.

There is no commercial grade of true PTFE wax that exhibits the combination of thermal stability and rheological properties required for application in extrudable pyrotechnic formulations.

Initial goals of this research were: 1) the production of a PTFE wax that can be melt-extruded at temperatures in the region of 100 °C to 150 °C and 2) to test the behaviour of such a wax in pyrotechnic formulations. The synthesis of PTFE wax requires the synthesis of low-molecular-weight PTFE chains, which may be achieved by either altering the polymerisation process conditions or by introducing a chain-transfer- or control agent to the polymerisation reaction.

The use of a chain-transfer- or chain control agent implies a cost increase and may result in a self-smothering wax due to excessive hydrogen content in the polymer. The preferred method for synthesis of a low-molecular-weight PTFE is the adjustment of the polymerisation process conditions, such as temperature, the ratio of monomer to initiator, and the concentrations of the monomer and initiator.

As the rheological- and thermal properties of polymers are strongly affected by the molecular-weight distribution, a detailed understanding of the effects of the polymerisation conditions on the molecular-weight distribution is desired. However, it is exceedingly difficult to determine the molecular-weight distribution of PTFE due to its insolubility, which prevents the use of molecular-weight characterisation techniques such as GPC, light scattering, and osmometry. Onerous rheological techniques are the only methods for determining the molecular-weight distribution of PTFE [5-8]. Thus, at minimum, some information is needed regarding the lower limit to which the M_n of PTFE can be pushed by changing the polymerisation operating conditions only.

At present, there appears to be no peer-reviewed papers in the open literature regarding the effects of reaction conditions on the molecular-weight distribution of PTFE prepared by precipitation polymerisation. While some kinetics literature exist in old Russian-, Japanese-, and Mandarin language journals, the online, publically accessible, English language literature has practically no articles concerning the effects of temperature, pressure, initiator chemistry, monomer- and initiator concentration on the reaction kinetics, morphology of the product PTFE, or its physical properties.

Indeed, the articles by Kim and co-workers [9, 10] are the only literature sources addressing the effects of reaction conditions on the properties of the resultant PTFE that could be found. However, these articles deal with the emulsion polymerisation of TFE under a continuous dosing regime and do not report any data on the molecular-weight distribution. Furthermore, the expressions for number-average molecular weight as a function of operating conditions reported by Kim *et al.* are reactor dependent. Consequently, their trends cannot be used to predict what will occur in a laboratory scale autoclave under batch suspension polymerisation conditions.

The Tobolsky polymerisation rate equation [11] indicates that the controllable factors in polymerisation are temperature, monomer concentration, and initiator concentration. If we assume that for TFE in water the effects of solvent abstraction and termination to the monomer is null, then polymer chain termination can only occur *via* mutual radical termination (dead-end polymerisation). Under these conditions, effects of the controllable factors on the rates of propagation and simple termination, and in turn, their effect on the molecular-weight distribution of the product polymer can be determined using a radical initiator for which the rates of decomposition and efficiency is known (*i.e.* ammonium persulfate (APS) in water).

The primary goal of the research presented in this chapter is to attempt to elucidate the effects of polymerisation conditions on the molecular weight of PTFE synthesised under laboratory-scale, batch-type suspension polymerisation conditions. Furthermore, the literature on reactions of magnesium/PTFE pyrotechnical formulations was compiled using commercial grades of PTFE, and there are only limited reports on the pyrotechnic behaviour of systems containing custom-synthesised PTFE.

A set of simple experiments in two variables (temperature and initiator concentration) was conducted for evaluation of the effect of polymerisation-condition control on the molecular weight of PTFE, as well as to answer questions concerning the lower limits of molecular weight obtainable by precipitation polymerisation.

A comparison of the burning characteristics between commercial PTFE and low-molecular-weight PTFE synthesised *via* APS was also made.

4.2 Experimental

4.2.1 Materials

Tetrafluoroethylene was produced by an in-house generation unit *via* the vacuum (< 1 Pa) pyrolysis of pure PTFE. The PTFE (PTFE 807NX) was purchased from DuPont/Chemours and used as received. The product gas was analysed using a Perkin Elmer Clarus 680 GC/MS fitted with a Porapak Q 60-80 micropacked column and found to consist of, at minimum, 94 % tetrafluoroethylene and 6 % hexafluoropropylene, with an average composition of 98 % TFE and the remainder a mixture of HFP and OFCB.

Deionised water with a resistivity of $18 \text{ M}\Omega\cdot\text{cm}^{-1}$ was supplied by an in-house purification unit (Barnstead Easypure 2).

Ammonium persulfate (>98 %), sodium tetraborate (>98 %), acetone (>99 %), and cyclohexane (>99 %) were supplied by Sigma Aldrich and used as received. The persulfate was stored at sub-zero conditions and used as needed.

Micronized silicon powder with an effective surface area of $20 \text{ m}^3\cdot\text{g}^{-1}$ was supplied by AEL and was used as received.

4.2.2 Polymerisation apparatus

The autoclave polymerisation reactions were conducted in a Parr Instruments (Moline, Illinois) stirred reactor (SS 316). The reactor was fitted with a duplex J-type thermocouple directly in contact with the polymerisation medium, an inlet valve, a vent valve, a 3000 psi rupture disc, and a pressure transducer with a range of 0 to 40 bar absolute. Temperature control was achieved by way of a heating jacket connected to a PID controller.

4.2.3 Synthesis of PTFE by free-radical polymerisation

4.2.3.1 Autoclave polymerisation

Polytetrafluoroethylene was synthesised *via* non-transfer, uncontrolled free-radical polymerisation using ammonium persulfate in water. Experimental conditions are presented in Table 12. The design is also presented graphically in Figure 50. Two sets of these experiments were performed to permit evaluation of the statistical significance of the data and the reproducibility of the polymerisation conditions.

For each run, 100 mL of deionised water was charged with the required amount of initiator and the borax buffering agent (0.48 g), and the mixture was loaded into the autoclave. The assembled autoclave was pressure tested for 1 hour with N₂ at 6 bar before TFE was loaded to ensure the seals were working properly. The autoclave was degassed using three freeze-thaw cycles (cooled by liquid nitrogen) with the frozen reactor being kept under vacuum for 10 minutes in each cycle. The entire system was cooled a final time and kept under vacuum for 20 minutes before the required mass of TFE was frozen in. Connection to the loading reservoir was maintained for 20 minutes to ensure all the TFE was carried over to the autoclave.

In all cases, after degassing, the reactor was installed in its stand and permitted to warm up slowly to ambient temperature (~22 °C) over the course of an hour before being fitted with the heating mantle and the heating control started at the desired set point, e.g., 50 °C. The reactions were left running over-night (~12 hours) at a stirring speed of 700 rpm. Afterward, the reactor was cooled to ambient and degassed before being opened.

After polymerisation, the product polymer was washed with water three times with stirring in a round-bottomed flask before being rinsed with acetone and dried under vacuum at 60 °C.

4.2.3.2 *Carius tube polymerisation*

For the TFE experiments, 3 mL of deionised water was added to the tube with the initiator (1 % APS) pre-dissolved therein. For the VDF experiment, 10 mL of deionised water was added to the tube with the initiator (1 % APS) pre-dissolved therein.

In both cases, a flea type stirring bar, purchased from Sigma Aldrich, was also added to the tube to permit stirring of the liquid. Each tube was connected to the Carius manifold, subjected to three degassing cycles using liquid nitrogen, before being charged with 0.5 g of monomer. The Carius tubes were sealed under frozen vacuum using an oxy-acetylene torch and placed in a fumehood inside a steel blast container to warm up to ambient temperature over the course of an hour.

Each tube was suspended in an oil bath and brought to 65 °C while stirring and kept isothermal for 24 hours. Afterward, the tubes were slowly cooled to ambient temperature.

Table 12: *Experimental conditions for the synthesis of PTFE via non-transfer uncontrolled free-radical polymerisation.*

Experiment number	Temperature (°C)	TFE amount (mmol)	Initiator ratio (%)
1	50	50	5.5
2	55	50	5.5
3	65	50	5.5
4	75	50	5.5
5	80	50	5.5
6	65	50	1
7	65	50	2.3
8	65	50	5.5
9	65	50	8.7
10	65	50	10
11	55	50	8.7
12	55	50	2.3
13	75	50	8.7
14	75	50	2.3
15	65	50	5.5

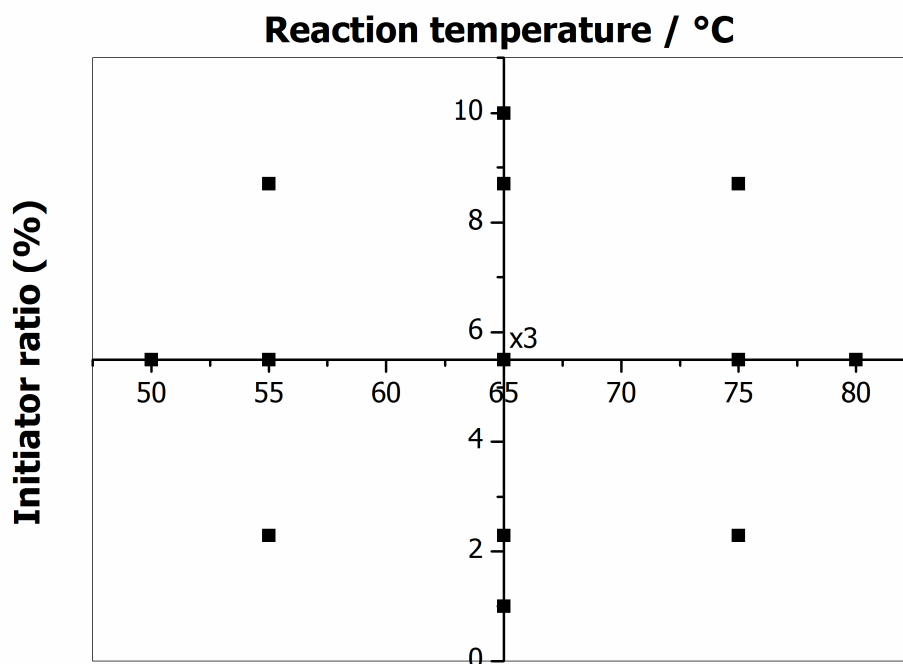


Figure 50: Graphical representation of the experimental design for the non-transfer, uncontrolled free-radical synthesis of PTFE using APS in water.

4.2.4 Differential scanning calorimetry

Differential scanning calorimetry was performed on a Perkin Elmer DSC4000 with ~ 12 mg of dried polymer sample. The samples were heated from 20 °C to 430 °C at a rate of 10 °C·min⁻¹ before being cooled to 20 °C at a rate of 10 °C·min⁻¹, all under a nitrogen atmosphere flowing at a rate of 20 mL·min⁻¹. Each sample was subjected to three of these heating/cooling cycles to erase any thermal history in the sample, and the heat of crystallisation was determined by integrating the crystallisation peak on the third cycle.

The number-average molecular weight of the polymer was determined from the enthalpy of crystallisation using the correlation of Wiegel *et al.* as recommended by Lappan *et al.* [12].

4.2.5 Thermogravimetric analysis

Thermogravimetric analysis was performed using a Hitachi STA7300 TGA-DTA instrument. Approximately 10 mg of sample was used for each run. Each sample was heated from 30 °C to 1000 °C at a rate of 10 °C·min⁻¹ under a nitrogen atmosphere flowing at 200 mL·min⁻¹.

4.2.6 Fourier-transform infrared analysis

Fourier transform infrared analysis was performed on 25 mm diameter discs of PTFE powder cold pressed under 5 metric tons of pressure (~0.5 g of powder per disc) for 10 minutes,

resulting in a disc thickness in the region of 250 μm . The discs were inserted into the transmission cell of a Perkin Elmer Spectrum 100 instrument and scanned from 4000 to 450 cm^{-1} at a resolution of 2 cm^{-1} , collecting and averaging 32 spectra per sample.

4.2.7 Pyrotechnic burn tests

Commercial PTFE as well as PTFE synthesised by the method mentioned in Section 5.2.3.1 was mixed with silicon powder in an 80:20 ratio. The powders were placed in a mortar and pestle along with sufficient cyclohexane to wet the powders, then ground together for approximately 5 minutes. The mixture was left in a fume hood for 1 hour to permit the cyclohexane to evaporate. Approximately 5 g of powder was prepared per compounding.

The pyrotechnic mixture was scraped into a 3-cm line loosely packed in a 4-mm wide, 2-mm deep square-cut groove cut into a pyrophyllite brick and having a graded background. The mixture was ignited by heating one end with a small butane torch. Burn rates were measured optically using a high-speed Canon Powershot SX 260 HS camera. The camera lens was covered by a metalised polypropylene foil.

4.3 Results & discussion

The products were all isolated as clumps of granular, off-white to light yellow, hydrophobic powders, and substantially increasing the initiator concentration (up to 20 %) did not change the observed morphology of the particles or the product colour. A small portion of the product was fine, spherical powder, bright white in appearance, and this portion tended to increase with increasing temperature. Figure 51 shows an example of the isolated polymer product. When pressed into discs, the polymer exhibited a range of hues, from pale yellow to deep orange, with these discs being extremely brittle (*cf.* the bright white and mechanically tough discs obtained from commercial PTFE). The disc colour deepened with increasing initiator concentration and, furthermore, all the discs darkened significantly upon sintering at 360 $^{\circ}\text{C}$.

Interestingly, PTFE synthesised at 65 $^{\circ}\text{C}$ with 5.5 % APS, but without borax buffer, behaved similar to commercial PTFE in that it was bright white and ductile when pressed, but slightly darkened upon sintering, though much less than the borax-buffered PTFE. Furthermore, the discs made from commercial PTFE were opaque, whereas the synthesised PTFEs produced discs that were transparent and glassy in appearance before sintering.

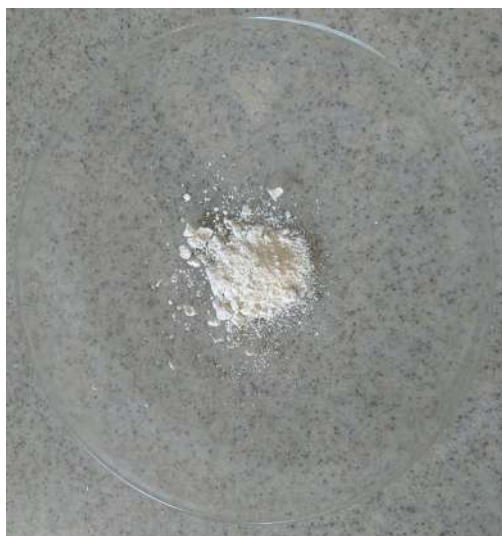


Figure 51: *Photograph showing an example of the PTFE synthesised by aqueous, free-radical polymerisation at 80 °C.*

4.3.1 Molecular weight

4.3.1.1 Molecular weight determined by thermal analysis

The molecular weights for PTFE synthesised at 65 °C, determined by DSC, are presented in Figure 52 as a function of square root of initiator concentration, and the thermograms for these polymers are presented in Figure 53.

Noticed immediately from Figure 52 is the increase in number-average molecular weight (M_n) with increasing initiator concentration, which is contrary to what is expected in a free radical polymerisation [11]. The above-mentioned trends in molecular weight also holds for the polymers produced at 55 and 75 °C. The molecular weight for all the PTFE produced here fell between 1×10^5 and 9×10^5 Da. The product molecular weight increases with decreasing reaction temperature, with the product produced at 50 °C and 5.5 % APS exhibiting a number-average molecular weight of 6×10^5 Da, whereas the product produced at 75 °C and 5.5 % APS exhibited a M_n of 3.5×10^5 Da. The molecular weight determined for commercial PTFE per the DSC method was 3×10^7 Da.

The thermograms (Figure 53) show mass loss at lower temperatures than observed for commercial PTFE, with the magnitude of the mass loss increasing with increasing initiator concentration.

Linear, unbranched perfluorocarbons are semi-ridged chains consisting of CF_2 moieties. These fluorocarbons undergo decomposition only *via* chain scission, or unzipping from the end-groups

[13]. For the homologous series of linear, unbranched fluorocarbons of the formula $\text{CF}_3-(\text{CF}_2-\text{CF}_2)_n-\text{CF}_3$, there is some value of n , below which there will be minimal entanglement between the fluorocarbon chains. There is also some value of n for which the normal boiling point of the fluorocarbon exceeds the decomposition temperature. If a mixture of linear, unbranched fluorocarbons containing a wide distribution of chain lengths (*i.e.* exhibit a large distribution of n values) is subjected to heating, all the chains with n values lower than the critical n value will evaporate from the mixture before decomposition occurs. Evaporation will not occur if the chains are sufficiently long for chain entanglement to restrict the diffusive mobility of the chain in the mixture. Also, evaporation of a fluorocarbon chain will not occur if its normal boiling point exceeds the decomposition temperature. The maximum value that n may attain is determined by the n value where either of the above-mentioned restrictions first start to occur.

This implies that the mass loss before 590 °C, as seen in Figure 53, is due to evaporation of low-molecular-weight PTFE chains. Thus, the thermograms imply an increase in the low-molecular-weight chain content with increasing initiator concentration. This observation is not unexpected and such a trend is anticipated from kinetic considerations.

The increasing number-average molecular weight presents a conundrum: Given that there is a finite amount of TFE present, an increase in initiator concentration will result in a general lowering of the number-average molecular weight. A broadening of the molecular-weight distribution may occur, but the general trend is the shifting of the molecular-weight distribution towards the low molecular weight end.

4.3.1.2 Infrared end-group analysis

Attempts to determine the number-average molecular weight from the end-groups using FTIR spectroscopy did not deliver any useful results: The FTIR spectra of the product PTFE did not exhibit the same absorption bands that Lappan indicates should be present, and hence, the method of Lappan [12] could not be used.

An example FTIR spectrum, for PTFE synthesised at 65 °C using an initiator ratio of 5.5 % is presented in Figure 54. Lappan reports the IR absorption band for a free carboxylic acid as 1815 and 1809 cm^{-1} , and the band for a bound carboxylic acid as 1777 cm^{-1} .

According to the end-group schemes laid out by Pianca *et al.* [14], the product PTFE should exhibit either carboxylic acid or amide end-groups due to the ammonium persulfate initiator.

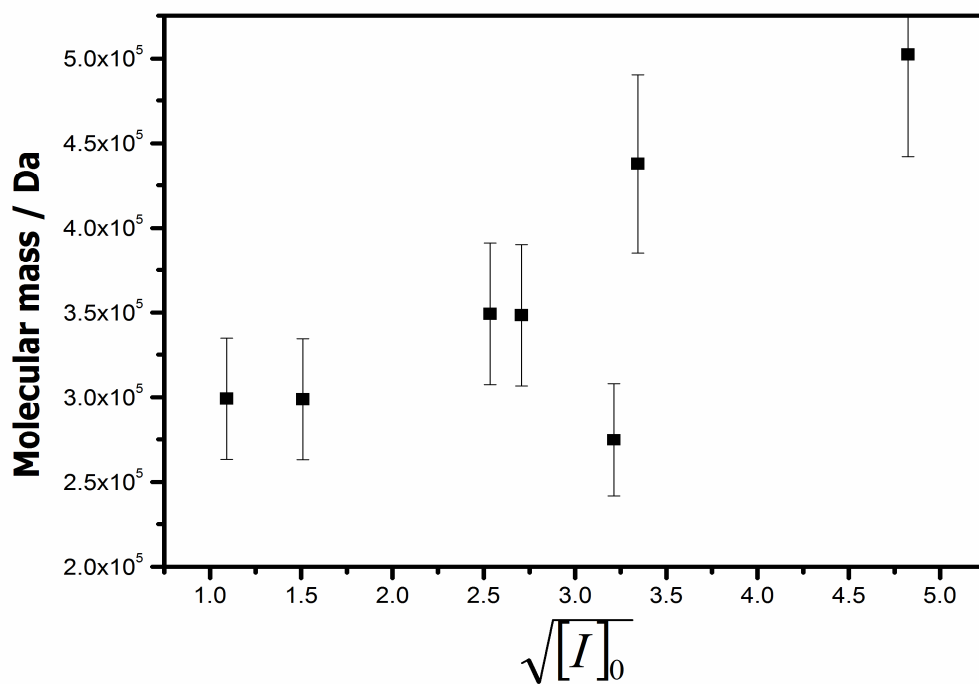


Figure 52: *Molecular weight of PTFE, as determined by DSC, as a function of the square root of the initiator concentration at 65 °C isothermal conditions, produced by aqueous, batch free-radical polymerisation using ammonium persulfate as initiator.*

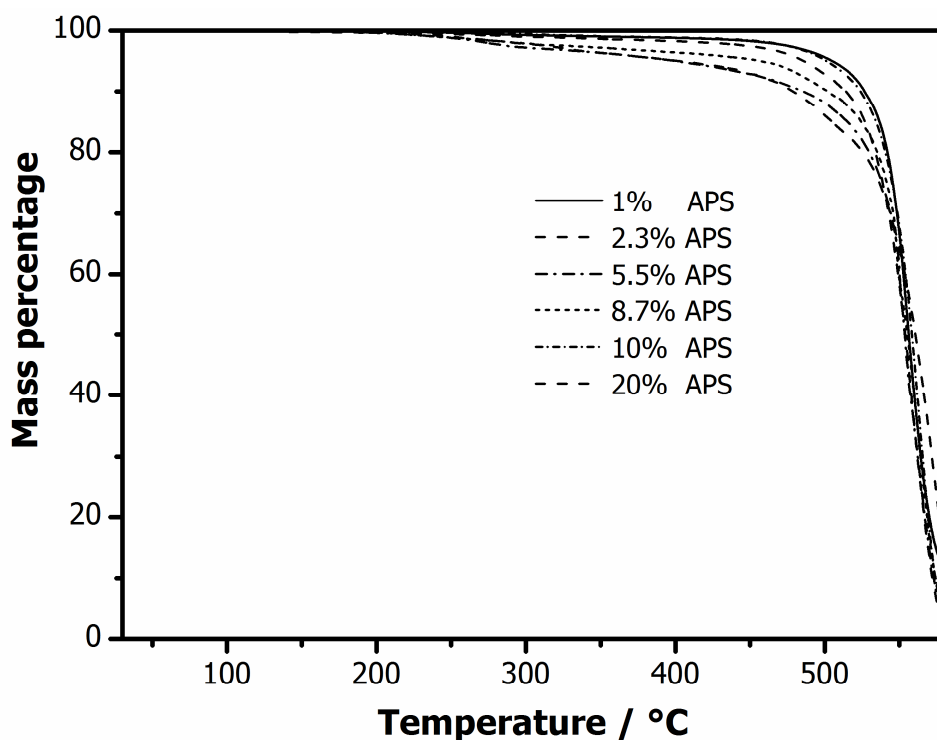


Figure 53: *Thermograms for PTFE synthesized at 65 °C at 1, 2.3, 5.5, 8.7, 10, and 20 mol % APS.*

The bands at 3557 and 1775 cm^{-1} corresponds to the free OH- and the C=O bond of a carboxylic acid group, respectively, while the bands at 3437 and 1665 cm^{-1} correspond to the various vibration modes for an amide, indicating a mixed termination situation. The bands at 2365 and 1545 cm^{-1} are due to the vibrations of the PTFE chain [15]. The band at 980 cm^{-1} does not correspond to the frequencies assigned to the intrinsic vibrations to the PTFE chain in the literature [15, 16]. The band at 980 cm^{-1} does correspond to a C-O-C moiety, found in end-groups generated by bis(perfluoro-2-n-propoxypropionyl) peroxide [17]. As pointed out by Xu *et al.* [17], this band is absent in PTFE prepared with aqueous initiators, so attributing the band at 980 cm^{-1} to a C-O-C moiety from the end-group makes no sense.

Even if the bands assigned by Pianca and co-workers to the end-groups of PTFE are used with Lappan's method, the molecular weights obtained differ by two orders of magnitude from the molecular weights obtained by DSC. Interestingly, the peak at 3512 cm^{-1} is present in all samples, except for the sample prepared *sans* borax and, therefore, it appears that the borax buffer is included in the end-group. This phenomenon does not seem to be reported in the literature. Understanding the end-group phenomena was deemed beyond the scope of the research brief, and it will not be explored further.

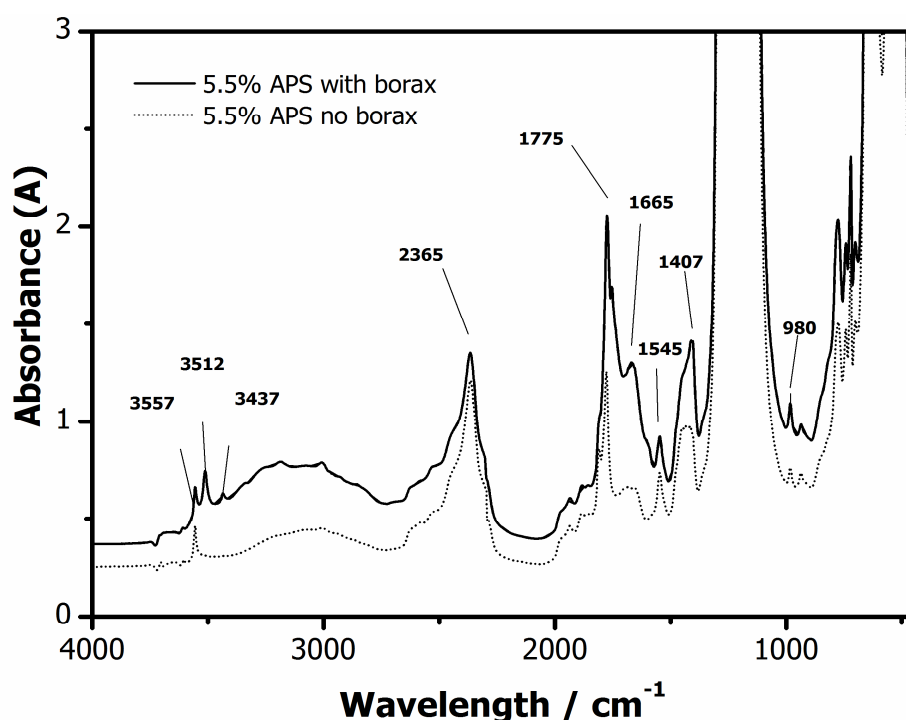


Figure 54: The transmission mode FTIR spectrum of a disc of PTFE produced by aqueous, batch free-radical polymerisation at 65 °C using 5.5 % ammonium persulfate as initiator.

The failure of end-group analysis by IR to corroborate the M_n obtained by thermal analysis suggests that the end-groups of PTFE are poorly understood. Furthermore, the literature

equations relating end-group absorbance to molecular weight are not universally applicable to all PTFEs.

4.3.2 Kinetic modelling of the TFE polymerisation process

The TGA and M_n data seem to indicate that it is not possible to tailor, in a facile manner, the molecular weight of PTFE prepared by aqueous free-radical polymerisation by altering the polymerisation conditions alone; and PTFE waxes suited to pyrotechnical applications cannot be produced in this manner. Contrast this with the facile control of the molecular weight of PTFE by sc-CO₂ [17]. However, the molecular weight data obtained from differential scanning calorimetry is unexpected, and the inability to corroborate the data by end-group analysis presents a conundrum. Given that, save for the initiator concentration, the experimental conditions were equal between runs, why is the M_n behaving opposite to what is expected?

As the M_n does not drop below the minimum value where Wiegel's equation is applicable ($\sim 10^5$), the result is not due to an extrapolation error. Both Suwa and Wiegel used the SSG method to determine the M_n of their polymers and correlated this M_n to the heat of crystallisation. The M_w was not known for these polymers, and the effect of M_w on the heat of crystallisation is poorly understood for PTFE. It may be that differences in the molecular-weight distribution between the low-molecular-weight PTFE and the calibrant PTFE used by Suwa and Wiegel give rise to the erroneous M_n values. On the other hand, the kinetics of TFE suspension homopolymerisation are also poorly understood, and it may be that the increase of molecular weight with increasing initiator concentration is not an analytical artefact.

An important question arises: Given that M_n is calculated from the molecular-weight distribution, can the data be explained by the kinetic behaviour and can the molecular-weight distribution (and the observed M_n) correctly be predicted for heterogeneous suspension polymerisation reactions, such as TFE?

Various possible forms of the molecular-weight distribution are shown in Figure 55. The preceding question is justified from the following considerations regarding these distributions: The assumption that PTFE has a symmetrical molecular-weight distribution (Panel A, Figure 55) is implicit in Suwa and Wiegel's equations, and this assumption is justified for some commercial PTFE grades (from the curves generated by Wu [5]). However, panel B shows a narrower distribution than what is shown in panel A, but with the same M_n value. These two curves are

not expected to show similar heats of crystallisation and may give different M_n results when Wiegels equation is applied.

Furthermore, there is no guarantee, no fundamental reason why the molecular-weight-distribution curves for PTFE should be symmetrical, and the low-molecular-weight waxes may also exhibit skewed distributions (shown in panels C and D in Figure 55). If the kinetics governing TFE polymerisation behave such that the skewness of the distribution is a function of the initiator concentration, then M_n may increase, even if the polydispersity and low-molecular-weight content of the PTFE increases.

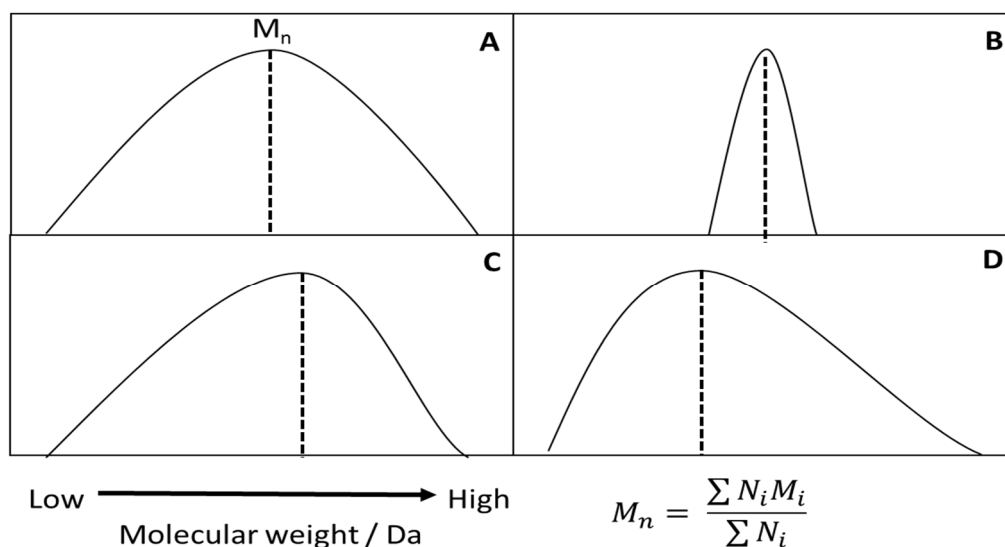


Figure 55: Possible shapes of a molecular-weight-distribution curve for PTFE.

The efficient tailoring of PTFE molecular-weight distribution by altering the polymerisation conditions only, is such an attractive proposition that the idea cannot simply be abandoned without at least attempting to ascertain to what extent the polymerisation conditions can control the distribution and to prove, or disprove, the assertion that PTFE may exhibit a skewed molecular-weight distribution. Presented below is a suggestion for deriving a kinetic expression that can predict the molecular-weight distribution of PTFE. As the rheological behaviour of the low-molecular-weight PTFE synthesised here was not satisfactory (see Section 4.3.4), this sub-project was abandoned and development of the kinetic expression was not pursued in full.

The endeavour to produce PTFE waxes shows that simple adjustments of the polymerisation process will not necessarily produce the hoped for low-molecular-weight PTFE waxes and it is no easy task to control the molecular-weight distribution of PTFE. Some other method will have to be used to tailor the molecular weight of PTFE.

4.3.2.1 Suggested route for kinetic model development

Tobolsky [11, 18] published a quantitative relation with which the molecular-weight distribution may be calculated. From Tobolsky's law (shown in Equation (24)) the equation for kinetic chain length (shown in Equation (25)) is derived [11, 18],

$$\frac{d[M]}{dt} = -k_p \sqrt{\left(\frac{fk_d[I]}{k_t}\right)} [M] \quad (24)$$

$$v = \frac{k_p[M]}{2\sqrt{(fk_d[I]k_t)}} \quad (25)$$

Here, $[M]$ is the concentration of the monomer in the medium, $[I]$ is the concentration of the initiator in the medium, k_p is the propagation constant on the monomer, k_d is the decomposition constant for the initiator, k_t is the termination constant of the polymer, f is the initiator efficiency factor, t is time and v is the kinetic chain length.

Applying this equation using the rate constants for TFE and APS reported in the literature [19] with the assumption that all the TFE is in the liquid phase, a kinetic chain length of $\sim 4 \times 10^9$ is obtained for the *initial phase* of polymerisation at 40 °C (TFE concentration is 1.5 mol·L⁻¹), which translates to an initial molecular weight of $\sim 8 \times 10^{11}$ Da when assuming that termination only occurs *via* mutual recombination (that is, $DP_n = 2v$).

The initial molecular weight predicted ($\sim 10^{11}$ Da) by the kinetic equation is far in excess of what is experimentally observed ($\sim 10^5$ Da), and it is inconceivable that the number-average molecular weight calculated from the distribution should approach the experimental values. There are multiple possible reasons for this discrepancy, of which the most salient are: 1) the kinetic data in the literature are wrong, 2) tetrafluoroethylene does not undergo dead-end polymerisation in aqueous media, and, 3) tetrafluoroethylene diffusion into the aqueous media is the rate limiting step in the polymerisation process.

Markevich *et al.* [20] indicated that Tobolsky's law is not strictly applicable to TFE polymerisation and that the termination constant, k_t , is a function of the monomer concentration and not an independent variable.

By modifying the kinetic equation to include Markevich's expression for k_t , Equations (29), (27), and (28) are obtained.

$$\frac{d[M]}{dt} = -k_p \sqrt{\left(\frac{fk_d[I]}{k_p[M]\xi}\right)} [M] \quad (26)$$

$$v = \frac{k_p[M]}{2\sqrt{(fk_d[I]k_p[M]\xi)}} \quad (27)$$

$$\xi = \lambda\alpha\left(1 + 4\pi\lambda\frac{r}{\alpha}\right) \quad (28)$$

Here λ is the C-C bond length in PTFE (2.64 Å), a is the cross section of the TFE molecule in the polymer (*ca.* 28.6 Å²), and r is the cage radius around the radical centre where recombination may take place (*ca.* 2 Å at 40 °C). The new equation gives an initial kinetic chain length of 2.93x10¹⁵ and a M_n of 5.88x10¹⁷ Da. This value is even more absurd than the first.

Tobolsky's law assumes that all the monomer is in solution and the most probable cause of the errors from the kinetic expressions is the incorrectness of assumption that all the TFE monomer is available for polymerisation. Diffusion of TFE into the liquid medium plays a critical role in the polymerisation process, and this is evident from the observed low solubility of tetrafluoroethylene in water (153 mg·L⁻¹) [21] and from the slow headspace pressure drop over time observed experimentally during autoclave polymerisation (see Figure 57).

However, solubility alone is not sufficient to prove the assertion. Kim *et al.* [9, 10] (and numerous statements in the patent literature) indicates that the gas-liquid surface area plays a crucial role in determining the rate of polymerisation. However, employees of DuPont/Chemours (personal communications made during various ACS Fluoropolymer conferences) have repeatedly stated that the actual polymerisation reaction occurs in the gas phase.

To test the extent to which mass transfer plays a role in the polymerisation of TFE, experiments were performed in Carius tubes to enable the visual observation of PTFE formation over time. Experiments were performed with both TFE and with VDF. The justification for using VDF is the greater solubility of VDF in water [22, 23]. The photographic results of these experiments are reproduced in Figure 56.

The experiments in Carius tube show that: 1) Mass transfer of monomer into the liquid phase is far slower than the actual polymerisation and 2) in the case of TFE, the polymerisation occurs

strictly at the gas-liquid interface, provided the radical source is solubilised in the liquid medium. Hence, monomer mass transfer cannot be ignored, and the kinetic equations must be modified to incorporate the effect of diffusion of TFE into the polymerisation medium.



Figure 56: Post-reaction Carius tubes loaded with TFE and with VDF using 1 % APS as initiator at 65°C.

No articles discussing the polymerisation kinetics of sparingly soluble monomers in water could be found. Therefore, a kinetic model was developed by adding a diffusion term to the Tobolsky equation. This diffusion term is simply the product of the mass flux through the surface and the interfacial area divided by the volume of the phase the monomer resides in, viz. $\frac{J_{TFE} \times A_s}{V}$. There are many diffusion models for gas flux into a liquid medium, but in the case of TFE, transient diffusion into a semi-infinite medium [24], although not completely accurate, best describes the monomer behaviour. The modified equations for monomer concentration as a function of time is given in Equations (29) and (30),

$$\frac{d[M]_l}{dt} = -k_p \sqrt{\left(\frac{fk_d[I]}{k_t}\right)} [M]_l + \frac{\sqrt{\frac{D_{TFE,Water}}{\pi t}} ([M]_l - [M]_g) A_s}{V_l} \quad (29)$$

$$\frac{d[M]_g}{dt} = -\frac{\sqrt{\frac{D_{TFE,Water}}{\pi t}} ([M]_l - [M]_g) A_s}{V_g} \quad (30)$$

Here, $[M]_l$ is the concentration of the monomer in the liquid medium, $[M]_g$ is the concentration of the monomer in the gas phase, A_s is the interfacial area between the gas and the liquid, V_l is

the volume of the liquid phase, V_g is the volume of the gas phase, and $D_{TFE,Water}$ is the diffusivity of TFE into water. The k_t term may be replaced with the relation derived by Markevich *et al.* [20], as per Equations (26), (27), and (28).

No articles in the publically accessible literature could be found that provide data for the diffusion coefficient of TFE in water. However, there are some “general purpose” correlations for the diffusion of non-electrolytes in water, the simplest of which is the correlation of Hayduk and Laudie [25], given in Equation (31),

$$D_{A,B} = 13.26 \times 10^{-5} \mu_B^{-1.14} (0.285 \times V_{cA}^{1.048})^{-0.589} \quad (31)$$

Here μ is the viscosity of water in cP and V_{cA} the critical volume of the solute in $\text{cm}^3 \cdot \text{g}^{-1}$. The temperature dependence of the viscosity of water is modelled by an Antoine equation with the parameters taken from Perry [26].

One major challenge is the determination of the gas-liquid interfacial area. Treybal [27] discusses numerous correlations for bubble formation and the concomitant interfacial area in aerated stirred tanks, but no equation or model could be found in the literature that is suitable to the case of a small, stirred gas-liquid batch reactor with transient pressure drop. Woods [28] provides some rules of thumb for the estimation of gas-liquid interfacial area in batch stirred reactors, indicating that a well-stirred reactor will have, maximally, an interfacial area of 4000 m^2 per m^3 of reactor volume and, at minimum an interfacial area of 50 m^2 per m^3 of reactor volume.

Since the $[M]_g$ term can be related to the pressure in the reactor, the suitability of the model to the prediction of TFE polymerisation can be assessed by comparing the calculated pressure-time curve to the experimental curves. The pressure as a function of time calculated by the foregoing equations are compared against the experimental pressure drop in Figure 57 for an experiment at $75 \text{ }^\circ\text{C}$ assuming an average interfacial area of 2000 m^2 . The kinetic reaction parameters from literature [19] were used.

Immediately noticeable in Figure 57 is the large error between experimental and predicted values during the first two hours. Furthermore, the experimental data shows an almost linear pressure drop during that time, and the same pressure drop phenomenon holds true for polymerisations at other temperatures and initiator concentrations.

The models derived here predict the general trend of the pressure curve, but they are not accurate enough to be used for the prediction of the molecular-weight distribution of PTFE produced by suspension polymerisation.

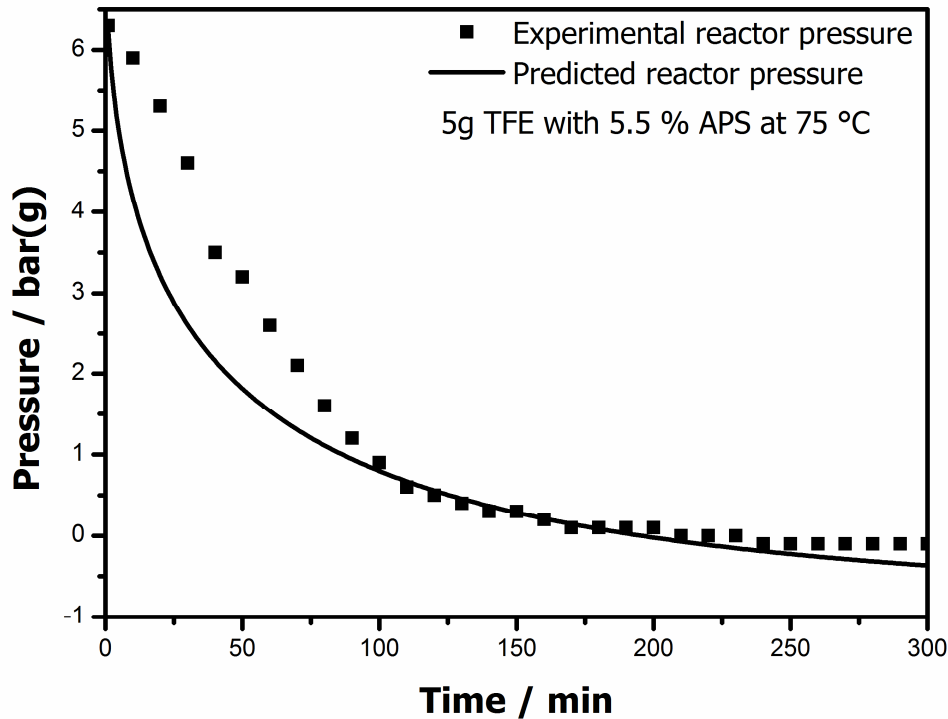


Figure 57: Comparison of the experimental pressure drop with the predicted pressure drop during the homopolymerisation of PTFE in water at 75 °C using 10 % APS as initiator.

The inaccuracies are due partly to the approximate nature of the flux term (in reality, the diffusion coefficient is affected by pressure and boundary shear effects) and partly to the assumption that the interfacial area remains constant throughout the polymerisation process.

Additionally, the initiator efficiency (f) was assumed to be constant throughout the polymerisation process. This assumption is incorrect.

The initiator efficiency is the ratio of rate of initiation of propagating chains to the rate of primary radical formation. If the polymerisation medium is stripped of monomer, the rate of propagating chain initiation decreases and, concomitantly, the initiator efficiency decreases. Hence, f is also a function of $[M]_t$. Furthermore, the termination reaction comprises two parts, *viz.* self-termination and radical-fragment termination.

The kinetic expression must also take into account radical-fragment termination, which is currently not the case and also predict the changing gas-liquid interfacial surface area.

4.3.3 Pyrotechnic behaviour

The mixtures prepared from commercial PTFE did not wet well with cyclohexane, being powdery even when wetted and had no structural integrity when dry, whereas the mixtures prepared with product PTFE wetted to some extent with cyclohexane, forming a viscous

mixture with the silicon that tended to maintain a flaky structure when dry. The mixture with commercial PTFE failed to ignite using a butane torch, only sputtering some ignited silicon embers. The low-molecular-weight PTFE ignited almost immediately upon heating with the butane torch, producing a steady, but low-intensity burn with an optically measured burn rate of $0.035 \text{ mm}\cdot\text{s}^{-1}$. The difference in behaviour of the product PTFE and commercial PTFE toward silicon is explained by two factors: 1) Increased contact between the Si and the product polymer owing to a reduction in mechanical rigidity of the polymer brought about by the effects of a lower molecular weight and 2) the effects of the end-group elimination on the oxygen passivation layer of the silicon.

In order to understand the effect of the abovementioned factors, the mechanism of metal fluorocarbon exchange must be discussed. The technology has been reviewed by Koch [3].

Metal-fluorocarbon-based pyrolants operate *via* a fluorine abstraction reaction. This reaction is complex. The current understanding is that the reaction takes place in three sequential steps, *viz.*: pre-heating (melting), pre-ignition, and rapid fluorine exchange. As there is a large difference in the temperatures required for these steps to proceed, metal-fluorocarbon pyrolants do not detonate; they rather deflagrate with a well understood combustion wave, detailed in Figure 58, and a well understood heat propagation, detailed in Figure 59.

Specifically for Magnesium/Teflon/Viton mixtures (MTVs), the mechanism of fluorine exchange involves a Grignard type metal insertion of magnesium into the C-F bond, followed by the rapid formation of magnesium fluoride and carbon [29]. A similar mechanism can be proposed for the reaction of silicon with PTFE. The ratios of magnesium to fluorine in the condensed product are highly non-stoichiometric and the carbon produced in this reaction is highly amorphous.

The fluorine exchange reactions do not occur in the condensed phase, but rather in an anaerobic gas phase comprising the immediate space around a magnesium particle imbedded in the PTFE. The reactions are presented schematically in Figure 60. The radical fluorocarbons are the product of the thermal decomposition of PTFE.

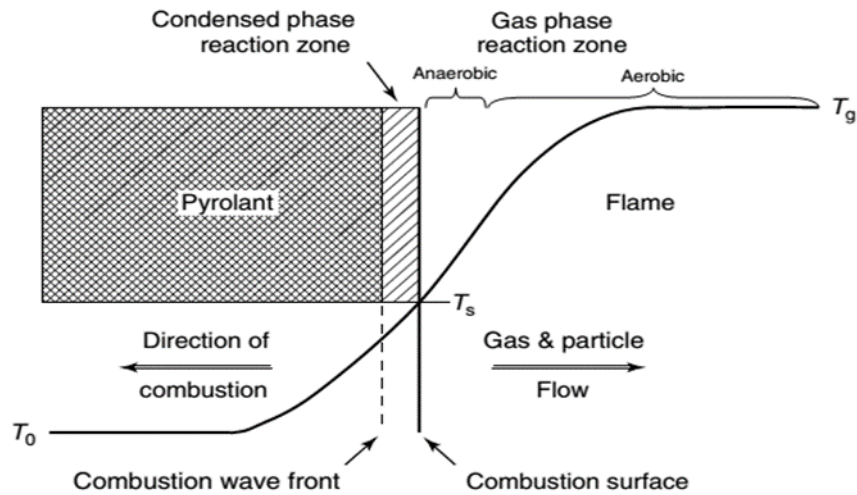


Figure 58: Structure of an MTV combustion wave (image taken from Koch [3]).

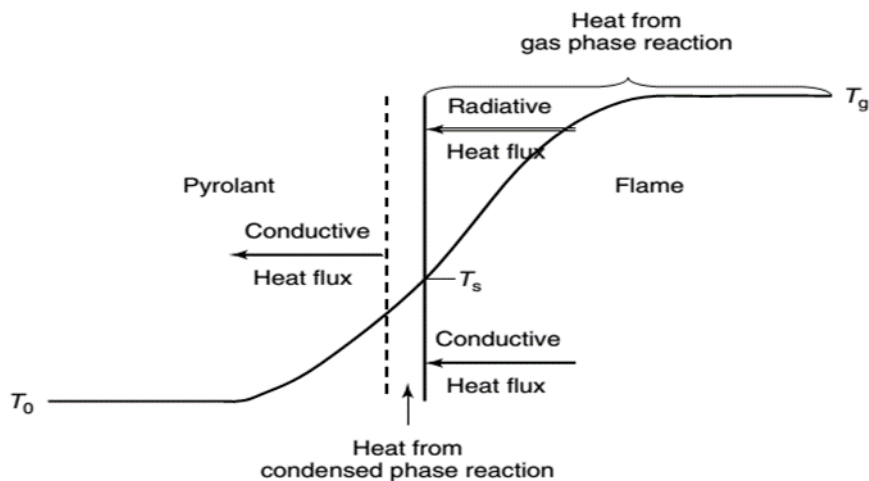


Figure 59: Temperature profile and structure of the heat transfer mechanisms for the combustion of an MTV pyrolant (image taken from Koch [3]).

The polymer chains in commercial PTFE are long and rigid, arranging themselves into large highly ordered regions (polymer crystallites) and next to no amorphous regions, with the apparent crystallinity of virgin PTFE being around 98 %. This is in contrast to polyethylene, whose strands form both crystalline, packed structures, and entangled, globular masses comprising its amorphous portions. When the commercial PTFE is ground together with a filler material, such as silicon metal particles, the PTFE agglomerates are ductile and resist agglomerative breakup, resulting in a mixture of silicon particles embedded in the interstices of large agglomerative particles.

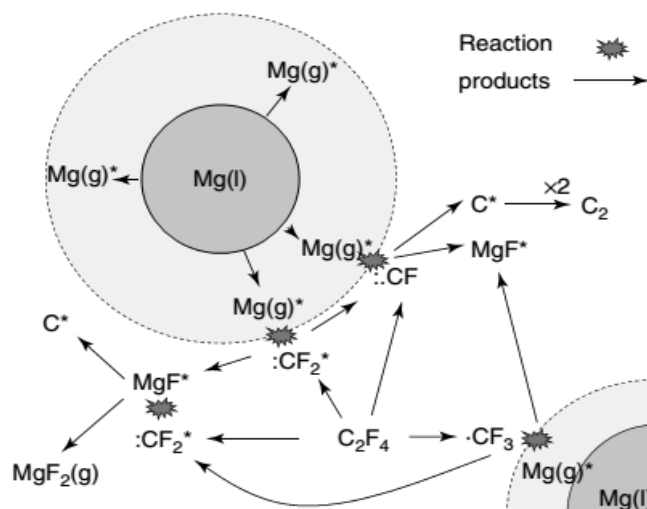


Figure 60: *Schematic representation of the gaseous reactions mediating fluorine exchange between fluorocarbons and magnesium in an MTV combustion reaction (image taken from Koch [3]).*

Shorter chains of PTFE produce smaller crystallites with more amorphous linkages, hence the more brittle behaviour of the low-molecular PTFE. This situation permits filler material to more easily penetrate agglomerated PTFE particles and permits a more even distribution of filler into the PTFE during grinding, which in turn will result in less severe mass-transfer effects of the metal-fluorine exchange reaction. Hence the improved ignitability and better burn characteristic of lower-molecular-weight PTFE.

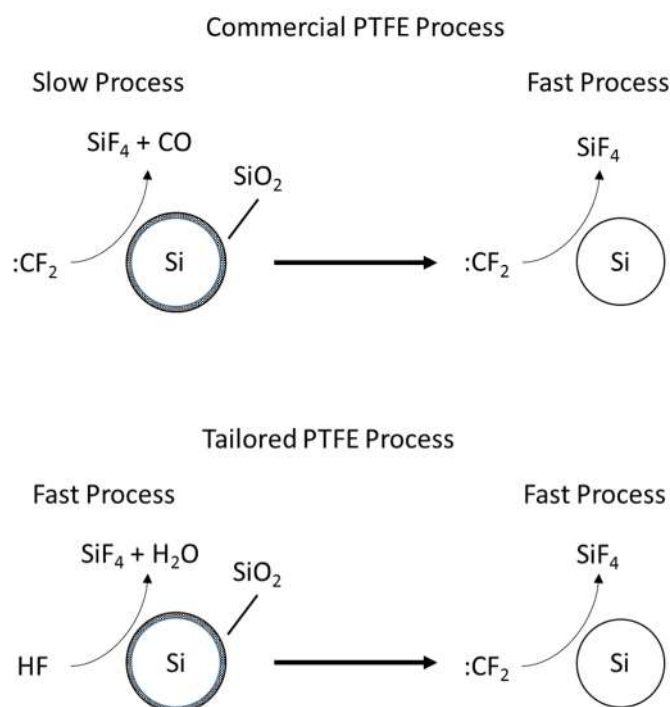
It must also be remembered that elemental silicon, on exposure to air, forms a passivation layer, a thin shell of SiO₂ on the surface of the silicon particle. The stripping of SiO₂ is a much slower process than the Si–fluorine reaction since it is more difficult for :CF₂ radicals to remove the oxygen from the layer.

The low-molecular-weight polymers were initiated with APS and contain carboxylic acid and carboxylic acid derivative end-groups [14]. These end-groups may eliminate, generating HF in the process.

This HF etches (strips) SiO₂ much faster than :CF₂, permitting quicker removal of the passivation layer and the concomitant increase of reactivity of the Si particle. This process is detailed in Scheme 10.

The caveat here is that, although under normal conditions HF elimination should occur first, the high temperatures achieved in the reaction zone and the rapidity of the heat generation implies that HF and :CF₂ will be liberated simultaneously. Hence, the etching of the SiO₂ layer is a combined mechanism, consisting of both :CF₂ and HF etching. The desirable HF mediated

etching becomes a deleterious competitive reaction for pure Si once the passivation layer is gone, so the amount of HF liberated from the polymer must be optimised to obtain the best reaction rates.



Scheme 10: *Reaction of PTFE breakdown products with Si particles, showing the HF stripping of the SiO₂ passivation layer.*

The first factor (better mechanical inclusion) is evident from the observed decreases in molecular weight resulting in better burn rates. The apparent lack of change in the FTIR spectra between pre- and post-sintered PTFE militates against the idea of HF release (the second factor). Some change must occur as there is a noticeable discoloration of the polymer, and what other change can there be except for end-group elimination? Therefore, the HF etching factor, while not entirely proven, must form part of the explanation for the improved reactivity towards silicon of the tailored PTFE over commercial PTFE.

4.3.4 Rheological characterisation

Attempts to perform rheological characterisation on discs pressed from the product PTFE failed as the discs disintegrated, even under low shear conditions, and the mechanical strength did not change significantly with temperature treatment, remaining brittle.

The low-molecular-weight PTFE produced here cannot be moulded or melt-extruded as the molecular weight is simply not low enough to impart wax-like mechanical properties to the polymer.

4.4 Conclusions

The preceding experimental work shows that the polymerisation of PTFE is mass-transfer limited, and the number-average molecular weight and the molecular-weight distribution of PTFE cannot be tailored easily by altering only the polymerisation conditions. However, the polydispersity of the polymer can be tuned by increasing or decreasing the initiator concentration, with increasing initiator concentration resulting in a larger polydispersity index, provided tetrafluoroethylene is polymerised in a batch operation. Therefore, proper control of the molecular weight is best effected by using either a chain-transfer agent, or by using a polymerisation-control agent such as is commonly employed in living-radical polymerisation.

Furthermore, the colour of the product and the end-groups present on the PTFE chain are a function of the polymerisation environment, with even seemingly innocuous additives, *i.e.* sodium tetraborate, incorporating in some way into the PTFE chain.

The preceding results also suggest that lowering the molecular weight, and permitting the generation of small amounts of HF during fluorocarbon/fuel combustion does improve both the reactivity and the burn rate of a PTFE-based pyrotechnic mixture.

However, lowering the number-average molecular weight of the product PTFE by two orders of magnitude with respect to the M_n of commercial PTFE did not produce the hoped for wax-like material, instead producing a brittle material that disintegrates when subjected to rheological characterisation and cannot be melt-extruded. Producing a PTFE wax will not just require lowering the number-average molecular weight, but also tailoring the polydispersity, preferably producing a monodisperse polymer in order to avoid the self-solubilisation of lower mass chains into higher mass chain (which results in a glassy material).

Furthermore, producing a thermally-stable low-molecular-weight polymer will require bridging the PTFE chains to ensure that the lower-molecular-weight chains do not evaporate prematurely and permit the chains to entangle, lending sufficient mechanical (tensile) strength to the product to withstand the stress exerted during extrusion.

4.5 References

- [1] Ebnesajjad, S., 2000, *Fluoroplastics, Volume 1: Non-melt Processible Fluoroplastics*, Elsevier Science, Norwich, New York.
- [2] Ebnesajjad, S., 2002, *Fluoroplastics, Volume 2: Melt Processible Fluoroplastics: The Definitive User's Guide*, Elsevier Science, Norwich, New York.
- [3] Koch, E.C., 2012, *Metal-Fluorocarbon Based Energetic Materials*, Wiley, New York.
- [4] Bunn, C.W., Cobbold, A.J., and Palmer, R.P., "The fine structure of polytetrafluoroethylene", *Journal of Polymer Science*, 1958, 28 (117), 365-376.
- [5] Wu, S., "Characterization of polymer molecular weight distribution by transient viscoelasticity: Polytetrafluoroethylenes", *Polymer Engineering & Science*, 1988, 28 (8), 538-543.
- [6] Tuminello, W.H., Treat, T.A., and English, A.D., "Poly(tetrafluoroethylene): molecular weight distributions and chain stiffness", *Macromolecules*, 1988, 21 (8), 2606-2610.
- [7] Tuminello, W.H. and Cudré-Mauroux, N., "Determining molecular weight distributions from viscosity versus shear rate flow curves", *Polymer Engineering & Science*, 1991, 31 (20), 1496-1507.
- [8] Starkweather, H.W. and Wu, S., "Molecular weight distribution in polymers of tetrafluoroethylene", *Polymer*, 1989, 30 (9), 1669-1674.
- [9] Kim, C.U., Lee, J.M., and Ihm, S.K., "Emulsion polymerization of tetrafluoroethylene: effects of reaction conditions on the polymerization rate and polymer molecular weight", *Journal of Applied Polymer Science*, 1999, 73 (5), 777-793.
- [10] Kim, C.U., Lee, J.M., and K. Ihm, S., "Emulsion polymerization of tetrafluoroethylene: effects of reaction conditions on particle formation", *Journal of Fluorine Chemistry*, 1999, 96 (1), 11-21.
- [11] Tobolsky, A.V., "Dead-end Radical Polymerization", *Journal of the American Chemical Society*, 1958, 80 (22), 5927-5929.
- [12] Lappan, U., Geißler, U., Häußler, L., Pompe, G., and Scheler, U., "The Estimation of the Molecular Weight of Polytetrafluoroethylene Based on the Heat of Crystallisation. A Comment on Suwa's Equation", *Macromolecular Materials and Engineering*, 2004, 289 (5), 420-425.
- [13] Puts, G., Crouse, P., and Ameduri, B., 2014, "Thermal degradation and pyrolysis of polytetrafluoroethylene", in D.W. Smith, Iacono, S.T., and Iyer, S.S. (eds.), *Handbook of Fluoropolymer Science and Technology*, John Wiley & Sons, Inc., New York.
- [14] Pianca, M., Barchiesi, E., Esposito, G., and Radice, S., "End groups in fluoropolymers", *Journal of Fluorine Chemistry*, 1999, 95 (1-2), 71-84.
- [15] Moynihan, R.E., "The Molecular Structure of Perfluorocarbon Polymers. Infrared Studies on Polytetrafluoroethylene¹", *Journal of the American Chemical Society*, 1959, 81 (5), 1045-1050.
- [16] Starkweather, H.W., Ferguson, R.C., Chase, D.B., and Minor, J.M., "Infrared spectra of amorphous and crystalline poly(tetrafluoroethylene)", *Macromolecules*, 1985, 18 (9), 1684-1686.
- [17] Xu, A., Yuan, W.Z., Zhang, H., Wang, L., Li, H., and Zhang, Y., "Low-molecular-weight polytetrafluoroethylene bearing thermally stable perfluoroalkyl end-groups prepared in supercritical carbon dioxide", *Polymer International*, 2012, 61 (6), 901-908.
- [18] Tobolsky, A.V., Rogers, C.E., and Brickman, R.D., "Dead-end Radical Polymerization. II", *Journal of the American Chemical Society*, 1960, 82 (6), 1277-1280.
- [19] Brandrup, J., Immergut, E.H., and Grulke, E.A., 2003, *Polymer Handbook*, Wiley, New York.

- [20] Markevich, A.M., Volokhonovich, I.Y., Kleimenov, N.A., Nosov, E.F., Mel'nikov, V.P., and Berlin, A.A., "The heterogeneous polymerization of tetrafluoroethylene", *Polymer Science U.S.S.R.*, 1975, 17 (11), 2909-2915.
- [21] Veretennikof, N.V., Reshetova, L.I., and Fil'chakova, T.A., "Solubility of different fluorine-containing compounds in water and aqueous solutions of fluoro-organic surfactants", *Fizika Khimiya*, 1984, 1984 (4), 112-114.
- [22] Ameduri, B., "From vinylidene fluoride (VDF) to the applications of VDF-containing polymers and copolymers: Recent developments and future trends", *Chemical Reviews*, 2009, 109 (12), 6632-6686.
- [23] Ameduri, B. and Boutevin, B., 2004, *Well-architected Fluoropolymers: Synthesis, Properties and Applications*, Elsevier Science, Amsterdam, The Netherlands.
- [24] Welty, J.R., Wicks, C.E., and Wilson, R.E., 1976, *Fundamentals of Momentum, Heat, and Mass Transfer*, Wiley, New York.
- [25] Hayduk, W. and Laudie, H., "Prediction of diffusion coefficients for nonelectrolytes in dilute aqueous solutions", *AIChE Journal*, 1974, 20 (3), 611-615.
- [26] Green, D. and Perry, R., 2007, *Perry's Chemical Engineers' Handbook*, McGraw-Hill Education, New York.
- [27] Treybal, R.E., 1980, *Mass-transfer Operations*, McGraw-Hill, New York.
- [28] Woods, D.R., 2007, *Rules of Thumb in Engineering Practice*, Wiley, New York.
- [29] Davis, S.R. and Liu, L., "Ab initio study of the insertion reaction of Mg into a C-F bond of tetrafluoroethylene", *Journal of Molecular Structure: THEOCHEM*, 1994, 304 (3), 227-232.

Chapter 5

**Radical copolymerisation of
chlorotrifluoroethylene with isobutyl vinyl
ether initiated by the persistent perfluoro-3-
ethyl-2,4-dimethyl-3-pentyl radical**

5.1 Introduction

As discussed in Chapter 1, PTFE waxes suitable to use in pyrotechnics require a zero shear viscosity of 10^4 Pa·s at the processing temperature. The effects of temperature and molecular-weight distribution on the viscosity of PTFE waxes are unknown; however, the zero shear melt viscosity of PTFE seems to be a function of M_w [1]. Wu's correlation indicates that, at the melt temperature, PTFE requires a M_w of 5×10^5 Da, and thus the target M_w must be below this value.

The commercial nature of this doctoral research precluded an initial, in-depth study of the effects of molecular-weight distribution on the rheology of PTFE, and it was assumed that an acceptable, pyrotechnic grade of PTFE could be produced simply by decreasing the molecular weight of PTFE. The low-molecular-weight PTFE synthesised in the preceding chapter did not exhibit the desired rheological properties required for use in pyrotechnical formulations, despite exhibiting an increased polydispersity and a relatively low molecular weight compared to commercial PTFE.

The counter-intuitive M_n values obtained by thermal analysis implies that the standard methods for determining PTFE's number-average molecular weight may be susceptible to grave errors and care must be taken when interpreting the calculated M_n values for PTFE systems with molecular-weight distributions significantly different from the distributions of the calibrant PTFEs. Furthermore, the M_w of PTFE is exceedingly difficult to determine. Objective values for M_w , independent of the other techniques [1-4] may come from the polymerisation kinetics, but the kinetic equations must be vetted against experimental values. At minimum, a believable kinetic relation must predict the M_n of PTFE accurately.

Accurate values of M_n can be obtained from end-group analysis, but the failure of IR end-group analysis in the previous chapter to corroborate the M_n values obtained by DSC, implies that an alternative end-group analysis method is required. Recently Patil *et al.* [5] utilised the persistent perfluoro-3-ethyl-2,4-dimethyl-3-pentyl radical (abbreviated as PFR [6], structure shown in Figure 61) to generate $\bullet\text{CF}_3$ radicals for polymerisation initiation. The resulting CF_3 end-groups were used in ^{19}F NMR spectroscopy for the determination of average molecular weights of VDF copolymers. The technique provides M_n values closer to the true molecular weight of the copolymers than SEC. In addition CF_3 labelling allows for the identification of the attack preferences of radical initiators on both co-monomers.

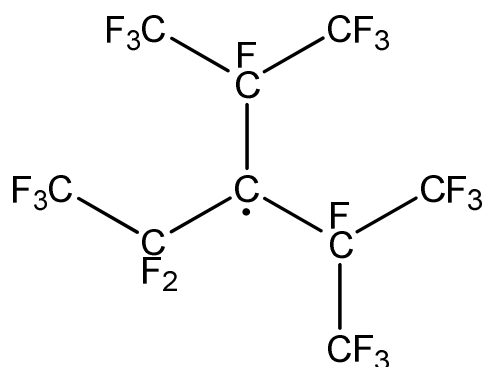


Figure 61: *Structure of the perfluoro-3-ethyl-2,4-dimethyl-3-pentyl persistent radical (PPFR).*

In the research reported in this chapter, the use of PPFR as initiator was extended to the copolymers of CTFE and isobutyl vinyl ether. The molecular weights as well as the attack preferences of $\bullet\text{CF}_3$ onto the co-monomers, and the polymers thermal properties was studied. The purpose of this work is to validate the use of the PPFR as an NMR spectroscopic tracer on polymers where the backbone contains large, continuous sections of fully halogenated moieties, as opposed to the partially fluorinated moieties found in VDF copolymers, with the final aim of applying PPFR to TFE polymerisation and determine, in a reliable manner, the M_n values of PTFE.

Additionally, the work in the preceding chapter showed that the synthesis of a low-molecular-weight, wax-like PTFE with a tailored molecular-weight distribution is not easy and cannot be accomplished by simply altering the polymerisation conditions. Alternative synthesis strategies will have to be employed, such as conducting reversible-deactivation radical polymerisation (living radical polymerisation) using a well-defined control agent, or by adding a chain-transfer agent to the reactor during polymerisation.

Unfortunately, the Fluoro-Materials Group (and South African in general) lacked sufficient expertise with these techniques to be able to successfully execute such syntheses. Skills transfer from France to South Africa regarding advanced fluoropolymer synthesis techniques was a second goal of the research laid out in this chapter.

This work was executed in the Laboratories of the Institute Charles Gerhardt of the CNRS at the École National Supérieur de Chimie de Montpellier in Montpellier, France and was performed under the supervision of Drs Bruno Ameduri and Gerald Lopez.

Part of this Chapter has been published as a research article in the journal RSC Advances [7].

5.2 Experimental

5.2.1 Materials

Chlorotrifluoroethylene $\geq 99\%$ (CTFE, CAS No 79-38-9) was kindly provided by Honeywell (Buffalo, USA) and used as received. Isobutyl vinyl ether 99 % (iBuVE, CAS No 109-53-5), potassium carbonate 99.99 % (K_2CO_3 , CAS No 584-08-7), dimethyl carbonate 99 % (DMC, CAS No 616-38-6), methanol $\geq 99.8\%$ (CH_3OH , ACS Reagent, Ph. Eur., CAS No 67-56-1), and acetone $\geq 99.5\%$ (CH_3COCH_3 , ACS Reagent, Ph. Eur., CAS No 67-64-1) were purchased from Sigma-Aldrich (Saint Quentin-Fallavier, France) and used as received. Distilled water was provided by an in-house purification system.

The PFR was kindly supplied by Prof. Taizo Ono of the Research Institute of Instrumentation Frontier in Nagoya. The PFR was prepared by direct fluorination of a hexafluoropropene trimer precursor mixture at room temperature using undiluted fluorine gas. The PFR solution was washed with 1 M aqueous Na_2CO_3 followed by distilled water, and then distilled under reduced pressure (25 mmHg). The distillate fraction boiling at 31–33 °C was used for this investigation. More information on the synthesis of the persistent radical may be found in Scherer *et al.* [6].

5.2.2 Polymerisation apparatus

The polymerisation reactions were conducted in a Parr Instruments (Moline, Illinois) stirred reactor (Hastelloy HC276). The reactor was equipped with an inlet valve and two outlet valves, a 3000 psi rupture disc, a Span bourdon type pressure gauge, and a thermowell. Temperature control was achieved by way of a heating jacket connected to a PID controller. A stainless steel sheathed (isolated) K-type thermocouple was used to monitor the temperature in the reactor.

5.2.3 Radical polymerisation procedure

The reactor was subjected to 24 hours of acetone wash at 90 °C before each polymerisation run and pressure tested at 20 bar nitrogen before being subjected to high vacuum for 1 hour.

The reaction mixture was prepared by dissolving 17.2 g of iBuVE and 0.0237 g of K_2CO_3 into 25 mL of DMC in a 50-mL round-bottom flask, with the PFR initiator (1 %, 5 %, 10 % and 20 %, molar basis with respect to total monomer charge) being added after the potassium carbonate had dissolved. The reaction mixture was degassed under nitrogen for 20 minutes using the balloon and septum method. The reaction mixture was introduced to the reactor *via* a funnel

tightly attached to the inlet valve with 25 mL of DMC used to wash out the degassing flask, ensuring that all the reagents were transferred to the vessel.

The reactor was immersed in liquid nitrogen until the DMC turned solid before the CTFE was transferred into the reactor. The mass of CTFE in the reactor was determined by weight difference (accurate to 0.5 g). The mass of CTFE was kept constant at 20 g in all the experiments.

The loaded reactor was left in a fume hood to warm to 25 °C over a 1 hour period before it was placed in the reactor stand. The reaction temperature was increased in a stepwise fashion to avoid overheating by first heating to 40 °C, then to 60 °C, then 80 °C, and finally to 90 °C, stirring all the while. The reactor was left at 90 °C for 24 hours and afterwards cooled to 25 °C using an ice bath before it was degassed and opened.

In all cases, addition of PFR to the solution of iBuVE in DMC resulted in an immediate yellowing of the solution. This is due to interaction between the π -orbitals of the vinyl ether and the PFR radical [8]. This interaction was considered to have no effect on the polymerisation reaction.

5.2.4 Product purification

The product solution from the reactor was evaporated in a rotary evaporator, leaving behind a viscous material. The impure polymeric material was thrice dissolved in acetone and evaporated, before being dissolved in sufficient acetone to produce a saturated solution that was precipitated by drop-wise addition of the solution into a flask of vigorously stirred, cold (~ 0 °C) methanol. The precipitate was filtered off, washed with methanol, precipitated a second time, filtered off, washed with methanol and dried under high vacuum at 80 °C. For the 20 % PFR experiment, distilled water rather than methanol was used as precipitating agent, as the product material dissolved in methanol.

The product from the 1 % PFR experiment was isolated as a hard, whitish, opaque solid. The products from the 5 % and 10 % PFR experiments were isolated as elastomeric, yellow to light orange solids, and the product from the 20 % PFR experiment was isolated as a dark brown wax.

5.2.5 Nuclear magnetic resonance spectroscopic characterisation

The nuclear magnetic resonance spectra were recorded on a Bruker AC 400 using deuterated chloroform. Coupling constants and chemical shifts are given in hertz (Hz) and parts per million (ppm), respectively. ^1H , ^{19}F , and proton-decoupled ^{19}F NMR spectroscopies were performed.

The experimental conditions for recording ^1H (or ^{19}F) NMR spectra were: flip angle 90° (or 30°); acquisition time of 4.5 s (or 0.7 s, pulse delay of 2 s, 32 scans (or 1024 scans); and a pulse width of 5 μs for ^{19}F NMR spectroscopy.

The samples for analysis by NMR spectroscopy were prepared by dissolving 100 mg of polymer material in 1 mL of CDCl_3 . The molecular weights determined by ^{19}F NMR spectroscopy were calculated using a similar procedure as previously reported [9].

5.2.6 Thermogravimetric analysis

Thermogravimetric analyses under nitrogen were performed using a Perkin Elmer TGA 4000 coupled to a Perkin Elmer Spectrum 100 FTIR spectrometer. Polymer samples (~ 50 mg) were heated from 25°C to 600°C at $10^\circ\text{C}\cdot\text{min}^{-1}$ in air flowing at a rate of $50\text{ mL}\cdot\text{min}^{-1}$. The IR spectra were recorded from 550 cm^{-1} to 4000 cm^{-1} every 6 seconds at a resolution of 4 cm^{-1} .

Thermogravimetric analyses under air were carried out on a TGA 51 apparatus from TA Instruments. Polymer samples (~ 15 mg) were heated from 25°C to 500°C at $10^\circ\text{C}\cdot\text{min}^{-1}$ in air flowing at a rate of $50\text{ mL}\cdot\text{min}^{-1}$.

5.2.7 Differential scanning calorimetry (DSC)

Polymer samples (~ 10 mg) were subjected to two heat-cool cycles under a nitrogen flow of $50\text{ mL}\cdot\text{min}^{-1}$. The polymer samples were heated from 25°C to 150°C at $10^\circ\text{C}\cdot\text{min}^{-1}$, held isothermally at 150°C for 5 min, cooled from 150°C to -150°C at $10^\circ\text{C}\cdot\text{min}^{-1}$, held isothermally at -150°C for 5 min, subjected to another heat-cool cycle before being heated from -150°C to 25°C at $10^\circ\text{C}\cdot\text{min}^{-1}$. T_g values were determined as the inflection point in the heat capacity jump.

5.2.8 Size-exclusion chromatography (SEC)

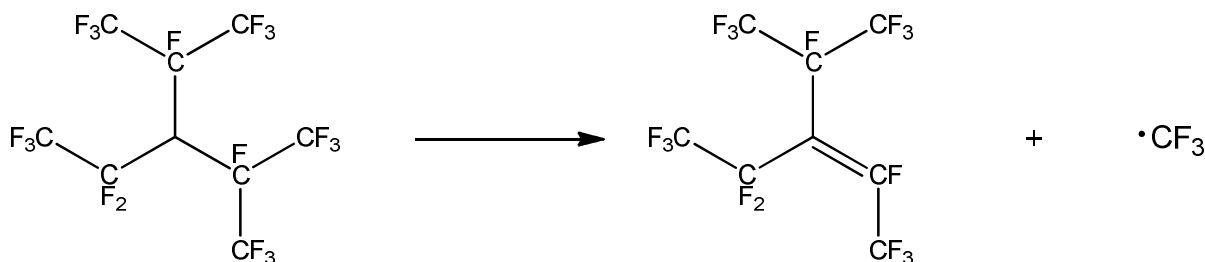
Size-exclusion chromatography was conducted using a GPC 50 from Polymer Labs (Now Agilent) with Cirrus software as well as an Agilent 1260 Infinity system equipped with a Varian 390 LC triple detection system. The two systems used 2 PL Gel Mixed C columns ($200 < M_w < 20\text{ Mg}\cdot\text{mol}^{-1}$) with tetrahydrofuran (THF) as the eluent at a flow rate of $1.0\text{ mL}\cdot\text{min}^{-1}$ at 35°C .

The RI and UV detectors were calibrated using polystyrene standards. The viscometry detector used a universal calibration. Samples were prepared by dissolving 15 mg of polymer into 3 mL of THF followed by filtering through a 20 μm commercial PTFE filter. Analyses were achieved by injection of 20- μL filtered solutions (5 $\text{mg}\cdot\text{mL}^{-1}$).

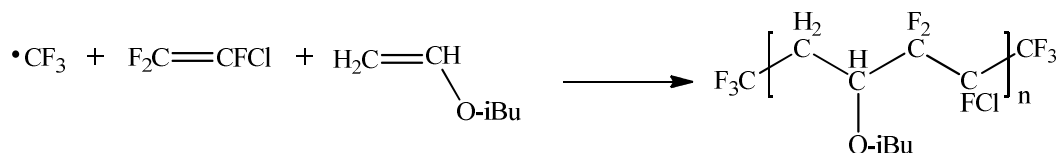
5.3 Results and discussion

The experimental conditions for the radical copolymerisation of chlorotrifluoroethylene (CTFE) with isobutyl vinyl ether (iBuVE) using PPFr as initiator, along with the characterisation results, are summarised in Table 13.

PPFR has a half-life of 1 hour at 100 $^{\circ}\text{C}$ [6], releasing $\bullet\text{CF}_3$ and a branched perfluorinated 2-pentene (Scheme 11). The CF_3 radical initiates the radical copolymerisation of CTFE with iBuVE from 90 $^{\circ}\text{C}$ (Scheme 12), taking into account that its half-life is 3 hours at this temperature. A 50 mol % feed of CTFE/iBuVE was chosen since the maximum rate of polymerisation is found at this ratio [10].



Scheme 11: β -scission elimination mechanism for the generation of $\bullet\text{CF}_3$ from PPFr.



Scheme 12: Expected copolymerisation reaction of CTFE and iBuVE initiated by $\bullet\text{CF}_3$ to yield a poly(CTFE-*alt*-iBuVE) alternating copolymer.

Table 13: Summary of experimental conditions and results obtained.

Experiment	Monomer CTFE+iBuVE (mol)	$\frac{[PPFR]_0}{[CTFE]_0 + [iBuVE]_0}$ (mol %)	Yield (%)	M_n^a (g·mol ⁻¹)	M_n^b (g·mol ⁻¹)	DP_n	PDI	$T_d^{c, 10\%}$ (°C)	T_g^d (°C)
1	0.171 + 0.171	1	64	85000	340000	1570	2.13	330	20
2	0.171 + 0.171	5	46	70000	237000	1100	1.58	340	23
3	0.171 + 0.171	10	58	66000	122000	560	1.62	344	24
4	0.171 + 0.171	20	20	59000	18000	84	2.19	322	23

Number-average molecular weight as determined by SEC^a and ¹⁹F NMR spectroscopy^b, ^c decomposition temperature at 10 % mass loss in air; ^d glass-transition temperature.

5.3.1 Nuclear magnetic resonance spectroscopic characterisation

The progression of ^{19}F NMR spectra going from 1 % to 20 % PPFR is presented in Figure 62. The $\text{CF}_3\text{-CH}_2$ signal is observed at -66 ppm in the 1 % PPFR spectrum with no other signals observed in the CF_3 range. Similarly for the 5 % and 10 % PPFR spectra only the signal at -66 ppm is noted. For the 20 % PPFR spectrum five signals are observed, *viz.* four major signals at -66, -77, -78, and -83 ppm. There is also one minor signal at -73 ppm. The ^1H NMR spectra for 1 % and 10 % PPFR are presented along with that of pure iBuVE in Figure 63. As expected from the literature [11, 12] both the ^{19}F and ^1H NMR spectra display signal broadening on the asymmetric carbons of CTFE and iBuVE units (in the range of -107 and -115 ppm for CTFE, and 4.5 ppm for iBuVE). The spectra agree with what is expected for poly(CTFE-*alt*-iBuVE) copolymer and demonstrates that the system produced *via* $\bullet\text{CF}_3$ radical initiation is alternating, as evidenced by the absence of any peaks in the -127 ppm range, indicative of CFCl groups in CTFE-CTFE dyads, in the ^{19}F NMR spectrum [12-15].

The five peaks present in the ^{19}F NMR spectrum for 20 % PPFR are unexpected. There are two plausible explanations: 1) The signals arise from $\bullet\text{CF}_3$ additions to carbon sites other than CH_2 or 2) the signals arise from CTFE or iBuVE reaction with the PPFR elimination products of trans- and cis-perfluoro-3-ethyl-4-methyl-2-pentene. The ^1H NMR spectra of poly(CTFE-*alt*-iBuVE) exhibit the absence of signals centered at 6.53, 4.20, and 3.95 ppm characteristic of unreacted VE vinylic protons (upper spectrum). However, their polymerised unit can be found between 2.50 and 3.2 ppm, and between 4.3 and 4.7 ppm for the methylene and methyne protons, respectively [11, 12, 14-16].

Both signals are broad arising from the presence of two types of asymmetric carbons leading to two diastereoisomers, which makes these protons anisochronous (*i.e.* nonequivalent). Methylene groups adjacent to the oxygen atoms, CH groups and both methyl groups in iBuVE are located at 3.45-3.65 ppm, 1.85 ppm, and 0.90 ppm, respectively. There are several very small signals between 1.5 and 1 ppm. Several satellite signals near the signal assigned to the $\underline{\mathbf{e}}$ carbons are observed in the neat iBuVE spectrum. The small signals in the polymer spectra are ascribed to cumulative intensities of the small signals seen in the iBuVE spectrum. These signals are due to $^1\text{H}\text{-}^{13}\text{C}$ coupling.

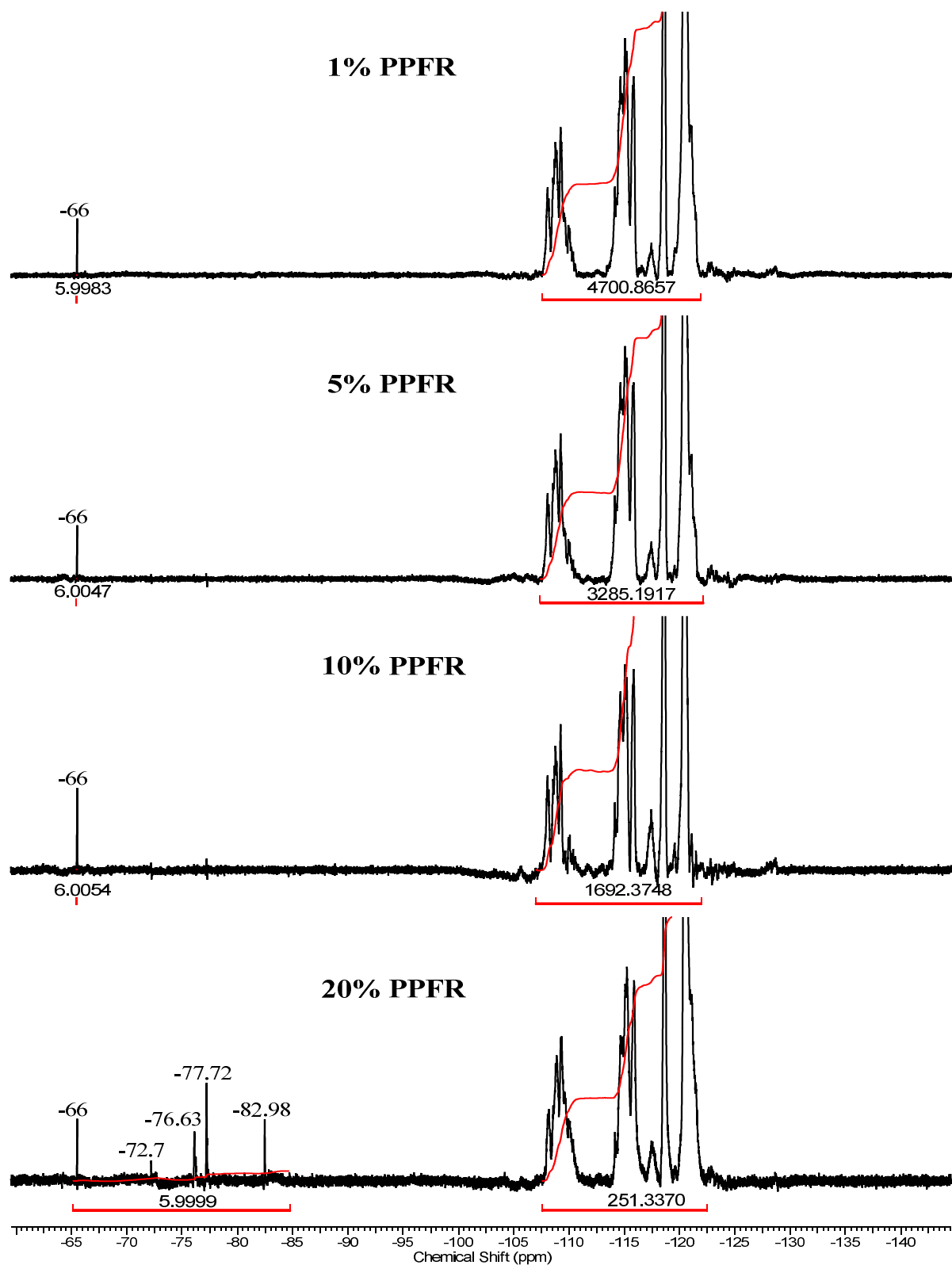


Figure 62: ^{19}F NMR spectra of poly(CTFE-*alt*-iBuVE) copolymers showing the progression of the CF_3 ^{19}F NMR signal with increasing initiator concentration from 1 mol % (top spectrum) to 20 mol % (bottom spectrum).

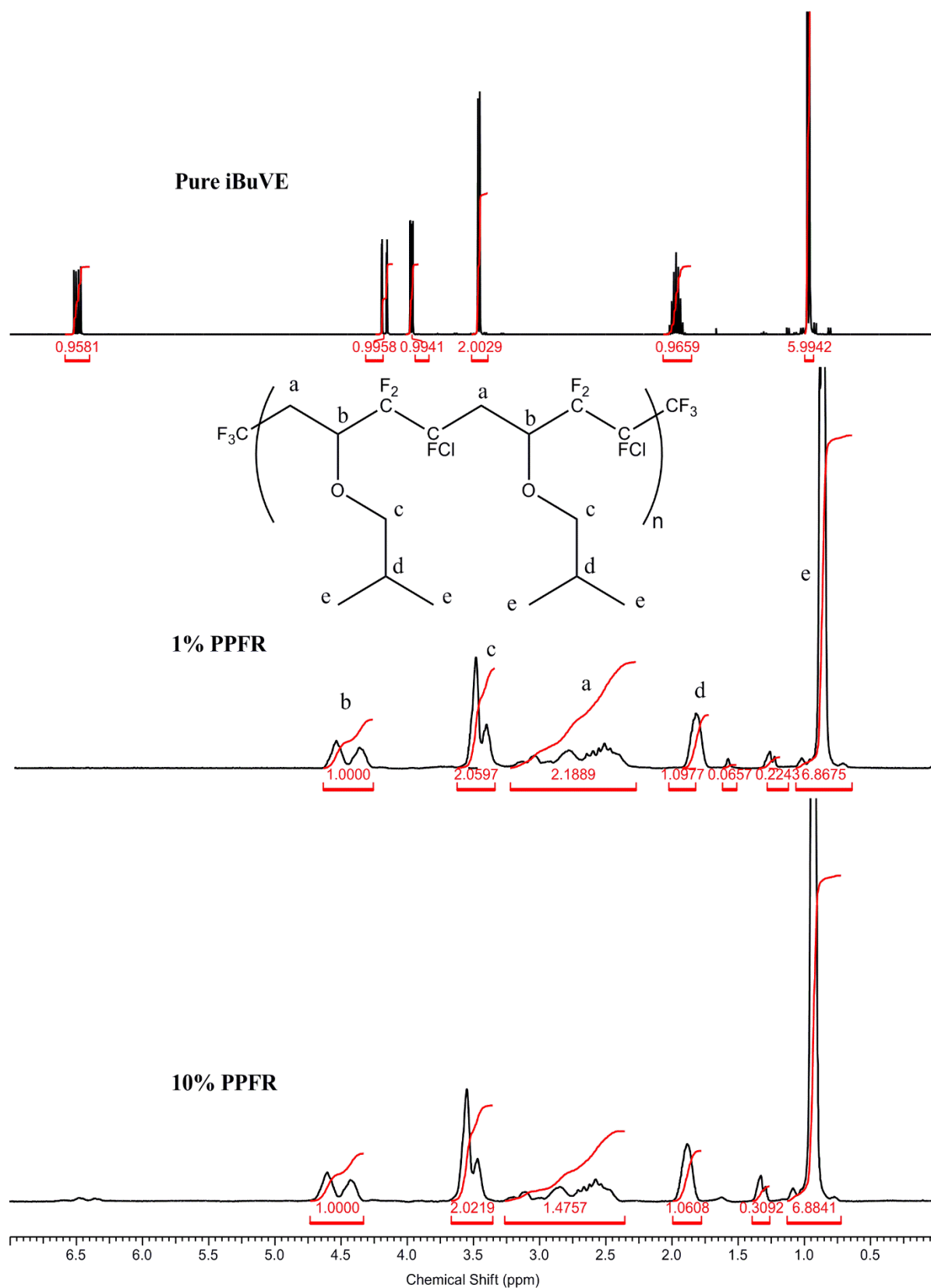
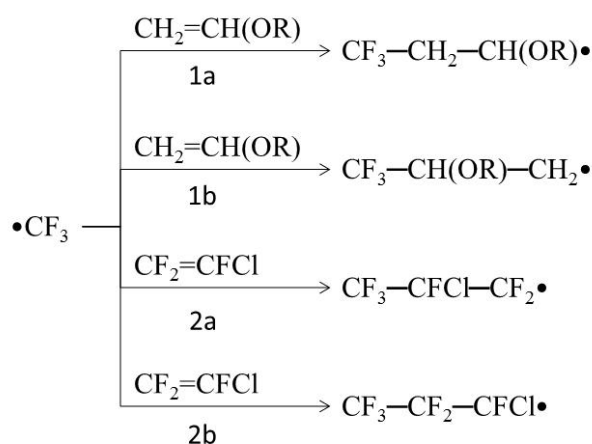


Figure 63: ^1H NMR spectra of poly(CTFE-alt-iBuVE) copolymers at 1 % and 10 % PPFR concentration compared to that of isobutyl vinyl ether (top spectrum).

5.3.2 Addition preferences of $\bullet\text{CF}_3$ radicals to the CTFE/iBuVE charge transfer complex

The possible attack patterns of $\bullet\text{CF}_3$ on the CTFE/iBuVE acceptor-donor complex [13, 17, 18] are presented in Scheme 13. Of these possible addition pathways, path 1a is considered the most likely as the highly electrophilic $\bullet\text{CF}_3$ radicals should preferentially attack the most electron donating, least hindered site in the monomer mixture [5, 19-22]. In the case of the vinyl ether, known to be a donating monomer [22], the preferred site will be the CH_2 carbon, as it is not sterically hindered and it is electron rich.

The literature [5, 9] indicates that, if the polymerisation occurs in a regioselective way *via* path 1a, there should be only one ^{19}F NMR signal for CF_3 , centered at -63 ppm. Work done on the telomerisation of CTFE with CF_3CFCII [23, 24] showed that the signals for CF_3 should be in the region of -77 ppm if it forms part of the $\text{CF}_3\text{CFCICF}_2$ motif and should be in the region of -82 ppm if it forms part of the $\text{CF}_3\text{CF}_2\text{CFCl}$ end-group. If the other pathways (such as attack onto the CTFE) are sufficiently viable, then there should be ^{19}F NMR signals at around -77 to -78 ppm as well. The assignments of the signals in the 20 % PFR spectrum and their relative abundance are presented in Table 14. The relative abundances were calculated by initially setting the integration of the -66 ppm signal to 6 and then dividing the integral of each CF_3 signal by the sum of the integrations of all the CF_3 signals.



Scheme 13: Possible addition reactions of $\bullet\text{CF}_3$ radicals onto the CTFE/iBuVE.

Table 14: CF_3 signal assignments and percentage relative abundance in the copolymer made with 20 % PPF_R.

Chemical shift (ppm)	Structural assignment ^a	Relative abundance (%)
-66	$\underline{CF}_3\text{---CH}_2\text{---CH(O-iBu)---CF}_2\text{---CFCl---R}$	6
-73	$\underline{CF}_3\text{---CH(O-iBu)---CH}_2\text{---CF}_2\text{---CFCl---R}$	5
-77	$\underline{CF}_3\text{---CFCl---CF}_2\text{---CH(O-iBu)---CH}_2\text{---R}$	37
-78	$\underline{CF}_3\text{---CFCl---CF}_2\text{---CH}_2\text{---CH(O-iBu)---R}$	47
-83	$\underline{CF}_3\text{---CF}_2\text{---CFCl---R}$	5

^a Assignments based on the NMR spectra for the telomerisation of $CF_2=CFCl$ with CF_3CFCl and considerations from the literature [23, 25].

Assuming that the signals in the ^{19}F NMR spectrum for 20 % PPF_R are only due to different $\bullet CF_3$ additions, then the NMR spectroscopic results show that at low initiator concentrations, pathway 1a is favoured, but at higher initiator concentrations pathway 2a becomes dominant. The low prevalence of attack *via* 2b is due to electronic effects, the CF_2 carbon being electron poor. The low occurrence of attack *via* 1b is due to steric and electronic effects.

The effect of initiator concentration is remarkable in that there are no electronic or steric considerations that shift the regioselectivity away from CH_2 towards $CFCl$ attack. The previous work with VDF and PPF_R was done in halogenated solvents, so the current reaction behaviour is possibly governed by kinetic effects arising from solubility considerations.

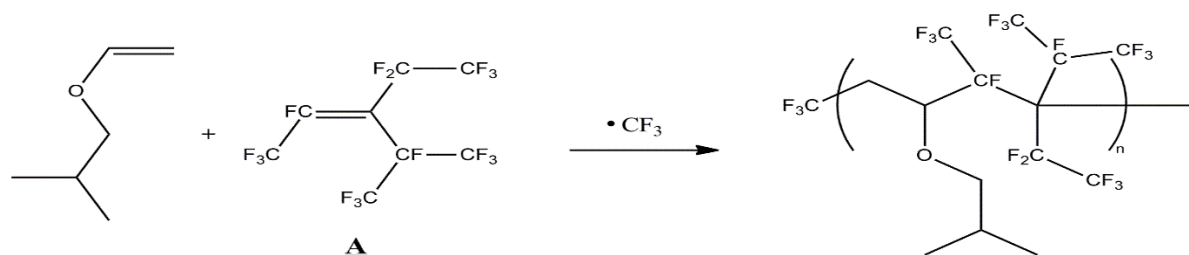
PPF_R is a fully fluorinated species that dissolves in dimethylcarbonate (DMC) at low concentrations. However, at higher concentrations, a two-phase system exists at standard conditions. The phase behaviour of large, sterically hindered, fully fluorinated molecules in contact with DMC at elevated temperatures and pressures is not known, but it is suspected that there exists, under the reaction conditions used here, a two-phase system, one phase being DMC rich and the other being fluorous.

The solubility of CTFE in the fluorous phase should be an order of magnitude higher than its solubility in DMC. The “regioselectivity” at higher initiator concentrations is then ascribed simply to the much higher abundance of CTFE over *i*BuVE near to the initiator molecules.

5.3.3 Reaction of *i*BuVE with PFR elimination products

At low initiator concentrations, any effect of the elimination products on the reaction is overshadowed by the much greater abundance of other monomers. However, at concentrations of 20 % PFR, the molar quantities of unsaturated fluorinated elimination product cannot be ignored when interpreting the results.

The decomposition reaction of PFR is shown in Scheme 11. The by-product from $\bullet\text{CF}_3$ elimination is a sterically hindered, unsaturated fluorocarbon. Normally, such hindered fluorocarbons do not homopolymerise under radical conditions, as is the case with hexafluoropropylene (HFP) or perfluoroalkylvinyl ethers (PAVEs). However, it has been shown that even HFP and PAVEs readily produces alternating copolymers with vinyl ethers [26, 27]. Accordingly, there exists a distinct possibility that *i*BuVE may react with the unsaturated elimination product **A** to produce a copolymer. A possible reaction is shown in Scheme 14.



Scheme 14: Possible polymerisation reaction between *i*BuVE and perfluoroolefin **A**.

However, the terminal radical that would form on product **A** in such a reaction should be unreactive as its environment is sterically very similar to the radical centre of PFR. A much more plausible scenario is the addition of *i*BuVE onto **A** to form a stable, radically capped monoadduct instead of a polymer.

If such a product did exist, there should be ^{19}F NMR signals at around -175 ppm. Since no such signals are detected, this reaction did not occur, and the unexpected ^{19}F NMR signals for CF_3 observed in the ^{19}F NMR spectrum for 20 % PFR cannot be due to incorporation of the PFR elimination product into the polymer.

5.3.4 Effect of initiator concentration on molecular weight

The normalised size-exclusion chromatograms (SEC or GPC) are displayed in overlaid form in Figure 64. The expected decrease in molecular weight with increasing initiator ratio is noted. However, the initiator concentration beyond 5 % is observed to have a limited effect on

molecular weight, displaying a significant drop in molecular weight from 1 % to 5 % (with M_n ranging from 85,000 to 70,000 $\text{g}\cdot\text{mol}^{-1}$), but showing a nearly linear correlation for decreasing molecular weight with increase of the square root of the ratio of initiator concentration to the monomer concentration from 5 % to 20 % (with M_n ranging from 66,000 to 59,000 $\text{g}\cdot\text{mol}^{-1}$). This trend is presented graphically in Figure 65.

The molecular weights determined by ^{19}F NMR spectroscopy also show the expected decrease in molecular weight with increase in initiator concentration, with the trend being nearly linear in the region of 1 % to 10 % initiator (with M_n ranging from 340,000 to 122,000 $\text{g}\cdot\text{mol}^{-1}$).

As expected, since the GPC standards are polystyrene, there is a very large difference between the M_n values derived from SEC (or GPC) and NMR spectroscopy.

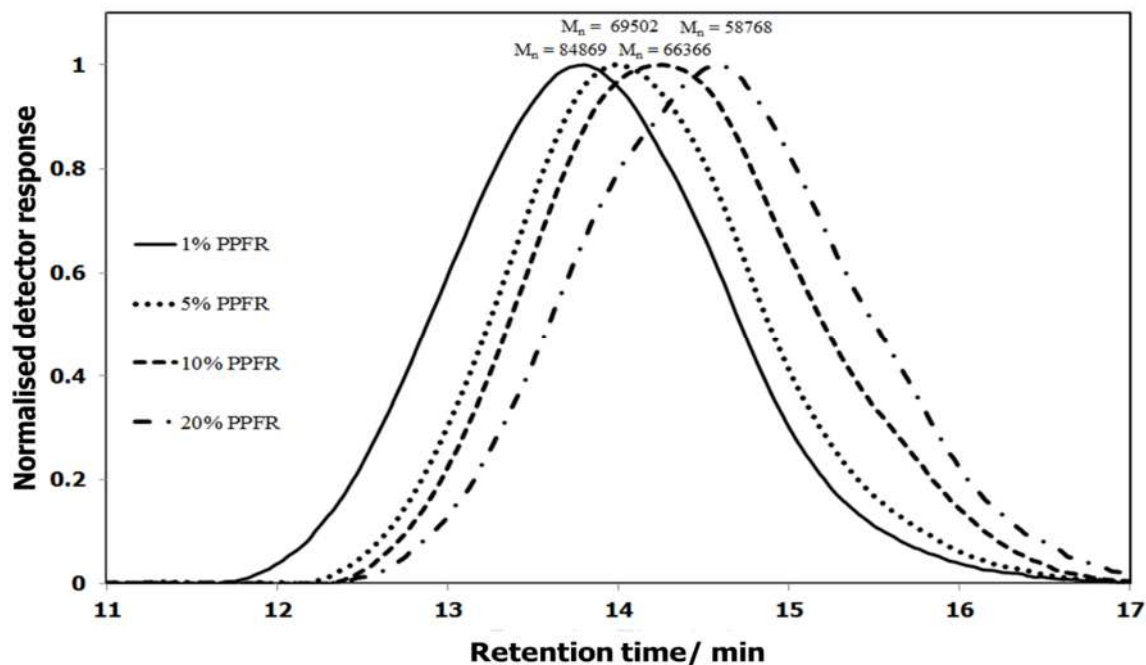


Figure 64: *Size-exclusion chromatograms showing the number-average molecular weights of poly(CTFE-*alt*-iBuVE) copolymers prepared from various amounts of PPF radical molar percentages.*

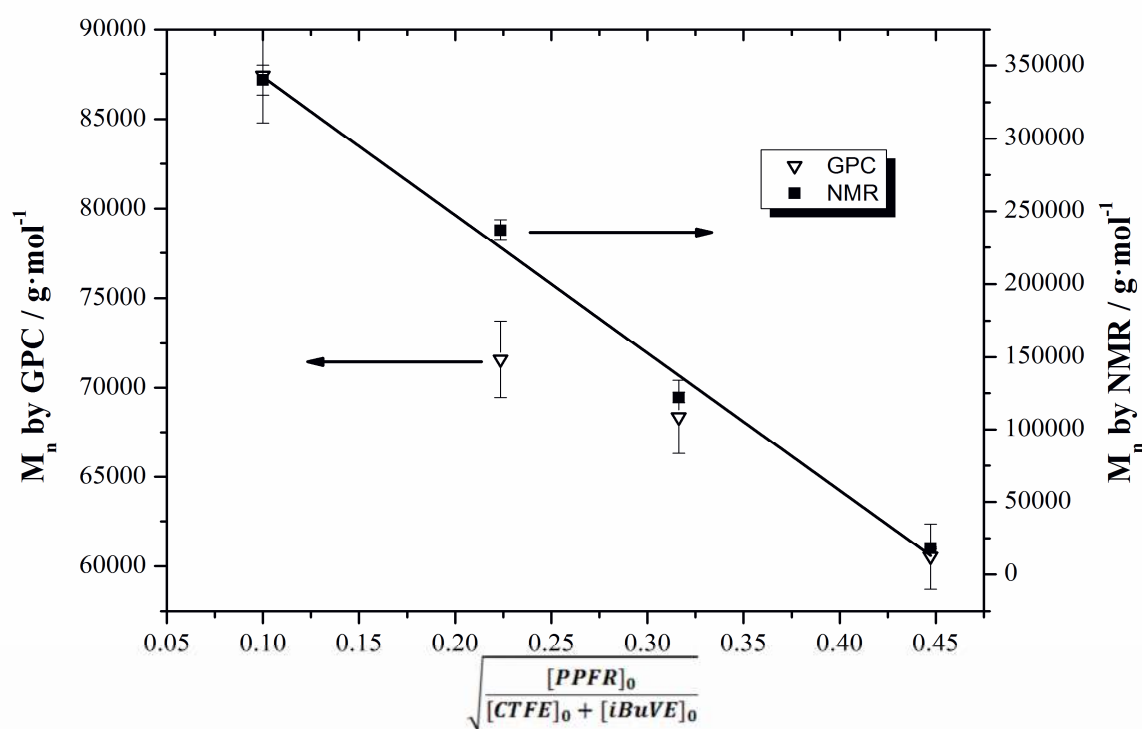


Figure 65: Correlation of M_n decrease as PPFR ratio increases as determined by both SEC (Δ) and ^{19}F NMR spectroscopy (\blacksquare).

5.3.5 Thermal properties of CF_3 terminated poly(CTFE-*alt*-iBuVE) copolymers

5.3.5.1 Thermogravimetric analysis coupled to Fourier transform infrared spectroscopy.

The thermograms for the thermal decomposition under nitrogen of the poly(CTFE-*alt*-iBuVE) alternating copolymers made with 1 mol %, 5 mol %, and 10 mol % PPFR are presented in Figure 66. Fourier-transform infrared spectra of the evolved gases from the thermal decomposition of the poly(CTFE-*alt*-iBuVE) alternating copolymers, taken at the point of maximum absorbance are presented in Figure 67.

The thermal degradation behaviour and degradation mechanism of fluoropolymers are dependent on the chemical nature of the polymer, the chain length, and the morphology of the chains [28]. For fully fluorinated polymers, the usual degradation routes involve either unzipping from the chain ends or breakdown due to random chain scission, while for partially fluorinated polymers, dehydrofluorination is usually the main mechanism of degradation [29, 30]. Polymers synthesised *via* non-fluorinated initiators are highly susceptible to unzipping from the chain ends or to oxidative attack initiated at the non-fluorinated chain ends.

The use of CF_3 as terminal group enables the gauging of the degradation behaviour of poly(CTFE-*alt*-iBuVE) free from breakdown initiated at the chain ends. The thermograms show that the polymer produced with 1 mol % PPFRR is the most stable, with a degradation onset temperature of 387 °C, as is expected considering that its molecular weight is the largest of all the polymers. Interestingly, the 5 mol % and 10 mol % polymers show nearly the same degradation onset temperature (367 °C). The 20 mol % polymer is not shown as the polymer underwent significant mass loss, *via* evaporation of the low-molecular-weight chains, long before the other polymers started degrading, with the onset of loss temperature for the higher-molecular-weight fraction of the 20 mol % PPFRR polymer being in the region of 325 °C.

The 10 % mass loss temperatures of the four copolymers are reported in Table 13, and the data demonstrate that the thermal behaviour of the 5 mol %, and 10 mol % polymers are nearly identical under both air and nitrogen. The differences in onset temperatures between heating in air and in inert atmosphere demonstrates that the alternating poly(CTFE-*alt*-iBuVE) copolymer undergoes combustion long before the polymer chains start degrading, implying that in the event of combustion during service, the subsurface polymer material will remain in serviceable condition when the surface combustion is extinguished. Also, the differences in degradation onset temperatures between the 1 mol % PPFRR, 5 mol % and 10 mol % PPFRR polymers demonstrates that the degradation behaviour is dependent on molecular weight.

Furthermore, these results indicate that the intrinsic oxidative thermal stability of the poly(CTFE-*alt*-iBVE) backbone is quite good for a partially fluorinated polymer, being comparable to the stability achieved by fully fluorinated polymers. For comparison, the onset of degradation temperature for PTFE is around 550 °C [31] under the same conditions. The infrared spectra of the evolved gases display the expected release of HF and HCl. The infrared absorbance bands for CO and CO₂ are also observed, at 2142 and 2336 cm⁻¹, respectively. The peak at 1748, 3084, 2964 and 1116 cm⁻¹ is indicative of a C=O group, a C=C-H stretch, a CH₂ stretch and of =C-H bends, respectively. Also, no peaks for an O-H bond, usually seen at around 3600 cm⁻¹ are observed.

While the gas phase is obviously a mixture of species, the FTIR spectra indicate that the major component of the organic pyrolysis products is something akin to isobutenal. Given that CO and CO₂ are also produced, other minor components like isobutylene and ethers of isobutene must also be present in the gas phase. The literature [29, 30] indicates that monofluorides and monochlorides of these compounds should also be present in some small quantity.

The work of Zulfiqar *et al.* [29, 30, 32] focused on the random copolymers of CTFE with methyl methacrylate, VDF, and styrene. These polymers are all random copolymers. It was noticed there that the degradation of CTFE-MMA copolymers occurs in a two-step process, with HCl being eliminated first, followed by depolymerisation of the polymer chain to MMA and chlorofluorocarbons. No mention is made of the elimination of HF.

The thermal decomposition of polyvinyl alcohol and polyvinyl acetate (model polymers approximating vinyl ethers) also occur in a two-step process. Polyvinyl alcohol first releases water, forming double bonds in the polymer chain and afterward undergoing chain scission to produce unsaturated aldehydes and ketones. Polyvinyl acetate first releases acetic acid to form an unsaturated, ketenic polymer backbone, followed by elimination of ketones from the unsaturated chain [33, 34].

In the case of poly(CTFE-*alt*-iBuVE), the breakdown is seen to be one step with HCl, HF, and the pendant ether group eliminated from the polymer chain concurrently.

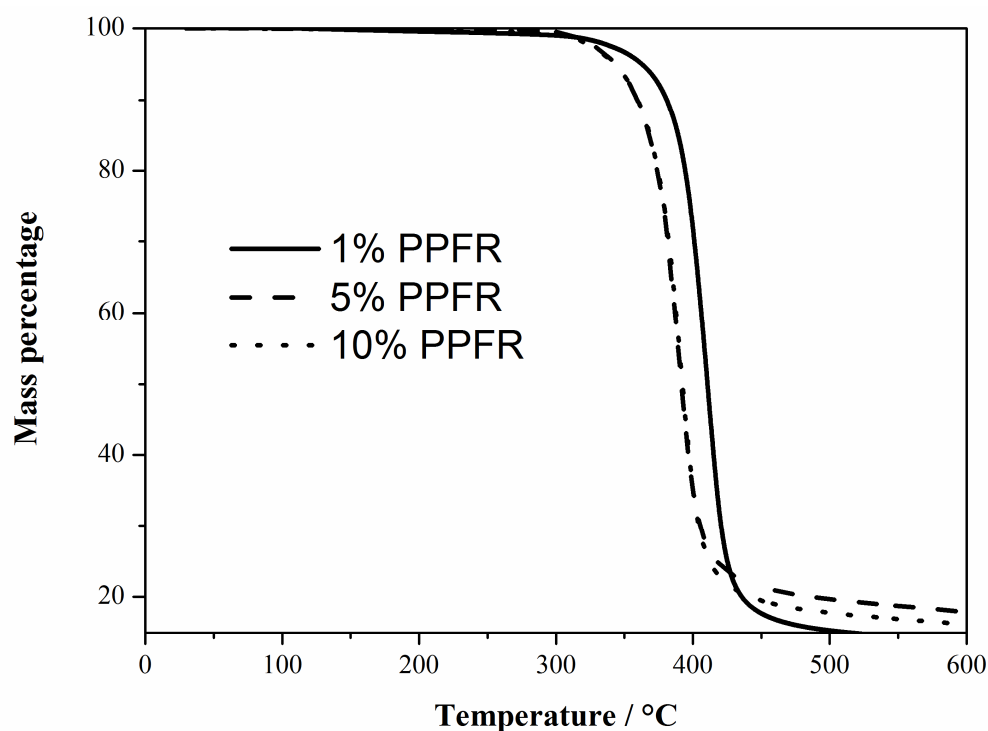


Figure 66: TGA thermograms for the poly(CTFE-*alt*-iBuVE) copolymers under N₂ at 10 °C/min.

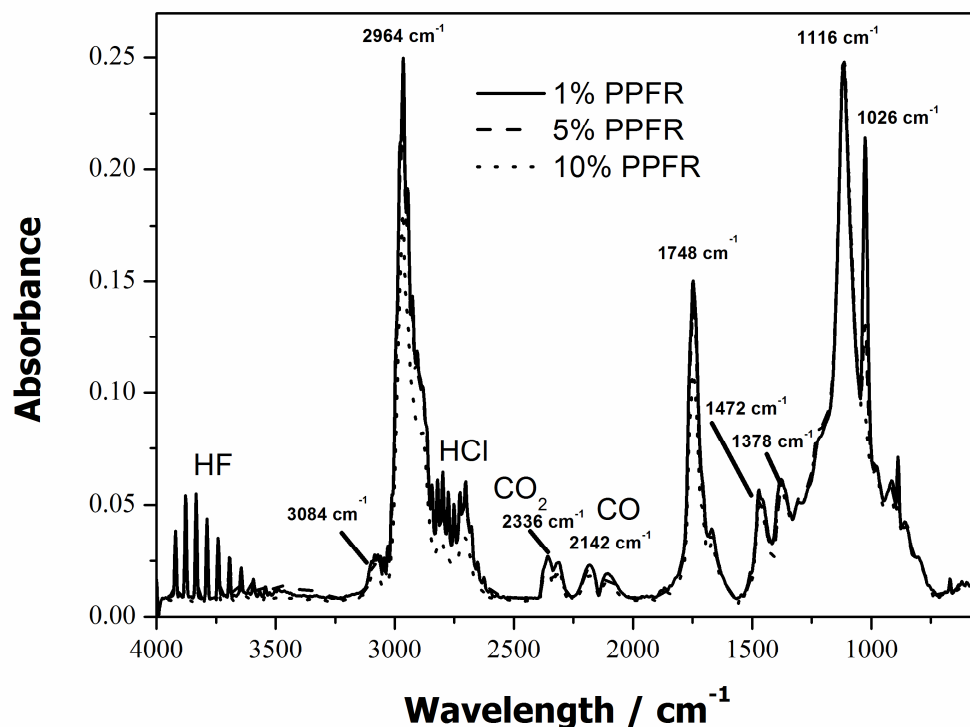


Figure 67: *Fourier-transform infrared spectrum of the evolved gases from the thermal decomposition of the poly(CTFE-*alt*-iBuVE) alternating copolymers, taken at the point of maximum absorbance, showing, among other species, the evolution of HF, HCl, CO and CO₂.*

5.3.5.2 Differential scanning calorimetry (DSC)

The main calorimetric parameter of importance to the poly(CTFE-*alt*-iBVE) copolymers is the glass-transition temperature, which in this case is shown to be nearly independent of polymer molecular weight. The glass-transition temperatures for the poly(CTFE-*alt*-iBVE) copolymers are around 23 °C. This invariance is in agreement with the expected behaviour [35], given that the glass transition is not so much dependent on molecular weight as it is dependent on polymer composition, which in this case remains constant at a 1:1 ratio of CTFE:iBuVE.

5.4 Conclusions

A series of poly(CTFE-*alt*-iBuVE) alternating copolymers were synthesised in good yield *via* radical polymerisation initiated by •CF₃ released from the β-scission of perfluoro-3-ethyl-2,4-dimethyl-3-pentyl persistent radical at 90 °C. The addition behaviour of •CF₃ radicals onto the CTFE/iBuVE is highly dependent on the initiator-to-monomer ratio. It was demonstrated that •CF₃ radicals preferentially attack the methylene site in the vinyl ether monomer to initiate chain

cross propagation when using low initiator concentrations. At initiator concentrations of 20 % it was shown that there is significant deviation from the expected behaviour, ascribed to the effects of initiator. The usefulness of CF_3 end-groups as labels for molecular weight determination in poly(CTFE-*alt*-iBVE) copolymers by ^{19}F NMR spectroscopy was demonstrated and compared to results obtained by SEC. The polymerisation initiated by PFR persistent radical exhibiting the expected tendency for the molecular weight of the copolymers to increase with decreasing initiator concentration.

It is expected that application of PFR to the polymerisation of TFE will permit the determination of the M_n of PTFE *via* ^{19}F NMR spectroscopy. This will provide an alternative method for determining the M_n of PTFE, which can corroborate the M_n values derived from the kinetic expression.

Furthermore, the experience gained with advance fluoropolymer synthesis techniques in France will enable the Fluoro-Materials Group to undertake the reversible-deactivation radical polymerisation of TFE to produce PTFE polymers with well-defined molecular weights.

5.5 References

- [1] Wu, S., "Characterization of polymer molecular weight distribution by transient viscoelasticity: Polytetrafluoroethylenes", *Polymer Engineering & Science*, 1988, 28 (8), 538-543.
- [2] Tuminello, W.H., Treat, T.A., and English, A.D., "Poly(tetrafluoroethylene): molecular weight distributions and chain stiffness", *Macromolecules*, 1988, 21 (8), 2606-2610.
- [3] Starkweather, H.W. and Wu, S., "Molecular weight distribution in polymers of tetrafluoroethylene", *Polymer*, 1989, 30 (9), 1669-1674.
- [4] Tuminello, W.H. and Cudré-Mauroux, N., "Determining molecular weight distributions from viscosity versus shear rate flow curves", *Polymer Engineering & Science*, 1991, 31 (20), 1496-1507.
- [5] Patil, Y., Alaaeddine, A., Ono, T., and Ameduri, B., "Novel Method to Assess the Molecular Weights of Fluoropolymers by Radical Copolymerization of Vinylidene Fluoride with Various Fluorinated Comonomers Initiated by a Persistent Radical", *Macromolecules*, 2013, 46 (8), 3092-3106.
- [6] Scherer, K.V., Ono, T., Yamanouchi, K., Fernandez, R., and Henderson, P., "F-2,4-Dimethyl-3-ethyl-3-pentyl and F-2,4-dimethyl-3-isopropyl-3-pentyl; stable tert-perfluoroalkyl radicals prepared by addition of fluorine or trifluoromethyl to a perfluoroalkene", *Journal of the American Chemical Society*, 1985, 107 (3), 718-719.
- [7] Puts, G., Lopez, G., Ono, T., Crouse, P., and Ameduri, B., "Radical copolymerisation of chlorotrifluoroethylene with isobutyl vinyl ether initiated by the persistent perfluoro-3-ethyl-2,4-dimethyl-3-pentyl radical", *RSC Advances*, 2015, 5 (52), 41544-41554.
- [8] Ono, T. and Ohta, K., "Spectroscopic observation of charge transfer complex formation of persistent perfluoroalkyl radical with aromatics, olefin, and ether", *Journal of Fluorine Chemistry*, 2014, 167 (0), 198-202.
- [9] Boschet, F., Ono, T., and Ameduri, B., "Novel source of trifluoromethyl radical as efficient initiator for the polymerization of vinylidene fluoride", *Macromolecular Rapid Communications*, 2012, 33 (4), 302-308.
- [10] Tabata, Y. and Du Plessis, T.A., "Radiation-induced copolymerization of chlorotrifluoroethylene with ethyl vinyl ether", *Journal of Polymer Science Part A-1: Polymer Chemistry*, 1971, 9 (12), 3425-3435.
- [11] Couture, G., Campagne, B., Alaaeddine, A., and Ameduri, B., "Synthesis and characterizations of alternating co- and terpolymers based on vinyl ethers and chlorotrifluoroethylene", *Polymer Chemistry*, 2013, 4 (6), 1960-1968.
- [12] Alaaeddine, A., Couture, G., and Ameduri, B., "An efficient method to synthesize vinyl ethers (VEs) that bear various halogenated or functional groups and their radical copolymerization with chlorotrifluoroethylene (CTFE) to yield functional poly(VE-alt-CTFE) alternated copolymers", *Polymer Chemistry*, 2013, 4 (16), 4335-4347.
- [13] Tiers, G.V.D. and Bovey, F.A., "Polymer NMR spectroscopy. VII. The stereochemical configuration of polytrifluoroethylene", *Journal of Polymer Science Part A: General Papers*, 1963, 1 (3), 833-841.
- [14] Carnevale, D., Wormald, P., Ameduri, B., Tayouo, R., and Ashbrook, S.E., "Multinuclear magnetic resonance and DFT studies of the Poly(chlorotrifluoroethylene-alt-ethyl vinyl ether) copolymers", *Macromolecules*, 2009, 42 (15), 5652-5659.
- [15] Gaboyard, M., Hervaud, Y., and Boutevin, B., "Photoinitiated alternating copolymerization of vinyl ethers with chlorotrifluoroethylene", *Polymer International*, 2002, 51 (7), 577-584.
- [16] Boschet, F. and Ameduri, B., "(Co)polymers of chlorotrifluoroethylene: synthesis, properties, and applications", *Chemical Reviews*, 2013, 114 (2), 927-980.

- [17] Ameduri, B. and Boutevin, B., 2004, *Well-architected Fluoropolymers: Synthesis, Properties and Applications*, Elsevier Science, Amsterdam, The Netherlands.
- [18] Rzaev, Z.M.O., "Complex-radical alternating copolymerization", *Progress in Polymer Science*, 2000, 25 (2), 163-217.
- [19] Takeyama, Y., Ichinose, Y., Oshima, K., and Utimoto, K., "Triethylborane-induced stereoselective radical addition of perfluoroalkyl iodides to acetylenes", *Tetrahedron Letters*, 1989, 30 (24), 3159-3162.
- [20] Cape, J.N., Greig, A.C., Tedder, J.M., and Walton, J.C., "Free radical addition to olefins. Part 14.-Addition to trifluoromethyl radicals to fluoroethylenes", *J. Chem. Soc. Faraday Trans. 1: Phys. Chem. Cond. Phases*, 1975, 71 (0), 592-601.
- [21] Miura, K., Takeyama, Y., Oshima, K., and Utimoto, K., "Triethylborane Induced Perfluoroalkylation of Silyl Enol Ethers and Ketene Silyl Acetals with Perfluoroalkyl Iodides", *Bulletin of the Chemical Society of Japan*, 1991, 64 (5), 1542-1553.
- [22] Hill, D.J.T., O'Donnell, J.J., and O'Sullivan, P.W., "The role of donor-acceptor complexes in polymerization", *Progress in Polymer Science*, 1982, 8 (3), 215-275.
- [23] Amiry, M.P., Chambers, R.D., Greenhall, M.P., Ameduri, B., Boutevin, B., Caporiccio, G., Gornowicz, G.A., and Wright, A.P., 1993, "The peroxide initiated telomerization of chlorotrifluoroethylene with perfluorochloroalkyl iodides", presented at the ACS Division of Polymer Chemistry Meeting 205, Polym. Prep. (ACS Polym. Div.), American Chemical Society.
- [24] Haszeldine, R.N., "Fluoro-olefins. Part IV. Synthesis of polyfluoroalkanes containing functional groups from chlorotrifluoroethylene, and the short-chain polymerisation of olefins", *Journal of the Chemical Society (Resumed)*, 1955 (0), 4291-4302.
- [25] Dolbier, W.R., 2009, *Guide to Fluorine NMR for Organic Chemists*, Wiley, New York.
- [26] Valade, D., Boschet, F., and Améduri, B., "Synthesis and Modification of Alternating Copolymers Based on Vinyl Ethers, Chlorotrifluoroethylene, and Hexafluoropropylene†", *Macromolecules*, 2009, 42 (20), 7689-7700.
- [27] Alaaeddine, A., Boschet, F., Ameduri, B., and Boutevin, B., "Synthesis and characterization of original alternated fluorinated copolymers bearing glycidyl carbonate side groups", *Journal of Polymer Science Part A: Polymer Chemistry*, 2012, 50 (16), 3303-3312.
- [28] Crompton, T.R., 2010, *Thermo-oxidative Degradation of Polymers*, iSmithers, Akron, Ohio.
- [29] Zulfiqar, S., Rizvi, M., Munir, A., Ghaffar, A., and McNeill, I.C., "Thermal degradation studies of copolymers of chlorotrifluoroethylene and methyl methacrylate", *Polymer Degradation and Stability*, 1996, 52 (3), 341-348.
- [30] Zulfiqar, S., Zulfiqar, M., Rizvi, M., Munir, A., and McNeill, I.C., "Study of the thermal degradation of polychlorotrifluoroethylene, poly(vinylidene fluoride) and copolymers of chlorotrifluoroethylene and vinylidene fluoride", *Polymer Degradation and Stability*, 1994, 43 (3), 423-430.
- [31] Puts, G.J. and Crouse, P.L., "The influence of inorganic materials on the pyrolysis of polytetrafluoroethylene. Part 1: The sulfates and fluorides of Al, Zn, Cu, Ni, Co, Fe and Mn", *Journal of Fluorine Chemistry*, 2014, 168, 260-267.
- [32] Zulfiqar, S., Rizvi, M., and Munir, A., "Thermal degradation of chlorotrifluoroethylene-styrene copolymers", *Polymer Degradation and Stability*, 1994, 44 (1), 21-25.
- [33] Holland, B.J. and Hay, J.N., "The thermal degradation of poly(vinyl acetate) measured by thermal analysis-Fourier transform infrared spectroscopy", *Polymer*, 2002, 43 (8), 2207-2211.
- [34] Holland, B.J. and Hay, J.N., "The thermal degradation of poly(vinyl alcohol)", *Polymer*, 2001, 42 (16), 6775-6783.
- [35] Nicholson, J.W., 2012, *The Chemistry of Polymers*, Royal Society of Chemistry, London, United Kingdom.

Chapter 6

**Free-radical and controlled-radical
copolymerisation of tetrafluoroethylene with
isobutyl vinyl ether**

6.1 Introduction

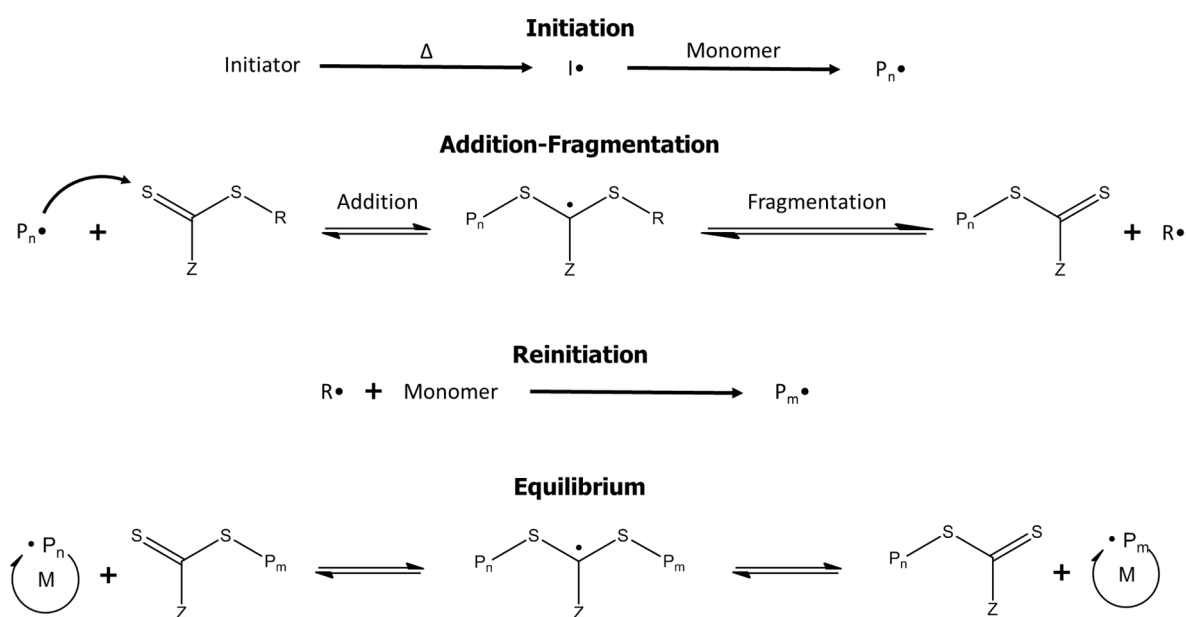
Chapter 4 showed that control of the molecular weight of PTFE cannot easily be accomplished by manipulating the polymerisation conditions. Furthermore, the determination of the molecular-weight distribution of PTFE is not easily accomplished, requiring onerous rheological characterisation [1-4]. The effects of temperature and molecular-weight distribution on the viscosity of PTFE waxes below the melting point are unknown; however, the zero shear viscosity of PTFE seems to be a function of M_w [1]. The rheological shortcomings of the low-molecular-weight PTFE synthesised in Chapter 4 necessitates a better understanding of the molecular-weight distribution on the rheological properties of PTFE.

TFE polymers are usually synthesised *via* radical polymerisation, and a number of methods are available to conduct controlled-radical polymerisation (also known as reversible-deactivation radical polymerisation or RDRP) [5-7]. Significant work has been carried out in the last couple of decades on the controlled homo- and copolymerisation of fluoroolefins using iodine transfer polymerisation (ITP) and RAFT/MADIX methods [8-17].

Telomerisation of TFE, and to a certain extent, the controlled-radical polymerisation of TFE using ITP (pioneered by Tatemoto [8, 9, 18]) with various iodated chain-transfer agents (CTA) has been reviewed by Ameduri [19]. CTAs such as H_2 and methanol are already used in industry to cap unreacted, immobilised fluoromacroradicals [20, 21], while numerous others have been applied to the telomerisation of TFE, but according to the chain-transfer constant value, these CTAs tend to broaden the polydispersity and their effect on the polydispersity is not strictly controllable. The control of the molecular-weight distribution of TFE homopolymer has heretofore not been studied significantly beyond the oligomeric stage. Hence, synthesis of a low-molecular-weight PTFE with a tailored polydispersity will require the use of a polymerisation-control agent.

Proper control of the molecular-weight distribution of PTFE may permit the synthesis of a linear, unbranched perfluoropolymer with a custom temperature-viscosity relationship. The applications of PTFE with such bespoke properties extend beyond their use in extrudable fluorocarbon-based pyrotechnics, and may include high-tech fluorocarbon lubricants. Also, if the molecular-weight distribution can be properly manipulated to produce a monodisperse PTFE, then both the M_n and M_w of the polymer can be determined from end-group analysis using solid-state ^{19}F NMR spectroscopy. In turn, the effects of M_w on the viscosity of PTFE at temperatures below the melting point can be studied. Therefore, there is both a purely technological, as well as a commercial interest in more effectively controlling the molecular-weight distribution of PTFE.

RAFT/MADIX polymerisation proceeds *via* a degenerative chain-transfer mechanism in which a double equilibrium favours control of the polymerisation with high efficiency (Scheme 15) [22-28]. Recently, RAFT/MADIX polymerisation using O-ethyl-S-(1-methyloxycarbonyl)ethyl xanthate has been applied in the RDRP of vinylidene fluoride homo- and copolymers to great effect [11, 17, 29-32], and the limits to which VDF lends itself to controlled polymerisation has been explored. Furthermore, Bai *et al.* investigated the RAFT/MADIX copolymerisations of chlorotrifluoroethylene (CTFE) and hexafluoropropylene (HFP) with butyl vinyl ether initiated by ^{60}Co γ -rays using S-benzyl O-ethyl dithiocarbonate as CTA [15, 16].



Scheme 15: Mechanism of reversible addition-fragmentation chain transfer polymerisation (RAFT) / macromolecular design via the interchange of xanthates (MADIX).

So far, no study has been reported on the RAFT/MADIX homo- or copolymerisation of TFE, and the application of RAFT/MADIX agents to TFE is a logical next step in the controlled polymerisation of fluoroolefins. However, homopolymers of TFE are completely insoluble in any solvent and cannot be subjected to any analysis technique for the determination of molecular-weight distribution, such as size-exclusion chromatography (SEC), viscosimetry, light scattering, or vapour-pressure osmometry. Before attempting to apply a xanthate chain-control agent to the TFE homopolymerisation process, it would be useful to determine if such a CTA can indeed be used to control the polymerisation in a soluble polymer system where TFE is present. The RDRP of TFE that can alternate with a non-fluorinated monomer has never been reported in the literature. As isobutyl vinyl ether (iBuVE) was previously employed with CTFE and its chemistry is known (this product is marketed by Daikin as Zeffle[®]), this monomer was

selected for use with TFE to render the polymer soluble and thus subjectable to liquid-state NMR spectroscopy and SEC analysis.

The aim of the work reported in this chapter is to examine the behavior of the RAFT/MADIX copolymerisation of TFE with a vinyl ether with a xanthate CTA, with the emphasis on determining if control of the molecular-weight distribution and the identity of the chain end is possible, and the limits to which the molecular weight can be controlled.

6.2 Experimental

6.2.1 Materials

Tetrafluoroethylene (TFE) was produced by an in-house generation unit *via* the vacuum (< 1 Pa) pyrolysis of pure PTFE. The PTFE (PTFE 807NX) was purchased from DuPont/Chemours and used as received.

Dimethyl carbonate (99 %), acetone (99 %), benzoyl peroxide (~75 %, remainder water), isobutyl vinyl ether (iBuVE) (99 %), K_2CO_3 (99 %), and $CDCl_3$ (99 %) were purchased from Sigma Aldrich. The benzoyl peroxide was dried under high vacuum at 30 °C for 24 hours before use, and all other chemicals were used as received. O-Ethyl-S-(1-methyloxycarbonyl)ethyl xanthate was synthesised according to the method of Liu *et al.* [33]. All the chemicals were stored in a fridge at 4 °C, except for the benzoyl peroxide (stored in a freezer at -25 °C).

6.2.2 Free-radical copolymerisation of tetrafluoroethylene with isobutyl vinyl ether

The experimental conditions are summarised in Table 15. For a typical reaction, TFE was copolymerized with iBuVE in a 1:1 molar ratio in thick Carius tubes at 85 °C using benzoyl peroxide (BPO) as initiator and dimethyl carbonate (DMC) as solvent. The reaction temperature of 85 °C was chosen as this is as close to the 3 hour half-life of the initiator. In all experiments, K_2CO_3 was added to the Carius tubes as an acid scavenger to prevent cationic homopolymerisation of iBuVE [34].

The Carius tubes were loaded with K_2CO_3 (0.13 g, 0.94 mmol) along with iBuVE (0.5 g, 0.5 mmol) and BPO dissolved in 5 mL of DMC. The tubes were subjected to three cycles of degassing *via* the freeze thaw method. Then, TFE ($\Delta P = 0.7$ bar, 0.5 g) was frozen into the tube using liquid N_2 , and the tubes was flame sealed under vacuum. After this, the Carius tubes were permitted to warm slowly to ambient and installed in their blast tubes in the shaking oven.

After the reaction time had been completed, the tubes were cooled to ambient, frozen in liquid nitrogen, and cut open. The resulting copolymer was dried, redissolved in the minimum of acetone, and precipitated into cold water, dried, precipitated once more, dried again, and subjected to vacuum (~ 0.1 Torr) at $80\text{ }^{\circ}\text{C}$ to remove any remaining volatiles. Interestingly, and contrary to the behavior of poly(CTFE-*alt*-iBuVE) copolymers, the TFE-based copolymers all produced clumpy material during the first precipitation, but formed a cloudy, white suspension during the second precipitation. This suspension did not settle out over time (~ 8 hours observation at $22\text{ }^{\circ}\text{C}$) and did not separate out during centrifugation.

Furthermore, all copolymers exhibited strong adhesive behavior, sticking to glass, metal, gloves, and skin alike.

6.2.3 Copolymerisation of TFE with iBuVE by RAFT/MADIX

TFE was copolymerised with iBuVE in thick Carius tubes with the same method as above, using O-ethyl-S-(1-methyloxycarbonyl)ethyl xanthate as a CTA. The reaction temperature of $85\text{ }^{\circ}\text{C}$ was chosen as this is close to the 3 hour half-life of the initiator. In all experiments, K_2CO_3 was added to the Carius tubes as an acid scavenger to prevent cationic homopolymerisation of iBuVE. The reactions and their conditions are summarised in Table 16.

6.2.4 Nuclear magnetic resonance spectroscopy

Proton decoupled ^{19}F and ^1H NMR spectra were collected using a Bruker Ultrashield 400 NMR spectrometer equipped with a 5-mm broadband observe (BBO) probe. The experimental conditions for recording ^1H , (or ^{19}F) spectra were: flip angle 90° (or 30°); acquisition time of 4.5 s (or 0.7 s), pulse delay of 2 s, 512 scans (or 1024 scans); and a pulse width of $5\text{ }\mu\text{s}$ for ^{19}F NMR spectroscopy.

Samples for NMR were prepared by dissolving 20 to 50 mg of copolymer in 1 mL of CDCl_3 .

6.2.5 DP_n and $M_{n(\text{NMR})}$ calculations using benzoyl end-group analysis

The average number degree of polymerisation (DP_n) can be calculated from ^1H NMR spectroscopy using the integrals for the signals corresponding to the methyl groups of the vinyl ether (singlet centred at *ca.* 0.81 ppm) and the ortho position hydrogens on the benzene ring of the benzoyl end-group (centred at *ca.* 8.02 ppm) according to Equation (32), with the molecular weight being calculated according to Equation (33), where $M_n(\text{BPO}) = 242.23\text{ g}\cdot\text{mol}^{-1}$, $M_n(\text{TFE}) = 100.02\text{ g}\cdot\text{mol}^{-1}$, and $M_n(\text{iBuVE}) = 100.16\text{ g}\cdot\text{mol}^{-1}$.

$$DP_n(BPO) = \frac{\frac{1}{6} \times \int_{0.6}^{0.95} CH_3(VE)}{\frac{1}{2} \times \int_{7.9}^{8.2} H(Ortho)} \quad (32)$$

$$M_{n,NMR}(BPO) = M_n(BPO) + DP(BPO) \times M_n(TFE + iBuVE) \quad (33)$$

6.2.6 DP_n and $M_{n(NMR)}$ calculations using R and Z end-group analysis

Alternatively, the DP_n can be calculated from 1H NMR spectroscopy using the integrals for the signals corresponding to the methyl groups of the vinyl ether (centered at *ca.* 0.81 ppm) and the methyl group on the CTA R-group (centered at *ca.* 1.15 ppm) according to Equations (34) and (35), where $M_n(CTA R) = 208.3 \text{ g}\cdot\text{mol}^{-1}$. Similarly, the DP_n and M_n can be calculated from the CTA Z-group *via* the integral of the methyl group centred at 1.36 ppm and the six methyl protons of the vinyl ether (Equations (36) and (37)).

$$DP(CTA R) = \frac{\frac{1}{6} \times \int_{0.6}^{0.95} CH_3(VE)}{\frac{1}{2} \times \int_{1.05}^{1.25} CH_3(CTA R)} \quad (34)$$

$$M_{n,NMR}(CTA R) = M_nCTA + DP(CTA R) \times M_n(TFE + iBuVE) \quad (35)$$

$$DP(CTA Z) = \frac{\frac{1}{6} \times \int_{0.6}^{0.95} CH_3(VE)}{\frac{1}{2} \times \int_{1.25}^{1.45} CH_3(CTA Z)} \quad (36)$$

$$M_{n,NMR}(CTA Z) = M_nCTA + DP(CTA Z) \times M_n(TFE + iBuVE) \quad (37)$$

6.2.7 Theoretical molecular weight

The theoretical molecular weight for the RAFT copolymerisation was calculated using Equation (38) using the yields listed in Table 16.

$$M_{n,the o} = M_nCTA + \frac{[TFE + iBuVE]_0}{[CTA]_0} \times yield \times M_n(TFE + iBuVE) \quad (38)$$

6.2.8 Differential scanning calorimetry

DSC measurements were performed using a Netzch DSC 200 F3 instrument. Polymer samples (~10 mg) were subjected to two heat-cool cycles under a nitrogen flow of 50 mL·min⁻¹. The polymer samples were heated from 25 °C to 120 °C at 20 °C·min⁻¹, held isothermally at 120 °C for 5 min, cooled from 120 °C to -120 °C at 20 °C·min⁻¹, held isothermally at -120 °C for 5 min, subjected to another heat-cool cycle before being heated from -120 °C to 25 °C at 20 °C·min⁻¹. T_g values were determined as the inflection point in the heat capacity jump.

6.2.9 Thermogravimetric analysis

Thermogravimetric analysis was performed with a Hitachi STA7300 TGA-DTA instrument using α -alumina crucibles. Approximately 10 mg of sample was used for each run. Each sample was heated from 30 °C to 1000 °C at a rate of 10 °C·min⁻¹ under a nitrogen atmosphere flowing at 200 mL·min⁻¹.

6.2.10 Size-exclusion chromatography

SEC was conducted in DMF using a Varian Prostar HPLC system coupled to a Kontron Instruments model 430 UV detector and a Shodex RI-101 refractive-index detector, equipped with 2 columns in series having a total separation range of 200 to 400 kDa kept at 70 °C. The solvent was supplied at 0.8 mL·min⁻¹, and analyses were achieved by injection of 20 μ L filtered solution (5 mg·mL⁻¹).

6.2.11 Particle-size analysis

Particle-size analysis and zeta-potential determination were carried out using a Malvern Zetasizer instrument fitted with a zeta-potential cuvette.

6.2.12 MALDI-TOF Spectroscopy

MALDI-TOF mass spectra were recorded with a Bruker Ultraflex III time-of-flight mass spectrometer using a nitrogen laser for MALDI (λ 337 nm). The measurements in positive ion mode were performed with voltage and reflector-lens potentials of 25 and 26.3 kV, respectively. For negative-ion mode, the measurements were performed with ion-source- and reflector-lens potentials of 20 and 21.5 kV, respectively. Mixtures of peptides were used for external calibration.

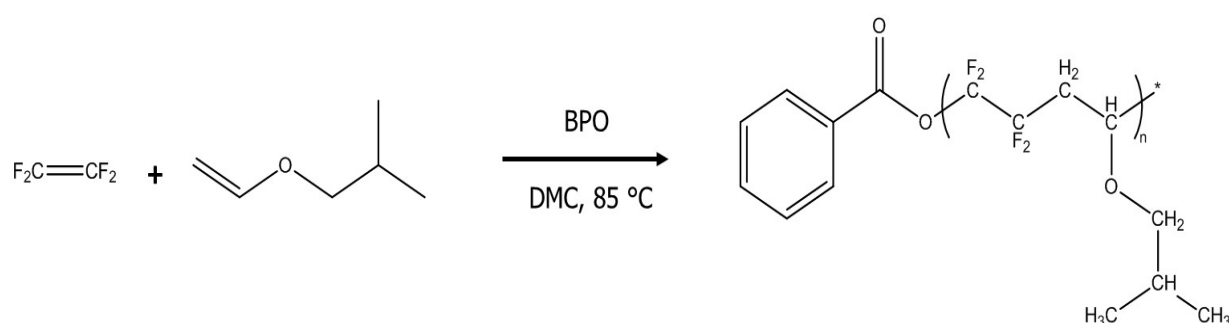
The matrix and cationizing agent were trans-2-[3-(4-tertbutylphenyl)-2-methylprop-2-enylidene]malononitrile (DCTB) (10 mg/mL in CHCl_3) and LiCl (10 mg/mL in methanol), respectively. The polymer concentration was 10 mg/mL in dimethylformamide (DMF). The polymer and matrix were mixed in a 4:10 volume ratio, and LiCl was first deposited on the target. After evaporation of the solvent, the mixture (composed of polymer, matrix, and cationising agent) was placed on the matrix-assisted laser-desorption ionization (MALDI) target. The dry droplet sample preparation method was used.

6.3 Results and discussion

6.3.1 Free-radical copolymerisation of tetrafluoroethylene with isobutyl vinyl ether

The experimental conditions for the free-radical copolymerisation of tetrafluoroethylene (TFE) with isobutyl vinyl ether (iBuVE) using BPO as initiator, along with the characterisation results, are summarised in Table 15. The expected structure of the product is shown in Scheme 16.

Benzoyl peroxide has a half-life of *ca.* 3 hours at 85 °C in benzene, decomposing into two benzoyl radical that may initiate polymerisation. The decomposition kinetics for benzoyl peroxide in dimethyl carbonate are unknown, but it is reasonable to expect the kinetics to be similar to those in benzene. A polymerisation temperature of 85 °C was chosen to ensure that the reaction rates in this study are comparable to the work reported with CTFE and persistent perfluoro-3-ethyl-2,4-dimethyl-3-pentyl radical [35, 36]. A 50 mol % feed of TFE to iBuVE was chosen since the maximum rate of polymerisation is found at this ratio [37, 38].



Scheme 16: Radical copolymerisation of tetrafluoroethylene with isobutyl vinyl ether initiated by benzoyl peroxide (BPO) in dimethyl carbonate (DMC) leading to a poly(TFE-*alt*-iBuVE) alternating copolymer.

All polymers were isolated as highly viscous, yellow liquids, with the viscosity increasing as initiator concentration decreased. Precipitation into water did not alter the appearance of the

final product. Attempts to precipitate in solvents besides water all met with failure. Indeed, cold pentane, n-hexane, cyclohexane, and methanol all solubilised the resulting polymers. Likewise, the copolymer was soluble in DMSO, chloroform, acetone, THF, DMF, DMA, and a range of alcohols.

Measurement of the zeta potential for the polymer synthesised with 5 % BPO gave a potential value of -20 mV, indicating an incipiently stable suspension [39, 40]. Particle-size analysis of the polymer suspension returned a d_{50} particle size of ~200 nm.

6.3.1.1 Nuclear magnetic resonance spectroscopic characterisation of poly(TFE-*alt*-iBuVE) copolymers prepared by conventional free-radical method.

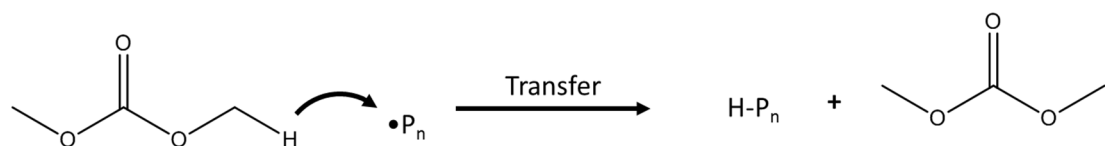
Figure 68 and Figure 69 exhibits the ^1H NMR spectra for poly(TFE-*alt*-iBuVE) copolymers prepared with 1 % and 30 % initiator, while the ^{19}F NMR spectra are shown in Figure 70 & Figure 71. Figure 68 shows the absence of signals centred at 6.6 ppm, which is assigned to the vinyl C-H proton of iBuVE. The signals centred at *ca.* 4.0, 3.4, 2.43, 1.77, and 0.83 ppm correspond to the expected signals for iBuVE in a poly(TFE-*alt*-iBuVE) copolymer [38]. The tiny signal at -138 ppm in the ^{19}F NMR spectrum corresponds to the $\text{CF}_2\text{-CF}_2\text{-H}$ moiety [41]. This observation is reinforced by the presence of some small signals at 6.1 ppm ($^2J_{\text{HF}} = 54.3$ Hz) in the proton NMR spectrum corresponding to $\text{CF}_2\text{-CF}_2\text{-H}$ [41, 42].

Guerre *et al.* [31] demonstrated that transfer from the solvent occurred with VDF polymerisation in DMC, as shown in Scheme 17, to produce a polymer dead chain and a radical DMC fragments, that may initiated further polymerisation or terminate other macroradicals by recombination. In the ^1H NMR spectrum, where 1 % BPO was used, signals ranging between 3.5 and 3.8 ppm are observed, assigned to $\text{CH}_3\text{-O-(C=O)-O-R}$ moieties. These signals are quite small and indicate that proton transfer from the solvent (proton abstraction from DMC by polymer radicals) is quite negligible in the 1 % BPO.

The ^1H NMR spectrum for 30 % BPO exhibits numerous small signals which do not correspond to any protons in the expected structure, and this NMR spectrum also includes the signals for the protons on the benzene ring. The ratio between the signals at *ca.* 3.5 and 3.8 ppm and the signals corresponding to iBuVE is large, indicating a significant percentage of the chains are terminated by solvent fragments.

Furthermore, the signal at *ca.* 4.5 ppm indicates a CH containing moiety that is not part of the vinyl ether in the backbone. This, in conjunction with the signals at *ca.* 1.2 ppm, implies that

there is significant proton transfer from the vinyl ether monomer to produce monomer fragments, which also terminate the macroradical.



Scheme 17: Mechanism of proton transfer from DMC onto macroradicals to produce a polymer dead chain and radical fragments.

The calculated number-average molecular weight for 30% BPO (calculated by Equations (32) and (33)) from the NMR spectrum gives a DP_n of ~ 5 (~ 1000 Da). The same calculation indicates a DP_n of ~ 100 ($\sim 20,000$ Da) for the polymer initiated with 1 % BPO. Table 15 lists the calculated number-average molecular weight of the other copolymers. The calculations assume a chain termination by recombination, as is the case for PTFE [43].

The stereochemistry of the poly(TFE-*alt*-iBuVE) copolymer backbone as viewed from a CF_2 unit is shown in Figure 69 along with an enlargement of the region from 3 to 3.5 ppm for the 1 % BPO polymer showing both the normal proton and ^{19}F decoupled proton signals. The signals for the CH_2 in the polymer backbone remain unchanged with fluorine decoupling of the protons, indicating that the $^3J_{HF}$ coupling is negligible for the CH_2 protons.

The ^{19}F NMR spectra display signals at -75 ppm, assigned to the CF_2 groups adjacent to the initiator moiety ($Ph-(C=O)-O-CF_2-CF_2-$). This chemical shift is in agreement with that of the (OCF_2CF_2) units in perfluoropolyether [44].

The region from -110 ppm to -125 ppm is shown in enlarged form in Figure 72 along with the splitting patterns. The signals can be explained from the stereochemistry of the chain, depicted in Figure 73. Given that the polymer backbone contains a stereocentre, splitting of the fluorine signals due to magnetic non-equivalence is expected. First, geminal coupling ($^2J_{FaFa'}$) between Fa and Fa' is observed at 280.4 Hz. Second, from the stereochemistry, Fa is expected to undergo vicinal and gauche coupling with Fb and Fb' , respectively, while Fa' is expected to undergo gauche and anti-position coupling with Fb and Fb' , respectively. Based on the limits for these types of couplings given in the literature, the potential 3J coupling constants for Fa fall in the range of 0-36 Hz and that for Fa' in 16-31 Hz. This is in agreement with the findings of Tabata *et al.* [38].

Table 15: Experimental conditions and results obtained for the free-radical copolymerisation of TFE with *i*BuVE initiated by BPO at 85 °C in DMC.

Experiment No.	Monomer TFE + <i>i</i> BuVE (mmol)	$\frac{[BPO]_0}{[TFE]_0 + [iBuVE]_0}$ (mol %)	Yield (%)	M_n^a (g·mol ⁻¹)	M_n^b (g·mol ⁻¹)	$T_d^{10\%,c}$ (°C)	PDI
1	9.98	1	14	11000	20250	305	1.44
2	9.98	5	21	8000	12550	275	1.62
3	9.98	10	25	6100	3050	225	1.29
4	9.98	15	33	5100	1950	225	2.18
5	9.98	30	46	4400	1050	180	1.03

^a M_n as determined by GPC (or SEC) ^b M_n as determined by ¹H NMR spectroscopy from equations (32) and (33)

^cDecomposition temperature at which the polymer has undergone 10 % mass loss.

The mode of termination is of some importance and four of the six possible modes are presented in Scheme 18. TFE to TFE recombination results in a signal at approximately -122 ppm. However, no such signal is noted in the ^{19}F NMR spectrum of the copolymer prepared from 1% BPO in Figure 70. This implies that, normally, TFE to TFE recombination does not occur.

The signals at 4.65 and 4.4 ppm in the 30 % BPO ^1H NMR spectrum may correspond to the CH-CH moieties of head-to-head termination. The signal at 1.52 ppm in the 1 % BPO ^1H NMR spectrum is attributed to the $\text{CH}_2\text{-CH}_2$ moieties of tail-to-tail termination. The preferred mode of termination in free-radical polymerisation of poly(TFE-*alt*-iBuVE) seems to be either a TFE-vinyl ether recombination or termination *via* tail-to-tail recombination of the vinyl ether.

6.3.1.2 Addition preferences of the benzoyl radicals to the TFE/iBuVE monomer mixture

Benzoyl peroxide undergoes decomposition to form two kinds of radicals, as detailed in Scheme 19 [45-47]. The fast decarboxylation of the benzoyl radical to give a benzene radical generally occurs only at high temperatures ($>90\text{ }^\circ\text{C}$), and thus, it is very slow at the reaction temperature where this work was conducted. Hence, the possibility of benzene radical attack is not considered here. Besides this, the signal for a $\text{CF}_2\text{-CF}_2\text{-Ph}$ moiety is expected at -111.6 ppm [48]. Since this region also contains the signals for other CF_2 groups, it is nearly impossible to determine the extent to which initiation by phenyl radical may have occurred.

Scheme 20 details the three possible additions of benzoyl radicals onto the monomer mixture. The expected chemical shifts for the CH_2 in path 1a is around 4.5 ppm, while for CH in path 1b it is around 6.4 ppm. A Ph-CO-O-CF_2 moiety will exhibit a ^{19}F NMR chemical shift in the region of -74 ppm [49].

The expected attack preference should be *via* path 1a as the benzoyl radical is electrophilic and the CH_2 of iBuVE is the sterically less hindered site. Concomitantly, attack *via* TFE is not expected to occur due to its electron poor nature. In contrast, the proton NMR spectrum of the copolymer obtained from for 1 % BPO does not exhibit a signal at 4.5 ppm nor at 6.4 ppm.

The ^1H and ^{19}F NMR spectra of copolymer obtained from 30 % BPO seems to show attack *via* all three pathways, and this is ascribed to an overabundance of benzoyl radicals, stripping the DMC solution of TFE and concomitantly attacking any available double bond, as well as abstracting hydrogen atoms from the vinyl ether monomer. This implies that, even in a solvent such as DMC, the limiting factor for the free-radical polymerisation of TFE with iBuVE is the mass transfer of TFE into the solution.

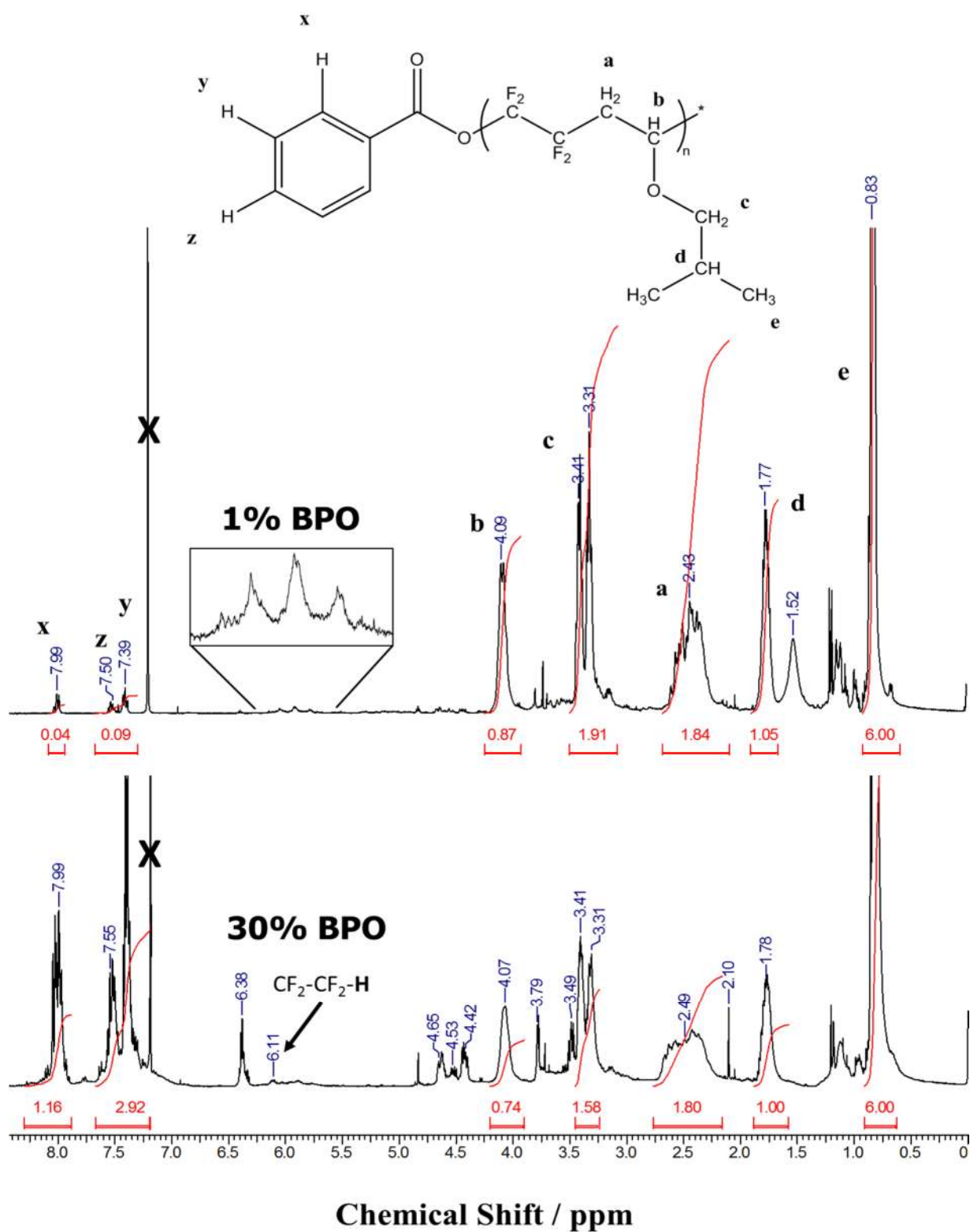


Figure 68: ^1H NMR spectra of poly(TFE-alt-iBuVE) copolymers achieved from 1 and 30 % BPO (recorded in CDCl_3).

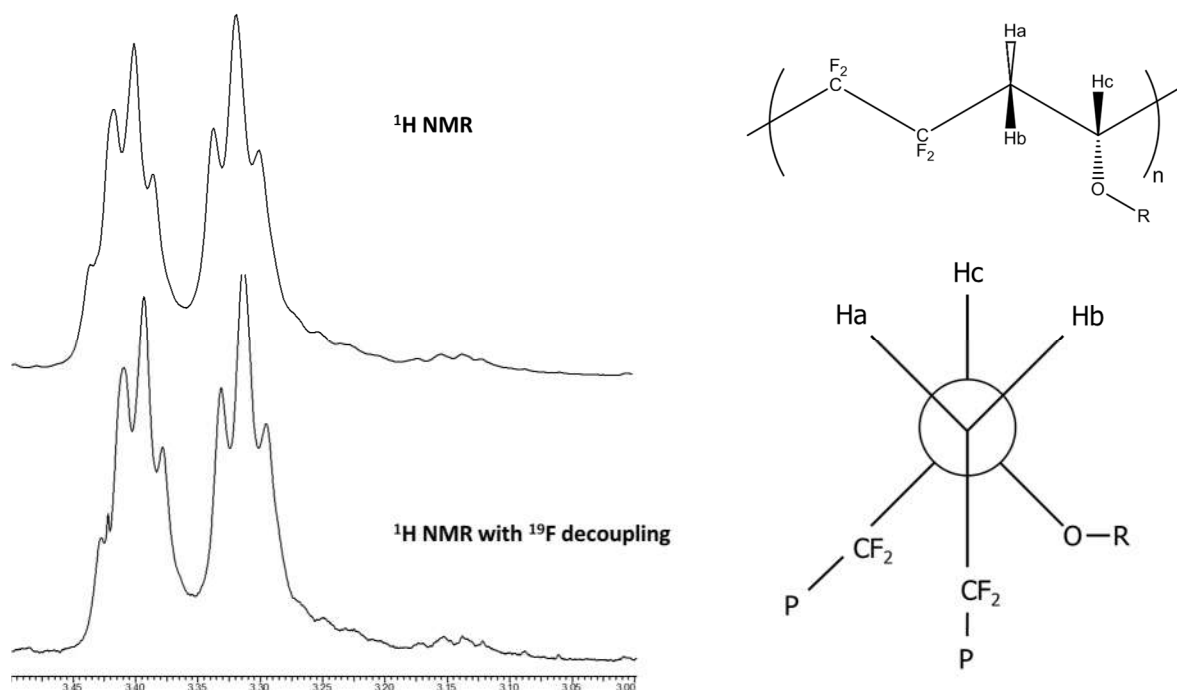


Figure 69: Expansion of the ^1H NMR spectra of poly(TFE-*alt*-iBuVE) copolymer achieved from 1 % BPO (3.00 to 3.50 ppm) showing the stereochemistry of the polymer backbone as viewed from the CF_2 group.

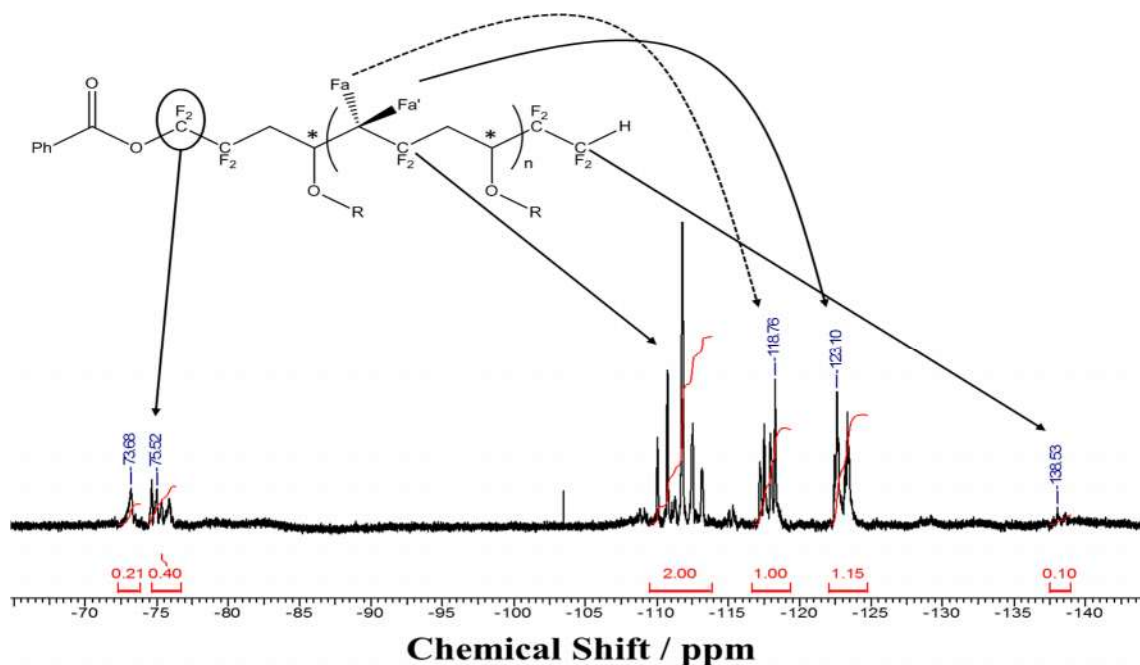


Figure 70: ^{19}F NMR spectrum of poly(TFE-*alt*-iBuVE) copolymers at 1 % BPO (recorded in CDCl_3).

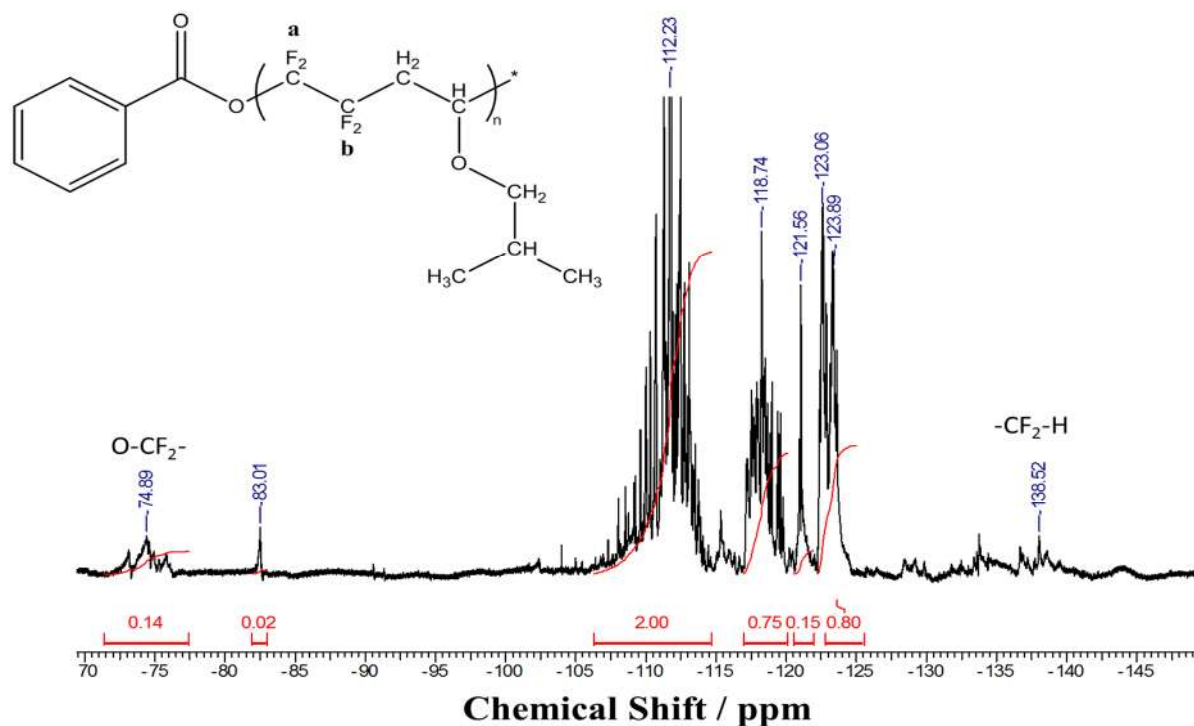


Figure 71: ^{19}F NMR spectrum of poly(TFE-alt-iBuVE) copolymers at 30% BPO (recorded in CDCl_3).

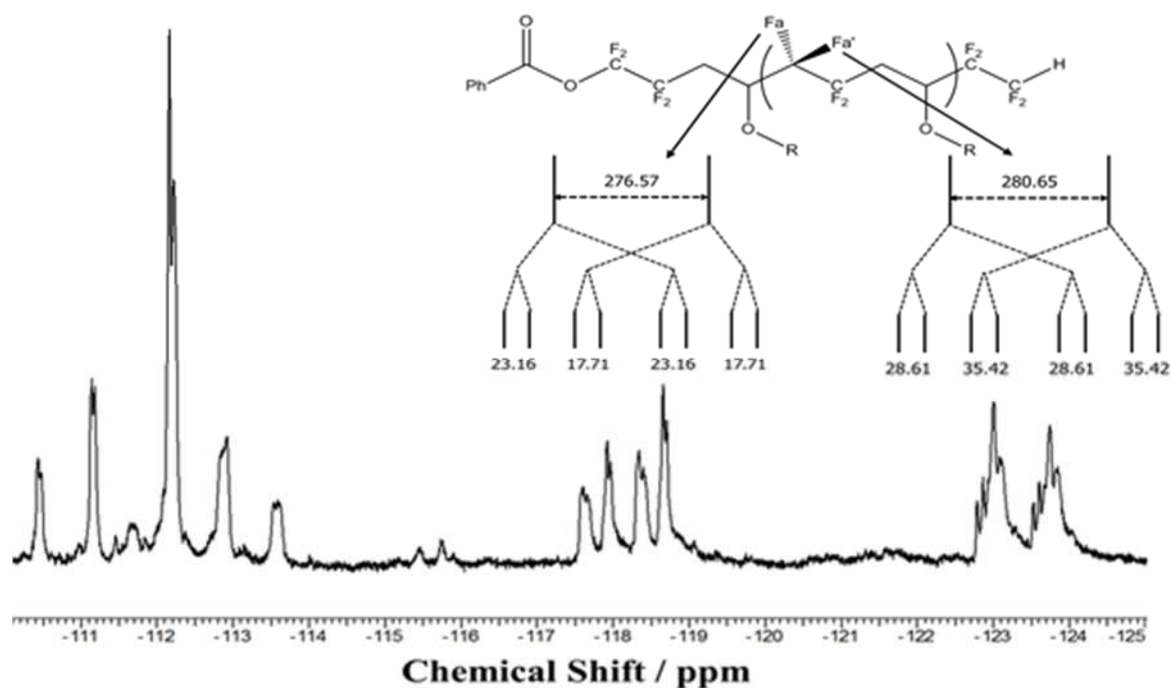


Figure 72: Enlargement of the region from -110 to -125 ppm for the ^{19}F NMR spectrum of poly(TFE-alt-iBuVE) copolymers at 1% BPO, showing the multiplicities and coupling constants.

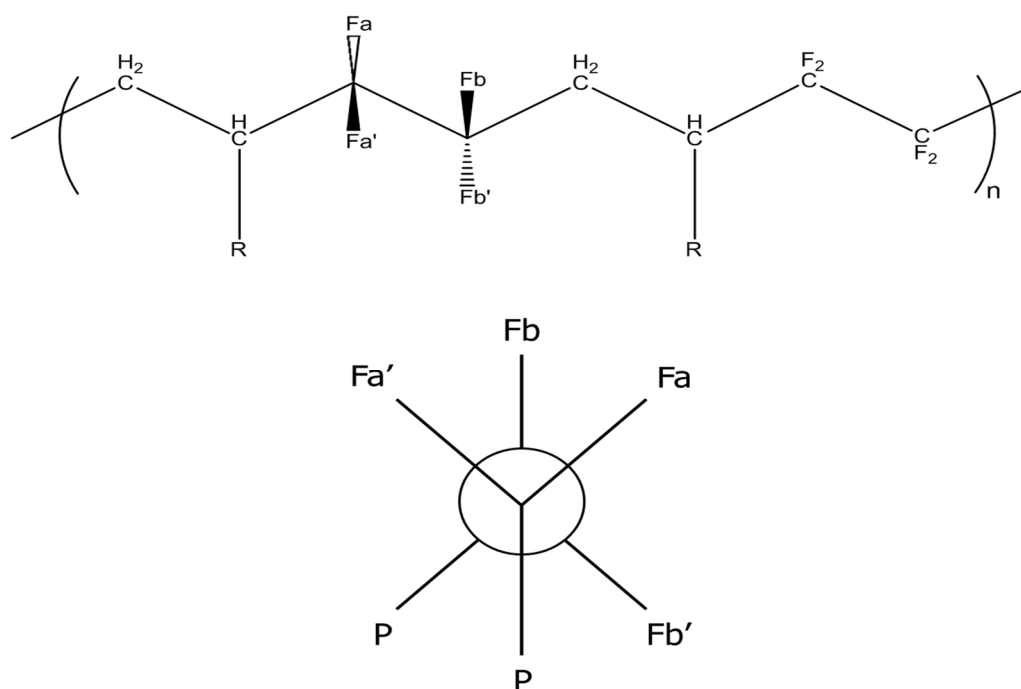
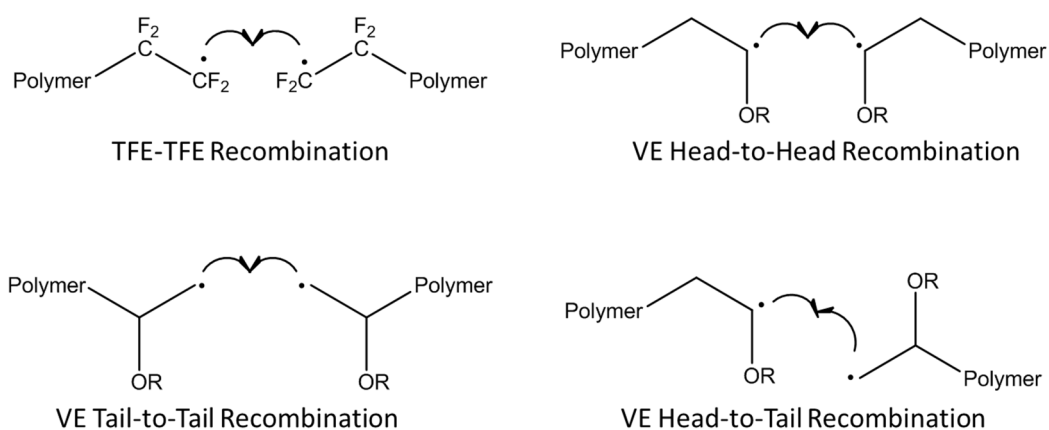
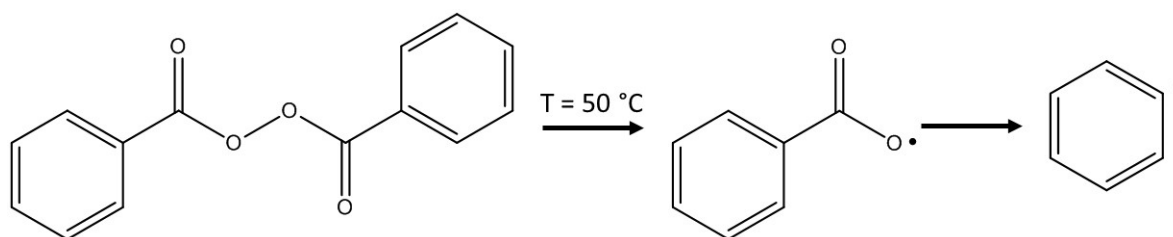


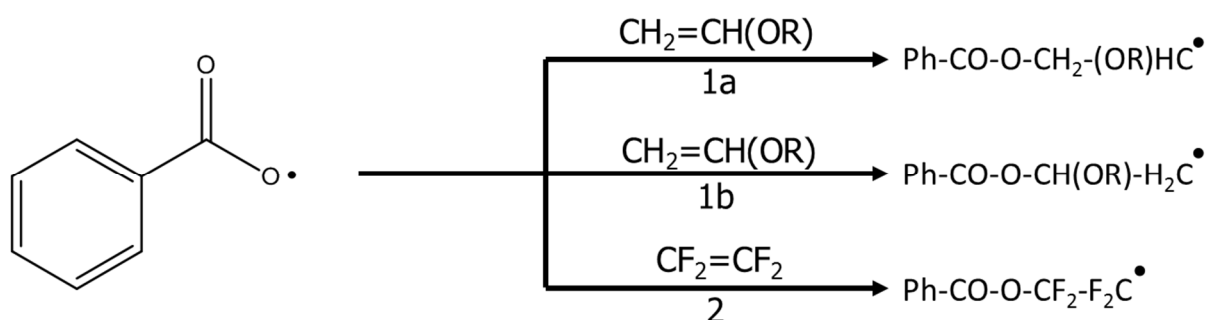
Figure 73: Stereochemistry of the polymer backbone of poly(TFE-*alt*-iBuVE) copolymer as viewed from the C-H group.



Scheme 18: Non-trivial modes for the termination by recombination of macroradicals for poly(TFE-*alt*-iBuVE) copolymer.



Scheme 19: Thermal decomposition process of benzoyl peroxide [45-47].



Scheme 20: Possible addition reactions of benzoyl radicals onto the TFE/iBuVE mixture.

6.3.1.3 MALDI-TOF mass spectrometry

Characterisation of the structures of poly(TFE-*alt*-iBuVE) copolymers synthesised *via* free radical polymerisation was performed by matrix-assisted laser desorption/ionisation coupled time-of-flight mass spectrometry (MALDI-TOF) using both positive and negative ion modes. The MALDI-TOF mass spectrum of poly(TFE-*alt*-iBuVE) copolymer synthesised with 30 % BPO (Table 15, experiment 5) recorded in negative ion mode displays two distributions in the form of deprotonated adducts (M-H)⁻ as presented in the spectrum between 500 and 3000 m/z. The more intense distribution corresponds to oligomers of formula HO(CH₃)CH[CF₂CF₂CH₂CHOCH₂CH(CH₃)₂]_mCF₂CF₂OC₆H₅ (marked with a triangle, Figure 74), and the second distribution is attributed to formula HO(CH₃)CH[CF₂CF₂CH₂CHOCH₂CH(CH₃)₂]_mOC₆H₅ (marked with a circle, Figure 74). All distributions display the repeat unit mass between two consecutive peaks ($\Delta m/z = 200$ Da) that confirm the presence of [CF₂CF₂CH₂CHOCH₂CH(CH₃)₂] blocks. No oligomers were detected in the positive ion mode. The MALDI data confirm that benzoyl radicals do indeed preferentially attack TFE to initiate the polymer chain. This corroborates the M_n determined by NMR spectroscopy.

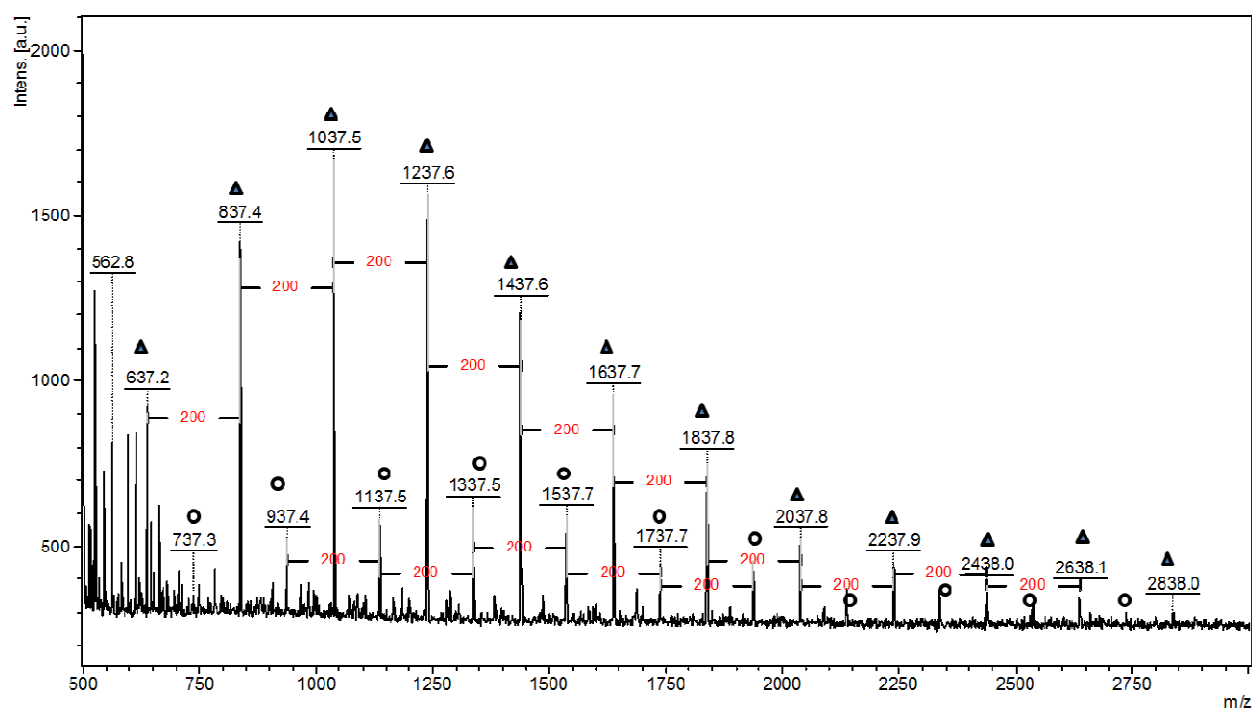


Figure 74: Negative ion MALDI-TOF mass spectrum of poly(TFE-*alt*-iBuVE) synthesised by free radical copolymerisation (Table 15, experiment 5) with DCTB as matrix and LiCl as cationic agent.

6.3.1.4 Effect of initiator concentration on the molecular weight

The number-average molecular weights as determined by ^1H NMR spectroscopy (using the benzoyl end-group as a label) and as assessed by GPC are compared in Figure 75. Polydispersities are summarised in Table 15. According to Tobolsky's law [50, 51] (Equation (39)), the molecular weight of a polymer depends upon several parameters *viz.* the reactant concentrations, the efficacy of the initiators (f), the propagation rate of the monomers (k_p), decomposition rate of the initiator (k_d), and the termination rate (k_t) with $a = 1$ when termination by recombination is assumed.

$$\text{Instantaneous } DP_n = \frac{(1 + a)k_p[\text{Monomer}]}{2\sqrt{(fk_d[\text{BPO}]k_t)}} \quad (39)$$

As expected, for increasing BPO concentrations, the molecular weight decreases, but there is little correlation between the M_n determined *via* GPC and *via* NMR spectroscopy, due to the difference between the hydrodynamic volume of the polymer and PMMA standards. However, the PDIs are rather narrower than what would be expected for a free-radical polymerisation, although considerable variance exists in the PDI data, indicating that the copolymerisation of

TFE with iBuVE is not an inherently well-behaved system with respect to abstraction and termination.

6.3.1.5 *Thermal properties of poly(TFE-*alt*-iBuVE) copolymers terminated by benzoyl groups*

The thermograms for the decomposition of poly(TFE-*alt*-iBuVE) synthesised with 1, 5, 10, 15 and 30 mol % BPO under a nitrogen atmosphere are presented in Figure 76. These copolymers exhibit satisfactory thermal stability, being thermally stable up to 200 °C, before undergoing elimination of HF and, subsequently, the scission of the polymer backbone to produce the breakdown products, as reported by Zulfiqar *et al.* [52-54]. Importantly, the effect of molecular weight is strongly observed, with the evaporation of low-molecular-weight material occurring well before proper thermal decomposition. As with the CTFE copolymers [36], thermal decomposition temperatures remained the same whether the samples were run in air or in nitrogen.

6.3.2 Copolymerisation of TFE with iBuVE by RAFT/MADIX

The experimental conditions for the RDRP of TFE and iBuVE using BPO as initiator and O-ethyl-S-(1-methyloxycarbonyl)ethyl xanthate as RAFT/MADIX CTA, along with the characterisation results, are summarised in Table 16. The structure of the expected copolymers is shown in Figure 77. The benzoyl-peroxide-initiated polymers were all isolated as highly-viscous, yellow liquids, showing stickiness and a propensity to form an emulsion in water similar to the uncontrolled polymers. Due to the nature of the xanthate, all polymers exhibited a strong smell, even after solvent removal under vacuum.

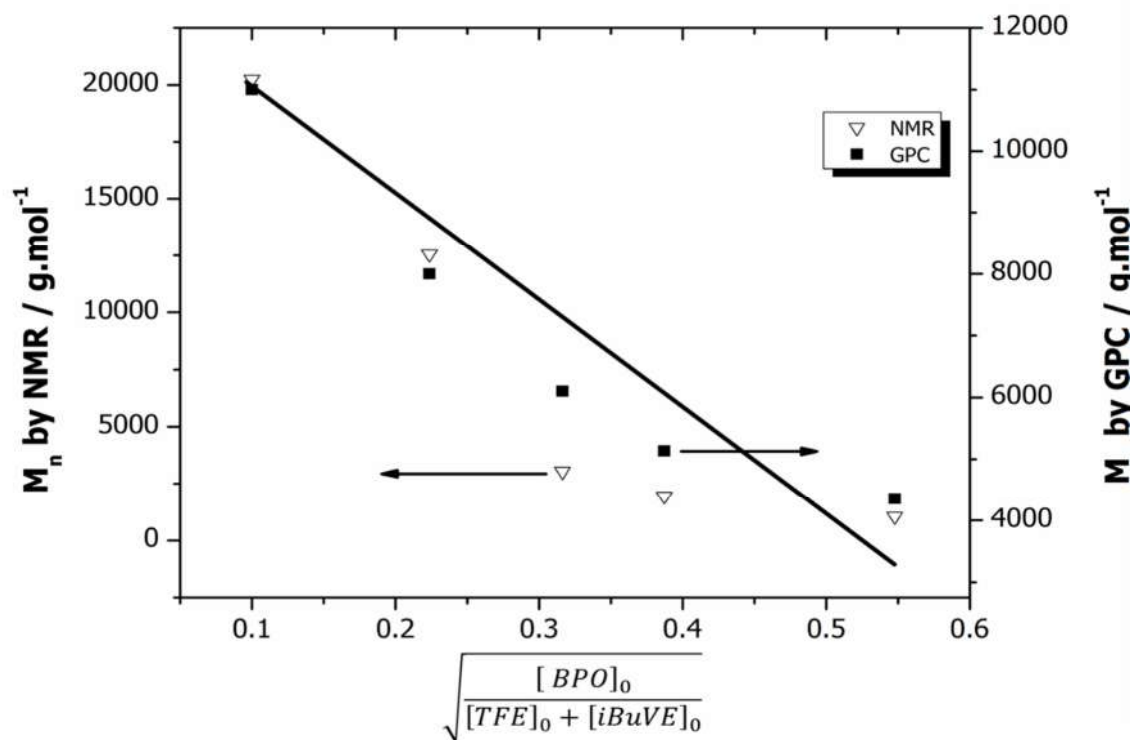


Figure 75: Correlation of M_n decrease as BPO ratio increases, determined by both SEC (■) and ^{19}F NMR spectroscopy (Δ).

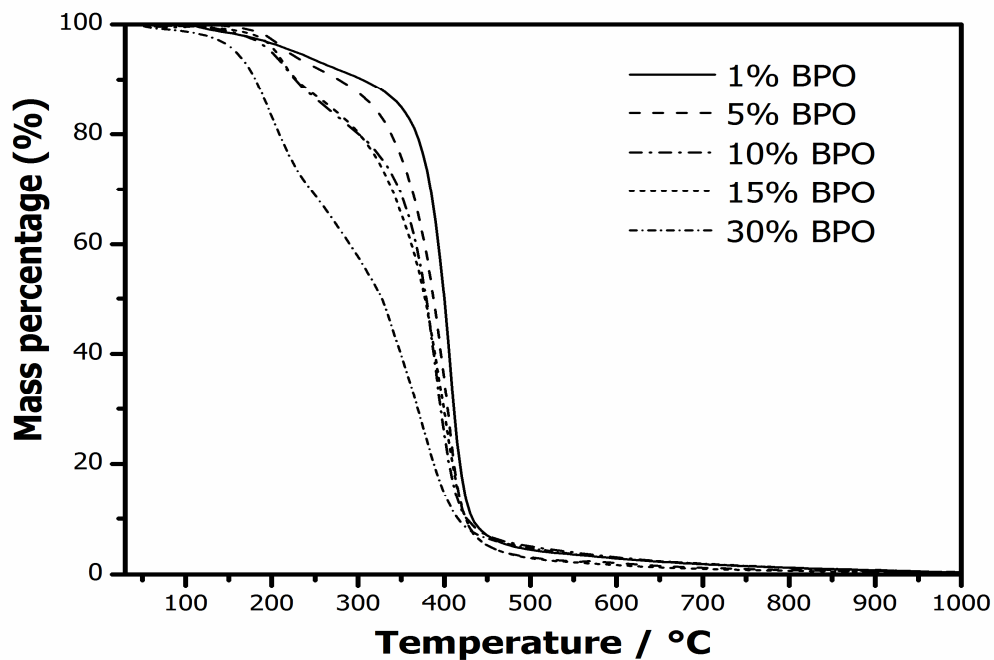


Figure 76: TGA thermograms of poly(TFE-*alt*-iBuVE) copolymers synthesised with 1, 5, 10, 15, and 30 mol % BPO under an N_2 atmosphere.

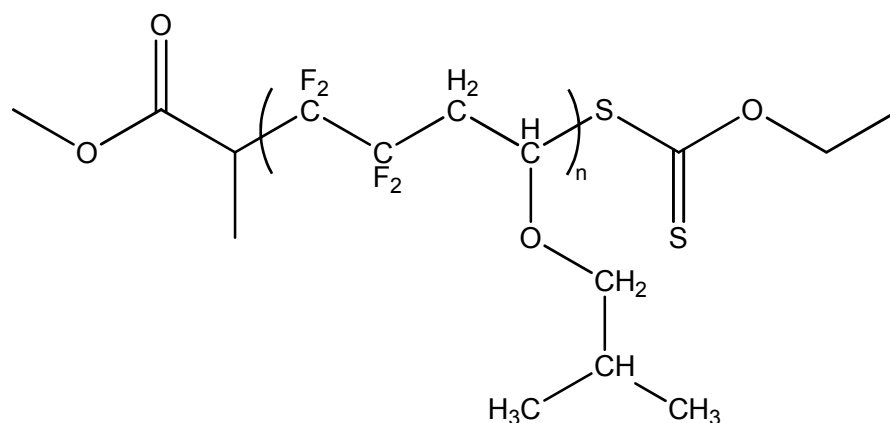


Figure 77: Expected structure of poly(TFE-*alt*-iBuVE) alternating copolymer from the RAFT copolymerisation reaction of TFE and iBuVE initiated by benzoyl radical and controlled by *O*-ethyl-*S*-(1-methyloxycarbonyl)ethyl xanthate.

6.3.2.1 Nuclear magnetic resonance spectroscopic characterisation of poly(TFE-*alt*-iBuVE) synthesised via RAFT/MADIX

The ^1H and ^{19}F NMR spectra for poly(TFE-*alt*-iBuVE) copolymer controlled by xanthate taken at 15 minutes is presented in Figure 78 and Figure 79, and enlargements of various regions of interest are given in Figure 80 along with the coupling constants and structural assignments. The structural assignments for the xanthate end-groups are based on the assignments reported by Guerre *et al.* [29-31].

The nature of the moiety to which the Z-group of the xanthate binds is of significant interest as this functionality determines the long term reactivity of the macroradical [31]. For the RAFT/MADIX polymerisation of VDF, it is possible to switch the end moiety from CF_2 to CH_2 if the VDF adds to the macroradical in a manner that produces head-to-head chain defects (and thus allows CH_2 -xanthate to accumulate in the medium). Depending on the manner in which the chain initiates and the nature of the addition of the monomers to the chain end, a poly(TFE-*alt*-iBuVE) copolymer may have either CF_2 or CH end moieties. The evolution of the end moieties with time is of interest, as it will reveal if the monomers add to the chain in a concerted manner, or if only one monomer at a time adds to the chain end.

The signal at 1.15 ppm appears to be comprised of two doublets (which belong to the $\text{CO-CH}(\text{CH}_3)$ - group) that almost overlap. This indicates that the CH moiety is attached to two different chemical systems, which arise from a mixed initiation mode by the R group. The relative intensities of these doublets are nearly equal and do not change with time, indicating a binary initiation regime, with R group attack on TFE and iBuVE to be equally likely.

Table 16: Experimental conditions and results obtained for the RAFT copolymerisation of TFE with *i*BuVE in a 1:1 ratio initiated by BPO at 85 °C controlled by *O*-ethyl-*S*-(1-methyloxycarbonyl)ethyl xanthate. $[Monomers]_0 : [CTA]_0 : [BPO]_0$ ratio of 20:1:0.1.

Experiment No.	Monomer TFE + <i>i</i> BuVE (mmol)	$\frac{[BPO]_0}{[TFE]_0 + [iBuVE]_0}$ (mol %)	Xanthate (mmol)	Reaction time (minutes)	Yield (%)	M_n^a	M_n^b	PDI
1	9.98	0.5	0.499	15	43	2700	1200	1.08
2	9.98	0.5	0.499	30	50	2760	1400	1.08
3	9.98	0.5	0.499	60	55	2950	1600	1.09
4	9.98	0.5	0.499	120	65	3200	1800	1.10
5	9.98	0.5	0.499	1440	73	3300	2000	1.11

^a M_n as determined by GPC ^b M_n as determined by ¹H NMR spectroscopy using R group analysis ((**34**) and (**35**)).

The low field signals at -75 ppm, assigned to $\text{CF}_2\text{-CF}_2\text{-S-(C=S)}$, are nearly identical to that of CF_2 in $\text{Ph-(C=O)-O-CF}_2\text{-CF}_2$. The signals at 3.49 and 3.21 ppm indicate that a vinyl ether unit is attached to the Z group.

Furthermore, there are signals at *ca.* 4.6 ppm that correspond to $\text{CH}_3\text{-CH}_2\text{-O-(C=S)-S-}$. These signals show two overlapping quartets. The lower field and more intense of these quartets is assigned to $\text{CH}_3\text{-CH}_2\text{-O-(C=S)-S-CF}_2\text{-CF}_2\text{-}$, whereas the less intense and more upfield quartet is assigned to $\text{CH}_3\text{-CH}_2\text{-O-(C=S)-S-CH}_2\text{-CH(OCH}_2\text{-CH(CH}_3\text{))}_2\text{-}$.

Figure 81 details the evolution of these signals with conversion. Almost no change occurs in the ratio of these signals with time, implying a mixed termination mode and that both vinyl ether and TFE units are equally useful as end-groups for propagating the macroradical (unlike in the case for PVDF [31]). Despite the near time invariance of these signals, there is still a noticeable difference in the ratio between them, indicating that the TFE end-group is preferred.

The complex signals centred at 3.64 ppm, assigned to CH_3 in $\text{CH}_3\text{-O-(CO)-O-CH}_2\text{-R}$, arise from DMC addition on to the macroradical. The observation of such a transfer is reinforced by the presence of the signal at -138 ppm in the ^{19}F NMR spectra assigned to $\text{CF}_2\text{-CF}_2\text{-H}$. This indicates that transfer from the solvent to the macroradical or the initiator occurs readily during RAFT/MADIX. This is also observed in the RAFT polymerisation of VDF [31].

Three mechanisms have been proposed for acceptor-donor copolymerisation. The first one involves the formation of a charge-transfer complex (CTC) that adds to the growing macroradical [55, 56]. The second mechanism suggests that electrostatic interactions and polarity differences between the radical chain end and the inserting monomer result in vastly different activation energies that energetically favor alternating monomer addition [57]. The third mechanism proposes that both free monomers and a charge transfer complex take part in the polymerisation.

The TFE/iBuVE system has not been shown to exhibit CTC formation, but it does show acceptor-donor (AD) behavior [19]. The second AD mechanism is only practical if both monomers are difficult to homopolymerise, but since TFE readily propagates, the second mechanism seems not to be applicable. Taking into account that both mixed-initiation and mixed-termination modes occur, it appears that once the chain has been initiated, then a concerted insertion of iBuVE and TFE takes place on the macroradical. This seems to indicate that TFE copolymerises with iBuVE *via* the CTC-addition mechanism to produce an alternating copolymer.

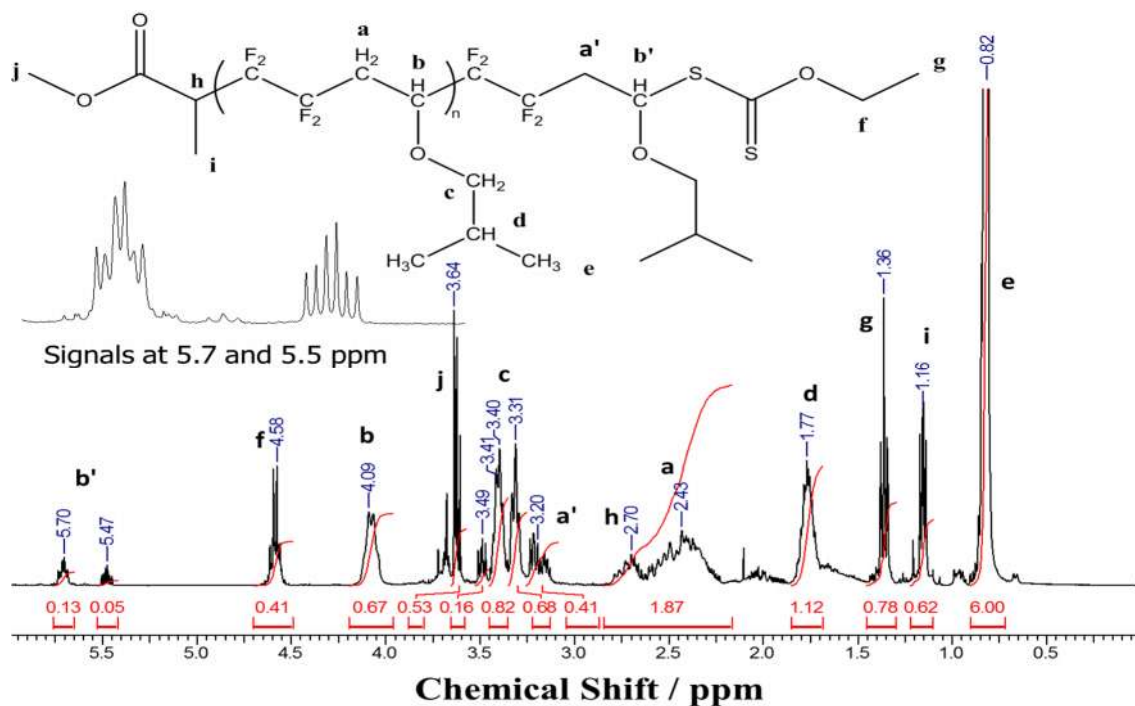


Figure 78: ^1H NMR spectrum of RAFT copolymerisation of TFE with *i*BuVE controlled by xanthate, taken at 15 min (recorded in CDCl_3).

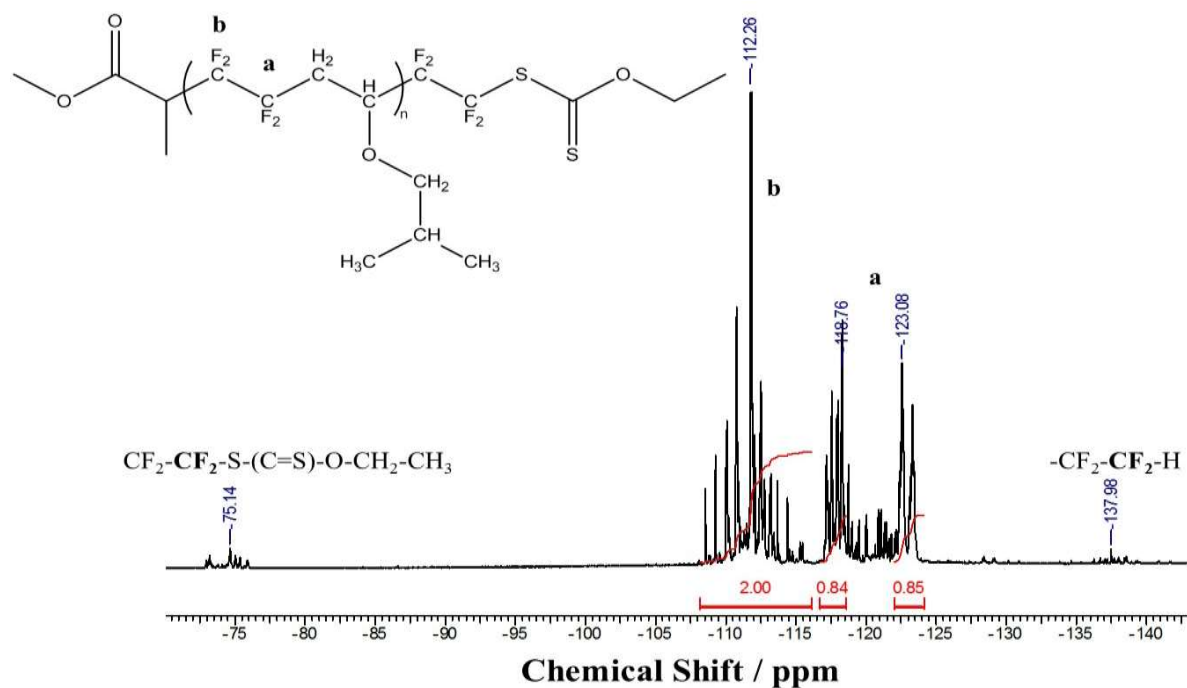


Figure 79: ^{19}F NMR spectrum of the total product mixture of the radical copolymerisation of TFE with *i*BuVE initiated by BPO and controlled xanthate, controlled poly(TFE-*alt*-*i*BuVE), taken at 15 min (recorded in CDCl_3).

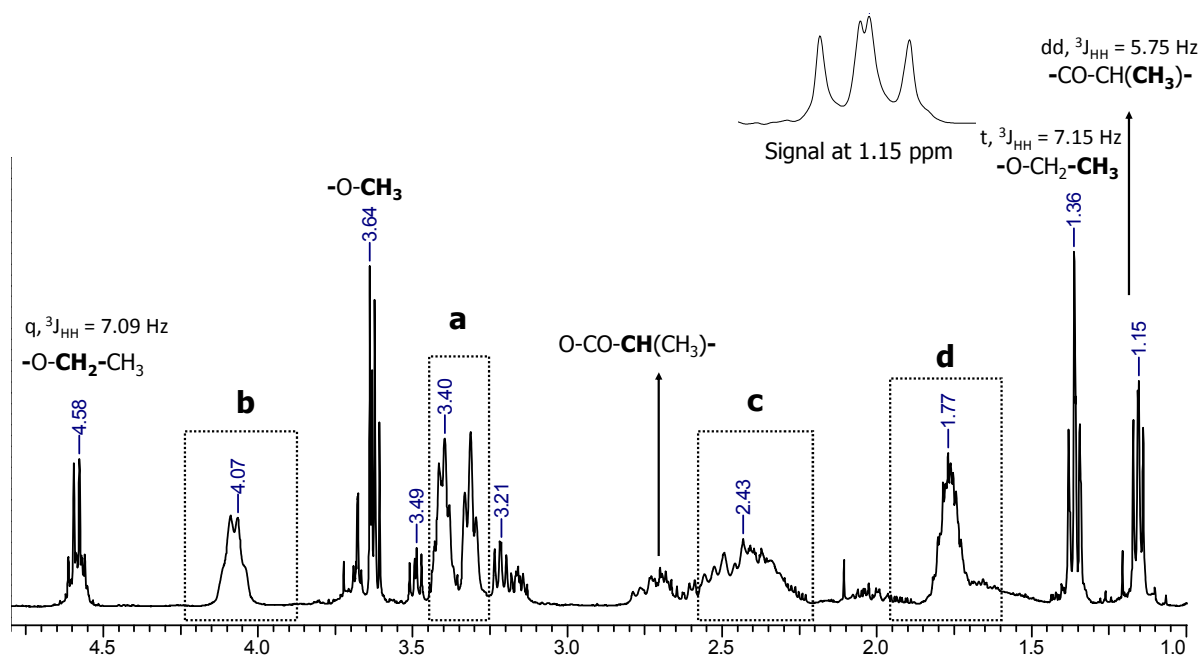


Figure 80: Enlargement of the region from 1 to 4.75 ppm for the ^1H NMR spectrum of poly(TFE-*alt*-iBuVE) copolymer controlled by xanthate, taken at 15 minutes (recorded in CDCl_3).

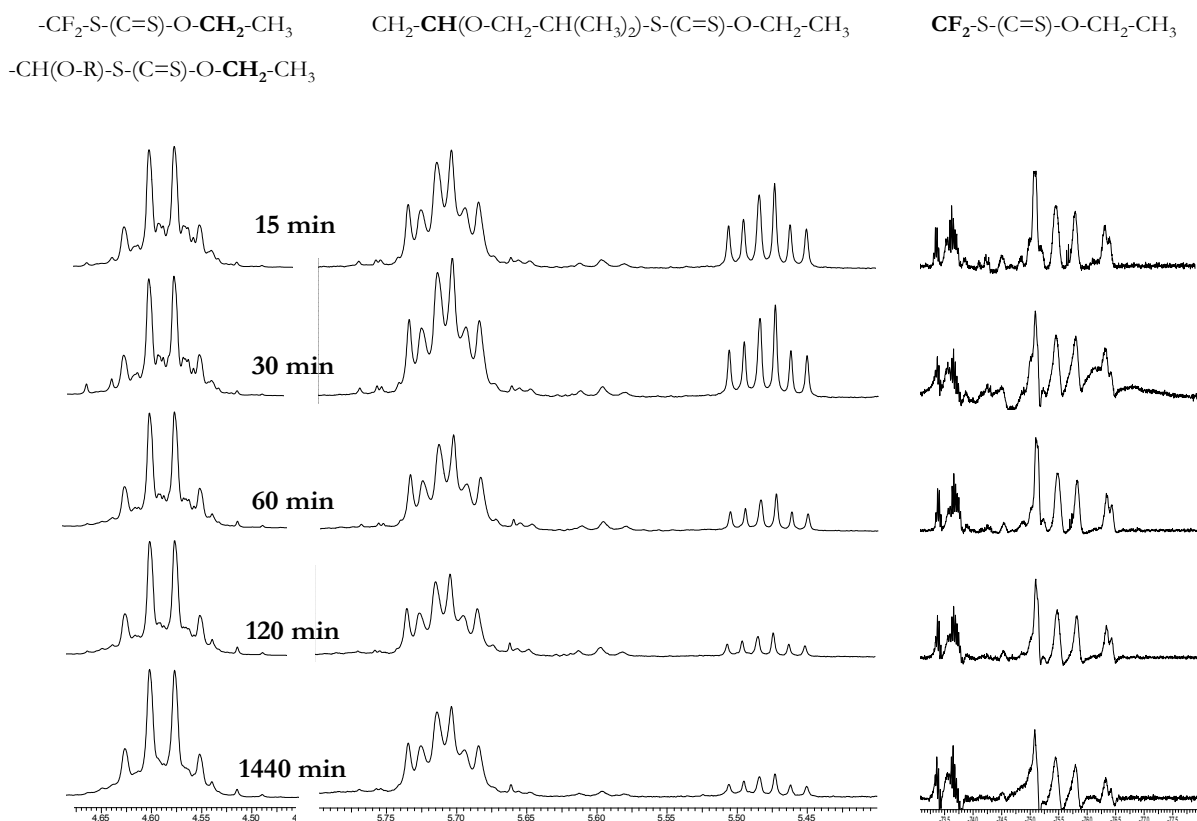


Figure 81: Evolution of selected ^1H and ^{19}F NMR signals with conversion of poly(TFE-*alt*-iBuVE) copolymers synthesised via MADIX polymerisation using a 1:1 ratio of monomers and a $[\text{Monomers}]_0:[\text{CTA}]_0:[\text{BPO}]_0$ ratio of 20:1:0.1, with O-ethyl-S-(1-methoxycarbonyl)-ethylthiocarbonate as CTA.

6.3.2.2 MALDI-TOF mass spectrometry

Characterisation of the structures of poly(TFE-*alt*-iBuVE) copolymers synthesised *via* MADIX polymerisation was performed by matrix-assisted laser-desorption/ionization-coupled time-of-flight mass spectrometry (MALDI-TOF) using both positive- and negative-ion modes. The MALDI-TOF mass spectrum recorded in negative-ion mode of poly(TFE-*alt*-iBuVE) recovered after 15 minutes (Table 16, experiment 1) is presented in Figure 82, and it displays four distributions as presented in the spectrum between 1250 and 1670 m/z. All distributions display the repeat unit mass between two consecutive peaks ($\Delta m/z = 200$ Da) that confirms the presence of $(CF_2CF_2CH_2CHOCH_2CH(CH_3)_2)_m$ blocks. The most intense distribution corresponds to oligomers of formula $CH_3OOC(CH_3)CH[CF_2CF_2CH_2CHOCH_2(CH_3)_2]_n CF_2CF_2SH$ (marked with a star) and the second distribution corresponds to oligomers of formula $CH_3OOC(CH_3)CH[CF_2CF_2CH_2CHOCH_2(CH_3)_2]_n S(C=S)OCH_2CH_3$ (marked with a triangle). The oligomer of formula $CH_3OOC(CH_3)CH[CF_2CF_2CH_2CHOCH_2(CH_3)_2]_n SH$ (marked with a circle) and the oligomer of formula $CH_3OOC(CH_3)CH[CF_2CF_2CH_2CHOCH_2(CH_3)_2]_n CF_2CF_2S(C=S)OCH_2CH_3$ are the least intense.

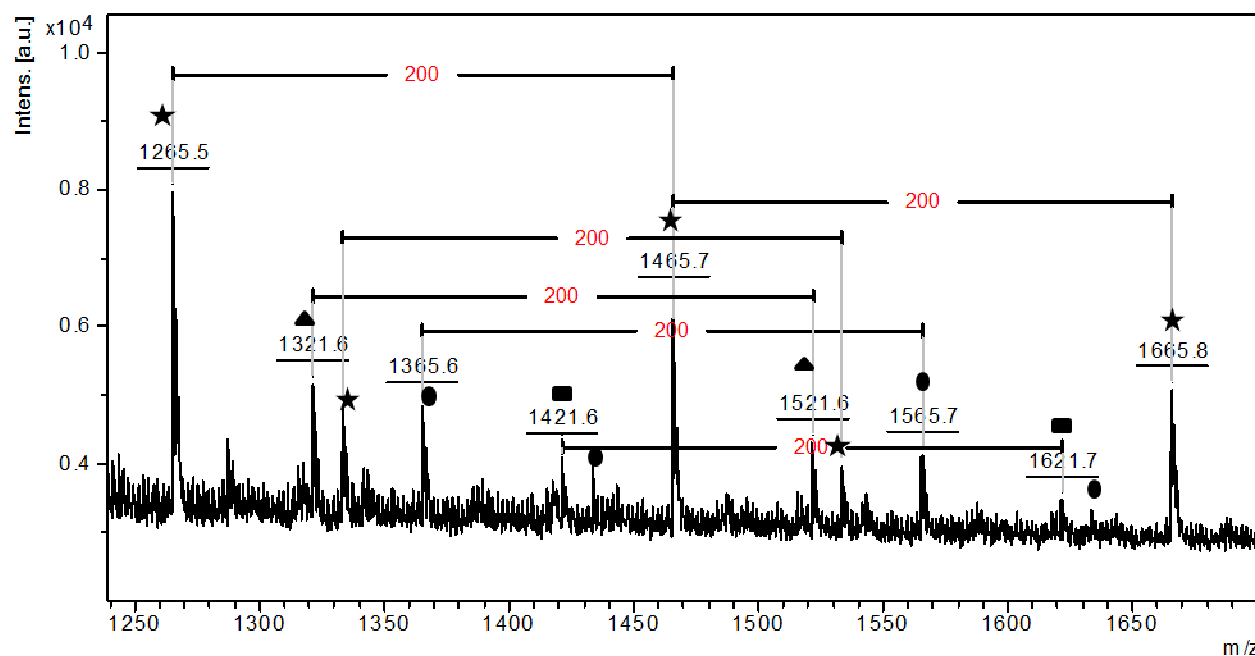


Figure 82: Negative ion MALDI-TOF mass spectrum of poly(TFE-*alt*-iBuVE) synthesised by MADIX polymerisation (Table 16, experiment 1) with DCTB as matrix and LiCl as cationic agent.

6.3.2.3 Evolution of the molecular weights of poly(TFE-*alt*-iBuVE) copolymers synthesised via RAFT/MADIX

The evolution of M_n and the polydispersity (\mathcal{D}) as a function of conversion for the MADIX copolymerisation of TFE and iBuVE are shown in Figure 83. The theoretical molecular weight was calculated according to Equation (38). The molecular weight determined *via* NMR spectroscopy was calculated from the R group concentration (Equations (34) and (35)) and from the Z-group concentration (Equations (36) and (37)). M_n increases linearly with conversion, and the PDI is surprisingly narrow, hovering very close to 1, indicating that the TFE/iBuVE system is well behaved in RAFT/MADIX polymerisation and control of the molecular weight can be achieved.

The molecular weights, as determined by NMR spectroscopy are summarised in Table 17. The experimental M_n values agree well with each other, but differ substantially from the theoretical M_n and the M_n determined by GPC.

Table 17: *Molecular weights of xanthate controlled poly(TFE-*alt*-iBuVE) copolymers as determined by NMR spectroscopy and by GPC versus the theoretical molecular weight.*

Time (min)	Conversion (%)	M_n Theoretical ($\text{g}\cdot\text{mol}^{-1}$)	M_n by GPC ($\text{g}\cdot\text{mol}^{-1}$)	M_n by Z-group analysis ($\text{g}\cdot\text{mol}^{-1}$)	M_n by R-group analysis ($\text{g}\cdot\text{mol}^{-1}$)
15	43.0	1900	2700	1000	1200
30	50.1	2200	2760	1200	1400
60	54.6	2400	2950	1400	1600
120	64.7	2800	3200	1600	1800
1440	72.7	3100	3300	1800	2000

In the RAFT polymerisation of VDF [30, 31, 44], the propagation proceeds from the PVDF macroradical especially generated from the CF_2 -xanthate end-group. Due to head-to-head addition, the chain terminates in a CH_2 -xanthate moiety, which cannot fragment again to form an active macroradical and produces a dead polymer chain [31]. These dead chains accumulate over time, thus broadening the PDI. In the RAFT copolymerisation of TFE with iBuVE, no

accumulation of dead chain ends seems to occur, and the slight increase in polydispersity is due to the generation of new polymer chains by the initiator. This may also account for the discrepancy between the theoretical molecular weight and the actual molecular weight.

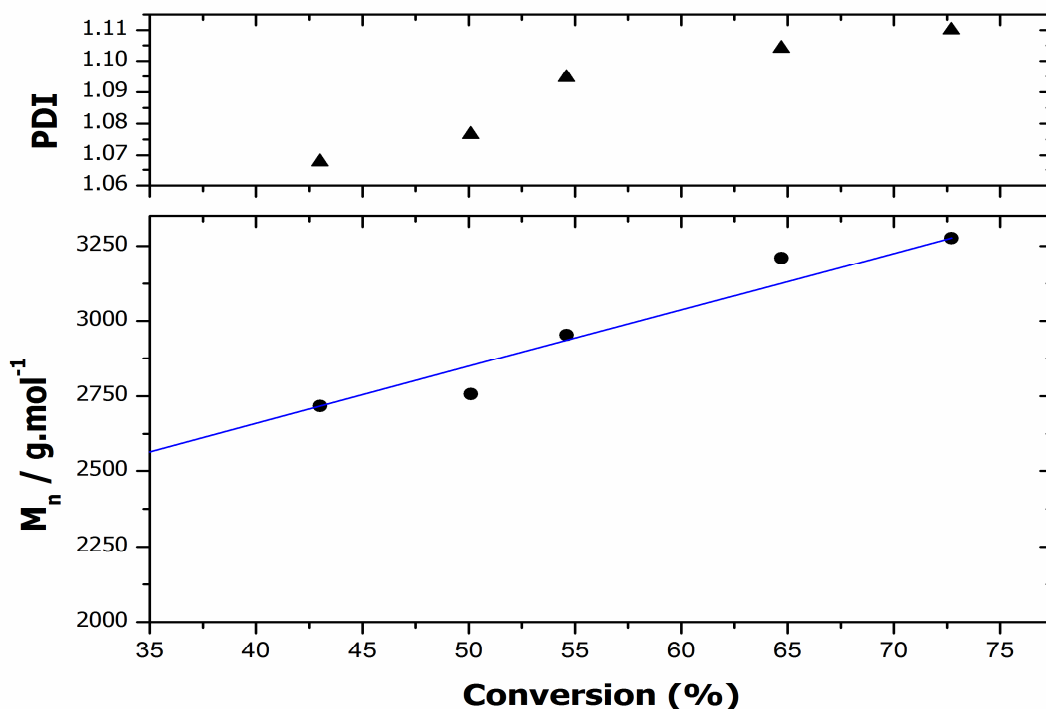


Figure 83: Evolution of M_n and \mathcal{D} as a function of conversion for the MADIX copolymerisation of TFE and *iBuVE* using a 1:1 ratio of monomers and a $[\text{Monomers}]_0:[\text{CTA}]_0:[\text{BPO}]_0$ ratio of 20:1:0.1, with *O*-ethyl-*S*-(1-methoxycarbonyl)-ethylthiocarbonate as CTA.

6.3.2.4 Thermal properties of poly(TFE-*alt*-*iBuVE*) controlled by xanthate

The TGA thermograms of poly(TFE-*alt*-*iBuVE*) copolymers prepared *via* RAFT/MADIX using *O*-ethyl-*S*-(1-methoxycarbonyl)-ethylthiocarbonate are presented in Figure 84. The initial mass loss is more pronounced, as compared to the initial mass loss of the copolymers prepared by free-radical synthesis, due to the greater contribution of the xanthate end-group to the low-temperature elimination, as evidenced by the decrease in low-temperature mass loss with increasing conversion. This behaviour is comparable to that found for PVDF synthesised *via* RAFT/MADIX as the $T_d^{10\%}$ values approach a maximum (*ca.* 170 °C for PVDF and *ca.* 230 °C for poly(TFE-*alt*-*iBuVE*)) with increasing DP_n , but do not exceed this value regardless of how much the molecular weight increases beyond the molecular weight where the elimination of xanthate becomes the determining factor in thermal stability [31].

The curves are all nearly the same shape, which is due to the nearly monodispersed nature of the copolymer chains. This implies that, even at a relatively low DP_n , the thermal stability of poly(TFE-*alt*-iBuVE) is improved by narrowing the molecular-weight distribution. The TGA thermograms obtained under N_2 atmosphere do not differ substantially from the thermograms obtained under air.

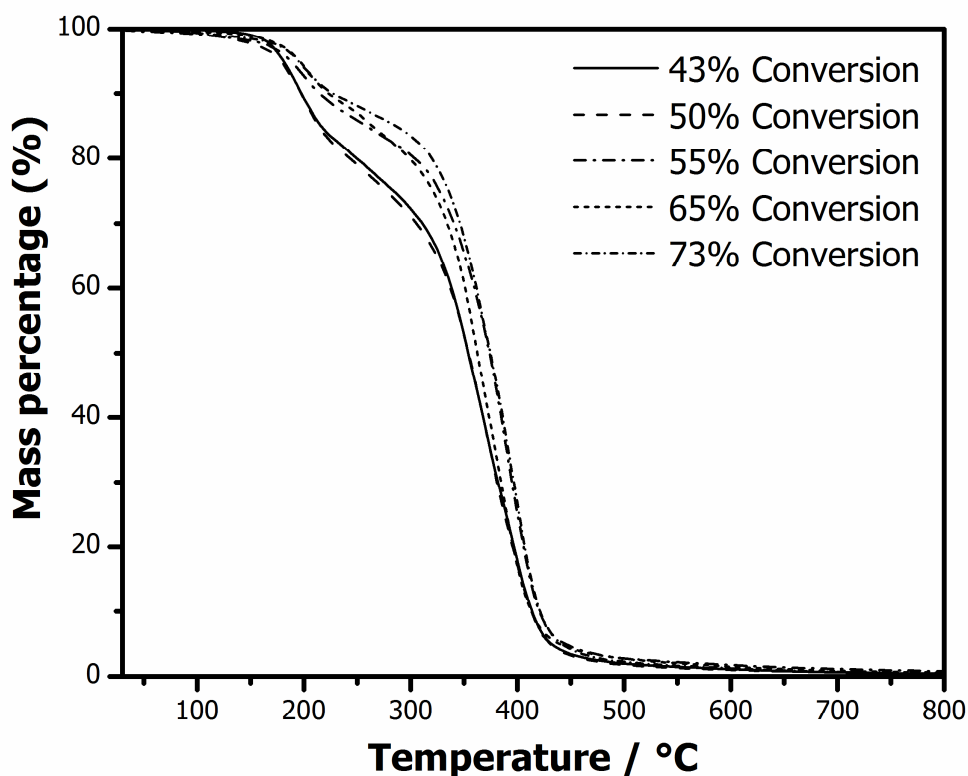


Figure 84: TGA thermograms of poly(TFE-*alt*-iBuVE) copolymers prepared via RAFT/MADIX using *O*-ethyl-*S*-(1-methoxycarbonyl)-ethylthiocarbonate at 15, 30, 60, 120, and 1440 minutes reaction time under N_2 atmosphere.

6.4 Conclusions

The main goal of this study was to demonstrate the unprecedented RAFT/MADIX copolymerisation of TFE with isobutyl vinyl ether using *O*-ethyl-*S*-(1-methoxycarbonyl)-ethylthiocarbonate in DMC. This included an in-depth NMR study on the stereochemistry and the end-group functionality of the poly(TFE-*alt*-iBuVE) system, both in uncontrolled- and in RAFT/MADIX copolymerisation. The ability of *O*-ethyl-*S*-(1-methoxycarbonyl)-ethylthiocarbonate to control the copolymerisation of TFE with iBuVE to produce nearly monodispersed, low-molecular-weight copolymers with a linear evolution of the molecular weight

with conversion, concluded the controlled nature of such a copolymerisation. In contrast to TFE homopolymers, copolymers of TFE with iBuVE are soluble and permit the study of the molecular-weight distribution by liquid-state NMR spectroscopy and GPC. In all cases, alternating copolymers were obtained.

The end-group functionality was invariant with conversion, which implies that, unlike with VDF, termination by the non-fluorinated monomer does not inhibit the ability of the RAFT agent to control the polymerisation.

Compared to the PDIs of PVDF produced with the same chain-transfer agent, which range from 1.05 to 1.34, the PDIs for poly(TFE-*alt*-iBuVE) copolymers obtained *via* RAFT copolymerisation are exceptionally narrow, ranging from 1.08 to 1.11.

Significant proton transfer from the DMC and the vinyl ether monomer on to the macroradical was observed in uncontrolled polymerisation, whereas much less proton transfer was observed with RAFT polymerisation. This is comparable to the results obtained for the RAFT polymerisation of PVDF.

Additionally, it was shown that benzoyl peroxide radicals preferentially attack onto TFE to initiate free radical polymerisation and that a mixed mode of initiation exists in the xanthate controlled polymerisation, with attack onto TFE or iBuVE being equally present. Furthermore, it appears that there was a concerted addition of the monomers to the growing macroradical, producing a mixed end-group functionality. However, TFE appears to be the more favoured end-group, with the ratio of TFE to vinyl ether end-groups nearly invariant with time.

Further work on the limits of this RAFT copolymerisation (to achieve higher molecular weights) as well as the application of the O-ethyl-S-(1-methoxycarbonyl)-ethyldithiocarbonate to the homopolymerisation of TFE may present an interesting avenue of research.

The application of RAFT/MADIX polymerisation to the homopolymerisation of TFE using O-ethyl-S-(1-methoxycarbonyl)-ethyldithiocarbonate is a promising technique for the synthesis of PTFE with well-defined molecular-weight distributions. This method may enable the synthesis of low-molecular-weight, wax-like PTFE suitable for use in extrudable pyrotechnical formulations.

6.5 References

- [1] Wu, S., "Characterization of polymer molecular weight distribution by transient viscoelasticity: Polytetrafluoroethylenes", *Polymer Engineering & Science*, 1988, 28 (8), 538-543.
- [2] Tuminello, W.H., Treat, T.A., and English, A.D., "Poly(tetrafluoroethylene): molecular weight distributions and chain stiffness", *Macromolecules*, 1988, 21 (8), 2606-2610.
- [3] Starkweather, H.W. and Wu, S., "Molecular weight distribution in polymers of tetrafluoroethylene", *Polymer*, 1989, 30 (9), 1669-1674.
- [4] Tuminello, W.H. and Cudré-Mauroux, N., "Determining molecular weight distributions from viscosity versus shear rate flow curves", *Polymer Engineering & Science*, 1991, 31 (20), 1496-1507.
- [5] Klumperman, B., 2002, "Reversible Deactivation Radical Polymerization", in (eds.), *Encyclopedia of Polymer Science and Technology*, John Wiley & Sons, Inc., New York.
- [6] Jenkins, A., D., Jones, R., G., and Moad, G., "Terminology for reversible-deactivation radical polymerization previously called "controlled" radical or "living" radical polymerization (IUPAC Recommendations 2010)", *Pure and Applied Chemistry*, 2009, 82 (2), 483.
- [7] Braunecker, W.A. and Matyjaszewski, K., "Controlled/living radical polymerization: Features, developments, and perspectives", *Progress in Polymer Science*, 2007, 32 (1), 93-146.
- [8] Tatemoto, M., "Development of Iodine Transfer Polymerization and Its Applications to Telechelically Reactive Polymers", *KOBUNSHI RONBUNSHU*, 1992, 49 (10), 765-783.
- [9] Oka, M. and Tatemoto, M., 1984, "Vinylidene fluoride — hexafluoropropylene copolymer having terminal iodines", in W.J. Bailey and Tsuruta, T. (eds.), *Contemporary Topics in Polymer Science: Volume 4*, Springer, Boston, Massachusetts.
- [10] Arcella, V. and Apostolo, M., "Branching and pseudo-living technology in the synthesis of high performance fluoroelastomers", *Rubber World*, 2001, 224 (5), 27.
- [11] Boyer, C., Valade, D., Sauguet, L., Ameduri, B., and Boutevin, B., "Iodine transfer polymerization (ITP) of vinylidene fluoride (VDF). Influence of the defect of VDF chaining on the control of ITP", *Macromolecules*, 2005, 38 (25), 10353-10362.
- [12] Asandei, A.D., Adebolu, O.I., Simpson, C.P., and Kim, J.-S., "Visible-Light hypervalent iodide carboxylate photo(trifluoro)methylations and controlled radical polymerization of fluorinated alkenes", *Angewandte Chemie International Edition*, 2013, 52 (38), 10027-10030.
- [13] Kostov, G., Boschet, F., Buller, J., Badache, L., Brandsadter, S., and Ameduri, B., "First Amphiphilic Poly(vinylidene fluoride-co-3,3,3-trifluoropropene)-b-oligo(vinyl alcohol) Block Copolymers as Potential Nonpersistent Fluorosurfactants from Radical Polymerization Controlled by Xanthate", *Macromolecules*, 2011, 44 (7), 1841-1855.
- [14] Girard, E., Marty, J.-D., Ameduri, B., and Destarac, M., "Direct synthesis of vinylidene fluoride-based amphiphilic diblock copolymers by RAFT/MADIX polymerization", *ACS Macro Letters*, 2012, 1 (2), 270-274.
- [15] Liu, L., Lu, D., Wang, H., Dong, Q., Wang, P., and Bai, R., "Living/controlled free radical copolymerization of chlorotrifluoroethene and butyl vinyl ether under ⁶⁰Co [gamma]-ray irradiation in the presence of S-benzyl O-ethyl dithiocarbonate", *Chemical Communications*, 2011, 47 (27), 7839-7841.
- [16] Wang, P., Dai, J., Liu, L., Dong, Q., Jin, B., and Bai, R., "Xanthate-mediated living/controlled radical copolymerization of hexafluoropropylene and butyl vinyl ether under ⁶⁰Co [gamma]-ray irradiation and preparation of fluorinated polymers end-capped with a fluoroalkyl sulfonic acid group", *Polymer Chemistry*, 2013, 4 (6), 1760-1764.
- [17] Patil, Y. and Ameduri, B., "First RAFT/MADIX radical copolymerization of tert-butyl 2-trifluoromethacrylate with vinylidene fluoride controlled by xanthate", *Polymer Chemistry*, 2013, 4 (9), 2783-2799.

- [18] Tatemoto, M., 15-16 February, 1979, presented at the The First Regular Meeting of Soviet-Japanese Fluorine Chemists, Tokyo, Japan.
- [19] Ameduri, B. and Boutevin, B., 2004, *Well-architected Fluoropolymers: Synthesis, Properties and Applications*, Elsevier Science, Amsterdam, The Netherlands.
- [20] Brinker, K.C. and Bro, M.I., (E.I. du Pont de Nemours and Company) 1958, *Process for polymerizing perfluorinated monomers*, GB805115.
- [21] Cardinal, A.J., Van Dyk, J.W., and Edens, W.L., (E.I. du Pont de Nemours and Company) 1961, *Novel tetrafluoroethylene resins and their preparation*, GB885809.
- [22] Moad, G., Rizzardo, E., and Thang, S.H., "Radical addition-fragmentation chemistry in polymer synthesis", *Polymer*, 2008, 49 (5), 1079-1131.
- [23] Destarac, M., Bliidi, I., Coutelier, O., Guinaudeau, A., Mazières, S., Van Gramberen, E., and Wilson, J., 2012, "Aqueous RAFT/MADIX polymerization: same monomers, new polymers?", in (eds.), *Progress in Controlled Radical Polymerization: Mechanisms and Techniques*, American Chemical Society, Washington, District Columbia.
- [24] Moad, G., Rizzardo, E., and Thang, S.H., "Living Radical Polymerization by the RAFT Process", *Australian Journal of Chemistry*, 2005, 58 (6), 379-410.
- [25] Moad, G., Rizzardo, E., and Thang, S.H., "Living Radical Polymerization by the RAFT Process A First Update", *Australian Journal of Chemistry*, 2006, 59 (10), 669-692.
- [26] Moad, G., Rizzardo, E., and Thang, S.H., "Living Radical Polymerization by the RAFT Process A Second Update", *Australian Journal of Chemistry*, 2009, 62 (11), 1402-1472.
- [27] Moad, G., Rizzardo, E., and Thang, S.H., "Living Radical Polymerization by the RAFT Process – A Third Update", *Australian Journal of Chemistry*, 2012, 65 (8), 985-1076.
- [28] Hill, M.R., Carmean, R.N., and Sumerlin, B.S., "Expanding the Scope of RAFT Polymerization: Recent Advances and New Horizons", *Macromolecules*, 2015, 48 (16), 5459-5469.
- [29] Guerre, M., Wahidur Rahaman, S.M., Ameduri, B., Poli, R., and Ladmiral, V., "RAFT synthesis of well-defined PVDF-b-PVAc block copolymers", *Polymer Chemistry*, 2016, 7 (45), 6918-6933.
- [30] Guerre, M., Rahaman, S.M.W., Améduri, B., Poli, R., and Ladmiral, V., "Limits of Vinylidene Fluoride RAFT Polymerization", *Macromolecules*, 2016, 49 (15), 5386-5396.
- [31] Guerre, M., Campagne, B., Gimello, O., Parra, K., Ameduri, B., and Ladmiral, V., "Deeper Insight into the MADIX Polymerization of Vinylidene Fluoride", *Macromolecules*, 2015, 48 (21), 7810-7822.
- [32] Patil, Y., Ono, T., and Ameduri, B., "Innovative Trifluoromethyl Radical from Persistent Radical as Efficient Initiator for the Radical Copolymerization of Vinylidene Fluoride with tert-Butyl α -Trifluoromethacrylate", *ACS Macro Letters*, 2012, 1 (2), 315-320.
- [33] Liu, X., Coutelier, O., Harrisson, S., Tassaing, T., Marty, J.-D., and Destarac, M., "Enhanced Solubility of Polyvinyl Esters in scCO₂ by Means of Vinyl Trifluorobutyrate Monomer", *ACS Macro Letters*, 2015, 4 (1), 89-93.
- [34] Vandooren, C., Jérôme, R., and Teysslé, P., "Living cationic polymerization of 1H,1H,2H,2H perfluorooctyl vinyl ether", *Polymer Bulletin*, 1994, 32 (4), 387-393.
- [35] Boutevin, B., Cersosimo, F., and Youssef, B., "Studies of the alternating copolymerization of vinyl ethers with chlorotrifluoroethylene", *Macromolecules*, 1992, 25 (11), 2842-2846.
- [36] Puts, G., Lopez, G., Ono, T., Crouse, P., and Ameduri, B., "Radical copolymerisation of chlorotrifluoroethylene with isobutyl vinyl ether initiated by the persistent perfluoro-3-ethyl-2,4-dimethyl-3-pentyl radical", *RSC Advances*, 2015, 5 (52), 41544-41554.
- [37] Tabata, Y. and Du Plessis, T.A., "Radiation-induced copolymerization of chlorotrifluoroethylene with ethyl vinyl ether", *Journal of Polymer Science Part A-1: Polymer Chemistry*, 1971, 9 (12), 3425-3435.

- [38] Hikita, T., Tabata, Y., Oshima, K., and Ishigure, K., "Radiation-induced copolymerization of tetrafluoroethylene with vinyl ethers", *Journal of Polymer Science Part A-1: Polymer Chemistry*, 1972, 10 (10), 2941-2949.
- [39] Schramm, L.L., 2005, *Emulsions, Foams, and Suspensions: Fundamentals and Applications*, Wiley, Weinheim, Germany.
- [40] Hunter, R.J., 1981, "Chapter 6 - Applications of the Zeta Potential", in (eds.), *Zeta Potential in Colloid Science*, Academic Press, Cambridge, Massachusetts.
- [41] Dolbier, W.R., 2009, *Guide to Fluorine NMR for Organic Chemists*, Wiley, New York.
- [42] Shtarov, A.B., Krusic, P.J., Smart, B.E., and Dolbier, W.R., "Bimolecular Kinetic Studies with High-Temperature Gas-Phase ^{19}F NMR: Cycloaddition Reactions of Fluoroolefins", *Journal of the American Chemical Society*, 2001, 123 (41), 9956-9962.
- [43] Berry, K.L. and Peterson, J.H., "Tracer studies of oxidation—Reduction polymerization and molecular weight of "Teflon" tetrafluoroethylene resin", *Journal of the American Chemical Society*, 1951, 73 (11), 5195-5197.
- [44] Guerre, M., Lopez, G., Soulestin, T., Totée, C., Améduri, B., Silly, G., and Ladmiral, V., "A Journey into the Microstructure of PVDF Made by RAFT", *Macromolecular Chemistry and Physics*, 2016, 217 (20), 2275-2285.
- [45] Bawn, C.E.H. and Mellish, S.F., "A method of determination of the rate of molecular dissociation in solution. Parts I and II.-The rate of dissociation of benzoyl peroxide and 2, 2-azo-bis(isobutyronitrile) in various solvents", *Transactions of the Faraday Society*, 1951, 47 (0), 1216-1227.
- [46] Abel, B., Assmann, J., Botschwina, P., Buback, M., Kling, M., Oswald, R., Schmatz, S., Schroeder, J., and Witte, T., "Experimental and theoretical investigations of the ultrafast photoinduced decomposition of organic peroxides in solution: Formation and decarboxylation of benzoyloxy radicals", *The Journal of Physical Chemistry A*, 2003, 107 (26), 5157-5167.
- [47] Brown, D.J., "The thermal decomposition of benzoyl peroxide", *Journal of the American Chemical Society*, 1940, 62 (10), 2657-2659.
- [48] Ceretta, F., Zaggia, A., Conte, L., and Ameduri, B., "Optimization of the synthesis of 4'-nonafluorobutylacetophenone by metal catalysed cross-coupling reaction", *Journal of Fluorine Chemistry*, 2012, 135, 220-224.
- [49] Lopez, G., Guerre, M., Schmidt, J., Talmon, Y., Ladmiral, V., Habas, J.-P., and Ameduri, B., "An amphiphilic PEG-b-PFPE-b-PEG triblock copolymer: synthesis by CuAAC click chemistry and self-assembly in water", *Polymer Chemistry*, 2016, 7 (2), 402-409.
- [50] Tobolsky, A.V., "Dead-end Radical Polymerization", *Journal of the American Chemical Society*, 1958, 80 (22), 5927-5929.
- [51] Tobolsky, A.V., Rogers, C.E., and Brickman, R.D., "Dead-end Radical Polymerization. II", *Journal of the American Chemical Society*, 1960, 82 (6), 1277-1280.
- [52] Zulfiqar, S., Rizvi, M., and Munir, A., "Thermal degradation of chlorotrifluoroethylene-styrene copolymers", *Polymer Degradation and Stability*, 1994, 44 (1), 21-25.
- [53] Zulfiqar, S., Zulfiqar, M., Rizvi, M., Munir, A., and McNeill, I.C., "Study of the thermal degradation of polychlorotrifluoroethylene, poly(vinylidene fluoride) and copolymers of chlorotrifluoroethylene and vinylidene fluoride", *Polymer Degradation and Stability*, 1994, 43 (3), 423-430.
- [54] Zulfiqar, S., Rizvi, M., Munir, A., Ghaffar, A., and McNeill, I.C., "Thermal degradation studies of copolymers of chlorotrifluoroethylene and methyl methacrylate", *Polymer Degradation and Stability*, 1996, 52 (3), 341-348.
- [55] Bartlett, P.D. and Nozaki, K., "The polymerization of allyl compounds. III. The peroxide-induced copolymerization of allyl acetate with maleic anhydride", *Journal of the American Chemical Society*, 1946, 68 (8), 1495-1504.

- [56] Butler, G.B., Olson, K.G., and Tu, C.L., "Monomer orientation control by donor-acceptor complex participation in alternating copolymerization", *Macromolecules*, 1984, 17 (9), 1884-1887.
- [57] Walling, C., Briggs, E.R., Wolfstirn, K.B., and Mayo, F.R., "Copolymerization. X. The Effect of meta- and para-Substitution on the Reactivity of the Styrene Double Bond", *Journal of the American Chemical Society*, 1948, 70 (4), 1537-1542.

Chapter 7

**Radical copolymerisation of
tetrafluoroethylene with 1,4-butanediol divinyl
ether and isobutyl vinyl ether**

7.1 Introduction

The preceding chapters dealt with the production of wax-like PTFE suitable for the extrusion moulding of metal/fluorocarbon pyrotechnical formulations. In particular, Chapter 6 detailed the application of RAFT/MADIX to the copolymerisation of TFE with iBuVE using O-ethyl-S-(1-methoxycarbonyl)-ethyldithiocarbonate as chain-transfer agent. The RAFT/MADIX homopolymerisation of VDF [1], exhibit a defunctionalisation of the macroradicals *via* accumulation with time of CH₂ chain ends. Contrary to this, RAFT/MADIX of copolymerisation TFE seems to accumulate CF₂ chain ends, and no defunctionalisation was observed. Therefore, the application of a RAFT/MADIX approach to the control of the molecular-weight distribution of PTFE was investigated in pilot studies.

RAFT/MADIX homopolymerisation of TFE using O-ethyl-S-(1-methoxycarbonyl)-ethyldithiocarbonate as chain-transfer agent yielded wax-like, low-molecular-weight PTFE. Unfortunately, the thermal stability of the wax-like PTFE synthesised in the pilot studies was unsatisfactory (seen from Figure 90), with the majority of the polymer evaporating long before the ignition temperature for fluorine exchange between metals and fluorocarbons was reached.

As discussed in Chapter 4 (see Section 4.3.1.1), the low-temperature evaporation of low-molecular-weight, linear, unbranched fluorocarbons is due to the minimal chain entanglement present in the polymer. Furthermore, such low-molecular-weight PTFE exhibits poor tensile strength and metal filled rods extruded from this material are likely to break during processing or during handling.

Bridging of the PTFE chains is one possible method for overcoming this chain evaporation, but, thus far, attempts have not been reported to produce a bridged, low-molecular-weight PTFE. Bridging of high-molecular-weight PTFE has generally been effected by γ -ray- and electron-beam-induced chain scission and subsequent branching [2-10]. However, radiation bridged of PTFE is not suited to industrial-scale production of bridged polymer, and the C-F type γ -branches in radiation-bridged PTFE lower the thermal stability of the polymer.

A chemical-crosslinking method appears to be the more desirable route towards a thermally-stable, low-molecular-weight PTFE, but this crosslinking method must result in a polymer that can be facily melt-extruded and that is amenable to application in pyrotechnic devices. By these requirements, the novel tetrafluoroethylene polymer can only contain low levels of crosslinking agent, sufficient to link two to three individual chains together, but not forming a proper network polymer, as well as ensuring only minimal generation of HF during pyrolysis. If the

polymer is fully crosslinked (*i.e.* if each chain is connected to another chain and the entire mass counts as a single molecule), the material will become a hard thermoset. Hence, the term “bridged polymer” is employed, as the polymer chains are bridged together, as opposed to truly crosslinked.

The aim of the study reported in this chapter was to prepare bespoke low-molecular-weight, bridged PTFE suitable for use in time-delay elements, applicable to the South African mining industry. As a first attempt, the PTFE was bridged *in situ* during polymerisation using 1,4-butanediol divinyl ether.

The divinyl ether was chosen over other divinyl compounds as the TFE/vinyl ether system exhibits alternating copolymerisation behaviour [11-13] and incorporation of both vinyl groups into a PTFE chain is nearly certain. As was proven previously, the suppression of the molecular weight of PTFE by alteration of the polymerisation conditions alone did not yield polymers with acceptably-low molecular weight, and, therefore, controlled-radical polymerisation in the form of RAFT/MADIX [14-22] was employed using O-ethyl-S-(1-methyloxycarbonyl)ethyl xanthate as control agent to produce a tetrafluoroethylene wax.

7.2 Experimental

7.2.1 Materials

Tetrafluoroethylene was produced by an in-house generation unit *via* the vacuum (< 1 Pa) pyrolysis of pure PTFE. The PTFE (PTFE 807NX) was purchased from DuPont/Chemours and used as received.

Dimethyl carbonate (99 %), acetone (99 %), benzoyl peroxide (~75 %, remainder water), isobutyl vinyl ether (99 %), 1,4-butanediol divinyl ether (98 %), K_2CO_3 (99 %), ammonium persulfate (>98 %), sodium tetraborate decahydrate (>99 %), and $CDCl_3$ (99 %) were purchased from Sigma Aldrich. HCl (40 % in water) was purchased from ACE Chemicals. The benzoyl peroxide was dried under high vacuum at 30 °C for 24 hours before use. All other reagents were used as received. O-ethyl-S-(1-methyloxycarbonyl)ethyl xanthate was synthesised according to the method of Liu *et al.* [23]. All the chemicals were stored in a fridge at 4 °C, except for the benzoyl peroxide (stored in a freezer at -25 °C).

7.2.2 Free-radical copolymerisation of TFE with BDDVE

Tetrafluoroethylene (TFE) was copolymerized with 1,4-butanediol divinyl ether (BDDVE) in a Carius tube at 85 °C using benzoyl peroxide (BPO) as initiator and dimethyl carbonate (DMC) as solvent. The reaction temperature of 85 °C was chosen as this is close to the 3 hour half-life of the initiator. In all experiments, approximately 0.13 g of K_2CO_3 was added to the Carius tubes as an acid scavenger to prevent cationic homopolymerisation of 1,4-butanediol divinyl ether.

The Carius tubes were loaded with the K_2CO_3 along with the BDDVE and BPO dissolved in 5 mL of DMC. The tubes were subjected to three cycles of degasing *via* the freeze thaw method. The tetrafluoroethylene was then frozen in and the tubes flame sealed under vacuum, after which the Carius tubes were permitted to warm slowly to ambient, installed in their blast tubes within the shaking oven and heating commenced.

After the reaction time was completed, the tubes were cooled to ambient, frozen in liquid nitrogen and cut open. The polymer, being insoluble in acetone, DMC, and chloroform, was stirred rapidly in a 5 % HCl solution to remove the K_2CO_3 , washed with water, and dried *via* a rotavapor.

7.2.3 Free-radical terpolymerisation of TFE with BDDVE and iBuVE

Tetrafluoroethylene (TFE) was copolymerized with BDDVE and iBuVE in a Carius tube at 85 °C using benzoyl peroxide (BPO) as initiator and dimethyl carbonate (DMC) as solvent. The reaction temperature of 85 °C was chosen as this is close to the 3 hour half-life of the initiator. In all experiments, approximately 0.13 g of K_2CO_3 was added to the Carius tubes as an acid scavenger to prevent cationic homopolymerisation of the vinyl ethers.

The Carius tubes were loaded with the K_2CO_3 along with the iBuVE, BDDVE, and BPO dissolved in 5 mL of DMC. The tubes were subjected to three cycles of degasing *via* the freeze thaw method. The tetrafluoroethylene was then frozen in and the tubes flame sealed under vacuum, after which the Carius tubes were permitted to warm slowly to ambient temperature, installed in their blast tubes within the shaking oven, and heating commenced.

After the reaction time was completed, the tubes were cooled to ambient temperature, frozen in liquid nitrogen, and cut open. The resultant polymer was dissolvent in acetone, precipitated into a 5 % HCL solution before being collected, redissolved in acetone, and thoroughly dried using a rotavapor.

7.2.4 Free-radical synthesis of low-molecular-weight bridge PTFE in water, dimethyl carbonate, and perfluoroheptane

Tetrafluoroethylene was copolymerised with small amounts of 1,4-butanediol divinyl ether in a 300-mL Parr autoclave equipped with a set of baffles and a gas-entrainment impeller. With water as solvent, ammonium persulfate (APS) was used as initiator with a reaction temperature of 65 °C, so chosen because it is close to the 1-hour half-life of the initiator. With dimethyl carbonate and perfluoroheptane as solvent, benzoyl peroxide was used as the initiator with a reaction temperature of 85 °C, so chosen because it is close to the 3-hour half-life of the initiator. The reactor was charged with 100 mL of solvent for all experiments.

The reaction conditions were repeated for each of the three solvents used. In all cases, the solvent, initiator, and 0.13 g of K₂CO₃ (acting as acid scavenger to prevent the cationic homopolymerisation of 1,4-butanediol divinyl ether) were loaded into the reactor. The reactor pressured tested for 1 hour under 6 bar of N₂ before being subjected to three cycles of degassing *via* the freeze-thaw method. The tetrafluoroethylene was subsequently frozen in, after which the autoclave was installed within the reactor stand. The frozen autoclave was permitted to slowly warm to ambient conditions (~22 °C) before the heating mantle was fitted and heating commenced.

The reactions were left running overnight (~12 hours). Afterward, the reactor was cooled to ambient and degassed before being opened. After polymerisation, the product polymer was washed with water three times with stirring in a round-bottomed flask before being rinsed with acetone and dried under vacuum at 60 °C.

7.2.5 Synthesis of low-molecular-weight bridged PTFE in water, dimethyl carbonate, and perfluoroheptane by RDRP

The RAFT/MADIX polymerisation was carried out in a similar way to the method described for the aqueous polymerisations, substituting 10 mL of water with acetonitrile and using a molar amount of xanthate double that of the APS initiator. Two experiments were performed, *viz.* one with 10 mol % APS and one with 20 mol % APS, both at 65 °C. For the *in situ* crosslinking, 1 mol % and 2.5 mol % 1,4-butanediol divinyl ether, respectively, was added to a RAFT reaction mixture using 20 mol % initiator at 65 °C.

7.2.6 Thermogravimetric analysis

Thermogravimetric analyses were performed using a Hitachi STA7300 TGA-DTA instrument. Approximately 10 mg of sample was used for each run. Each sample was heated from 30 °C to 1000 °C at a rate of 10 °C·min⁻¹ under a nitrogen atmosphere flowing at 200 mL·min⁻¹.

7.2.7 Differential thermal analysis

Differential thermal analysis was performed with a Shimadzu DTA-50 instrument using 10 mg of sample. The polymer/Si mixtures were run from 20 °C to 1000 °C at a rate of 50 °C·min⁻¹ under a nitrogen atmosphere flowing at 20 mL·min⁻¹.

7.2.8 Swelling tests

Swelling capacity tests were performed by immersing 0.1 g of the product polymer in CHCl₃ at 25 °C for 20 minutes, then filtering off the polymer from the chloroform, dabbing the polymer surface dry of any remaining liquid, followed by weighing of the product. The swelling capacity was calculated as a percentage of the original polymer mass.

7.2.9 Pyrotechnic burn tests

Low-molecular-weight, marginally-bridged PTFE was mixed with silicon powder in an 80:20 ratio. The powders were placed in a mortar and pestle along with cyclohexane sufficient to wet the powders, then ground together for approximately 5 minutes. The mixture was left in a fume hood for 1 hour to permit the cyclohexane to evaporate.

The pyrotechnic mixture was scraped into a 3-cm line loosely packed in a 4-mm wide, 2-mm deep square-cut groove cut into a pyrophyllite brick. The brick had a graded background. The mixture was ignited by heating one end with a small butane torch. Burn rates were measured optically using a high-speed Canon Powershot SX 260 HS camera. The camera lens was covered by a metalized polypropylene foil.

7.3 Results and discussion

7.3.1 Copolymerisation of tetrafluoroethylene and butanediol divinyl ether

The experimental conditions for the free-radical copolymerisation of tetrafluoroethylene (TFE) with butanediol divinyl ether (BDDVE) using BPO as initiator, along with the characterisation results, are summarised in Table 18. The expected structure of poly(TFE-*co*-BDDVE) is shown

in Scheme 21, where the *m* and *l* repeat units are expected to be 0 for a TFE to BDDVE ratio of 1:2.

Benzoyl peroxide has a half-life of ~3 hours at 85 °C in benzene, decomposing into two benzoyl radical that may initiate polymerisation. The decomposition kinetics for benzoyl peroxide in dimethyl carbonate are unknown, but it is reasonable to expect them to be similar to the kinetics in benzene. A polymerisation temperature of 85 °C was chosen to ensure that the reaction rates in this work are comparable to the work done with chlorotrifluoroethylene and PPF. An initial 50 mol % feed of TFE/BDDVE was chosen since the maximum rate of polymerisation should be found at this ratio.

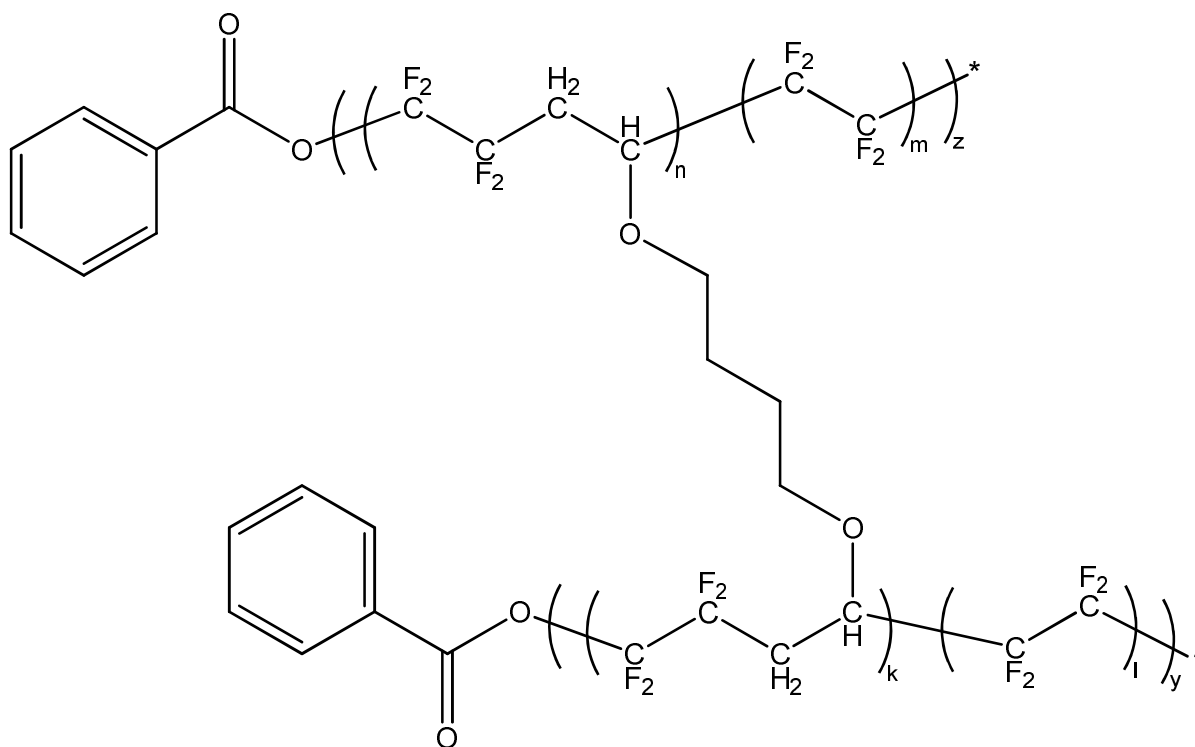
The tube with BDDVE present in a 1:2 ratio formed a clear, gelatinous deposit on the bottom of the tube, with the polymer morphology changing from gelatinous to a clear solution (change-over at 10 % BDDVE) as the amount of divinyl ether decreased. During vacuum drying, all the gelatinous polymers steadily shrank and dried to form a yellow-to-off-white solid, while the soluble polymers rapidly crystallised to form the same. The gelatinous polymers were rubbery when initially isolated from the Carius tubes, but when vacuum dried they became brittle and easily grindable solids, regardless of the BDDVE content. The only major difference between runs was the yield, it being a strong function of the amount of divinyl ether added to the system.

Interestingly, the poly(TFE-*co*-BDDVE) is optically active, exhibiting fluorescence. Taking a photograph with the camera flash on yields a green polymer, while the polymer remains yellow in the picture with the flash off. The photographs are reproduced in Figure 85. This is contrasted with the poly(TFE-*ter*-iBuVE-*ter*-BDDVE) and poly(TFE-*alt*-iBuVE), which do not exhibit such behaviour. Repeating this experiment using a UV-A lamp produced the same effect, as the polymer turns green under the action of near UV or after exposure to sunlight.

Attempts to dissolve the polymers in CHCl₃ were unsuccessful as the polymers simply did not dissolve, even when heat and violent agitation were applied. In all cases, the polymers physically disintegrated after exposure to chloroform, forming a clear to yellowish, wax-like layer on the surface of the CHCl₃. Consequently, neither liquid-state NMR spectroscopy nor swelling tests could be performed on the poly(tetrafluoroethylene-*co*-BDDVE) polymers.

Table 18: Summary of experimental conditions and results obtained for the free-radical copolymerisation of tetrafluoroethylene with butanediol divinyl in DMC.

Experiment No.	TFE mol	$\frac{[BDDVE]_0}{[TFE]_0}$ Mol %	$\frac{[BPO]_0}{[TFE]_0 + [BDDVE]_0}$ Mol %	$T_d^{10\%,c}$ (°C)	Yield (%)
1	0.00499	50	20	282	98
2	0.00499	50	2	380	94
3	0.00499	25	2	360	38
4	0.00499	10	2	330	28
5	0.00499	5	2	300	19
6	0.00499	2.5	2		0



Scheme 21: Expected copolymerisation reaction of TFE and BDDVE initiated by benzoyl radical to yield a poly((TFE-alt-BDDVE)-co-TFE) polymer.

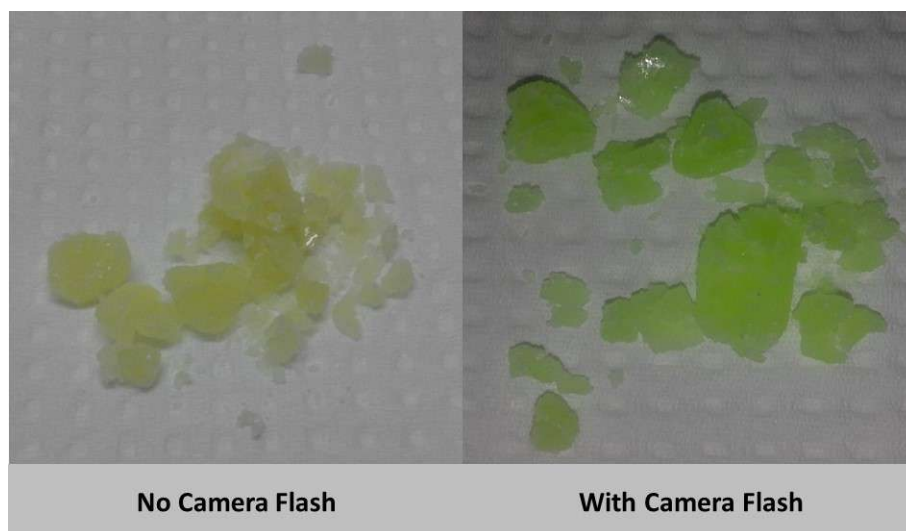


Figure 85: *Fluorescence of poly(TFE-co-BDDVE) under the action of a camera flash.*

The TGA thermograms for the thermal decomposition of poly(tetrafluoroethylene-*co*-BDDVE) polymers under inert atmosphere are presented in Figure 86. All the curves display a two-step decomposition similar to the decomposition found with poly(tetrafluoroethylene-*alt*-iBuVE) copolymers, with the first step being due to the elimination of HF and the decomposition of the pendant chain on the divinyl ether sections.

A vast difference exists in the ratio of the first decomposition step between polymer synthesised with 2 % BPO versus polymer synthesised with 20 % BPO. This is due to an increased ratio of divinyl ether to TFE in the copolymer, presumably due to the lower molecular weight of the 20 % BPO initiated polymer. Interestingly, the content of divinyl ether in the polymer seemingly increases with increasing ratio of TFE to BDDVE. Furthermore, the content of char (tarry, post-decomposition residue) is not related to the initiator concentration or to the ratio of TFE to BDDVE. While it cannot be confirmed without NMR spectroscopy, this is suspected to be due to the relative positions of the divinyl ethers within the copolymer chain as the char content of repeat run polymers synthesised under similar conditions did not show a tendency toward a particular char content and the final mass values were randomly scattered. Repeat runs did, however, show a repeatability on the ratio of BDDVE to TFE incorporated into the polymer (as determined by the ratio of the first decomposition step to the second decomposition step).

The implication here is that there is no uniformity of divinyl ether distribution within the polymer chain and that the polymer chains are randomly bridged.

The TGA results indicate that at sufficiently low BDDVE concentration, the desired copolymer, containing small amounts of randomly distributed divinyl ether interspersed with long-chain sections of TFE homopolymer, is obtained.

7.3.2 Terpolymerisation of tetrafluoroethylene, isobutyl vinyl ether, and butanediol divinyl ether

The experimental conditions for the free-radical copolymerisation of tetrafluoroethylene (TFE) with butanediol divinyl ether (BDDVE) using BPO as initiator, along with the characterisation results, are summarised in Table 19.

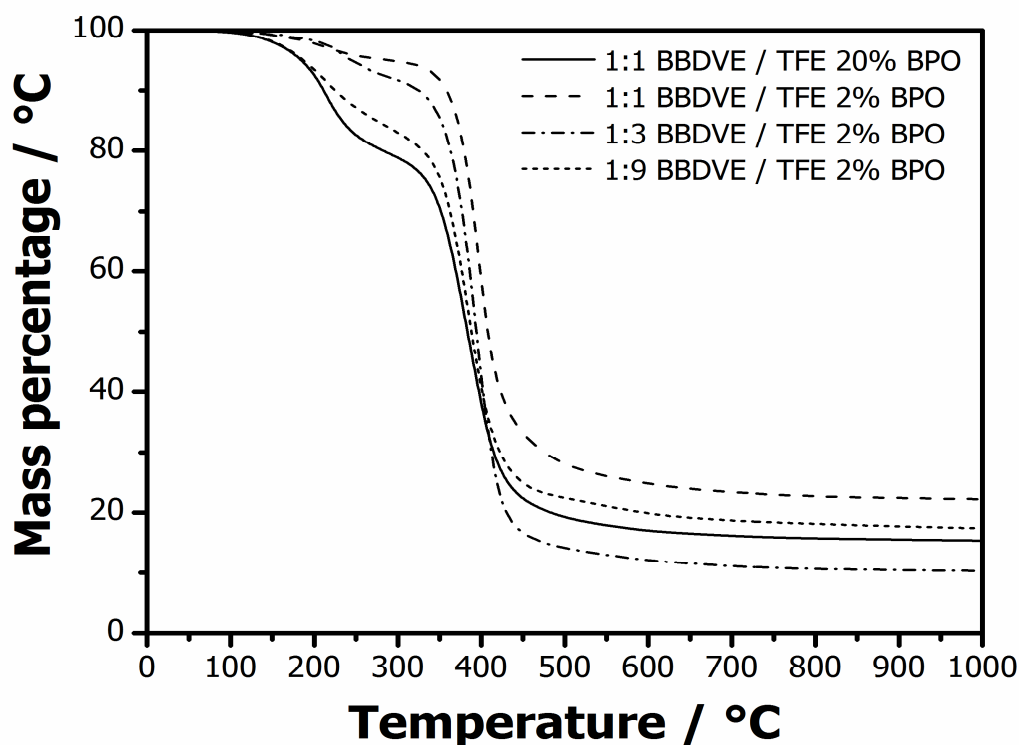


Figure 86: Thermograms for the decomposition of poly(TFE-co-BBVE) copolymers under N_2 atmosphere.

Table 19: *Summary of experimental conditions and results obtained for the free-radical terpolymerisation of tetrafluoroethylene with butanediol divinyl ether and isobutyl vinyl ether using benzoyl peroxide as initiator.*

Experiment No.	TFE + iBuVE Mol	$\frac{[BDDVE]_0}{[TFE]_0 + [iBuVE]_0}$ Mol %	$\frac{[BPO]_0}{[Monomer]_0}$ Mol %	Temperature °C	Yield %	Swelling %
1	0.01	25	20	85	-	N/A
2	0.01	25	2.5	85	62	246
3	0.01	12.5	2.5	85	85	230
4	0.01	5	2.5	85	80	524
5	0.01	2.5	2.5	85	-	N/A
6	0.01	1	2.5	85	-	N/A

The terpolymer morphology is dependent on the amount of divinyl ether and the amount of initiator present, with the product from 20 % initiator experiment isolated as a viscous, off-yellow liquid with crystalline precipitates, while the product from 2.5 % initiator experiments using between 25 % and 5 % divinyl ether were isolated as clear rubbery solids the tactile toughness of which increased with decreasing BDDVE content. The polymers with divinyl ether content below 5 % were isolated as viscous liquids, which formed some crystals with time on the shelf. Unlike poly(TFE-*co*-BDDVE) copolymers, the poly(TFE-*ter*-iBuVE-*ter*-BDDVE) terpolymers do not exhibit any kind of fluorescence. Photographic proof of this is given in Figure 87.

The terpolymers produced with a BDDVE feed content of 2.5 % were slightly soluble in chloroform, and these solutions were subjected to NMR spectroscopic analysis. The ¹H NMR spectrum (shown in Figure 88) exhibited numerous broad signals. The signals for iBuVE and BDDVE overlapped and no significant structural information could be obtained from the spectrum. Notably absent was the signal at 6.6 ppm, which corresponds to the vinyl C-H for both BDDVE and iBuVE. The absence of a vinylic proton indicates that BDDVE incorporates fully into the polymer and that there are insignificant amounts of dangling vinyl ether bonds.



Figure 87: Photograph detailing the rubbery, non-fluorescing poly(TFE-ter-iBuVE-ter-BDDVE) terpolymer.

The ^{19}F NMR spectrum exhibited no significant structural information other than what is expected for a poly(TFE-co-vinyl ether) copolymer (the spectrum is reproduced in Figure 89). The signals at *ca.* -134 ppm indicate a large population of $\text{CF}_2\text{-H}$ moieties. The ^{19}F NMR spectrum indicates much proton transfer on to the CF_2 macroradical.

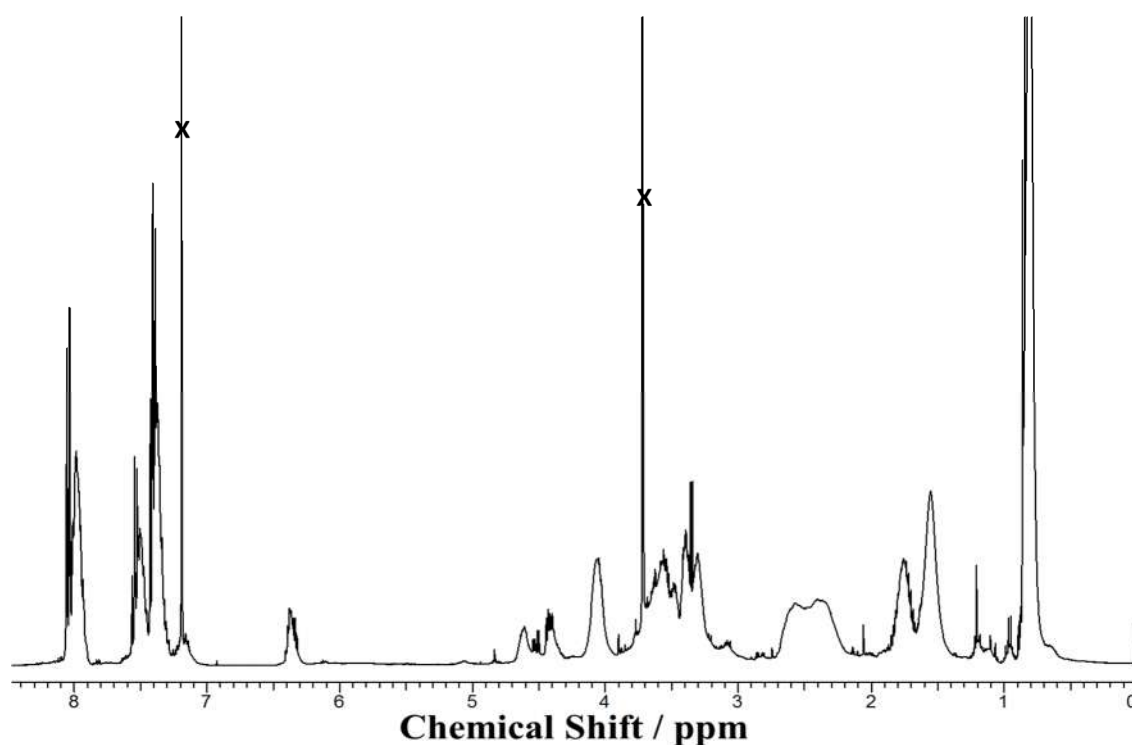


Figure 88: ^1H NMR spectrum for poly(TFE-ter-iBuVE-ter-BDDVE) terpolymer synthesised at 85 °C with a monomer ratio [TFE]:[iBuVE]:[BDDVE] of 20:20:1.

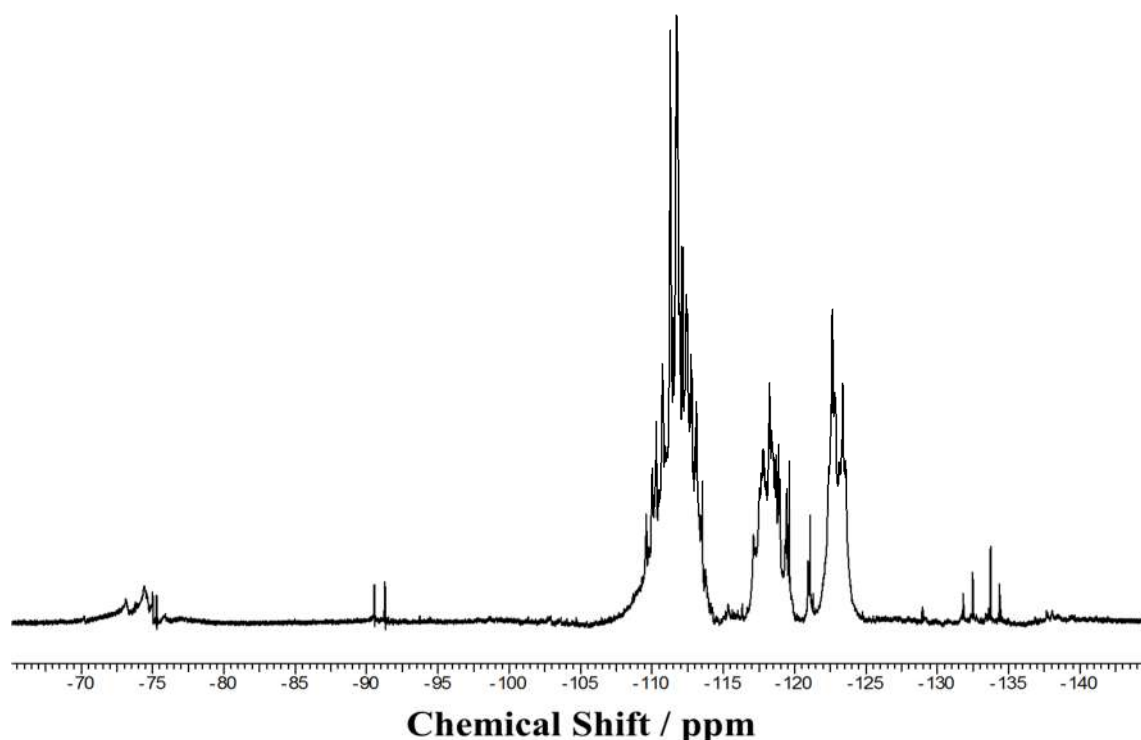


Figure 89: ^{19}F NMR spectrum for poly(TFE-ter-iBuVE-ter-BDDVE) terpolymer synthesised at 85 °C with a monomer ratio [TFE]:[iBuVE]:[BDDVE] of 20:20:1.

7.3.3 Synthesis of low-molecular-weight tetrafluoroethylene polymers marginally bridged with 1,4-butanediol divinyl ether

7.3.3.1 Free-radical synthesis of low-molecular-weight bridge PTFE in water, dimethyl carbonate and perfluoroheptane

The free-radical synthesis of marginally bridged, low-molecular-weight PTFE in perfluoroheptane did not yield any results due to the insolubility of the initiator in the medium, whereas the synthesis in DMC did proceed, but termination by proton abstraction from the dimethyl carbonate produced a clear, viscous compound, easily soluble in organic solvents. The DMC products decomposed before 250 °C in the TGA, and could not be used for burn tests.

The product isolated from aqueous media were powdery and insoluble in all solvents, having the same appearance as PTFE synthesised in water without a bridging agent and exhibited a melting point similar to commercial PTFE (*ca.* 320 °C, as determined by DSC). Burn tests on the free-radical PTFE from aqueous media also proceeded similar to the 20 % APS low-molecular-weight, unbridged PTFE.

The initial hope was that vigorous stirring on the reaction medium, coupled with elevated temperature would cause the BDDVE to dissolve sufficiently to participate in the polymerisation reaction, but the free-radical synthesised PTFE did not seem to have incorporated any bridging agent. Furthermore, this PTFE exhibited a molecular weight in the region of 10^5 dalton (as per the method of Wiegel), similar to the unbridged free-radical PTFE .

Hence, the synthesis of marginally bridged PTFE of low-molecular-weight by free-radical methods did not result in a polymer suitable for pyrotechnic applications.

7.3.3.2 RAFT/MADIX synthesis of low-molecular-weight bridge PTFE in water, dimethyl carbonate, and perfluoroheptane

The TFE homopolymers synthesized using *via* RAFT/MADIX with *O*-ethyl-*S*-(1-methyloxycarbonyl)ethyl xanthate in DMC is of such low molecular weight that most of the polymer evaporates long before 500 °C. The remaining mass is composed of char produced by the xanthate end-groups. The reactions in perfluoroheptane, again, did not result in any polymeric material. However, the reactions in the water/acetonitrile mixture did result in polymeric product, and both the bridged, and unbridged TFE polymer was yellow in colour and waxy in texture. The use of a co-solvent to solubilise the divinyl ether, although undesirable from a commercial standpoint, did result in the incorporation of the bridging agent. Synthesis solely by aqueous polymerisation is therefore not tenable for the production of bridged PTFE.

The thermogram for the decomposition of the PTFE synthesized *via* RAFT/MADIX using 1,4-butanediol divinyl ether, both *in situ* crosslinked (bridged) and unbridged, along with the thermograms for PTFE synthesised by free-radical methods are presented in Figure 90.

The *in situ* bridging PTFE synthesized *via* RAFT/MADIX using 1,4-butanediol divinyl ether exhibits some evaporation, similar to the case of 20 % initiator, but the evaporation is slow enough so that a large portion of the polymer is still present when the bulk decomposition temperature is reached. However, the unbridged PTFE rapidly evaporates (with a $T_{d,10\%}$ of 150 °C), leaving behind a little char from the xanthate end-groups.

The use of a RAFT/MADIX agent to control the molecular weight, coupled with the bridging of the polymer chains seems to lead to a polymer suitable for use in metal/fluorocarbon-based pyrotechnical formulations.

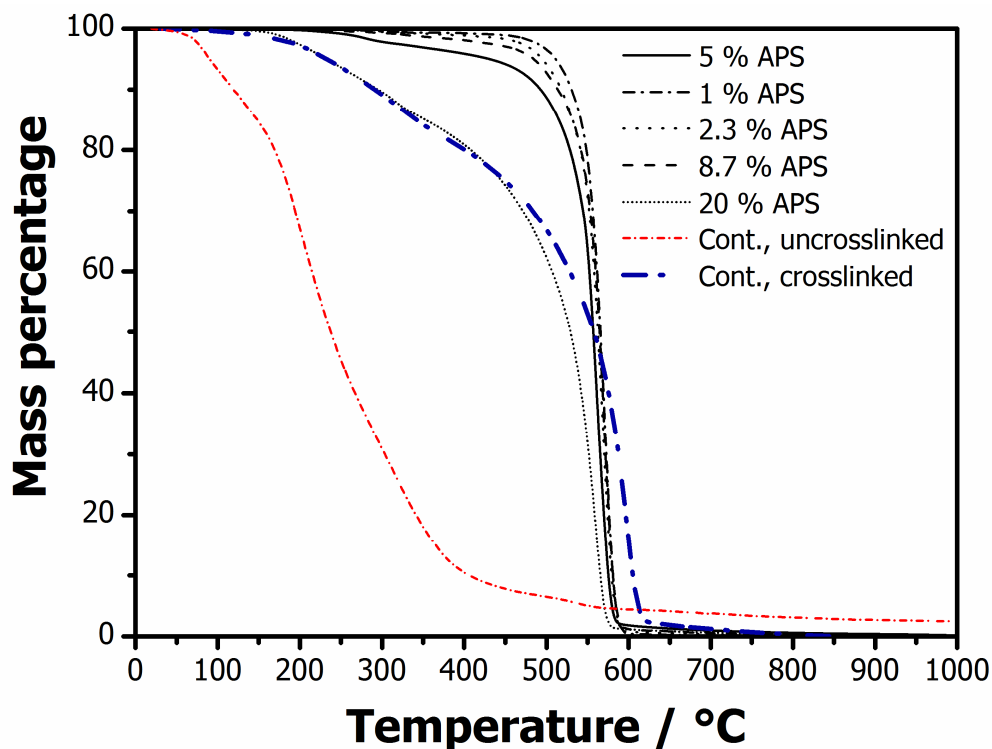


Figure 90: Thermograms for selected PTFE samples decomposed under nitrogen atmosphere.

7.3.4 Pyrotechnic behaviour of low-molecular-weight tetrafluoroethylene polymers marginally bridged with 1,4-butanediol divinyl ether

The burn test results for the various polymers with commercial Si powder are reported in Table 20. Commercial PTFE showed a reluctance to react, irrespective of the ignition method (*i.e.* open flame or electrical wire). The broad-distribution, low-molecular-weight PTFE synthesized with 20 % initiator does react, although slowly, and from this it seems that reducing the molecular weight by an order of magnitude immensely increases the polymer's reaction rate towards Si. The reasons for this behaviour have already been discussed in Section 4.3.3.

Unsurprisingly, and as expected from the thermograms, the unbridged low-molecular-weight PTFE produced *via* RAFT/MADIX evaporates before ignition is achieved. However, the *in situ* bridged PTFE shows a remarkable improvement in reactivity towards Si, with the burn rate being nearly two orders of magnitude faster.

The DTA curves for uncontrolled, low-molecular-weight PTFE with Si and controlled bridged PTFE with Si are reproduced in Figure 91. The curves indicate that only small differences exist between the thermal events for the broad-distribution, low-molecular-weight PTFE and tailored PTFE, with both mixtures exhibiting polymer melting and bulk reaction at roughly the same temperatures.

Table 20: *Summary of open-air ignition tests, and burn rates with electrical ignition, for selected PTFE samples with powdered silicon.*

Polymer	Open-flame ignition	Burn rate (mm·s ⁻¹)
Commercial PTFE	No ignition	No ignition
20 % initiator uncontrolled	Ignition, low-intensity flame	0.035
Controlled unbridged	No ignition	No ignition
Controlled bridged	Ignition, high-intensity flame	3.1

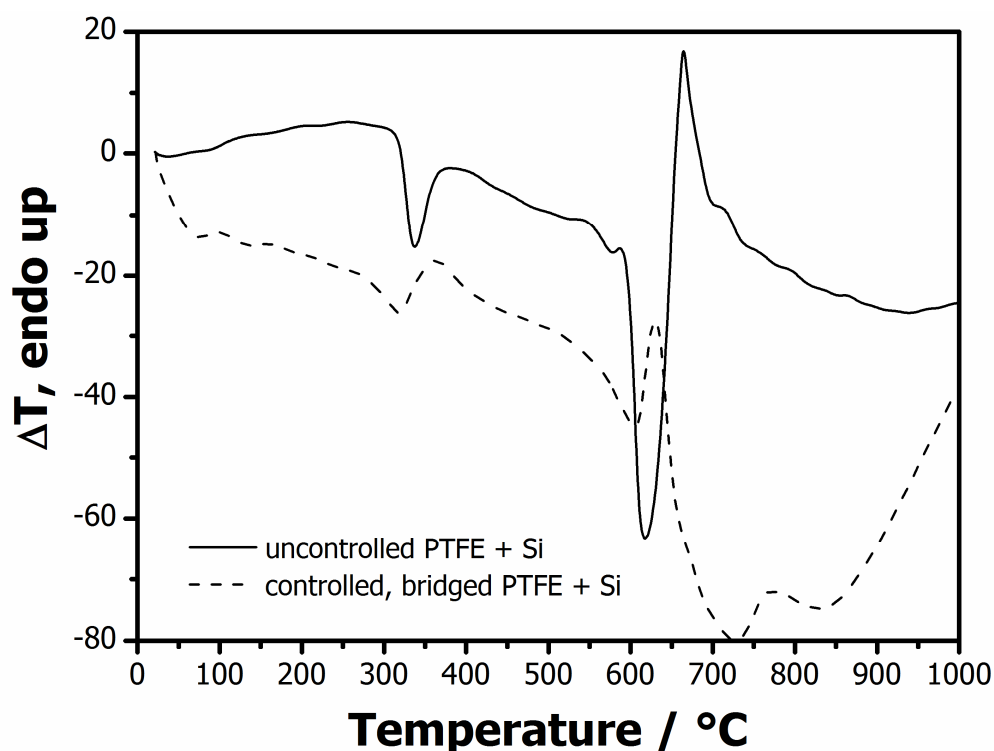


Figure 91: *Differential temperature curves for uncontrolled, low-molecular-weight PTFE/Si- and RAFT controlled, bridged PTFE/Si mixtures.*

As discussed in Section 4.3.3, the increased reactivity of the tailored PTFE towards silicon can be due to both an increased incorporation of Si particles into the polymer matrix or due to the elimination of HF from the end-groups, which removes SiO₂ from the surface of the Si particle,

leaving behind nascent Si. The lack of any significant pre-reaction in the differential thermograms indicates that the liberation of HF in the bridged, controlled polymer is not significantly greater than the HF liberation in the 20 % APS initiated PTFE.

This shows that the reactivity of the tailored PTFE cannot be attributed to any new reaction mechanism, and the improved reactivity should be attributed to the expected efficient incorporation of Si into the polymer matrix due to the breaking of the crystallinity usually associated with PTFE.

7.4 Conclusions

Although the product polymers have not been fully characterised, open-flame ignition tests and burn rates indicate that low-molecular-weight, marginally-crosslinked (bridged) PTFE, prepared using

O-ethyl-S-(1-methyloxycarbonyl)ethyl xanthate as RAFT/MADIX chain-transfer agent and 1,4-butanediol divinyl ether as crosslinker, is suitable for pyrotechnic applications.

The low molecular weight and bridged structure of the polymer results in more intimate mixing with the fuel and improves the processability of the fluorocarbon metal fuel mixture. The bridged nature of the polymer also prevents pre-ignition vapourisation, which has heretofore plagued the application of low-molecular-weight fluoropolymers to pyrotechnics.

Additionally, the conventional wisdom that generation of HF during metal fluorocarbon combustion is undesirable, may not strictly be true. Small amounts of HF may increase the reactivity of the metal fuel towards fluorine exchange with the fluorocarbon.

The insoluble nature of the poly(TFE-*alt*-BDDVE) copolymers makes NMR spectroscopic characterisation difficult. An investigation into the possible solubilisation of these copolymers with a fluorinated solvent was not undertaken due to time constraints. If it should be possible to solubilise the poly(TFE-*alt*-BDDVE) copolymers, NMR spectroscopic characterisation thereof presents an interesting avenue of research regarding the nature of the incorporation of the divinyl ether into the polymer backbone.

7.5 References

- [1] Guerre, M., Campagne, B., Gimello, O., Parra, K., Ameduri, B., and Ladmiral, V., "Deeper Insight into the MADIX Polymerization of Vinylidene Fluoride", *Macromolecules*, 2015, 48 (21), 7810-7822.
- [2] Oshima, A., Ikeda, S., Katoh, E., and Tabata, Y., "Chemical structure and physical properties of radiation-induced crosslinking of polytetrafluoroethylene", *Radiation Physics and Chemistry*, 2001, 62 (1), 39-45.
- [3] Oshima, A., Ikeda, S., Kudoh, H., Seguchi, T., and Tabata, Y., "Temperature effects on radiation induced phenomena in polytetrafluoroethylene (PTFE)—Change of G-value", *Radiation Physics and Chemistry*, 1997, 50 (6), 611-615.
- [4] Oshima, A., Ikeda, S., Seguchi, T., and Tabata, Y., "Change of molecular motion of polytetrafluoroethylene (PTFE) by radiation induced crosslinking", *Radiation Physics and Chemistry*, 1997, 49 (5), 581-588.
- [5] Oshima, A., Ikeda, S., Seguchi, T., and Tabata, Y., "Improvement of radiation resistance for polytetrafluoroethylene (PTFE) by radiation crosslinking", *Radiation Physics and Chemistry*, 1997, 49 (2), 279-284.
- [6] Oshima, A., Seguchi, T., and Tabata, Y., "ESR study on free radicals trapped in crosslinked polytetrafluoroethylene (PTFE)", *Radiation Physics and Chemistry*, 1997, 50 (6), 601-606.
- [7] Oshima, A., Seguchi, T., and Tabata, Y., "ESR study on free radicals trapped in crosslinked polytetrafluoroethylene(PTFE)—II radical formation and reactivity", *Radiation Physics and Chemistry*, 1999, 55 (1), 61-71.
- [8] Oshima, A., Tabata, Y., Kudoh, H., and Seguchi, T., "Radiation induced crosslinking of polytetrafluoroethylene", *Radiation Physics and Chemistry*, 1995, 45 (2), 269-273.
- [9] Oshima, A. and Washio, M., 2007, "Chemical and radiation cross-linking of polytetrafluoroethylene by containing fluorinated compound", in (eds.), *Polymer Durability and Radiation Effects*, American Chemical Society, Washington, District Columbia.
- [10] Bruk, M.A., "Radiation-thermal crosslinking of polytetrafluoroethylene", *High Energy Chemistry*, 2006, 40 (6), 357-369.
- [11] Ameduri, B. and Boutevin, B., 2004, *Well-architected Fluoropolymers: Synthesis, Properties and Applications*, Elsevier Science, Amsterdam, The Netherlands.
- [12] Boutevin, B., Cersosimo, F., and Youssef, B., "Studies of the alternating copolymerization of vinyl ethers with chlorotrifluoroethylene", *Macromolecules*, 1992, 25 (11), 2842-2846.
- [13] Gaboyard, M., Hervaud, Y., and Boutevin, B., "Photoinitiated alternating copolymerization of vinyl ethers with chlorotrifluoroethylene", *Polymer International*, 2002, 51 (7), 577-584.
- [14] Braunecker, W.A. and Matyjaszewski, K., "Controlled/living radical polymerization: Features, developments, and perspectives", *Progress in Polymer Science*, 2007, 32 (1), 93-146.
- [15] Destarac, M., Bliidi, I., Coutelier, O., Guinaudeau, A., Mazières, S., Van Gramberen, E., and Wilson, J., 2012, "Aqueous RAFT/MADIX polymerization: same monomers, new polymers?", in (eds.), *Progress in Controlled Radical Polymerization: Mechanisms and Techniques*, American Chemical Society, Washington, District Columbia.
- [16] Moad, G., Rizzardo, E., and Thang, S.H., "Living Radical Polymerization by the RAFT Process", *Australian Journal of Chemistry*, 2005, 58 (6), 379-410.
- [17] Moad, G., Rizzardo, E., and Thang, S.H., "Living Radical Polymerization by the RAFT Process A First Update", *Australian Journal of Chemistry*, 2006, 59 (10), 669-692.
- [18] Moad, G., Rizzardo, E., and Thang, S.H., "Living Radical Polymerization by the RAFT Process A Second Update", *Australian Journal of Chemistry*, 2009, 62 (11), 1402-1472.

-
- [19] Moad, G., Rizzardo, E., and Thang, S.H., "Living Radical Polymerization by the RAFT Process – A Third Update", *Australian Journal of Chemistry*, 2012, 65 (8), 985-1076.
- [20] Hill, M.R., Carmean, R.N., and Sumerlin, B.S., "Expanding the Scope of RAFT Polymerization: Recent Advances and New Horizons", *Macromolecules*, 2015, 48 (16), 5459-5469.
- [21] Klumperman, B., 2002, "Reversible Deactivation Radical Polymerization", in (eds.), *Encyclopedia of Polymer Science and Technology*, John Wiley & Sons, Inc., New York.
- [22] Moad, G., Rizzardo, E., and Thang, S.H., "Radical addition–fragmentation chemistry in polymer synthesis", *Polymer*, 2008, 49 (5), 1079-1131.
- [23] Liu, X., Coutelier, O., Harrisson, S., Tassaing, T., Marty, J.-D., and Destarac, M., "Enhanced Solubility of Polyvinyl Esters in scCO₂ by Means of Vinyl Trifluorobutyrate Monomer", *ACS Macro Letters*, 2015, 4 (1), 89-93.

Chapter 8

General conclusions

The overall aim of this work was the preparation of a tetrafluoroethylene-based polymer suitable for use in extrudable metal/fluorocarbon pyrotechnic mixtures. Metal/fluorocarbon mixtures are employed extensively in the pyrotechnics industry, among other applications, as the pyrolants comprising time-delay elements in detonators. The application of a melt-extrudable metal/fluorocarbon mixture to these time-delay components will result in a safer and more environmentally benign detonator, which is of immense commercial importance to the South African explosives industry, given that said industry supplies all of sub-Saharan Africa and most of the Middle East, with the detonators used in mining activities.

At present, the industry-standard metal/fluorocarbon mixture is high-molecular-weight PTFE mixed with metals like aluminium, silicon, and magnesium in particular, using Viton as a binding agent. This mixture is not amenable to extrusion moulding techniques, and therefore, detonators comprising a metal fluorocarbon pyrolant must be premade and transported to the usage site; this state of affairs has heretofore limited their use as detonators. Hence, there is a need for an extrudable metal fluorocarbon mixture.

A secondary, but vitally important objective of this research was to develop competency in the synthesis and characterisation of fluoropolymers, a skill set, which prior to this time, has been nearly completely absent in the South African fluorochemical industry.

This document comprises six distinct sections, *viz.*: 1) A review of the homopolymerisation of tetrafluoroethylene; 2) an overview of the construction of the facilities for the generation, safe handling, and polymerisation of TFE; 3) the synthesis of low-molecular-weight PTFE, 4) the synthesis of poly(CTFE-*alt*-iBuVE) copolymers; 5) the synthesis of poly(TFE-*alt*-iBuVE); and 6) the synthesis of marginally bridged, low-molecular-weight PTFE waxes.

1) The review of the homopolymerisation of tetrafluoroethylene, covering all the English language publication in the open literature, from the very first report by Dr Plunkett to the latest developments, details the reaction conditions, equipment, initiators, and additives, as well as the properties of tetrafluoroethylene homopolymers, and the analysis techniques specific to insoluble PTFE.

2) The overview of the facilities construction details the design and assembly of the equipment for the facile and safe generation of tetrafluoroethylene, as well as the equipment required for the homo- and copolymerisation of tetrafluoroethylene. The end result is a laboratory that can produce up to 100 g of tetrafluoroethylene with a purity of not less than 95 % and can polymerise the monomer in either Carius tubes or autoclaves.

3) The third section of this work details the investigation into the suppression of the molecular weight of PTFE by changing the polymerisation conditions (*e.g.* the temperature and initiator concentration). While it was possible to decrease the molecular weight significantly lower than that of commercial PTFE ($\sim 10^5$ as opposed to $\sim 10^7$), the kinetics of aqueous TFE polymerisation did not permit the synthesis of a PTFE wax with the molecular weight in the range required for extrusion. An attempt was made to develop a kinetic expression that could predict the molecular-weight distribution of PTFE by extending Tobolsky's law to admit a diffusion controlled reaction mechanism. The kinetic route was followed in an attempt to elucidate if it was possible to tailor the molecular weight distribution of PTFE by only adjusting the polymerisation conditions, and guide the selection of experimental parameters that would produce a wax-like PTFE with the desired properties. The sub-project was abandoned in favour of other, more promising synthetic routes.

4) The fourth section of this work details the synthesis of poly(CTFE-*alt*-iBuVE) copolymers using a perfluorinated persistent radical as initiator. This was undertaken firstly, to effect skills transfer from France to South Africa regarding advanced techniques for the synthesis of fluoropolymers and, secondly, to validate the use of the PPR as an NMR tracer on polymers where the backbone contains large, continuous sections of fully fluorinated moieties, as opposed to the partially fluorinated moieties found in VDF copolymers. PPR was found to be an excellent end-group marker for fluoropolymers, and number-average molecular weights were readily obtained from the NMR spectra. Application of PPR to TFE homopolymers was not attempted due to technical issues concerning the solid-state NMR spectroscopic analysis of the insoluble TFE homopolymers. Specifically, the SS-NMR spectrometer at the University of KwaZulu-Natal experienced a technical breakdown and is still not operational.

5) The fifth part of this work focuses on the use of RDRP techniques to effect control of the TFE polymerisation process, specifically the use of RAFT/MADIX techniques. As TFE homopolymers are insoluble, and the molecular weights therefore cannot be studied by the usual techniques such as GPC, light scattering, or osmometry, the ability of a MADIX agent to control a polymerisation where TFE is present was investigated by copolymerising TFE with iBuVE in DMC using O-ethyl-S-(1-methyloxycarbonyl)ethyl xanthate as RAFT/MADIX control agent. Not only can RAFT/MADIX techniques control the polymerisation of a monomer as reactive as TFE, but the resultant polymers have a tightly controlled molecular-weight distribution, much tighter than what is observed for VDF. Molecular weights in the region of 3300 Da and polydispersities in the region of 1.1 were achieved.

6) The sixth and final section of this work details the synthesis of low-molecular-weight PTFE synthesised *via* RAFT/MADIX, marginally bridged by butanediol divinyl ether, as well as a comparison of the performance of this polymer with those of commercial PTFE, and of an unbridged PTFE wax in the pyrotechnic combustion with silicon metal. The low-molecular-weight, marginally-bridged PTFE showed excellent thermal stability in relation to the low-molecular-weight, unbridged PTFE wax and also exhibited a much improved burn rate with silicon than either commercial PTFE or PTFE synthesised with 20 % APS. The marginally-bridged, low-molecular-weight PTFE exhibited a burn rate of $3.1 \text{ mm}\cdot\text{s}^{-1}$ whereas the unbridged, low-molecular-weight PTFE exhibited a burn rate of $0.035 \text{ mm}\cdot\text{s}^{-1}$.

The overall aim of this work has been met with the synthesis of the bridged PTFE wax and sets the stage for developing fluorocarbon wax/metal formulations to test in actual extrusion processing. This new material promises to open up a new section of industrial application for fluorocarbon-based pyrotechnics and may positively impact the South African explosives market.

Future research avenues emanating from the outstanding issues regarding the results reported here, are: the refinement of the diffusion constants, mass-transfer correlations, and the kinetic parameters for the polymerisation of tetrafluoroethylene in water; and the limits to which RAFT/MADIX techniques can grow the poly(TFE-*alt*-iBuVE) copolymer chains before the polymerisation reaction enters an uncontrolled regime

